

INTERACTION BETWEEN WOOD AND GEOPOLYMER

DISSERTATION

with the aim of achieving the degree of *Doctor rerum naturalium* at

University of Hamburg

Faculty of Mathematics, Informatics, Natural Sciences

Biology Department

submitted by

Bright Asante

born in Kumasi, Ghana

Hamburg 2022

Type: Cumulative dissertation
Title: Interaction between wood and geopolymer
Author: Bright Asante
Page count: 164
Date of submission: 22.10.2022
Date of defense: 19.01.2023

Advisor and examiner:

Prof. Dr. Andreas Krause

Head of Institute,
Thünen Institute for Wood Research
Hamburg- Germany.

Co-Examiner:

Prof. Martina Meincken

Stellenbosch University,
Cape Town- South Africa.

Other oral defense commission members

Prof. Dr. Elisabeth Magel

University of Hamburg
Faculty of Mathematics, Informatics, Natural
Sciences
Hamburg- Germany

Prof. Dr. Bodo Saake

University of Hamburg
Faculty of Mathematics, Informatics, Natural
Sciences
Hamburg- Germany

Dedicated to my family

ACKNOWLEDGEMENT

My sincere gratitude belongs to God Almighty, for the strength and health to complete what He started.

I would like to thank my supervisor, Prof. Dr. Andreas Krause, for his time and support, the valuable advice and recommendations which helped to make this work a success. It has been an outstanding opportunity to be one of your doctoral students. In addition to my dedicated and cheerful Project Coordinator, Dr. Göran Schmidt, I wish to acknowledge him for his significant help not only with this project but also with my thesis. I am grateful to Professor Krause and Dr. Schmidt for believing in me and accepting me to work on the BioHome project. The German Academic Exchange (DAAD) and DLR funded my research as part of the BioHome Project, and I am grateful for their assistance.

I really appreciate the help from the Former acting director of Thünen Institute, Dr. Johannes Welling for help and advice during my early years at the work place. Dr. Hanzhou Ye for the time we spent working together on geopolymer. It was a joy to learn a lot during this time. Also, my profound appreciation belongs to Prof. Bodo Saake and Dr. Michael Altgen for helping me get funds and support when I was out of funding. Your support was really helpful to carry me through the challenging times during the covid season.

A big thank you to Prof. Holmer Savastano Jr. (University of Sao Paulo) for all that you taught me in your lab in Brazil. Thank you to all coauthors who contributed to my publications. My work would not have been a success without the help of these technicians from University of Hamburg (UHH) and Thünen Institute: Johannes Beruda (UHH), Tanja Potsch (TI), Gabriele Circelli (TI) and Sabrina Heldner (TI). I appreciate your help.

A big thank you to Mrs. Vicki Marais, Syllas Lau (UHH), Emilin Joma Da Silva (TI), Marco De Angelis (UHH) and all the Doctoral students who were on the BioHome project (colleagues from Stellenbosch University and Addis Ababa Institute of Technology). Lastly, a big thank you to Mrs. Judith Schlegel, Mr. Asaac Assali, the Bergmann and Asante families for their emotional and additional support during this hectic time of my studies. Although your help was not directly related to my thesis, it helped me to make this dream a reality. Without all of you I might have given up already.

I thank everyone who contributed directly or indirectly to my success and wish you tenfold blessings.

ABSTRACT

Geopolymers are commonly produced by the alkaline activation of aluminosilicate materials, such as fly ash and metakaolin. However, adding wood in an alkaline environment, such as that found in a geopolymer, may lead to the simultaneous leaching of various extracts and structural and non-structural polysaccharides as well as the cross-effects of these substances in affecting the geopolymer matrix, making it more complicated to understand the mechanism of polymerization/hardening of the geopolymer wood composite (GWC). The influence of extractives and the bonding of wood to the geopolymer matrix may differ among wood species due to the complexity and variation within wood. Moreover, the varying moisture content and hydrophilicity of wood (An intrinsic wood property) can affect the production of GWC as well as its final properties.

The present thesis investigated how wood inherent properties and wood material preprocessing affect the properties of geopolymer wood composites. Class F Fly ash from coal and metakaolin were used as aluminosilicate precursor materials for the studies. The precursors were activated with a combination of sodium silicate and sodium hydroxide solution at a weight ratio of 2.5:1. The wood materials used included wood particles from pine and eucalypt, softwood fibers, C100 softwood flour, rotary veneer (spruce and beech) as well as wood extractives from softwood (i.e. pine and spruce), hardwood (i.e. eucalypt species (*E. grandis* and *E. camaldulensis*) and acacia species (*A. mearnsii* and *A. saligna*). The influence of specific extractives such as polyphenols, resin and fatty acids on the strength of pure geopolymer was also tested. Wood material preprocessing includes moisture conditioning of wood flour (i.e. 0 to 90% moisture content), hot water and NaOH pretreatment of wood particles as well as sanding of the wood veneer with grit sizes P60, 100 and 180.

From the results, physical properties (i.e. water absorption, apparent porosity and density) and strength (i.e. compressive and specific compressive strength) of the GWC were affected by the wood species used in composite manufacture. In general, the physical properties and strength of pine-based composites were lower than eucalyptus ones. However, with hot water pretreatment of the wood particles, there was a 27% and 3% increase in the specific strength of pine-based and eucalyptus-based composites respectively. With 1% NaOH pretreatment of pine sapwood and heartwood particles, there was a significant increase in the specific strength of the GWC with sapwood but no significant increase in strength of those with heartwood. The specific strength of pure fly ash-based geopolymer with hardwood extractives was not

significantly different from the control (i.e. pure fly ash-based geopolymer without extractive). However, there was a reduction in the specific strength of those containing softwood extractives from pine and spruce with the former having the highest reduction. Furthermore, all the tested polyphenols, resin and fatty acids recorded lower specific strengths when compared to the control without any extractive. Since all extractive compounds investigated in this study reduced the specific strength of the geopolymer, the combined effect of these specific extractives could even be greater.

During this study, it was found that water, which became a part of the GWC (i.e. structurally bound water), was not able to be removed after drying at 103 degrees. A higher initial MC of the wood flour used in producing GWC led to an increase in structurally bound water. The SEM images showed that forming fly ash-based GWCs using a higher wood MC led to inferior interface bonding (gaps) between the fly ash-based geopolymer matrix and the wood. Generally, the GWC with dried wood flour ($\approx 0\%$ MC) recorded the highest specific strength and lowest porosity. Additionally, the fiber pullout test was modified by using spruce and beech wood veneer to determine the interfacial bonding strength of metakaolin-based geopolymer-wood composites. In comparison with beech, the geopolymer displayed a higher interfacial bonding strength with spruce. By sanding with 60-grit sandpaper, an increase in the interfacial bond strength was successfully achieved, brought about by strong mechanical interlocking at the interface, this being confirmed by microscopy imaging. It was found out that dimensional changes in wood played a key role in the bonding of both spruce and beech veneer to the metakaolin-based geopolymer. Finally, using fly ash and metakaolin as discrete precursors, the present thesis investigated the effects of wood type (wood fibers and flour) and mixing parameters on strength and density profiles. Fly ash-based and metakaolin-based GWCs showed a nearly constant density profile and similar strength in all mixtures. In conclusion, when to add what raw material is of little importance in the formulation of geopolymer wood fiber/ flour composites, on the condition that the mixing time and amount of raw materials remain the same. This gives more flexibility during composite formulation or production.

Kurzfassung

Geopolymere werden in der Regel durch die alkalische Aktivierung von Alumosilikatmaterialien wie Flugasche und Metakaolin hergestellt. Die Zugabe von Holz in einer alkalischen Umgebung wie in einem Geopolymer kann jedoch zur gleichzeitigen Auslaugung verschiedener Extrakte, struktureller und nicht-struktureller Polysaccharide und zu Kreuzwirkungen dieser Substanzen auf die Geopolymermatrix führen, was das Verständnis des Mechanismus der Polymerisation/Härtung des Geopolymer-Holz-Verbundstoffs (GWC) erschwert. Der Einfluss der Extraktionsmittel und die Bindung des Holzes an die Geopolymermatrix kann sich aufgrund der Komplexität und der Variationen innerhalb des Holzes von Holzart zu Holzart unterscheiden. Darüber hinaus können der unterschiedliche Feuchtigkeitsgehalt und die Hydrophilie des Holzes (d. h. eine intrinsische Holzeigenschaft) die Herstellung von GWC sowie seine endgültigen Eigenschaften beeinflussen.

In der vorliegenden Arbeit wurde untersucht, wie sich die inhärenten Eigenschaften von Holz und die Vorverarbeitung des Holzmaterials auf die Eigenschaften von Geopolymer-Holz-Verbundwerkstoffen auswirken. Für die Untersuchungen wurden Flugasche der Klasse F aus Kohle und Metakaolin als Aluminosilikat-Vorstufenmaterialien verwendet. Die Vorprodukte wurden mit einer Kombination aus Natriumsilikat und Natriumhydroxidlösung im Gewichtsverhältnis 2,5:1 aktiviert. Zu den verwendeten Holzmaterialien gehören Holzpartikel aus Kiefer und Eukalyptus, Weichholzfasern, C100-Weichholzmehl, Schäl furnier (Fichte und Buche) sowie Holzextrakte aus Weichholz (d. h. Kiefer und Fichte) und Hartholz (d. h. Eukalyptusarten (*E. grandis* und *E. camaldulensis*) und Akazienarten (*A. mearnsii* und *A. saligna*)). Der Einfluss spezifischer Extrakte wie Polyphenole, Harz und Fettsäuren auf die Festigkeit von reinem Geopolymer wurde ebenfalls getestet. Die Vorbehandlung des Holzmaterials umfasst die Konditionierung des Holzmehls auf einen Feuchtigkeitsgehalt von 0 bis 90 %, die Vorbehandlung der Holzpartikel mit heißem Wasser und NaOH sowie das Schleifen des Holz furniers mit den Körnungen P60, 100 und 180.

Die Ergebnisse zeigen, dass die physikalischen Eigenschaften (d. h. Wasseraufnahme, scheinbare Porosität und Dichte) und die Festigkeit (d. h. Druckfestigkeit und spezifische Druckfestigkeit) des GWC durch die bei der Verbundstoffherstellung verwendete Holzart beeinflusst wurden. Im Allgemeinen waren die physikalischen Eigenschaften und die Festigkeit von Verbundwerkstoffen auf Kiefern basis geringer als die von Eukalyptus. Durch eine Vorbehandlung der Holzpartikel mit heißem Wasser konnte die spezifische Festigkeit von Verbundwerkstoffen auf Kiefern- bzw. Eukalyptus basis jedoch um 27 % bzw. 3 % erhöht

werden. Bei einer 1%igen NaOH-Vorbehandlung der Kiefern Splint- und -kernholzpartikel kam es zu einer signifikanten Erhöhung der spezifischen Festigkeit der GWC mit Splint, aber zu keiner signifikanten Erhöhung der Festigkeit derjenigen mit Kernholz. Die spezifische Festigkeit von reinem Geopolymer auf Flugaschebasis mit Hartholzextrakten unterschied sich nicht signifikant von der Kontrolle (d. h. reines Geopolymer auf Flugaschebasis ohne Extrakte). Die spezifische Festigkeit von Geopolymeren, die Weichholzextrakte aus Kiefer und Fichte enthielten, nahm jedoch ab, wobei erstere die stärkste Verringerung aufwiesen. Darüber hinaus wiesen alle getesteten Polyphenole, Harze und Fettsäuren niedrigere spezifische Festigkeiten im Vergleich zur Kontrolle ohne Extraktionsmittel auf. Da alle in dieser Studie untersuchten Extraktionsmittel die spezifische Festigkeit des Geopolymers verringerten, könnte die kombinierte Wirkung dieser spezifischen Extraktionsmittel sogar noch größer sein.

In dieser Studie wurde festgestellt, dass Wasser zu einem Teil des GWC wurde (d. h. strukturell gebundenes Wasser), das nach der Trocknung bei 103 Grad nicht entfernt werden konnte. Eine höhere anfängliche MC des Holzmehls, das zur Herstellung von GWC verwendet wurde, führte zu einem Anstieg des strukturell gebundenen Wassers. Die REM-Bilder zeigten, dass die Bildung von GWC auf Flugaschebasis mit einer höheren Holz-MC zu einer schlechteren Grenzflächenbindung (Lücken) zwischen der Geopolymermatrix auf Flugaschebasis und dem Holz führte. Im Allgemeinen wiesen die GWC mit getrocknetem Holzmehl ($\approx 0\%$ MC) die höchste spezifische Festigkeit und die geringste Porosität auf. Darüber hinaus wurde der Faserauszugstest durch die Verwendung von Fichten- und Buchenurnier modifiziert, um die Grenzflächenhaftung von Geopolymer-Holz-Verbundwerkstoffen auf Metakaolinbasis zu bestimmen. Im Vergleich zu Buche zeigte das Geopolymer eine höhere Grenzflächenhaftung mit Fichte. Durch Schleifen mit Schleifpapier der Körnung 60 konnte die Grenzflächenhaftung aufgrund einer starken mechanischen Verzahnung an der Grenzfläche erfolgreich erhöht werden, was auch durch mikroskopische Aufnahmen bestätigt wurde. Es wurde festgestellt, dass Dimensionsänderungen im Holz eine Schlüsselrolle bei der Verbindung von Fichten- und Buchenurnier mit dem Geopolymer auf Metakaolinbasis spielen. Schließlich wurden in der vorliegenden Arbeit unter Verwendung von Flugasche und Metakaolin als diskrete Ausgangsstoffe die Auswirkungen der Holzart (Holzfaser und -mehl) und der Mischungsparameter auf Festigkeits- und Dichteprofile untersucht. Flugasche- und Metakaolin-basierte GWCs zeigten ein nahezu konstantes Dichteprofil und ähnliche Festigkeit in allen Mischungen. Zusammenfassend lässt sich sagen, dass es bei der Formulierung von geopolymeren Holzfaser-Mehl-Verbundwerkstoffen nicht wirklich darauf ankommt, wann man welchen Rohstoff hinzufügt. Dies gilt, solange die Mischzeit und die Menge der Rohstoffe

gleich bleiben. Dies bietet mehr Flexibilität bei der Formulierung oder Herstellung von Verbundwerkstoffen.

Table of content

Acknowledgement	i
Abstract	ii
Kurzfassung	iv
Content	vii
CHAPTER 1 Introduction	1
1.1 Geopolymer matrix synthesis and chemistry	2
1.2 Kinds of geopolymers (matrix)	5
1.2.1 Fly ash and fly ash-based geopolymer	5
1.2.2 Metakaolin and Metakaolin-based geopolymer	7
1.2.3 Acid-based geopolymers	9
1.3 Geopolymerization process	9
1.4 Wood as a material	12
1.5 General information of wood species used in this present thesis work	14
1.5.1 Softwood species	14
1.5.2 Hardwood species	15
1.6 Composites materials	17
1.6.1 Wood-based composites	19
1.6.2 Inorganic bonded wood composites	19
1.6.2.1 Cement bonded wood composites	20
1.6.2.2 Geopolymer wood composites	21
1.7 Wood as a filler or reinforcement in inorganic bonded wood composites	23
1.8 Working Hypothesis and Integration of Publications	27
CHAPTER 2 Materials and methods	31
2.1 Materials	31
2.1.1 Wood materials	31
2.1.2 Geopolymer precursors	31
2.1.3 Alkaline solution and other reagents	31
2.2 Methods	32

CHAPTER 3	34
Chapter 3.1 Influence of wood pretreatment and fly ash particle size on the performance of geopolymer wood composite (Paper 1)	34
1 Introduction	36
2 Materials and Methods	38
3 Results and Discussion	40
4 Conclusions	46
Chapter 3.2 Influence of wood pretreatment, hardwood and softwood extractives on the compressive behavior of fly ash-based geopolymer composite (Submitted)	49
1 Introduction	51
2 Materials and Methods	54
3 Results and Discussion	60
4 Conclusions	76
CHAPTER 4 Influence of wood moisture content on the hardened state properties of GWC (Paper 2)	83
1 Introduction	85
2 Materials and Methods	86
3 Results and Discussion	87
4 Conclusions	91
CHAPTER 5 Interfacial bonding properties of the eco-friendly geopolymer-wood composites: influences of embedded wood depth, wood surface roughness, and moisture conditions (Paper 3)	94
1 Introduction	97
2 Materials and Methods	98
3 Results and Discussion	101
4 Conclusions	106
CHAPTER 6 Preliminary studies on the influence of processing (mixing) parameters on the properties of geopolymer wood composite	110
1 Introduction	110
2 Materials and Methods	113

3 Results and Discussion	116
4 Conclusions	121
CHAPTER 7 Discussion of the conducted research	124
7.1 Evaluation of how wood's inherent properties affect properties of geopolymer wood composites	124
7.1.1 <i>Effect of wood species on the properties of geopolymer wood composite</i>	124
7.1.2 <i>Effect of wood extractives on the properties of geopolymer wood composite</i>	126
7.1.3 <i>Effects of the portion of wood and pretreatment on the properties of geopolymer wood composite</i>	128
7.2 Evaluation of material preprocessing of geopolymer wood composites	129
7.2.1 <i>Effect of wood moisture content on the properties of geopolymer wood composite</i> ...	130
7.2.2 <i>Effect of wood surface roughness on the properties of geopolymer wood composite</i>	131
7.2.3 <i>Effect of dimensional instability in wood on the interfacial bonding strength</i>	134
7.2.4 <i>Influence of different mixing and manufacturing process on the density and strength of geopolymer wood composite</i>	135
CHAPTER 8 General conclusion from the research	137
List of Tables	140
List of Figures	142
Abbreviations	146
References	147
Declaration	164

CHAPTER 1

INTRODUCTION

Wood-based composites can be classified based on the polymers used as binder or matrix material. Conventional wood-based composite products, like high or medium density fiberboard and particleboard, use thermoset resins to bind the wood together. In Europe, wood-based composites based on thermoplastic polymers are commonly referred to as wood plastic composites. The binding agents for the wood components in these composites are thermoplastics such as polyethylene or polypropylene. In contrast to thermoplastic resins, thermoset resins occur in a liquid state prior to processing and form rigid solids after curing. After curing, unlike thermoplastics, they do not melt again. This calls for different processing technologies when manufacturing these composites.

Inorganic bonded wood composites (IBWC) remain as one group of materials utilized in the building and construction sector. Examples of IBWC include ceramic-bonded, gypsum-bonded, Magnesia-bonded and Portland cement-bonded wood composites. Common applications of IBWC include flooring, tiling, prefabricated houses, façade, ceilings, and exterior and partition walls. However, cement-bonded wood composites dominate the market share of IBWC (Sarmin et al. 2014). Ordinary Portland cement (OPC) remains the main binding agent in these composites. It is an undisputed fact that the production of OPC remains one of the major contributors of CO₂ emissions (Li et al. 2019b). With the keen search to find suitable replacements for this binder, recent research has shown that geopolymers, an alkali activated cement, serves as a possible alternative (Zhao et al. 2007; Giancaspro et al. 2009; Giancaspro et al. 2010).

Geopolymer wood composite (GWC) consists of a geopolymer binder serving as the matrix material with a wood component as a filler or reinforcement. GWC serves similar purposes as with all other inorganic bonded wood composites. The fact that the matrices part of GWC (i.e. geopolymers) are mostly produced from industrial residues such as coal fly and bottom ashes (Morla et al. 2021), aluminum waste (Leiva et al. 2019), furnace slag (Bouaissi et al. 2019) and mineral soils such as metakaolin (Medri et al. 2020) and red mud (Li et al. 2019a), put these materials at a great advantage over other IBWC. Whereas many of the IBWCs had been established commercially in the early 1900s, most of the works under GWC remain in the research and development phase. Some of the core difficulties in production and commercialization of standardized products are the variation in the sources of the aluminosilicate binder and the cost alkaline solution or the hardener reagent. However, in the last decades, research has been ongoing to ascertain the best way of utilizing this binding agent in IBWC (Berzins et al. 2017; Olayiwola 2021; Sarmin and Welling 2016; Sarmin 2016; Al Bakri Abdullah et al. 2012).

1.1 Geopolymer matrix synthesis and chemistry

At a high pH and in the presence of soluble alkali metal silicates, materials containing aluminosilicate oxides such as fly ash, slag, metakaolin etc. are dissolved into individual alumina and silicate species followed by the copolymerization (i.e. polycondensation) of the species to form a hardened product called a geopolymer (Purbasari et al. 2018). These reactions result in a three-dimensional tecto-aluminosilicate framework (Davidovits 1989) with the general formula:



Where M represents a cation (K^+ , Na^+ , Ca^{2+} etc.), n is the degree of polycondensation, z is 1, 2, 3 or >3 and w is the amount of binding water.

Such frameworks are called polysialates, where sialate stands for the silicon oxo- aluminate building unit. The sialate network consists of SiO_4 and AlO_4 tetrahedras linked by sharing all oxygen atoms (Fig. 1.1). Positive ions (Na^+ , K^+ , Li^+ , Ca^{2+} , Ba^{2+} , NH_4 , H_3O^+) must be present to balance the negative charge of Al in 4-fold coordination. Chains and rings may be formed and (Halas et al. 2011) cross-linked together, always through a sialate Si-O-Al bridge. The charge-balancing by cations is important in determining the structural integrity and fragility of geopolymers (Saidi et al. 2013).

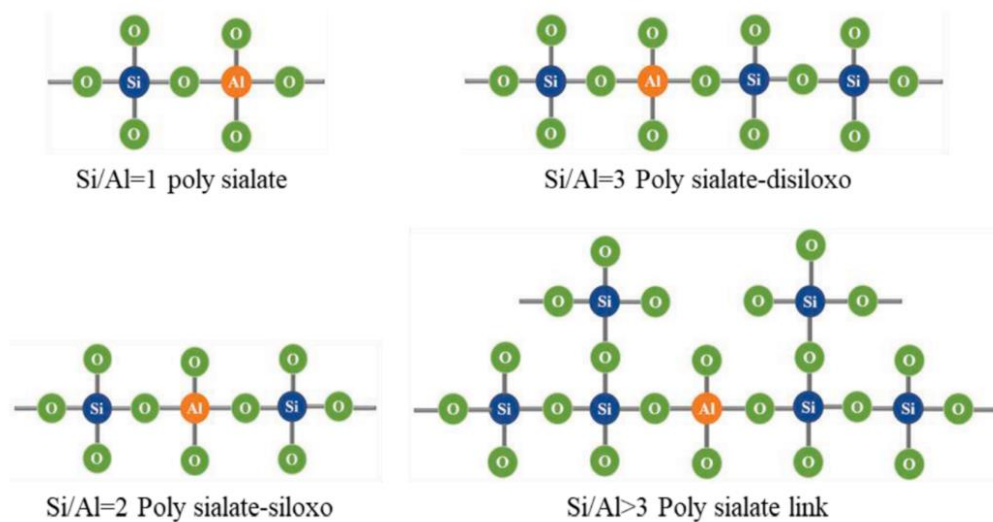


Fig. 1.1 Geopolymer systems based on the number of siloxo Si-O units [Photo adapted from Lan et al. 2022]

In most cases, cations are contributed by an alkali-silicate solution, which usually incorporates alkaline hydroxides ($NaOH$ or KOH) and silicates (Na_2SiO_3 or K_2SiO_3) (Barbosa et al. 2000; Xu and van Deventer 2002). The alkali hydroxide is required for the dissolution of

aluminosilicates, while the alkali silicate acts as a binder, alkali activator, and dispersant or plasticizer (Komnitsas and Zaharaki 2007). In addition, a certain amount of SiO₂ is supplied by the alkali silicate solution for the geopolymerization reaction (Singh et al. 2005).

Depending on the setting conditions, geopolymer compounds can be either crystalline or amorphous. At ambient temperature setting, the structure becomes amorphous, while crystalline poly (sialate) and poly (sialate-siloxo) result from hydrothermal setting conditions (Davidovits 1991). The silica to aluminum ratio has a great influence on the properties (esp. the strength) of the geopolymer. This ratio is greatly influenced by the aluminosilicate precursor material and the concentration of the alkali activator solution. However, it was established that not all the silica and aluminum ions react during the geopolymerization process (Fernández-Jiménez et al. 2006). The same discovered in an experiment using three different fly ashes from different steam power plants, that the percentage of reactive silica was the same in all systems but the percentage of reactive aluminum varied.

Alkaline activators such as potassium hydroxide, potassium silicate, sodium silicate, sodium hydroxide, sodium carbonate, sodium phosphate, and combinations of these activators (Bakharev et al. 1999; Purbasari et al. 2018) have all been used in the synthesis of geopolymers. However, a combination of sodium silicate and sodium hydroxide dissolved in water remains the most common alkaline solution activator used. Several synthesis and post-synthesis temperatures have been reported in the literature, ranging from room temperature curing to about 100°C, using different time intervals. However, the final geopolymer properties are very much dependent on the raw materials and the synthesis conditions i.e. chemical composition and morphology of the solid reactant (van Jaarsveld et al. 2002; Steveson and Sagoe-Crentsil 2005; van Deventer et al. 2007), SiO₂/Na₂O molar ratio (Dimas et al. 2009),

curing temperature (Sindhunata et al. 2006; Bakharev 2005a), Na/Al ratio (Stevenson and Sagoe-Crentsil 2005; Bakharev 2005a), water and soluble silicon in the aqueous phase, and alkali metal in the activation liquid (Stevenson and Sagoe-Crentsil 2005; van Jaarsveld and van Deventer 1999).

1.2 Kinds of geopolymers (matrix)

Geopolymers are amorphous and are made up of mineral compositions containing high amounts of aluminium (Al) and silicon (Si). They are made from natural minerals such as kaolinite and metakaolin, found in industrial wastes such as slag, biomass and coal fly and bottom ashes (Davidovits 1991; Cheah et al., 2015; Villaquirán-Caicedo and Gutiérrez, 2015) as the precursor aluminosilicate material. Geopolymer matrices are classified based on the precursor or starting raw material. However, the homogeneity and consistency of metakaolin and the abundance and ready availability of fly ashes, have made these two precursor materials the most commonly used in the synthesis of a geopolymer.

1.2.1 Fly ash and fly ash-based geopolymer

The wide scale of coal burning for energy makes fly ash an industrial waste available all over the world. In coal combustion, fly ash is collected in the chimney by electrostatic precipitators, while bottom ash is collected from the boilers. Of the coal ash generated, about 80% is fly ash with 20% being bottom ash (Kim and Lee). The annual production of fly ash in the world is estimated to be around 700 Mt (million tons) (Ferreira et al. 2003).

Fly ash mainly consists of Fe_2O_3 , SiO_2 , Al_2O_3 , with some potential toxic substances such as heavy metals from the coal and polyaromatic hydrocarbons that condense from the flue gas (Missengue et al. 2017). The coal's source, age, particle size, and combustion process all

influence the chemical composition and physical properties of fly ash. Fly ash has mainly been used as a replacement for Ordinary Portland cement (OPC) due to its beneficial properties, especially with respect to its high compressive strength compared to OPC (Abdullah et al. 2011). The incorporation of fly ash into OPC serves as a major industrial application for this inorganic residue in most countries (Rohde et al. 2006). There is a high probability that the quantity of fly ash will increase as a result of the low utilization potential and the operation of new coal-based thermal power plants, especially in developing countries (Izidoro et al. 2012). The replacement of OPC with fly ash up to 60% by mass is a notable development (Kumar et al. 2007).

In order to minimize waste and achieve a cleaner production process, more research is being conducted on fly ash as a precursor material for geopolymers. Most coal fly ashes are made up of an inhomogeneous mix of aluminosilicate and silica glasses together with small amounts of crystalline materials including mullite, quartz, hematite and magnetite (Song et al. 2000). The physical characteristics of fly ashes such as particle size distribution and particle fineness are the determining factors regarding their reactivity (Krizan et al. 2002).

Even though fly ash is one of the most popular precursors in geopolymer production, there is a notable variation in not only the chemical composition, but also the particle size and morphology (Zhuang et al. 2016). These qualities depend on the coal or fuel type used in the combustion process, the chemical composition as well as the combustion conditions (Fernández-Jiménez and Palomo 2003; Zhuang et al. 2016).

These properties and variations have a profound impact on the chemical and mechanical properties of the resulting geopolymer. In addition, the amount of unburned carbon content

within the fly ash, as well as the ratio of Si to Al play a major role in the geopolymerization process, and therefore are decisive as regards the strength and thermal properties of the resulting geopolymer (Fernández-Jiménez and Palomo 2003). According to Nath and Sarker (2014), the particle size and surface area of the ash particles have a profound effect on the reaction rate during geopolymerization. The smaller ash particle size results in a faster reaction time and subsequent curing time. The particle size also influences the resulting reaction products, which in turn influence the mechanical properties of the geopolymer (Rosas-Casarez et al. 2018). While initial steps have been made by the American Society for Testing and Materials to classify fly ashes, their grouping theory merely differentiates based on Ca content (Karayannis et al. 2018). While this is an important variable for the creation of geopolymers, the classification system is nowhere near exact enough to produce geopolymers with predictable qualities, as can be seen from the number of impactful variables mentioned above. One important technological challenge for the mass application of fly ash geopolymer is the high variation in the quality of ash itself (Komljenović et al. 2009; Vassilev and Vassileva 2009) as different ages, source, type and combustion conditions affect the obtained ash.

1.2.2 Metakaolin and metakaolin-based geopolymer

In contrast to fly ash-based geopolymers, where in most cases temperature post treatment is required (Palomo et al. 2004; Fernández-Jiménez and Palomo 2005), metakaolin remains the most used powdery solid precursor material for geopolymers where hardening has to take place at room temperature (Vogt et al. 2019). Metakaolin, also referred to as thermally treated kaolinite, is rich in amorphous SiO_2 and Al_2O_3 with a molar ratio of Si to Al of about 1, and displays a high reactivity, making it a great source material for the creation of geopolymers (Seiffarth et al. 2013; Ogundiran and Kumar 2015). According to Provis et al. (2010) the high

reactivity of the metakaolin results from the morphology and high specific surface area of the calcined kaolin particles.

Aside from the morphology and surface area of kaolinite, Fernandez et al. (2011) reported that the high content of hydroxyl groups in the structure also contributes to the high reactivity. Unlike fly ash material, the nature and morphology of metakaolin results in a high water demand by the powder (Provis et al. 2010) and a high viscosity of the resulting geopolymer paste (Cassagnabère et al. 2013). As the water needs to be expelled during the curing process, the higher water demand for metakaolin powder results in a higher porosity of metakaolin geopolymers.

In comparison to OPC, metakaolin requires far lower calcining temperatures and emits as little as 10 to 20% of the amount of CO₂ during calcination (Rovnaník 2010). Like all other geopolymers, the properties of metakaolin geopolymers depend on a variety of factors. For example, high Si to Al ratios negatively affect the density and physical strength properties of the final geopolymer (Duxson et al. 2005). The curing temperature has a profound effect on the hardening of metakaolin geopolymers (Rovnaník 2010; Chen et al. 2016). According to Chen et al. (2016), the optimal curing temperature for a metakaolin-based geopolymer is 60 °C, while Rovnaník (2010) stated that curing at 10 °C can increase the setting time by a factor of almost 20 when compared to ambient conditions. However, once fully hardened this does not affect the long-term mechanical properties. Nevertheless, higher long-term curing temperatures reduce the hardening time but cause a decrease in mechanical strength, although short influxes of temperature during curing can reduce the setting time without affecting the long-term mechanical properties (Rovnaník 2010).

1.2.3 Acid-based geopolymers

It is worth mentioning that geopolymers can also be categorised based on the solution used in the synthesis i.e. alkali solutions (such as NaOH/KOH with or without Na₂SiO₃/K₂SiO₃) or acid solution (such as phosphoric acid). [SiO₄]⁴⁻ is partially replaced by [PO₄]⁵⁻ in the morphology of acid-based geopolymers to form a Si-Al-P binder system, that has stronger bonding and better properties, including stronger compression strength, lower efflorescence, and higher thermal stability than an alkali-based geopolymer (Guo et al. 2016; Wang et al. 2017; Zhang et al. 2020a). The raw materials for the phosphate-based geopolymer mainly come from some calcined clay (e.g., metakaolin [Douiri et al. 2014], laterite [Lassinantti-Gualtieri et al. 2015], and halloysite [Zhang et al. 2020a]).

Conversely, the limited availability of the precursors (i.e. the natural minerals), makes large-scale production and application challenging (Wan et al. 2022). As a result of identifying precursors that have similar chemical properties, the raw materials for phosphate-based geopolymers can be extended beyond natural minerals to industrial wastes (Wan et al. 2022). In addition, Mathivet et al. (2021) reported that phosphate-based geopolymers are difficult to use for complex shapes due to the high viscosity of their reactive mixture. Nonetheless, the same authors stated that this could be overcome by the addition of water to the formulation. However, the present studies focused on a geopolymer produced using an alkaline solution.

1.3 Geopolymerization process

Fig. 1.2 describes the process of geopolymerization. Taking the reaction mechanism of alkali-activated silica-alumina phase components into account, Krivenko and Kovalchuk (2007) and Shi et al. (2011) proposed a five-stage model for the reaction process, consisting of dissolution, precipitation, recombination, gelation and polycondensation. These stages occur almost

simultaneously during the formation of the geopolymer and it is difficult to distinguish between the specific processes (Duxson et al. 2007). However, Zuhua et al. (2009) grouped these stages into two main periods: I- dissolution–hydrolysis and II- hydrolysis–polycondensation. Wang et al. (2005) and Zuhua et al. (2009) also confirmed that these two periods probably occur simultaneously once the solid material is mixed with the liquid solution (activator) making the exact separation of the periods difficult. For the sake of explanation and understanding, both periods will be explained separately.

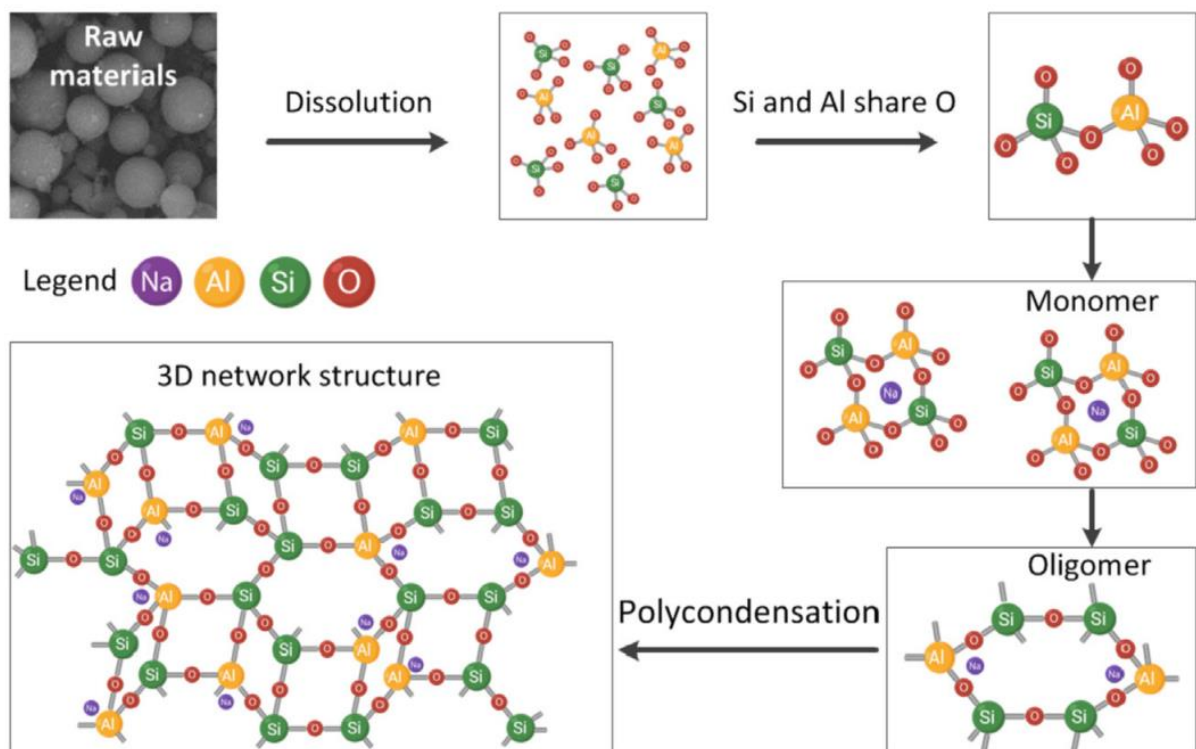


Fig. 1.2. Geopolymerization reaction process [Photo adapted from Zhang et al. 2020c]

The geopolymerization process starts with the dissolution of silicon and aluminum ions in the precursor aluminosilicate material. Once the precursor material comes into contact with the alkaline solution during mixing the process, it is activated. This indicates that the hydroxides are crucial in this stage, as pure water cannot activate this process (Fernández-Jiménez et al.

2006). The hydroxide concentration in the alkaline solution hydrolyzes or breaks the Si-O-Si, Al-O-Al, and Si-O-Al bonds that are present in the glasslike phase of the precursor binder and releases silica and aluminum ions in the solution. The free silicon and aluminum ions then form Si-OH and Al-OH groups (Fernández-Jiménez et al. 2006). The dissolution rate is mainly dependent on the pH of the alkaline solution and the composition of the precursor binder material (Saeed et al. 2010).

According to Provis et al. (2009), this dissolution process results in the formation of a disordered gel phase, which is a poorly networked gel (due to the added water) called the geopolymeric gel binder. The geopolymeric gel framework consists of a silicate and aluminate tetrahedral highly connected in a three-dimensional network (Silva et al. 2012). The presence of Al³⁺ in a fourth-fold coordination makes this network negatively charged. The Al³⁺ ions are localized on one or more of the bridging oxygen ions in each aluminate tetrahedron. The negative charge of this network is then balanced by the positively charged alkali metals from the activating solution such as Na⁺, K⁺, Li⁺, Ca²⁺, Ba²⁺, NH₄, H₃O⁺ (Provis et al. 2009; Davidovits 2009).

The final stage after the dissolution-hydrolysis period is the exothermic polycondensation reaction that occurs at room temperature or elevated temperatures. This exothermic reaction results in the formation of a three-dimensional macromolecular structure material of polymeric Si-O-Al bonds (Phair et al. 2003) (i.e. one of the backbones in Fig. 1.2) called a geopolymer. It is of interest to note that polycondensation reactions occurring for longer periods of time at an elevated temperature (i.e. above 70 degrees) appears to weaken the structure, suggesting that small amounts of structural water need to be retained in order to reduce cracking and maintain structural integrity (van Jaarsveld et al. 2002). Even though period I and II occur

simultaneously, more dissolution occurs at the early reaction stage compared with the formation of new bonds (polycondensation process). During period I, Al–O bonds are more readily hydrolyzed or broken than Si–O bonds (Fernández-Jiménez et al. 2006). The authors further explained that the rate of reaction will be very high when aluminium passes through a maximum in the solution (not all Al and Si ions are reactive). At the early stages of the alkaline activation, the possibility of forming Si–O–Al bonds is higher than Si–O–Si in the aluminosilicate gel (Fernández-Jiménez et al. 2006; Engelhardt and Michel 1987).

The reaction process releases water that was consumed during the dissolution stage in period I. Even though water is not incorporated directly in the geopolymer gel, it plays a very significant part in both periods. Zuhua et al. (2009) explained that more water with a considerable amount of OH⁻ anions accelerates the process in Period I (dissolution–hydrolysis). This means when there are enough OH⁻ anions, a high water liquid/solid ratio will speed up the process of period I due to water being consumed. The reaction will shift from water consumption (in period I) to the release of water (in period II) and too much water will therefore slow down the kinetics of hydrolysis– polycondensation. For this reason, period II favors systems with a lower liquid to solid ratio as these systems have both a high and early rate of polycondensation (Zuhua et al. 2009). The same authors found that the total energy emitted from systems with different liquid to solid ratios was about equal. However, the geopolymerization rates were different due to the differences in the water content.

1.4 Wood as a material

Wood is a natural composite comprised mainly of cellulose, lignin and hemicellulose as a structural component, as well as non-structural polysaccharides and other extractives. It displays a wide variety of characteristics, which vary greatly among species as well as between

trees of the same species (Stark et al. 2010). It can broadly be categorized into softwood and hardwood. While softwoods have a simpler basic structure with relatively little variation therein, hardwoods by comparison have a much greater structural complexity. They both have a greater number of basic cell types and a far greater degree of variability within the cell types. The most important difference between softwoods and hardwoods is the presence of a vessel element (or pore) which softwoods lack (Rowell 2013). In both softwood and hardwoods, the stem is divided into two distinct zones, sapwood and heartwood, based on functionality. In living trees, sapwood plays the role of sap conduction, storage of food (i.e. Photosynthate) and synthesis of biochemicals. Heartwood serves the function of long-term storage of biochemicals. The type of biochemicals stored varies depending on the wood species. They impart color to the wood, and some extend the durability. The biochemicals found in sapwood and hardwood are collectively called extractives (Rowell 2013).

Wood density is one of the most important physical properties of wood (Desch and Dinwoodie 1996; Bowyer et al. 2003) and therefore of any product made therefrom. Density is a measure of the quantity of cell wall material contained in a specific volume of a piece of wood (Hughes 1967). Density varies among wood species and along the wood stem (i.e. butt, middle and top) as well as between the sapwood and heartwood (Pong et al. 1986; Kärkkäinen 2003).

Wood is a hygroscopic material capable of holding or releasing water/moisture (Usta 2003). By absorbing liquid water, wood can undergo rapid changes in moisture content, as opposed to water vapor absorption, which causes slow changes. As wood absorbs liquid water above its fiber saturation point (i.e. the stage in the drying or wetting of wood at which the cell walls are saturated with water (bound water) and the cell cavities are free of water), air in the cell lumina

is replaced by water, a phenomenon known as capillary action or wicking (Forest Products Laboratory 2010).

Water interacts strongly with the wood cell wall and forms a concave meniscus within the lumen. Water absorption continues until the maximum moisture content is reached (Forest Products Laboratory 2010). Depending on the density and water diffusivity of wood, the amount of water absorbed varies. The water diffusivity coefficient describes the rate at which water moves from the surface to the interior of products (Khazaei 2007). Wood shrinks and swells because of liquid water and moisture/water vapor activities. As wood changes its moisture content in response to changes in the relative humidity of the atmosphere on a daily and seasonal basis, it shrinks and swells (Eckelman 1998). When the air is humid, wood absorbs moisture and swells; when the air is dry, wood shrinks. As water absorbs into wood, it enters the cell wall and hydrogen-bonds to the hemicelluloses and amorphous cellulose to cause swelling. Shrinking and swelling play important roles in the utilization of wood (Forest Products Laboratory 2010).

1.5 General information of wood species used in this present thesis work

1.5.1 Softwood species

Pinus taeda, also called Loblolly Pine, has a density of about 570 kg/m³. The heartwood is reddish brown while the sapwood is yellowish white (Meier 2022). Loblolly pine wood is commonly used in the construction of stringers, roof trusses, poles, joists and piles, as well as for interior applications like subflooring and sheathing (Meier 2022). The basic chemical composition of Loblolly pine wood is cellulose [43.6- 45.5%], hemicellulose [21.2- 23.0%], lignin [26.8- 28.0%] and extractive, [2.5- 3.2%] (Frederick et al. 2008; Huang et al. 2011).

Pinus Sylvestris, also known as Scots pine, has a density of about 550 kg/m³. The heartwood is light reddish brown, while the demarcated sapwood is pale yellowish white to nearly white (Meier 2022) and has a resinous odor when worked. In addition to utility poles and posts, the wood is widely used for flooring, as pulpwood and as construction lumber. The wood is made up of about 22.96- 35.17% lignin, 22.7- 26.9% hemicellulose, 35.94- 46.27% cellulose and 5.0% extractives (Dönmez et al. 2013; Raisanen and Athanassiadis 2013).

Picea abies, commonly known as Norway spruce, has a density of about 405 kg/m³. This variety of spruce is usually a creamy white with hints of yellow and/or red (Meier 2022). It is commonly used for paper (pulpwood), construction lumber, millwork, crates, Christmas trees and musical instrument soundboards. According to Raisanen and Athanassiadis (2013), the wood contains about 27.4% (± 0.7) lignin, 27.3% (± 1.6) hemicellulose, 42.0% (± 1.2) cellulose and 2.0% (± 0.6) extractives.

1.5.2 Hardwood species

Black wattle (*Acacia mearnsii*) and Port Jackson (*Acacia saligna*) are both hardwood species. Black wattle is an important plantation tree, used for a variety of timber and fiber applications as well as for forest management. The wood is light-brown in color and dense, with a straight, close grain, making it suitable for particle board as well as for pulp, timber, firewood, and furniture (Forest Legality Initiative 2022). The B. wattle wood has a density of about 730 kg/m³ (Meier 2022). According to Olayiwola (2021), B. wattle wood contains about 23.85% (± 1.25) lignin, 20.29% (± 0.11) hemicellulose, 33.72% (± 0.13) cellulose and 6.37% (± 0.58) extractives.

The Port Jackson wood is sometimes reported as sappy and, if larger, it would be suitable for cabinet-work (Maiden 1889). It has been successfully processed into particle board (Doran and

Turnbull 1997). The wood comprises about 25.47% (± 1.37) lignin, 13.13% (± 1.14) hemicellulose, 34.47% (± 0.66) cellulose, and 5.81% (± 0.31) extractives, according to (Olayiwola 2021).

Eucalyptus is also a hardwood species. In this thesis, two types of eucalypts were used, namely *Eucalyptus grandis* and *Eucalyptus camaldulensis*. *E. grandis* wood has a density of about 640 kg/m³ and is commonly referred to as rose gum. Heartwood is pink to reddish brown in color and the sapwood is sometimes indistinguishable from from it (Meier 2022). The wood is made up of about 29.8% (± 0.74) lignin, 22.0% (± 0.71) hemicellulose, 48.2% (± 0.25) cellulose and 4.1% (± 0.20) extractives (Pereira et al. 2013).

E. camaldulensis is popularly called River red gum. The wood of *E. camaldulensis* has a density of about 870 kg/m³. It is used for pulp and paper production. It is also planted for hardboard, fibreboard and particleboard (Orwa et al. 2009). In addition the wood is suitable for many structural applications, for example: railway sleepers, poles, posts, floorings, wharves, ship building and heavy construction (Orwa et al. 2009). The wood is made up of about 30.4% (± 0.33) lignin, 22.4% (± 0.89) Hemicellulose, 47.2% (± 0.68) cellulose and 3.1% (± 0.29) to 4.3% (± 0.24) extractives (Pereira et al. 2013).

Fagus sylvatica is more commonly known as European beech and has a density of about 710 kg/m³. The wood is a pale straw color, sometimes with a pink or brown hue. As the wood is usually prepared with steam before being sliced, a European beech wood veneer tends to be darker (Meier 2022). The use of beech wood includes veneers, plywood and furniture production, as well as internal design and for doors. Other common uses include lumber production, flooring, boatbuilding, cabinetry, musical instruments (piano pinblocks) and turned

objects. The compound composition of beech wood varies between 33.7- 46.4% cellulose, 11.6- 22.7% lignin, 11.8- 25.5% hemicelluloses and 3- 5% extractives, while inorganic compounds comprise 0.3% to 1.2% (Saranpää 1996).

1.6 Composites materials

Composites are materials made from two or more constituents or components. The components have remarkably dissimilar chemical or physical properties, but are combined to produce a material that is different from its individual components (Sabhadiya 2022; Sharma et al. 2020; Chawla 2012a). A composite is distinguished from a mixture or solid solution by the fact that the individual elements remain separate and distinct within the finished structure (Sabhadiya 2022). Composite materials may be preferred over traditional or common materials due to a number of reasons. Using composite materials instead of traditional materials for components is a great way to save weight (Sabhadiya 2022). However, composites can also be stronger than other materials, in addition to being lighter. For instance, reinforced carbon fibers can be 5 times as strong as steel 1020 grade and only one-fifth as heavy, making them ideal for structural applications (Sabhadiya 2022). Additionally, composites possess properties like thermal and chemical resistance, along with electrical insulation, which makes them more attractive than conventional materials (Sabhadiya 2022). They are also unique in that they can have multiple properties not commonly found in a single material, unlike traditional materials.

Composite materials are composed of two main phases, which are the matrix and the reinforcement (Fig. 1.3). Along with protecting the reinforcement from external and environmental harm, the matrix transfers load on the reinforcement, and for composites to perform better, the reinforcement phase must be well bonded to the matrix (Mallick 2012). The reinforcement provides strength and stiffness to the structure, strengthening it and preventing

cracks and fractures. In some cases, the matrix maintains the reinforcement to create the required shape. In addition, the reinforcement increases the matrix's mechanical characteristics as a whole. Matrixes are monolithic materials containing reinforcement that must be uniformly distributed throughout the matrixes (Sharma et al. 2020). Examples of matrix materials include metals, polymer resins, plastics, ceramics and inorganic materials.

According to Chawla (2012b) reinforcements used in composite manufacture need not necessarily be in the form of long fibers. They can also take the form of particles, flakes, whiskers, short fibers, continuous fibers, or sheets. However, in reality, many reinforcements used in composites production have a fibrous form because fibrous materials are stronger and stiffer than other forms of reinforcement (Chawla 2012b). Examples of materials used for reinforcement include inorganic fibers (glass fibers, basalt fibers, carbon fibers and asbestos fibers) and lignocellulosic materials (wood, hemp fibers, flax fibers, etc.).

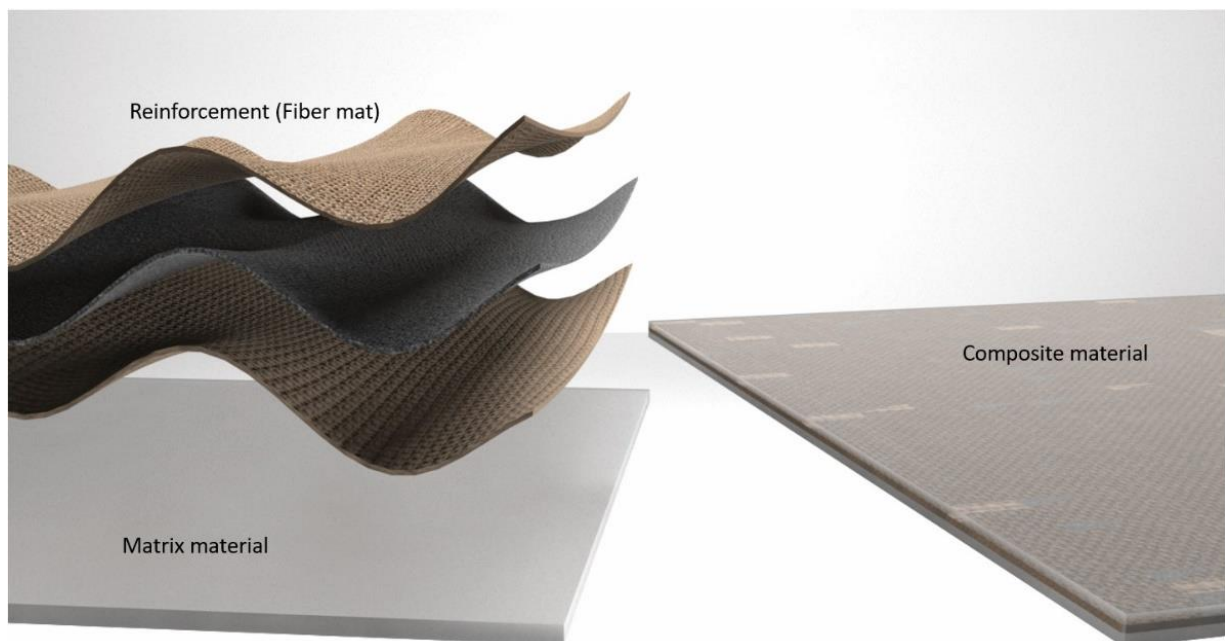


Fig. 1.3. Reinforcement/fiber, matrix and composite material

1.6.1 Wood-based composites

Wood-based composites are one broad category of composite materials. Youngquist (1999), Stark et al. (2010) and Irle et al. (2013) classified wood-based composites into veneer-based materials such as plywood and laminated veneer, laminates, composites such as flake board, fiberboard, particleboard, wafer board and oriented strand board, components such as beams and stress skin panels and wood-non wood composites such as wood plastics and inorganic bonded composites. Thermosetting resins (i.e. heat-curing resin or adhesives), are typically used to bind the lignocellulosic fibers together in conventional wood-based composites; the exception being wood plastic composites and fiber cement composites, which employ polymer resins (e.g. polypropylene, polyethylene etc.) and cement based (e.g. Portland cement, magnesia cement etc.) binder respectively. Commonly used thermosetting resin systems include phenol-formaldehyde, urea formaldehyde, melamine-formaldehyde, and isocyanate; the adhesives and binders selected being dependent on the product under consideration. Among the factors considered are the materials to be bonded together, the moisture content at the time the composite is bonded, its mechanical properties, its durability and certainly the cost of the resin system (Youngquist 1999).

1.6.2 Inorganic bonded wood composites

A typical inorganic-bonded composite contains between 30-90% inorganic binder and 10–70% wood component (Youngquist 1999). In the manufacturing of an inorganic bonded composite, reinforcement materials (i.e. wood or fibers) are mixed with inorganic materials in the presence of water and allowed to set into rigid masses to produce inorganic bonded composites (Amiandamhen 2017). The resulting products exhibit excellent or superior properties when the individual fibers are fully encapsulated in the inorganic matrix (Simatupang and Geimer 1990) and the matrix is continuous in order to obtain acceptable properties (Amiandamhen 2017). It

has been shown that these composites' properties are greatly affected by the amount and type of the inorganic binder, the wood/fiber element, as well as the target density of the composites (Stark et al. 2010). As stated earlier, current inorganic bonded composites include ceramic bonded composites, gypsum bonded composites, Portland cement bonded composites and magnesia cement bonded composites. The development of a new class of inorganic bonded composites is at an early stage (Olayiwola 2021). It consists of a geopolymer inorganic binder and a wood component (fibers or particles). The geopolymer bonded wood composites met the minimum technical requirements for cement bonded composites and showed the ability to compete with cement bonded composites (Olayiwola 2021).

Difference between OPC and geopolymer inorganic binders

Chemical bonding in ordinary Portland cement (OPC) differs from a geopolymer. Unlike the OPC, in which calcium silicate hydrates (C-S-H) gel is the main binding compound, geopolymer utilizes the polycondensation of Silica (SiO_2) and alumina (Al_2O_3) sources and a high-alkali environment to obtain structural strength (van Chanh et al. 2008; Nuaklong et al. 2020). In addition, the role of water in both binders is different. The water in a geopolymer acts as a catalyst (i.e. creates a medium for dissolution and movement of ions) and generally does not participate in the reaction. Water present in calcium silicate hydrate gel creates a part of C-S-H (Chen et al. 2018; Lingyu et al. 2021). That is to say, in the end, water is released from the polycondensation reaction in a geopolymer, whereas in an OPC reaction water is consumed.

1.6.2.1 Cement bonded wood composites

Cement bonded wood composites remain as the dominate products among the inorganic bonded wood composites. According to the geometry and source of the wood fibers or particles, many cement-bonded products have been created and given different names. These

include wood wool cement bonded composite, cement bonded particle board, cement bonded oriented strand board and cement bonded fiberboards amongst others (Olayiwola, 2021). Ridi et al. (2010) describe cement as a mixture of calcium silicates and aluminates. The most significant elements are tri-calcium silicate (Ca_3SiO_5 , C_3S), and di-calcium silicate (Ca_2SiO_5 , C_2S), which together comprise around 80% of the makeup of clinker (Van Oss and Padovani 2003). C_3S and C_2S , which are important for the early and long-term development of strength respectively, form hydrates when they come into contact with water (Van Oss and Padovani 2003; Ridi et al. 2010).

Wood fibers and other non-wood based lignocellulosic materials, when added to a cement matrix, slow down the production of cement hydrates, resulting in products with poor structural integrity (Jorge et al. 2004). Different strategies have been carefully investigated to address these compatibility issues. These included treating the wood with hot water to remove extractives and using a mild alkali with sodium hydroxide to treat hemicelluloses. In addition to these treatment methods, chemical accelerators like calcium chloride and magnesium chloride were also used.

1.6.2.2 Geopolymer wood composites

Similar to all other inorganic bonded wood composites, the wood in GWC serves as a means to reduce weight and thermal conductivity (Meng et al. 2011; Sarmin et al. 2014), whereas the geopolymer matrix binds the wood particles providing mechanical strength, low permeability, good chemical resistance, and excellent fire resistance behavior (Bakharev 2005b; Ryu et al. 2013; Shehab et al. 2016). The alkali solution commonly used in the geopolymer binder synthesis is sodium hydroxide (NaOH), with or without sodium silicate (Na_2SiO_3).

Generally, compressive strength and density decreases with increasing wood aggregate content (Sarmin and Welling 2016). A study by Halas et al. (2011) showed similar results, equating an increasing amount of sawdust with a decreasing in compressive strength of fly ash geopolymer specimens. Sarmin (2016) showed that the addition of wood flour, particles and fibers to geopolymer composites results in differences in physical and mechanical properties. The GWC with wood flour had the highest density and compressive strength, which was attributed to the micro-particles uniformly dispersed and filling up voids in the matrix, while the low performance of GWCs with fiber and particles were attributed to poor dispersion and agglomeration of the wood components. It was concluded that the particle geometry (i.e. size and shape of the wood aggregates) influenced the properties of geopolymer wood composites.

Duan et al. (2016) stated that wood waste had a positive effect on the main properties of a fly ash geopolymer. The authors corroborated, that the addition of wood particles without any special pretreatment, improved the cracking resistance and drying shrinkage especially at later ages. Sarmin et al. (2020) showed that when a *Picea abies* veneer was treated with NaOH, the de-bonding strength between the veneer and blend of fly ash/metakaolin geopolymer was reduced when compared to those of the untreated veneer. However, no de-bonding strength was observed for veneers treated with Na₂SiO₃, as they failed before any strengths were recorded. The authors further explained that visual analysis of each sample after testing revealed that the failure was located at the interface between the veneer and geopolymer matrix. Ye et al. (2018) found that hemicelluloses - one of the main components of wood - hinder geopolymerization. Treating wood with a NaOH solution is one possible way of removing this inhibitory substance in wood before its use in a GWC. However, the findings by Sarmin et al. (2020) on the treated veneer indicate otherwise.

Al Bakri Abdullah et al. (2012) studied the feasibility of producing GWCs using class C fly ash activated with a combination of 12M sodium hydroxide and sodium silicate. The authors added 10- 50% wood fibers to a geopolymer paste and concluded, that increasing the amount of wood leads to increased amount of water demand to achieve a given level of mix workability. However, this led to increased water absorption in GWCs with a high percentage of wood aggregates. Review of existing literature shows two major mixing technologies in the fabrication of GWCs:

- i) dry mixing the wood and aluminosilicate material, followed by addition of the activator solution with or without excess water (Sarmin and Welling 2016; Sarmin 2016; Furtos et al. 2021; Malenab et al. 2017; Alomayri and Low 2013).
- ii) activating aluminosilicate material before the addition of wood (Sá Ribeiro et al. 2016; Tan et al. 2019; Berzins et al. 2017).

Although the reasons behind these mixing technologies are not clearly stated by the authors, processing technologies in the production of composites has a profound effect on the final composites properties. In order to fully harness the potential of a geopolymer binder in wood composites, it is imperative that more research focuses on understanding the interactions between the properties of wood and the geopolymer binder. Understanding these interactions would help in the formulation of GWC products targeted at a specific end use.

1.7 Wood as a filler or reinforcement in inorganic bonded wood composites

In order to use fresh wood or post-industrial byproducts such as sawmill trimmings, logging trimmings, and chips for composites, the materials must be chipped and ground (Schwarzkopf and Burnard 2016). The wood structure is heavily altered during breakdown through mechanical and thermal treatment such as hammers, attrition mills, and refining aggregates.

The resultant wood geometry may take the form of particles or fibers, depending on the technology used. Despite this, the term “wood fiber” is often used in general as a general description for wood particles of any kind. From a biological or technical point of view, fibers can be defined differently. According to Schirp and Stender (2010) fibers are cell types that provide structural stability to trees, classified as softwood tracheids, hardwood tracheids and hardwood libriform fibers. Technically, wood fibers are derived through mechanical or chemical processes and contain single or bundles of anatomical fibers, whole fibers or fiber fragments. Fiber geometry varies according to the process (Mertens 2018). The present thesis uses the technical definition.

Commercially, wood fibers are produced using refiners, while wood flour and particles are often processed from mill waste (Amiandamhen 2017). Schwarzkopf and Burnard (2016) stated that wood flour grains (size 100-500 μm) are less than 1mm in length and have a wide distribution of length to diameter ratio (aspect ratio or Length/Diameter ratio). When compared to particles, wood fibers have a higher ratio of length to width, i.e. aspect ratio. A significant amount of the composite strength and stiffness is influenced by particle size characteristics, including aspect ratio, according to Stark and Rowlands (2003) and Nourbakhsh and Ashori (2008). This indicates that the different particle geometry is a crucial parameter influencing the mechanical properties. In addition to the hygroscopic nature of wood, mixing wood fibers, wood flour or wood particles with ever increasing wood content into an inorganic matrix may lead to wood distribution and orientation within the composite becoming unpredictable. For instance, mixing long fibers into a viscous inorganic matrix might lead to fiber entanglement and poor dispersion within the composite. During raw material mixing, the time of addition of raw materials (i.e. when to add what raw materials) may lead to effects such as:

- i) particle to particle interaction and increasing viscosity accompanied by high shear force in the mixer;
- ii) wood component not completely encased in the inorganic matrix;
- iii) poor distribution of the wood component the inorganic matrix;
- iv) poorly activated precursor material as a result of water/activator solution not having enough contact with the precursor material.

In spite of this, wood plays a very important role in inorganic bonded wood composites, acting either as an aggregate or reinforcing element. In addition to the geometry and size, wood characteristics, species and chemical compositions all have the capability of influencing the properties of the inorganic bonded wood composites (Jorge et al. 2004). Wood aggregates such as sawdust, flour and particles have all been used as fillers in geopolymer wood composites to reduce the density of the product (Sarmin 2016), while the addition of fibers improves tensile and flexural strength, toughness and energy absorption capacities through bridging cracks (Shaikh 2013). Halas et al. (2011) reported both positive and negative effects using sawdust as a filler in fly ash geopolymers. They also showed that a higher amount of sawdust had a negative effect on the compressive strength of the specimens. Duan et al. (2016) stated that wood residue had a positive effect on the main properties of fly ash geopolymer and showed that the addition of sawdust (without any special pretreatment) improved the cracking resistance while drying.

Despite the fact that wood reduces the density and improves on the strength properties of GWC, the utilization of wood in a high alkaline environment causes leaching of non-structural polysaccharides/ low molecular weight carbohydrates, extractive and some structural components like hemicellulose. Various extracts, sugars and structural and non-structural

polysaccharides may leach out simultaneously. The cross-effects of these inhibitory substances in affecting the matrix, make the understanding of the hardening mechanism when untreated wood is used in an alkaline inorganic bonded wood composite more complicated. The effects of these leachates and extractives are well-known for OPC wood composites. For example, inhibitory substances such as hemicelluloses, sugars, starch and phenols, hinder the setting and the formation of crystalline bonds in OPC composites (Fan et al. 2012). The nature of the extractive determines the extent of the inhibitory effect (Jorge et al. 2004), while the grade of inhibition depends on the type and amount of sugars (Sandermann and Brendel 1956). However, there is little to no established research about the influence of these inhibitory substances on geopolymer composites.

Among the structural components of wood, hemicellulose is the one that negatively affects the of geopolymer composites. Alkaline degradation of hemicellulose lowers the degree of geopolymerization (Ye et al. 2018). This drawback creates a necessity for different pretreatments and surface modifications of wood before utilization in high alkaline inorganic matrices. Different pretreatment and modification methods based on alkaline hydrolysis, extraction and retention of sugars and hemicelluloses, have been applied to minimize inhibition problems (Moslemi et al. 1983; Zhengtian and Moslemi 1985; Lee and Short 1989). Alkaline hydrolysis degrades hemicelluloses and sugars into non-inhibitory substances, while aqueous extraction removes inhibitory water soluble substances (Alberto et al. 2000). Retention treatment seals the inhibitory substances in the wood by forming a thin coating layer around the wood preventing the release of the inhibitory substances (Quiroga et al. 2016).

In addition to the wood species and the chemical composition, wood as a hygroscopic material has the tendency to hold water. During composite preparation, this water (held in the wood)

may be available for the interaction during the mixing and consolidation of the composite. In a case where the wood is dry or not saturated with water, it is likely to absorb water from the inorganic paste. For this reason, when adding wood to a composite, extra water is needed to complete the mixing process. Finding the correct amount of additional water needed is key in developing the composite.

Mixing wood particles directly with an inorganic mineral binder could potentially affect the water/solid ratio; this could limit the water available for geopolymerization due to migration of water into the wood particles (Alomayri and Low 2013). Hence, Tamba et al. (2001) proposed fully saturating the wood with water before use in inorganic bonded composites. However, this water from the wood adds up to the total water in the composite mixture. Nevertheless, it is a well-established fact the strength of most wood inorganic composite materials decreases with an increasing water/ solid ratio. This shows that wood moisture content (MC) may play a key role in the movement of water (containing ions) within the composite before the final hardening of the composite.

1.8 Working Hypothesis and Integration of Publications

Based on the introduction, there are indications that wood plays a very important role in inorganic bonded wood composites, acting either as aggregates or a reinforcing element. The interaction between wood and geopolymer is very important, as this has the ability to determine the properties of the resulting composites. As important as the control and manufacturing of the geopolymer matrix is, the wood's inherent characteristics and properties and their contributions to the composite manufacture are also of vital significance.

The efficacy of wood filler/ fiber reinforcement is based on the wood–matrix interactions. The understanding of these interactions is a challenging problem. This problem is sophisticated because of the following nonlinear interactions between the wood–geopolymer matrix as a result of the:

- Inherent properties of the wood such as wood species and wood chemical compositions, moisture content
- Geopolymer matrix properties such formulations and precursor materials used
- Interface/ interfacial de-bonding between geopolymer and wood

Therefore, the following working hypothesis was drafted:

“Depending on raw material selection and processing parameters, the geopolymer wood composite will show a wide variety of physical and mechanical properties.”

In order to confirm the drafted working hypothesis, this thesis is divided into two research scopes.

1. Evaluation of how wood’s inherent properties such as wood species and wood chemical compositions affect properties of geopolymer wood composites.
2. Evaluation of material preprocessing of geopolymer wood composites.

The present thesis is primarily based on three peer-reviewed publications, which are:

Paper I: Bright Asante, Goran Schmidt, Ronaldo Teixeira, Andreas Krause, Holmer Savastano Junior (2021). Influence of wood pretreatment and fly ash particle size on the performance of geopolymer wood composite (2021). *European Journal of Wood and Wood Products*. <https://doi.org/10.1007/s00107-021-01671-9>

Paper 2: Bright Asante, Hanzhou Ye, Martin Nopens, Goran Schmidt, Andreas Krause (2021). Influence of wood moisture content on the hardened state properties of geopolymer wood composites (2021). Composites Part A. <https://doi.org/10.1016/j.compositesa.2021.106680>

Paper 3: Hanzhou Ye, Bright Asante, Goran Schmidt, Andreas Krause, Yang Zhang, Zhiming Yu (2021). Interfacial bonding properties of the eco-friendly geopolymer-wood composites: influences of embedded wood depth, wood surface roughness, and moisture conditions (2021) - Journal of Materials Science. <https://doi.org/10.1007/s10853-021-05775-8>

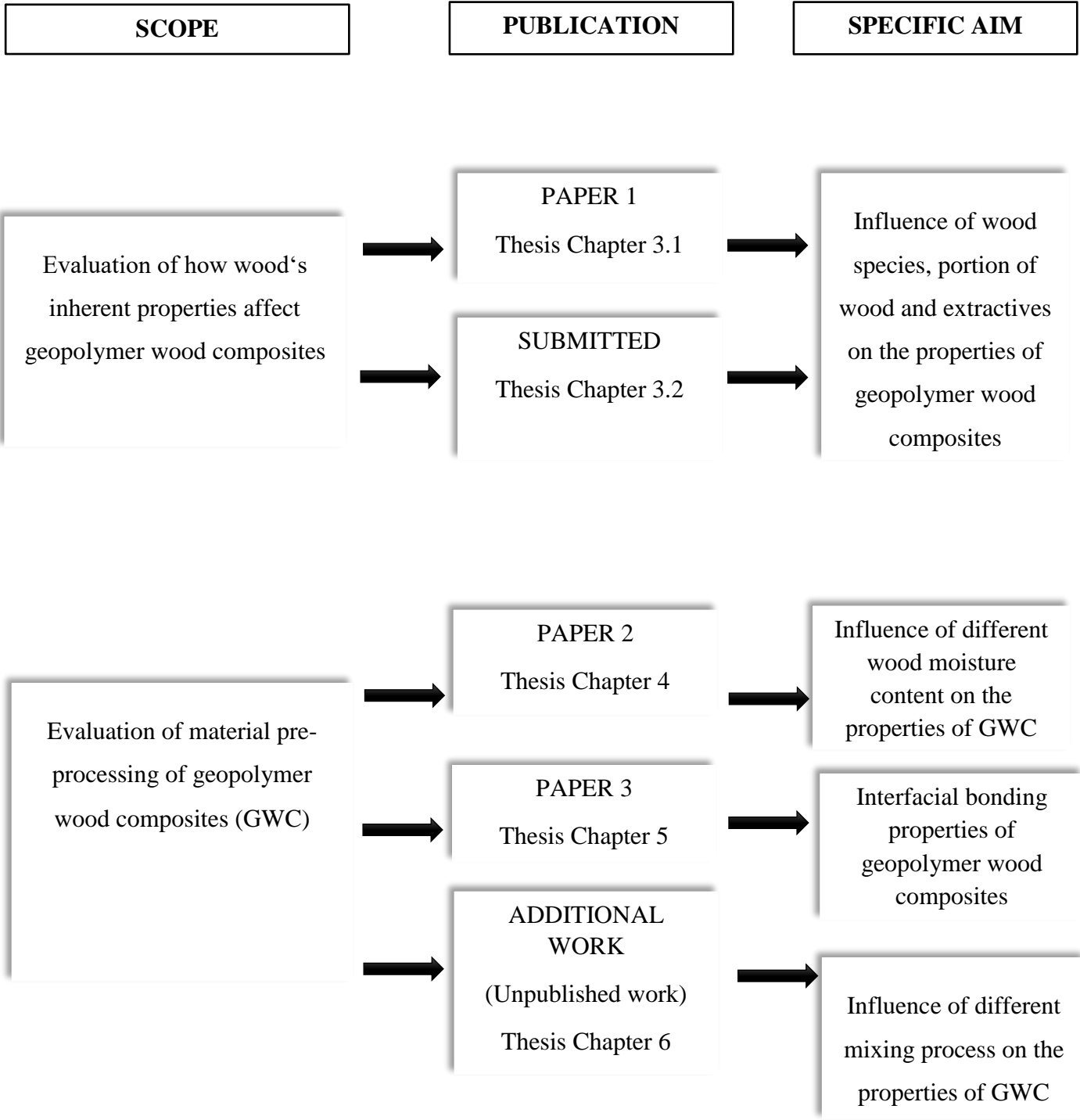
Additionally, the thesis includes one submitted and one additional work (unpublished work), which are:

Chapter 3.2: Influence of wood pretreatment, hardwood and softwood extractives on the compressive behavior of fly ash-based geopolymer composite (**Submitted**).

Chapter 6, additional work: Effects of different mixing and processing designs on the strength and density of geopolymer wood composite (**Unpublished work**).

Integration of the publications

The peer-reviewed publications are integrated into the present thesis and refer to the defined scopes and following the below shown scheme. The discussion of the entire conducted research is unified finally in Chapter 7.



CHAPTER 2

MATERIALS AND METHODS

2.1 Materials

2.1.1 Wood materials

Wood materials used in this work are Scot pine wood (*Pinus sylvestris*), Norway spruce rotary veneer (*Picea abies*) and common beech rotary veneer (*Fagus sylvatica*); all from Germany. Wood flour (Arbocel C100) was obtained from Rettenmaier & Sohne " GmbH + Co KG, Rosenberg, Germany. The other wood materials used in this study included alien invasive wood species. These wood species included Black wattle (*Acacia mearnsii*), Port Jackson (*Acacia saligna*) and *Eucalypt camaldulensis*. The Black wattle, Port Jackson and *E. camaldulensis* were harvested during the invasive clearing operations along the Berg river banks in Cape Town and supplied by Casidra, Paarl, Western Cape, South Africa. *Eucalypt grandis* and *Pinus taeda* was supplied by the Wood and Wood Structures Laboratory, São Carlos Engineering School of the University of São Paulo (USP).

2.1.2 Geopolymer precursors

Geopolymer starting materials used in this present thesis included commercial metakaolin (MK) (Metamax, BASF SE, Germany) and two low calcium fly ash (Class F fly ash) sourced from Pozo Fly, Brazil and the GK Kiel GmbH power plant in Kiel, Germany. The chemical compositions of these aluminosilicates materials are presented in Chapter 3-6.

2.1.3 Alkaline solution and other reagents

A combination of sodium silicate (Na_2SiO_3) and sodium hydroxide (NaOH) was used as the alkaline solution to activate the aluminosilicate materials. Sodium silicate solution (Betol 50

T, Woellner GmbH, Germany), Sodium silicate pellets (SiO_2 63%, Na_2O 18%), sodium hydroxide (NaOH) pellets (98.0%, VWR, Germany) and sodium hydroxide pellets (NaOH, 98%) were supplied by Dinâmica (Brazil) were used in this present thesis. 1% NaOH solution was used for the extraction of wood extractives and wood particles pretreatment.

2.2 Methods

This section will give an overview on the methods used to confirm the hypothesis. However, detailed information about the methods can be found in both published and unpublished works of the present study in the corresponding Chapters.

1. Evaluation of how wood's inherent properties affect properties of geopolymer wood composites

GWCs with a wood particle content of 20% (mass %) were produced by the dry mixing of fly ash and the wood before alkali activation and addition of water. Both softwoods and hardwoods particles and their extractives as well as wood flour were used. Hot water (Chapter 3 part 1) and 1% NaOH solutions (Chapter 3 part 2) were used for the pretreatment for wood particles. Accelerated solvent extraction method (ASE method) as well as Gas chromatograph mass spectrometry– flame ionization detection (GCMS–FID) – were used to quantify and identify the chemical composition of wood extracts respectively. In all the experiment conducted under this section, compressive strength, specific strength and scanning electron microscopy (SEM) were used as a means for comparison.

2. Evaluation of material preprocessing of geopolymer wood composites

In order to confirm this scope of the study, both fly ash-based and metakaolin-based geopolymers were used as the binding agent for wood. Wood of different forms (i.e. wood

veneer, flour, fibers and particles) were used in this scope of the study. Softwood flours in five (5) different moisture content levels were used to investigate the influence of wood moisture content on the hardened state properties of fly ash-based GWC (Chapter 4). Rotary veneers were used to study the interfacial bonding properties of metakaolin-based GWC (Chapter 5), while wood particles and fibers were used for the influence of different mixing process on both fly ash-based and metakaolin-based GWCs (Chapter 6). Sanding of wood veneers with different grit sizes (sandpapers P60, P100 and P180) (i.e. mechanical treatment) and moisture conditioning of wood flour were used as treatment. Five (5) different mixing processes were tested and evaluated for fly ash based and metakaolin-based GWCs. Compressive strength testing, x-ray density profiling and SEM were used for the characterization of the composites. Pull out force and strength were used for accessing the interfacial bonding properties between wood veneers and metakaolin-based geopolymer (Chapter 5).

CHAPTER 3

CHAPTER 3.1

Influence of wood pretreatment and fly ash particle size on the performance of geopolymer wood composite (**Paper 1**)

Authors' contribution

	CD	EX	ED
Bright Asante	75%	75%	60%
Goran Schmidt	5%	5%	15%
Ronaldo Teixeira	5%	10%	5%
Andreas Krause	5%	5%	10%
Holmer Savastano Junior	10%	5%	10%

CD: Conceptual Design

EX: Conducting experiments

ED: Editing



Prof. Andreas Krause

(Supervisor)

Originally published in: European Journal of Wood and Wood Products. Volume 79. First published online 10 March 2021. <https://doi.org/10.1007/s00107-021-01671-9>.

Changes to original published work

To conform to the systematic numbering in the present thesis, all figures and tables in the original published work are preceded by the thesis chapter number.

The text ‘figure’ in full was shortened to Fig. Other than this, no changes were made to the text.

NB: These changes might have moved some text positions.



Influence of wood pretreatment and fly ash particle size on the performance of geopolymer wood composite

Bright Asante^{1,2} · Goran Schmidt³ · Ronaldo Teixeira² · Andreas Krause^{1,3} · Holmer Savastano Junior²

Received: 27 August 2020 / Accepted: 11 February 2021
© The Author(s) 2021

Abstract

In search for greener building materials, geopolymer wood composites (GWC) were produced through alkali activation of fly ash, using pine and eucalypt wood particles. The study examined the influence of grinding fly ash, wood species and hot water treatment of wood particles on the physical properties and specific compressive strength of GWC before and after 200 cycles of soaking and drying. Ash-grinding affected particle size distribution, as the hot water pretreatment of the wood affected its extractives. The particle size analysis showed that grinding decreased the mean particle size of raw ash by 55% and played a major role in the composite's properties, as lower densities and specific strength with high water absorption were recorded for GWC from raw ash than from ground ash. The ash-grinding step doubled the specific strength of the composites before the aging test. A decrease in specific strength (15–32%) was observed for all composites after the soaking and drying cycles. Hot water washing of the wood resulted in a 47% and 67% reduction in the extractive content of the pine and eucalypt particles, respectively. An improvement of 27% and 3% was noted in specific strength values respectively for GWC with treated pine and eucalypt particles. In general, lower specific strength was recorded for pine-based composites than eucalypt ones, due to the fast impregnation and high water absorption from the mixture by pine particles. It was revealed that hot water treatment of wood improves GWC properties less compared to wood species or fly ash particle size.

1 Introduction

Current research aims at finding solutions to the ever-increasing population and its demand for infrastructure and accommodation, coupled with high waste accumulation. The cascade use of secondary resources, such as postconsumer thermoplastic waste or combustion byproducts, helps avoid solid wastes, keeps carbon in the material cycle and upcycles low value resources by substituting imported virgin building products. The production of Ordinary Portland Cement (OPC) contributes to a significant amount of CO₂ in the

environment. These emissions from OPC production and the environmental awareness of climate change have compelled society to seek for second generation materials with less environmental impact, with geopolymer being one of the prominent alternatives. Geopolymer (an alkali-activated cement) is estimated to produce about 55–75% less CO₂ compared to OPC (Yang et al. 2013). Since the discovery of geopolymer by Davidovits in 1970s, research has been ongoing to ascertain how best to utilize this cementitious building material.

Geopolymers are made-up of mineral compositions containing high amounts of aluminium (Al) and silicon (Si) and they are amorphous. In general, they can be produced of any material source that is rich in Si and Al. Currently, major research efforts for this binder focus on utilizing industrial wastes such as slag and fly ash as an alternative to natural raw material minerals such as kaolinite (Kumar et al. 2010; Kielè et al. 2020). Geopolymer is produced by alkaline activation of any aluminosilicate source material (Bakharev 2005). The reaction process results in the dissolution of the reactive aluminosilicate. The dissolved slurry undergoes polycondensation to produce a material with desired mechanical properties (Sofi et al. 2007). During the reaction

✉ Bright Asante
bright.asante@uni-hamburg.de

¹ Institute of Wood Sciences, University of Hamburg, Leuschnerstrasse 91c, 21031 Hamburg, Germany

² Department of Biosystems Engineering, University of São Paulo, Av. Duque de Caxias Norte 225, Jd. Elite, Pirassununga, SP 13635-900, Brazil

³ Johann Heinrich Von Thünen Institute, Federal Research Institute for Rural Areas, Forestry and Fisheries, Institute of Wood Research, Leuschnerstrasse 91, 21031 Hamburg, Germany

process, there is a gradual release of water. The geopolymer forms an amorphous three-dimensional network of aluminate and silicate units with charge balancing cation. Curing happens at ambient temperature and accelerates at elevated temperature (Sarmin et al. 2014).

Since geopolymer may be produced from many different raw material resources, specific characterization, pretreatment and processing procedures need to be considered. Each source of raw material differs in composition (e.g. alkali metal content and ratio), particle size and morphology. The geopolymerization varies with its raw materials and hence results in different microstructure, chemical and mechanical properties (Vickers et al. 2015).

The annual production of fly ash in the world from coal combustion is estimated to be around 700 Mt (million tons) (Ferreira et al. 2003; Argiz et al. 2015). Fly ash has mainly been used as a replacement for OPC because of its beneficial properties, especially with respect to its high compressive strength compared to cement (Abdullah et al. 2011). The replacement of OPC with fly ash up to 60% by mass is a notable development (Kumar et al. 2007). At present, multiple researches are focused on fly ash utilization as a precursor material for geopolymer, with large interest in cleaner production and minimizing waste.

In Brazil, about 4 Mt of fly ash are generated per year with the annual utilization for incorporation into cement and concrete accounting for about 30% of total fly ash production (Izidoro et al. 2012) and serves as a major industrial application for this inorganic residue in the country (Rohde et al. 2006). The low utilization potential and the operation of new coal-based thermal power plants are likely to increase the quantity of fly ash (Izidoro et al. 2012). Fly ash mainly consists of Fe_2O_3 , SiO_2 , Al_2O_3 with some potential toxic substances such as heavy metals from the coal and polyaromatic hydrocarbons that condense from the flue gas (Misengue et al. 2016). The large-scale storage and improper disposal of this waste act as a major source of air, water and land pollution (Ahmaruzzaman 2010). This present study is intended to not only mitigate and minimize the accumulation of fly ash but also to address the utilization of this waste in the synthesis of a high value added product.

The physical properties of fly ash—such as particle sizes and surface area—affect its reactivity, as well as the chemical and mechanical behavior of the geopolymer product formed (Erdođdu and Türker 1998; Van Jaarsveld et al. 2003). This indicates that particle size of the material is an important factor when it comes to the material selection, as it influences the reaction rate. According to Rosas-Casarez et al. (2018), it influences the rate of dissolution of aluminosilicate in the precursor material as the smaller particle size requires less time, hence a faster polymerization reaction.

For this reason, Rosas-Casarez et al. (2018) proposed that the activation and reactivity of fly ash could be improved by

adequate grinding. Mechanical grinding affects the microstructure of ash, causing a weakening in the vitreous chemical bonds of Si–O or Al–O. Beside the fact that it accelerates the dissolution of these bonds, it shortens the equilibrium time, gelation time, and the structuring of the new crystalline phases and the different reaction products, specifically the hydrated sodium aluminosilicate gel, which is known as the reaction product that gives the mechanical properties to the geopolymer (Rosas-Casarez et al. 2018).

Another way of steering geopolymer composite properties is the addition of lignocellulosic raw materials. Wood particles have been used as fillers in geopolymer wood composites (GWC) to reduce the density of the product (Sarmin 2016; Kielè et al. 2020). Halas et al. (2011) reported both positive and negative effects of the fly ash geopolymer with sawdust as filler. Halas et al. (2011) showed that a higher amount of sawdust had a negative effect on the compressive strength of the specimens. Duan et al. (2016) stated that lignocellulosic waste had a positive effect on the main properties of fly ash geopolymer and showed that the addition of sawdust (without any special pretreatment) improved the cracking resistance while drying. Wood as a lignocellulosic material mainly consists of lignin, cellulose, hemicellulose and extractives. Ye et al. (2018) studied the effect of lignin, cellulose and hemicellulose on geopolymer composites. The authors concluded that the degree of geopolymerization was clearly lowered by the alkaline degradation of hemicellulose, and higher concentrations of lignin and hemicellulose had a negative effect on the flexural and compressive strength of the geopolymer composites.

Although fly ash geopolymers have shown their applicability to wood, the variation in wood species and the complexity of wood offer drawbacks such as compatibility and long-term durability issues for these composites. The wood component, upon contact with the high alkali environment in the fly ash geopolymer, will lead to the leaching of non-structural polysaccharides and extractives from the wood. This might affect the interfacial reactions between geopolymer and wood, and the GWC properties. However, the intensity and the components (non-structural polysaccharides and extractives) that may leach out from the wood may differ among wood species. To avoid this negative impact from the non-structural polysaccharides and extractives, Ferraz et al. (2011) suggested removing these inhibitors by hot water (100 °C) pretreatment; this remains one of the cheapest extraction methods for wood. The easy accessibility and availability of water (as a solvent) make this pretreatment method more sustainable compared to other pretreatment methods. Hot water alters the chemical composition and the surface morphology of the biomass (Therasme et al. 2018) by removing some of the components—mainly extracts. To date, no report has been found neither in relation to the effect of pretreating the raw materials nor a comparison of these effects (i.e. wood species, hot water treatment of

wood together with fly ash particle size) on the performance of GWC.

This research investigates the influence of preparation of raw material on the physical properties, specific compressive strength and durability of geopolymer wood composites (GWC). The study of raw material focused on fly ash particle size (pre and post grinding) and hot water treatment of wood. In addition, the effect of two wood species on the GWC properties was assessed.

2 Materials and methods

2.1 Materials

Sodium silicate (Na₂SiO₃) pellets (SiO₂ 63%, Na₂O 18%) and sodium hydroxide pellets (NaOH, 98%) were supplied by Dinâmica (Brazil), debarked sawn wood (*Eucalyptus grandis* W.Hill and *Pinus taeda* L.) was supplied by the Wood and Wood Structures Laboratory, São Carlos Engineering School (LAMEM/EESC) of the University of São Paulo (USP). Class F fly ash was supplied by Pozo Fly (Brazil).

2.1.1 Fly ash composition

The fly ash was divided into two groups. One group was ground further using an Astecma (model mb 20) ball mill for 1 h, whereas the other group remained in its raw state. The composition of the chemical oxides of the starting material (raw fly ash) was detected by X-ray fluorescence (XRF), using a PANalytical Axios Advanced. The results are shown in Table 3.1.1.

2.1.2 Characterization of wood particles and fly ashes

The morphology of the wood particles pre and post treatment was assessed using the field emission scanning electron microscope (FESEM) Quanta FEG Type 250, FEI Electron Optics (SN: D9122), Netherlands. The wood samples were gold-coated before imaging. Particle size distribution (PSD) and X-ray diffraction (XRD) studies were carried out on the raw and ground fly ashes. The PSD and XRD studies were done in a Partica Laser Scattering Particle Size Distribution Analyzer LA-950V2 and Rigaku Miniflex600 diffractometer, respectively. The XRD was carried out using a Cu- K α wavelength, 40 kV and 20 mA, in a 2 θ range of 5°–70°. Scanning electron microscopy (SEM) was conducted on both sets of ashes. SEM was carried out using the LEO 1525 GEMINI test machine. The fly ash samples were carbon-coated before imaging.

Table 3.1.1 Chemical composition (% by mass) of fly ash from XRF test

Component	Al ₂ O ₃	SiO ₂	SO ₃	K ₂ O	Na ₂ O	CaO	TiO ₂	Fe ₂ O ₃
Share (%)	22.47	64.29	0.81	2.97	0.51	1.74	1.36	6.31

2.1.3 Lignocellulose materials processing and hot water pretreatment

Sawn wood pine and eucalypt boards with densities of 0.39 g/cm³ and 0.56 g/cm³ respectively, were cut to dimensions of 25 mm × 30 mm × 50 mm. These pieces of wood were milled and later sieved with a Manupen sieve vibrator for 1 h to separate the wood into different particle size fractions. Wood particles that could pass through the 1 mm sieve but which were retained in the 0.6 mm sieve were used for both pine and eucalypt. Hot water pretreatment was carried out on both sets of sieved particles according to the method described by Cabral et al. (2017). Water was heated up to 100 °C in a 3.5 L container and 31.25 g of wood particles were introduced per 1 L water for 30 min. Finally, the recovered particles were washed with 1 L of tap water and placed in an oven at 60 °C, until a moisture content of around 10% was reached.

2.1.4 Chemical composition of lignocellulose materials

The extract content of the wood samples was analyzed using the Accelerated Solvent Extraction (ASE 350) from Thermo Fisher Scientific (Dionex). Extraction was done using 2 g of wood under the conditions stated in Table 3.1.2. Wood particles that could pass through the 1 mm sieve but which were retained in 0.6 mm sieve were used for both pine and eucalypt in the extraction process. Extraction was first done using petrolether, followed by acetone/ water and lastly with water alone. The total extract was the summation of the extract content in these processes. The extractive-free wood was hydrolyzed for sugars using the method described by Lorenz et al. (2016). The extractive-free samples were then finely ground (vibrating mill, Duke).

Pre-hydrolysis Approximately 200 mg was weighed into a reaction vessel. The sample was mixed with 2 mL of 72% cold H₂SO₄ after which it was hydrolyzed in a thermostat for 1 h at 30 °C. After one

Table 3.1.2 Extraction conditions for extractive content

Solvent	Petrolether	Acetone/H ₂ O (9:1)	H ₂ O
Static [min]	10	10	10
Cycles	2	2	2
Pressure [bar]	100	100	100
Temperature [°C]	70	70	90

hour, the reaction of the pre-hydrolysis was stopped by the addition of 6 mL of distilled water. Next, the suspension was transferred together with 50 mL of water into a volumetric flask and the samples were post-hydrolyzed by autoclave at 120 °C under 1.2 bar pressure (40 min for pine and 30 min for eucalyptus). After cooling the volumetric flasks, the condensed lignin was filtered off as a hydrolysis residue by means of a G4 glass filter crucible. From the filtrate, about 1 ml was taken for the sugar analysis. The hydrolysis residue was washed thoroughly with distilled water, dried at 105 °C and determined gravimetrically.

2.2 Composite preparation

The alkaline solution for activation was prepared using molar solutions of 3 M Na₂SiO₃ and 12 M NaOH in a weight ratio of 2.5:1. The solution was allowed to cool to ambient conditions prior to use. Fly ash was first dry-mixed with 20 wt% wood particles for 2 min. Water was then added to the solid mixture of fly ash and wood for an additional 2 min. The ratio of water to solid material was kept constant at 0.16 for all mixtures. Finally, the mixture was activated for 2 min at an alkaline solution to fly ash ratio of 0.47 for all mixtures. The activated mixture was cast in a 50 mm × 100 mm cylinder mold and allowed to stand at 25 ± 2 °C for 2 h before oven curing for 4 h at 103 ± 2 °C. To avoid cracks forming due to rapid moisture loss, samples were kept in plastic before oven curing. The oven-cured samples were kept in the climate chamber (20 °C, 65% RH) for 7 days before all physical and compressive strength tests were carried out.

2.3 Compositetesting

2.3.1 Water absorption, density and apparent porosity

In determining water absorption, dry bulk density and apparent porosity, the recommendations based on Testing Methods for Fiber Reinforced Cement-based Composites (RILEM 1984) were used. 7-day old 50 mm × 100 mm specimens were removed from the climate chamber (20 °C and 65% RH) and cut to ~ 50 mm × 25 mm (diameter × height). The specimens were submerged in water for 24 h at room temperature. The specimen was then suspended in water and the immersed mass (Mi) was measured. The wet mass (Mu) was measured by withdrawing the sample from the water and lightly wiping its surface to remove excess water using a clean, dry cloth. After drying the specimen (to a constant mass) in an oven with air circulation (105 ± 5 °C), the dry mass (Ms) was obtained. The following equations were used to obtain the water absorption, apparent density and apparent porosity of the specimens.

$$\text{Water absorption}(\%) = \frac{Mu - Ms}{Ms}, \quad (1)$$

$$\text{Dry bulk density}(\text{g/cm}^3) = \frac{Ms}{Mu - Mi} \times d, \quad (2)$$

$$\text{Apparent porosity}(\%) = \frac{Mu - Ms}{Mu - Mi}. \quad (3)$$

2.3.2 Specific compressive strength

The compressive strength of 7-day old cylindrical samples (50 × 100 mm) was measured using an Emic DL30000N. The samples were compressed using a 300 kN load cell and a constant loading rate of 1 mm/min. The specific compressive strength (specific strength) was calculated by dividing the compressive strength by the sample density (mass per volume). An average of six samples was reported for each group.

2.3.3 Accelerated aging testing

The accelerated aging test involved a comparative analysis of the mechanical performance of the composites, before and after 200 soak/dry cycles. Specimens were successively immersed in water at 20 ± 5 °C over the course of 170 min, followed by a resting phase of 10 min, after which they were exposed to a temperature of 70 ± 5 °C for 170 min in a ventilated oven; the final resting phase being 10 min. This procedure was based on the recommendations of the EN 494 (1994) standards. Each soak/dry set represents one cycle and was performed for 200 cycles (Teixeira et al. 2012).

2.4 Statistics and data presentation

Statistical analysis was performed with JMP 14.2 software from the SAS Institute. All values presented in this study are mean values. Error bars are represented with the standard deviations. Statistical analysis (ANOVA) was applied to identify differences in density, water absorption, porosity and specific compressive strength between pine-based and eucalypt-based GWC, hot water treated and untreated GWC and for GWC from ground and raw fly ash. Comparisons of means were performed using the Tukey test at 5% significance level.

3 Results and discussion

3.1 Characterization of raw materials

3.1.1 Characterization of wood particles before and after treatment

The morphology and appearance of the pine and eucalypt wood particles before and after hot water treatment are presented in Fig. 3.1.1. From Fig. 3.1.1 it can be seen the major difference arose from the color change of wood particles. With hot water treatment of the particles, the wood color changed from light yellowish to dark yellowish for the pine and from light brown to dark brown for eucalypt particles. This color change might be a result of the removal of some extracts and drying of particles after treatment. FESEM images (Fig. 3.1.2) show that the pine particles appeared to be shorter in length while the eucalypt particles were slender and longer. The properties (density, fiber length, shear

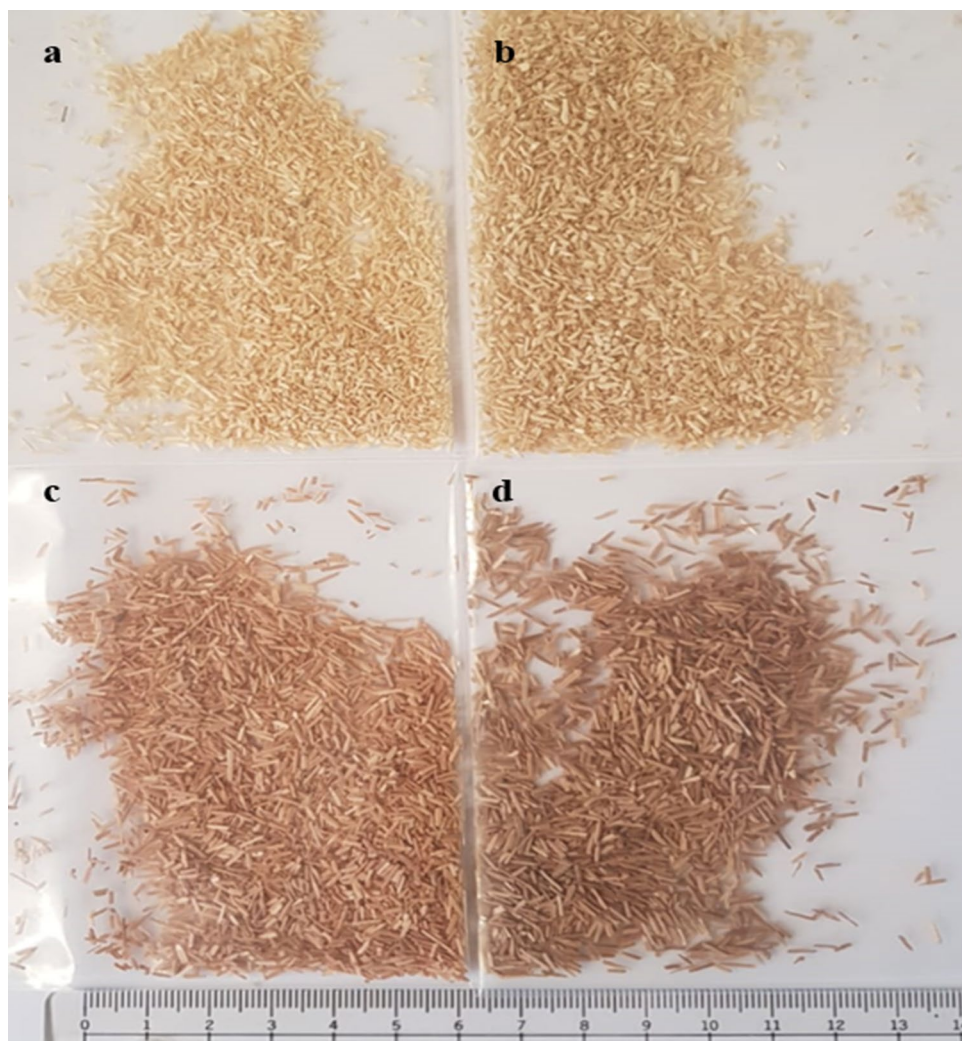
strength) of the wood itself might have influenced the shape of the particles obtained with the same milling system. No observable changes were seen on the surfaces of the wood particles, indicating that morphology effects due to mechanical interlocking do not affect strength changes.

3.1.2 Characterization of raw and ground fly ashes

Fig. 3.1.3 shows the particle size distribution and SEM of raw (a, b) and ground (c, d) fly ash. In this work, the particle size distribution was determined by the mean diameter as well as the cumulative percentage below a certain grain diameter (CPFT). The CPFT was classified for the diameter below 10% (D10), 50% (D50) and 90% (D90). The mean size of raw fly ash was 28.54 μm and 12.95 μm for ground fly ash. Through grinding, there was a 54.6% decrease in the mean particle size.

The fine ash particle fraction in D10 shifted from 2.95 to 1.78 μm . The major reason for the decreased mean particle size is found in the D90 class. Fig. 3.1.1a shows

Fig. 3.1.1 Wood particles before and after hot water treatment: **a** untreated pine; **b** treated pine; **c** untreated eucalypt; **d** treated eucalypt



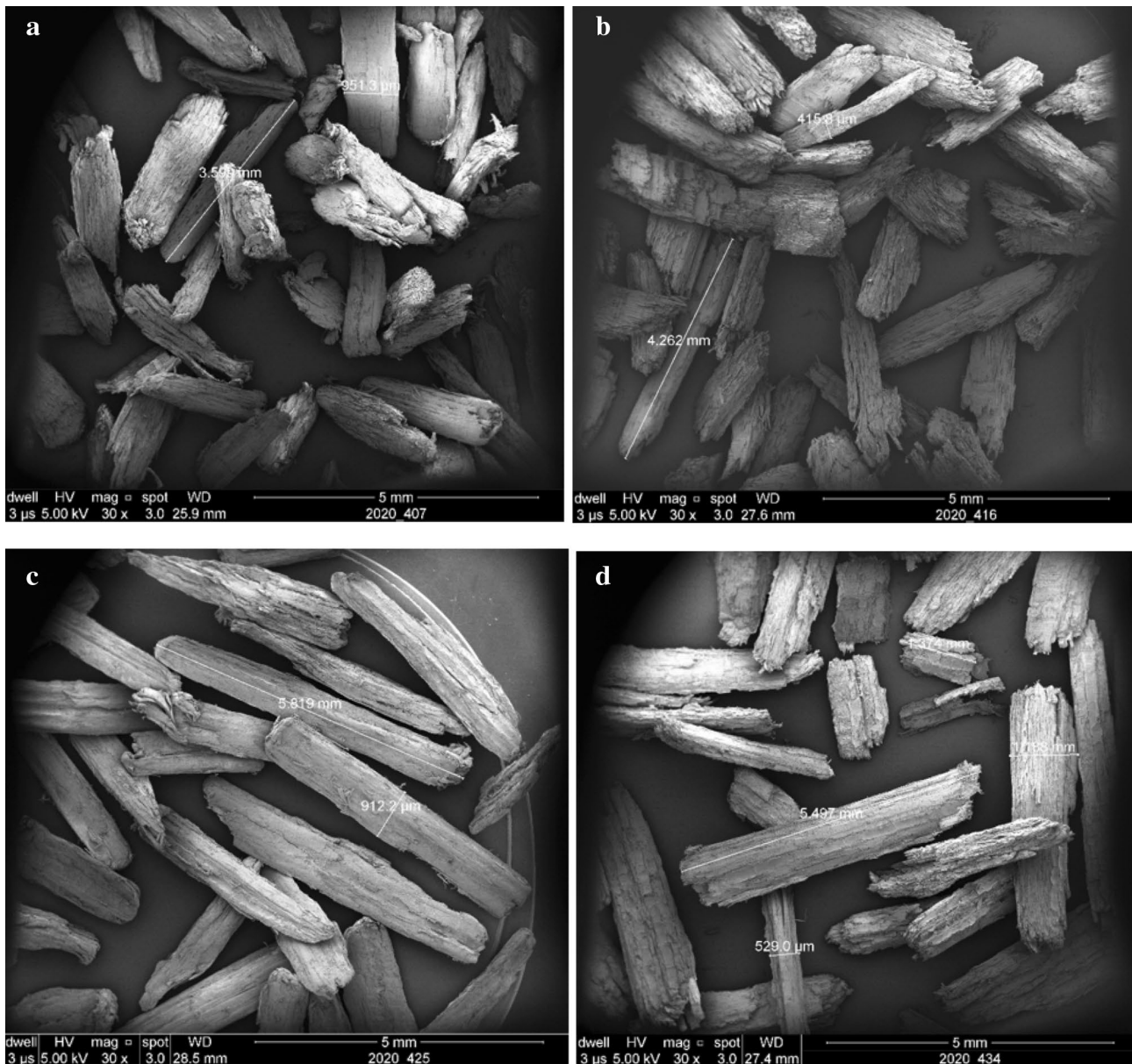


Fig. 3.1.2 FESEM images of wood particles before and after hot water treatment: **a** untreated pine; **b** treated pine; **c** untreated eucalypt; **d** treated eucalypt

a peak at roughly 100 μm , whereas this peak practically disappears after being ground (Fig. 3.1.3c). The grinding process might not only reduce the particle size of the fly ash but homogenize the grain structure, which may facilitate the alkaline activator to access the aluminosilicate. The surface and particles were studied using a SEM test. At the same magnification, the ground fly ash showed a smaller shape and more uniform particles than the raw fly ash (Fig. 3.1.3b and d). XRD was used to identify the crystallinity of the ash materials (Fig. 3.1.4). The identification phases obtained (with Match Phase Identification 3.8.0.137) showed that the main compounds in both the raw and ground ashes are mullite (M) and quartz (Q).

There was no apparent change in the mineralogy of ground material; Rosas-Casarez et al. (2018) made similar observations.

3.2 Characterization of geopolymer wood composite

3.2.1 Effect of species and pretreatment on physical properties

Table 3.1.3 shows the resulting water absorption, bulk density and apparent porosity of the GWC based on untreated and treated pine and eucalypt. The GWC based on pine gave a lower dry bulk density compared to those

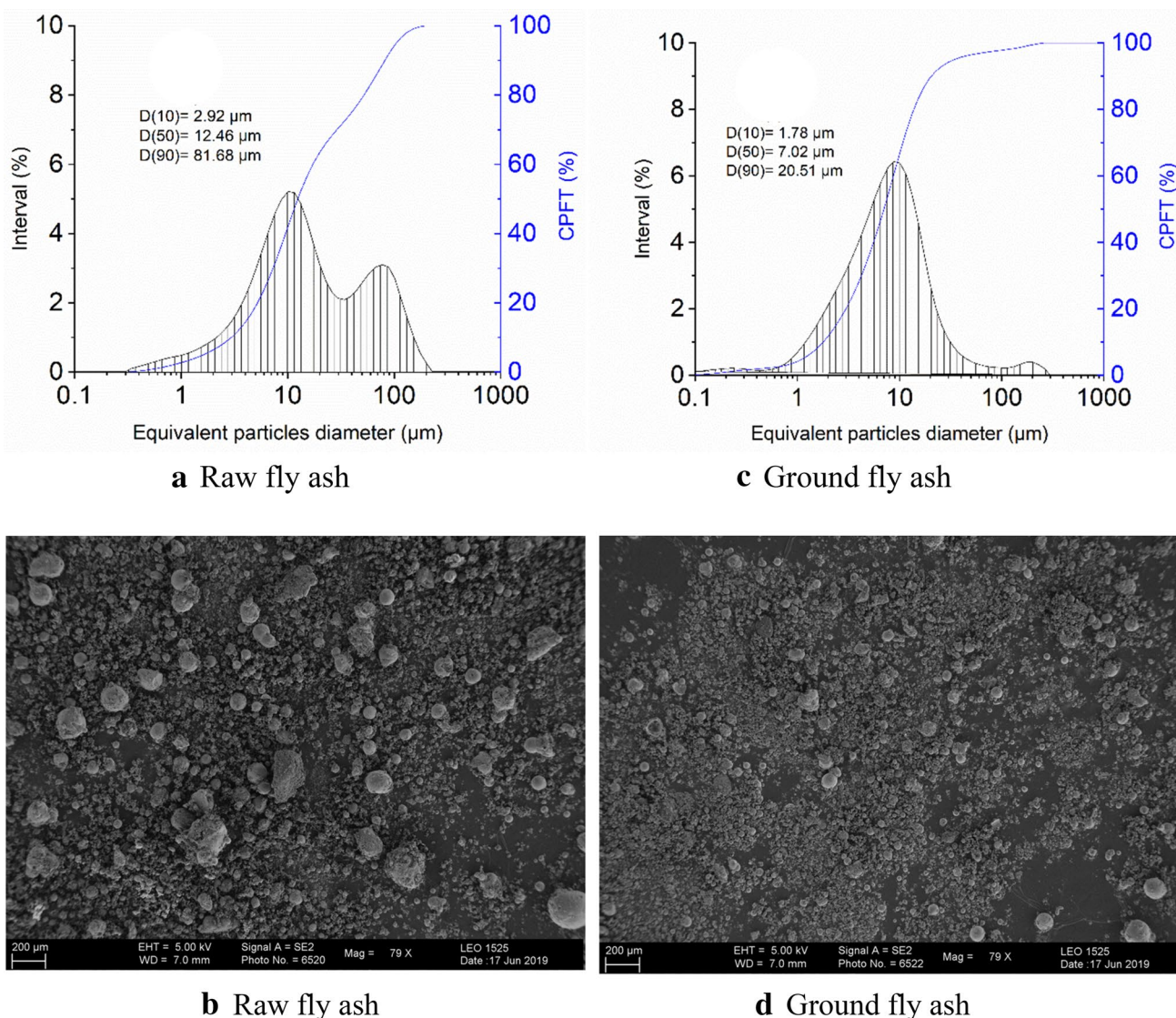


Fig. 3.1.3 Particle size distribution and SEM for raw (a, b) and ground (c, d) fly ash

from eucalypt. The results indicate a significant difference in density between pine-based and eucalypt-based composites. Eucalypt had a higher apparent density (0.56 g/cm^3) than pine (0.39 g/cm^3), which might have contributed to the final bulk density of the GWC. Similar densities were obtained for hot water treated and untreated samples for both wood species. There was no significant difference between composites formed from hot treated and untreated wood species.

Comparable porosity was recorded for all samples, with no significant difference between species and treatments. This porosity measurement with water might work for pure concrete or mortar but is no good for mortar containing a high amount of wood, as in this case. This is because in pure geopolymer mortar, the water might easily fill the voids

after 24 h immersion. In a GWC, the wood might hold some amount of water, which adds up to the water in the void. This might have accounted for the higher porosity values in all samples. After 24 h water immersion, pine-based GWC had the greatest water absorption rates (about 53%), while eucalypt recorded the lowest water absorption rates (about 46%). This difference in water absorption between the pine-based and eucalypt-based composites seems to arise from the different densities of the GWC. This clearly shows an inverse relation between water adsorption and density, that is, an increase in the density of the composite made from eucalypt led to a reduction in its water absorption. Sarmin (2016) reported similar observations: that denser GWC from wood flour had a lower water absorption rate compared with a less dense GWC from wood particles.

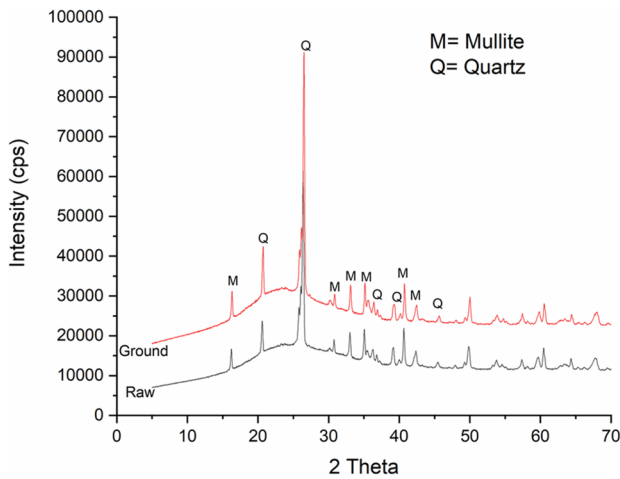


Fig. 3.1.4 X-ray (powder) diffraction analysis of raw and ground fly ashes

Another possible reason for the differences in water absorption could be a property of the wood itself, as it is well known that lower density coniferous wood takes up more water than higher density broadleaved wood species. Hence, the lower apparent density of pine than eucalypt might have led to a higher water uptake in the pine-based composite than in the eucalypt. Moslemi et al. (1995) ascertained that wood cement incompatibility leads to a large amount of free internal spaces within the wood cement matrix and could be a possible cause for great moisture adsorption of composites. Mahzabin et al. (2013) further reported that, without proper encasing of wood particles by cement particles, the hygroscopic nature of wood complicates the water absorption outcome among poorly compacted composites. Therefore, the low water absorption of the eucalypt-based composite could be due to the greater compatibility of this species with the geopolymer matrix. However, there was no significant difference between hot water treated and untreated GWC within the same wood species.

3.2.2 Effect of species and pretreatment on specific compressive strength

Pine-based composites recorded a compressive strength of 1.15–1.50 N/mm² while eucalypt-based composites had 2.49–2.59 N/mm², untreated – treated GWC respectively.

Table 3.1.3 Mean comparison (standard deviation) of physical properties of geopolymer wood composites (GWC) from ground fly ash

GWC	Wood treatment	Bulk density (g/cm ³)	Water absorption (%)	Porosity (%)
Pine	Untreated	0.88 ^a (0.03)	53.53 ^a (5.04)	47.21 (2.80)
Pine	Treated	0.88 ^a (0.01)	51.99 ^a (2.80)	45.76 (1.96)
Eucalypt	Untreated	1.03 ^b (0.02)	46.01 ^b (2.48)	47.13 (1.45)
Eucalypt	Treated	1.02 ^b (0.03)	45.93 ^b (2.29)	46.79 (1.09)

Means in the same column with same letters are not significantly different ($p > 0.05$)

The eucalypt composite density is 16% higher than that of pine, which may have risen from the different wood species' densities. The density difference affects the composite strength. Hence, density effects shall be eliminated for better comparability of the species and pretreatment effect on strength. Fig. 3.1.5 shows the resulting specific compressive strength of the GWC based on untreated and treated pine and eucalypt particles. In this study, the selection of wood species was found to have a significant influence on the strength of composites formed. Eucalypt-based composites recorded significantly higher specific compressive strength compared to pine-based composites. The hot water pretreatment increased specific strength by 27.4% for pine-based and 3.1% for eucalypt-based GWC. However, a significant difference was only observed between hot water treated and untreated pine-based GWC. This shows that the pretreatment was relatively effective for pine compared to eucalypt. GWC with treated wood had a higher specific strength, which could be due to the wood particle's improved compatibility with the geopolymer, which resulted in effective bonding and increased maximum load transfer capacity.

The chemical composition of the treated and untreated wood particles is summarized in Table 3.1.4. It is a fact that

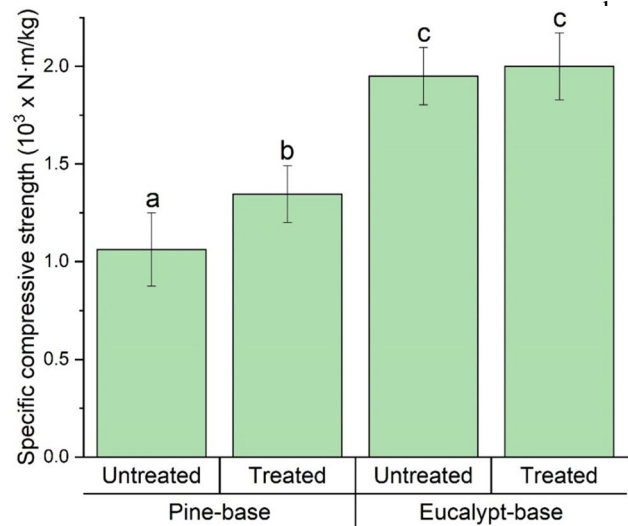


Fig. 3.1.5 Specific compressive strength of geopolymer wood composites from ground fly ash

Table 3.1.4 Chemical composition of treated and untreated wood particles (%)

Component (%)	Species			
	Pine untreated	Pine treated	Eucalypt untreated	Eucalypt treated
Hydrolysis residue	29.20	29.20	28.10	29.20
Xylose	7.18	7.29	11.12	11.53
Glucose	42.42	42.61	47.89	50.05
Mannose	9.36	9.57	1.02	1.03
Galactose	2.00	2.07	0.79	0.90
Arabinose	1.22	1.27	0.20	0.22
Rhamnose	0.15	0.14	0.20	0.22
Acid soluble lignin	0.45	0.46	2.41	2.60
Other extracts	2.79	1.47	4.08	1.33

hot water extraction alters the chemical composition of wood by fractionating accessible sugars and hemicelluloses (Pelaez-Samaniego et al. 2013, 2014). Due to the solvent polarity, it was expected that the hot water treatment would remove water-soluble extracts, such as non-structural carbohydrates, their saccharic acids, inorganic components and degradation products (alcohols, ketones) (Sluiter et al. 2008, 2010; Davison et al. 2013). The xylose, glucose, mannose, galactose, arabinose and rhamnose however, remained unaffected. The main portion of those sugars form part of the structural macromolecules and the apparent perceptual increase after treatment is an effect of the removal of other extracts. The hot water treatment removed 1.32 and 2.75% for pine and eucalypt, respectively. The analytical extraction agents, water, acetone–water and petrol ether reflect the range of polar to non-polar solvents. Aprotic polar solvents such as acetone cover a wider range of reactions due to their inter-mediate polarity. The extracted substances might comprise tannins, gums, sugars, starches and color producing chemicals (TAPPI 2007). Although a difference in strength was observed for pine, the extract yield was twice as high in eucalypt. This indicates, that one of the above-mentioned pine specific extracts causes the lower incompatibility of this species with the geopolymer matrix. Further investigations must focus on identifying the exact substance interacting with the geopolymerization.

Hot water treatment of wood particles by boiling is a similar process to cooking of wood chips in pulping, which

is largely influenced by wood density. Zañão et al. (2019) stated that the density differences between eucalypt and pine significantly affect the impregnation of these two woods. Low-density woods are impregnated faster than high-density woods when boiling in water. A similar phenomenon might have occurred in this study, as the fast impregnation and high water absorption by the pine particles might have decreased the amount of water available for ionic transport within the mixture and led to the lower specific strength. By this same principle, it was expected that pine-based GWC show higher water absorption (Table 3.1.3), with more advantages regarding specific strength increase with the hot water treatment than eucalypt-based GWC. Wilson and White (1986) reported that hardwoods are usually strong in compression, tension and shear, while softwoods are strong in tension but weak in shear. This might have contributed to the difference between the two composites. Since no observable changes were seen on the surfaces of the wood particles (Fig. 3.1.1) after treatment, it can be concluded that the morphology effects caused by mechanical interlocking did not affect changes in strength; rather, the wood species, shape of the wood particles and the removal of extracts did.

3.2.3 Effect of fly ash particle size on physical properties

For this test, the eucalypt-based GWC were used since they performed better than the pine-based GWC. Table 3.1.5 shows that composites made from ground fly

Table 3.1.5 Effect of fly ash particle size on the mean (standard deviation) of the physical properties of geopolymer wood composites (GWC) made with eucalypt

Type of fly ash	Eucalypt treatment	Bulk density (g/cm ³)	Water absorption (%)	Porosity (%)
Raw	Untreated	0.91 ^a (0.02)	53.13 ^a (1.60)	48.11 (0.62)
Raw	Treated	0.92 ^a (0.02)	50.96 ^a (2.17)	47.18 (1.11)
Ground	Untreated	1.03 ^b (0.03)	46.01 ^b (2.66)	47.13 (1.57)
Ground	Treated	1.02 ^b (0.03)	45.93 ^b (2.42)	46.79 (1.16)

Means in the same column with same letters are not significantly different ($p > 0.05$)

ash recorded greater densities than those from raw ash. After 24 h water immersion, composites from raw fly ash had the greatest water absorption rates while ground fly ash recorded the lowest water absorption rates. Significant differences were observed in densities and water absorption of composites from ground and raw fly ashes. The differences in water absorption may be attributed to the different densities of the GWC, owing to the smaller particles of the ground ash getting closely packed to fill up spaces within the composite thereby increasing the density with a reduction in water absorption. Another possibility might be the reduction of particle size through grinding, which resulted in an increased polymerization reaction and forming of a dense structure, with decreased water absorption. However, within the same fly ash group no significant differences were found between hot water treated and untreated composites. The apparent porosity ranged from 46.79 to 47.13% for ground fly ash and 47.18–48.11% for the samples from raw fly ash (Table 3.1.5), with no significant differences between the composites.

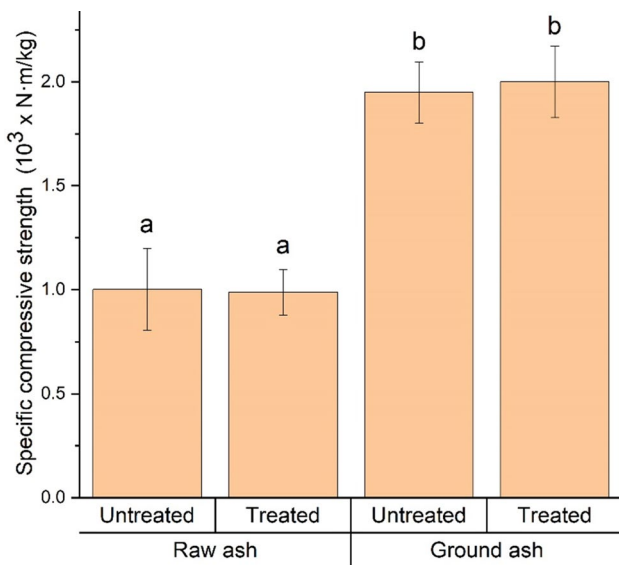


Fig. 3.1.6 Effect of fly ash particle size on specific compressive strength of GWC made from eucalypt

3.2.4 Effect of fly ash particle size on specific compressive strength

Compressive strength is 1.10–1.19 N/mm² (composites from raw ash) and 2.49–2.59 N/mm² (composites from ground ash), untreated—treated GWC, respectively. Hence, density effects shall be eliminated for better comparability of the grinding on the strength results. The ash-grinding step doubled the specific compressive strength (Fig. 3.1.6). Using raw fly ash resulted in about 1×10^3 N m/kg whereas ground fly ash yielded about 2×10^3 N m/kg. With the same ash group, no significant difference was observed for hot water treated and untreated GWC. However, significant differences were observed between the GWC from ground and raw fly ash. The 54.63% decrease in the mean particle size by grinding led to a 94.9% (untreated) and 102.4% (treated) increase in the specific strength.

Grinding results in a larger surface area, which allows for a greater dissolution of alumina and silica in alkaline activation of the fly ash. In addition, smaller particle size requires less time to produce crystalline structures and gels that provide stability to the geopolymer, as well as more homogeneity in the matrix and more rigid bonds (Rosas-Casarez et al. 2018). Kim and Lee (2017) who made a similar observation, discovered that geopolymer from finer ground bottom ash had the highest compressive strength compared to medium and coarse ground bottom ashes. The lower strength from the raw fly ash may be compensated by prolonging the reaction-mixing time to promote dissolution (Ziegler et al. 2016) and adding more soluble silica to dissolve the large particles (Kim and Lee 2017). Additionally, the particle fraction with diameters beyond 100 μ m could be sieved out prior to processing.

3.3 Effect of accelerated aging on specific compressive strength of GWC

The specific compressive strengths of eucalypt-based geopolymer composites after 200 cycles of soak/dry accelerated aging test are shown in Table 3.1.6. A significant difference was observed between the strength of composites from ground and raw ash. A similar pattern to the specific strength Fig. 3.1.6) was observed after the aging

Table 3.1.6 Mean comparison (standard deviation) of eucalypt-based geopolymer wood composite before and after 200 cycles of soak/dry conditions

Species	Type of fly ash	Wood treatment	Specific compressive strength (10 ³ × N m/kg)		% decrease
			Before aging test	After aging test	
Eucalypt	Raw	Untreated	1.00 ^a (0.20)	0.83 ^a (0.22)	17.00
Eucalypt	Raw	Treated	0.99 ^a (0.11)	0.84 ^{ab} (0.16)	15.15
Eucalypt	Ground	Untreated	1.95 ^b (0.15)	1.32 ^{bc} (0.14)	32.31
Eucalypt	Ground	Treated	2.00 ^b (0.17)	1.67 ^c (0.10)	16.50

Means in the same column with same letters are not significantly different ($p > 0.05$)

test, as GWC from ground ash yielded higher strength before and after the 200 cycles than those from raw ash. This difference may be attributed to the difference in water absorption of the GWC samples. Water absorption by composites containing wood particles has several effects on their properties and affect the long-term performance. According to Lin et al. (2002), moisture penetration may degrade the mechanical proper-ties of composites by three different mechanisms. The first involves the diffusion of water molecules inside the micro gaps between the polymer chain, while the second involves capillary transport into gaps and flaws at fiber and matrix interface. Lastly, it may induce swelling of wood particles, which propagates microcracks in the matrix.

Water absorption is related to specific compressive strength as GWC from raw fly ash recorded the highest water absorption and lower specific strength values before and after the accelerated aging test. By increasing reactive surface through grinding, a denser composite material was formed with reduced water absorption and increased compressive strength. Thokchom et al. (2009), who studied the effect of water absorption on the durability of fly ash based geopolymer mortar, made similar observations. The authors found that samples with higher water absorption had the lowest compressive strength. A decrease in this specific strength could be observed for all composites after the cyclic test. However, the highest percentage decrease in strength was recorded for the GWC from ground and untreated wood. The specific strength after aging for ground fly-ash and water treatment decreased notably. In contrast to the previous results on specific strength, these results indicate that there are eucalypt-specific factors that affect the geopolymerization. Nevertheless, this effect is negligible compared to pine. Apart from this, no significant differences were observed between hot water treated and untreated composites.

4 Conclusion

This study analyzed the influence of grinding fly ash, wood species and hot water wood pretreatment on geopolymer wood composite (GWC) properties. It revealed that hot water treated wood improves GWC properties less compared to wood species or ash grinding.

Grinding decreased the mean particle size of raw fly ash by more than 50% and homogenized the particle size dis-tribution. There was an increase in the specific surface area of the fly ashes with grinding, which contributed to their reactivity. Consequently, specific compressive strength doubled for all GWC made from ground ash.

The wood species significantly influenced the GWC's specific compressive strength, as eucalypt-based composites yielded strength nearly double as high as pine ones.

Furthermore, the wood species affected the composite's densities and played a vital role in the water absorption of the GWC. The eucalypt composite density was 16% higher than the pine counterpart, which rose from the different wood species densities. The lower apparent density of pine led to a higher water uptake in the pine-based composite than in the eucalypt-based composite.

The hot-water pre-treatment markedly increased (27%) the specific compressive strength of pine-based GWC, but not those of the eucalypt-based GWC. Washing out the pine-specific extracts led to a better compatibility between geopolymer and wood. Further investigations must focus on identifying the extract substance interacting with the geopolymerization. Alternative wood and non-wood (such as bamboo and bagasse) species shall be screened for their suitability.

Acknowledgements This work was supported by the German Federal Ministry of Education and Research, under the grant no 01DG17007A and in DAAD project 57359374. The authors express their gratitude to Prof. Antonio Francisco Rocco Lahr (LAMEM/USP—Brazil) for the provision of the wood materials used in the research and National Council for Scientific and Technological Development for supporting our lab. In addition, the contribution from Mrs. Bettina Steffen (Thünen Institute- Germany) is acknowledged for helping with the statistical analysis. The last author is grateful to CNPq—National Brazilian Research Agency for the financial support (process #303723/2017-8).

Funding Open Access funding enabled and organized by Projekt DEAL.

Compliance with ethical standards

Conflict of interest On behalf of all authors, the corresponding author states that there is no conflict of interest.

Open Access This article is licensed under a Creative Commons Attribution 4.0 International License, which permits use, sharing, adaptation, distribution and reproduction in any medium or format, as long as you give appropriate credit to the original author(s) and the source, provide a link to the Creative Commons licence, and indicate if changes were made. The images or other third party material in this article are included in the article's Creative Commons licence, unless indicated otherwise in a credit line to the material. If material is not included in the article's Creative Commons licence and your intended use is not permitted by statutory regulation or exceeds the permitted use, you will need to obtain permission directly from the copyright holder. To view a copy of this licence, visit <http://creativecommons.org/licenses/by/4.0/>.

References

- Abdullah MMA, Kamarudin H, Bnhussain M, Khairul Nizar I, Rafiza AR, Zarina Y (2011) The relationship of NaOH Molarity, Na₂SiO₃/NaOH ratio, fly ash/alkaline activator ratio, and curing temperature to the strength of fly ash-based geopolymer. *AMR* 328–330:1475–1482. <https://doi.org/10.4028/www.scientific.net/AMR.328-330.1475>

- Ahmaruzzaman M (2010) A review on the utilization of fly ash. *Progress Energy Combust Sci* 36(3):327–363. <https://doi.org/10.1016/j.pecs.2009.11.003>
- Argiz C, Menéndez E, Moragues A, Sanjuán MA (2015) Fly ash characteristics of Spanish coal-fired power plants. *AFINIDAD* 572:269–277
- Bakharev T (2005) Geopolymeric materials prepared using Class F fly ash and elevated temperature curing. *Cement Concr Res* 35:1224–1232. <https://doi.org/10.1016/j.cemconres.2004.06.031>
- Cabral MR, Nakanishi EY, Fiorelli J (2017) Evaluation of the effect of accelerated carbonation in cement–bagasse panels after cycles of wetting and drying. *J Mater Civ Eng* 4017018:1–7. [https://doi.org/10.1061/\(ASCE\)MT.1943-5533.0001861](https://doi.org/10.1061/(ASCE)MT.1943-5533.0001861)
- Davison BH, Parks J, Davis MF, Donohoe BS (2013) Plant cell walls: basics of structure, chemistry, accessibility and the influence on conversion. In: Wyman CE (ed) *Aqueous pretreatment of plant biomass for biological and chemical conversion to fuels and chemicals*. Wiley, Chichester, pp 23–38
- de Izidoro JC, Fungaro DA, dos Santos FS, Wang S (2012) Characteristics of Brazilian coal fly ashes and their synthesized zeolites. *Fuel Process Technol* 97:38–44. <https://doi.org/10.1016/j.fuproc.2012.01.009>
- Duan P, Yan C, Zhou W, Luo W (2016) Fresh properties, mechanical strength and microstructure of fly ash geopolymer paste reinforced with sawdust. *Constr Build Mater* 111:600–661
- EN 494 (1994) *Fibre-cement profiled sheets and fittings for roofing—products specification and test methods*. European Committee for Standardization BSI—British Standard Institution London, UK
- Erdoğan K, Türker P (1998) Effects of fly ash particle size on strength of portland cement fly ash mortars. *Cement Concr Res* 28:1217–1222. [https://doi.org/10.1016/S0008-8846\(98\)00116-1](https://doi.org/10.1016/S0008-8846(98)00116-1)
- Ferraz JM, Menezzi CHD, Teixeira DE, Martins SA (2011) Effects of treatment of coir fiber and cement/fiber ratio on properties of cement-bonded composites. *BioResources* 6:3481–3492
- Ferreira C, Ribeiro A, Ottosen L (2003) Possible applications for municipal solid waste fly ash. *J Hazard Mater* 96:201–216
- Halas O, Benes L, Minar L (2011) Sawdust as a filler to alkali-activated fly-ash. In: *Annals of DAAAM and proceedings of the 22nd international DAAAM symposium*, pp 797–799
- Kielé A, Vaičiukynienė D, Tamošaitis G et al (2020) Wood shavings and alkali-activated slag bio-composite. *Eur J Wood Prod* 78:513–522. <https://doi.org/10.1007/s00107-020-01516-x>
- Kim H, Lee J-Y (2017) Effect of ash particle size on the compressive strength and thermal conductivity of geopolymer synthesized with alkali activated low calcium ground coal bottom ash. In: *2017 World of coal ash*. Lexington, KY
- Kumar B, Tike GK, Nanda PK (2007) Evaluation of properties of high-volume fly-ash concrete for pavements. *J Mater Civ Eng* 19:906–911
- Kumar S, Kumar R, Mehrotra SP (2010) Influence of granulated blast furnace slag on the reaction, structure and properties of fly ash based geopolymer. *J Mater Sci* 45:607–615. <https://doi.org/10.1007/s10853-009-3934-5>
- Lin Q, Zhou X, Dai G (2002) Effect of hydrothermal environment on moisture absorption and mechanical properties of wood flour-filled polypropylene composites. *J Appl Polym Sci* 85:2824–2832. <https://doi.org/10.1002/app.10844>
- Lorenz D, Erasmy N, Akil Y, Saake B (2016) A new method for the quantification of monosaccharides, uronic acids and oligosaccharides in partially hydrolyzed xylans by HPAEC-UV/VIS. *Carbohydr Polym* 140:181–187. <https://doi.org/10.1016/j.carbpol.2015.12.027>
- Mahzabin MS, Hamid R, Badaruzzaman WHW (2013) Evaluation of chemicals incorporated wood fiber cement matrix properties. *J Eng Sci Technol* 8:385–398
- Missengue RNM, Losch P, Sedres G, Musyoka NM, Fatoba OO, Louis B, Pale P, Petrik LF (2016) Transformation of South African coal fly ash into ZSM-5 zeolite and its application as an MTO catalyst. *C R Chim*. <https://doi.org/10.1016/j.crci.2016.04.012>
- Moslemi AA, Souza MR, Geimer R (1995) Accelerated ageing of cement-bonded particleboard. In: *Inorganic bonded wood and fiber materials*. Forest Products Society Spokane, 4:83–88
- Pelaez-Samaniego MR, Yadama V, Lowell E, Espinoza-Herrera R (2013) A review of wood thermal pretreatment to improve wood composite properties. *Wood Sci Technol* 47(6):1285–1319
- Pelaez-Samaniego MR, Yadama V, Garcia-Perez T, Lowell E, Amidon T (2014) Effect of hot water extracted hardwood and softwood chips on particleboard properties. *Holzforschung* 68(7):807–815
- RILEM (1984) *Testing methods for fiber reinforced cement-based composites*. Recheches sur les matériaux et les constructions Matériaux et Constructions, Paris, pp 441–456
- Rohde GM, Zwonok O, Chies F, Silva NIW (2006) Cinzas de carvão fóssil no Brasil—aspectos técnicos e ambientais. *CIENTEC*, Porto Alegre, p 202
- Rosas-Casarez C, Arredondo-Rea S, Cruz-Enríquez A, Corral-Higuera R, Pellegrini-Cervantes M, Gómez-Soberón J, Medina-Serna T (2018) Influence of size reduction of fly ash particles by grinding on the chemical properties of geopolymers. *Appl Sci* 8(365):1–12. <https://doi.org/10.3390/app8030365>
- Sarmin SN (2016) The influence of different wood aggregates on the properties of geopolymer composites. *KEM* 723:74–79. <https://doi.org/10.4028/www.scientific.net/KEM.723.74>
- Sarmin SN, Welling J, Krause A, Shalbfan A (2014) Investigating the possibility of geopolymer to produce inorganic-bonded wood composites for multifunctional construction material—a review. *BioResources* 9:7941–7950
- Sluiter A, Ruiz R, Scarlata C, Sluiter J, Templeton D (2008) Determination of extractives in biomass: laboratory analytical procedure (LAP). Technical Report NREL/TP-510-42619
- Sluiter JB, Ruiz RO, Scarlata CJ, Sluiter AD, Templeton DW (2010) Compositional analysis of lignocellulosic feedstocks. 1. Review and description of methods. *J Agric Food Chem* 58:9043–9053. <https://doi.org/10.1021/jf1008023>
- Sofi M, van Deventer JSJ, Mendis PA, Lukey GC (2007) Engineering properties of inorganic polymer concretes. *Cement Concr Res* 37:251–257. <https://doi.org/10.1016/j.cemconres.2006.10.008>
- TAPPI (2007) *Solvent extractives of wood and pulp (T204)*. Technical Association of the Pulp and Paper Industry, Atlanta, pp 7–10
- Teixeira RS, Tonoli GHD, Santos SF, Fiorelli J, Savastano H, Lahr FR (2012) Extruded cement based composites reinforced with sugar cane bagasse fibers. *KEM* 517:450–457. <https://doi.org/10.4028/www.scientific.net/KEM.517.450>
- Therasme O, Volk TA, Cabrera AM, Eisenbies MH, Amidon TE (2018) Hot water extraction improves the characteristics of willow and sugar maple biomass with different amount of bark. *Front Energy Res* 6(93):1–13. <https://doi.org/10.3389/fenrg.2018.00093>
- Thokchom S, Ghosh P, Ghosh S (2009) Effect of water absorption, porosity and sorptivity on durability of geopolymer mortars. *ARPN J Eng Appl Sci* 4:28–32
- Van Jaarsveld JGS, van Deventer JSJ, Lukey GC (2003) The characterization of source materials in fly ash-based geopolymers. *Mater Lett* 57:1272–1280. [https://doi.org/10.1016/S0167-577X\(02\)00971-0](https://doi.org/10.1016/S0167-577X(02)00971-0)
- Vickers L, van Riessen A, Rickard WDA (2015) *Fire-resistant geopolymers: Role of fibers and fillers to enhance thermal properties*. Springer, Singapore
- Wilson K, White DJB (1986) *The anatomy of wood: Its diversity and variability*. Stobart, London
- Yang K-H, Song J-K, Song K-I (2013) Assessment of CO₂ reduction of alkali-activated concrete. *J Clean Prod* 39:265–272. <https://doi.org/10.1016/j.jclepro.2012.08.001>

- Ye H, Zhang Y, Yu Z, Mu J (2018) Effects of cellulose, hemicellulose, and lignin on the morphology and mechanical properties of metakaolin-based geopolymer. *Constr Build Mater* 173:10–16. <https://doi.org/10.1016/j.conbuildmat.2018.04.028>
- Zanão M, Colodette JL, Oliveira RC, Almeida DP, Gomes FJB, Carvalho DM (2019) Evaluation of kraft-PS cooking for eucalypt and pine wood chip mixtures. *J Wood Chem Technol* 39:149–165. <https://doi.org/10.1080/02773813.2018.1533979>
- Ziegler D, Formia A, Tulliani J-M, Palmero P (2016) Environmentally-friendly dense and porous geopolymers using fly ash and rice husk

ash as raw materials. *Mater* 9(466):1–21. <https://doi.org/10.3390/ma9060466>

Publisher's Note Springer Nature remains neutral with regard to jurisdictional claims in published maps and institutional affiliations.

CHAPTER 3.2

Influence of wood pretreatment, hardwood and softwood extractives on the compressive behavior of fly ash-based geopolymer composite (**Submitted**)

Authors' contribution

	CD	EX	ED
Bright Asante	80%	65%	65%
Jörn Appelt	10%	20%	15%
Libo Yan	0%	5%	5%
Andreas Krause	10%	10%	15%

CD: Conceptual Design

EX: Conducting experiments

ED: Editing

Influence of wood pretreatment, hardwood and softwood extractives on the compressive behavior of fly ash-based geopolymer composite

Bright Asante^{a,b}, Jörn Appelt^c, Libo Yan^{b,d}, Andreas Krause^c

^a University of Hamburg, Institute of Wood Sciences, Leuschnerstrasse 91, 21031 Hamburg, Germany

^b Technische Universität Braunschweig, Department of Organic and Wood-Based Construction Materials, Hopfengarten 20, 38102 Braunschweig, Germany

^c Johann Heinrich von Thünen Institute; Federal Research Institute for Rural Areas, Forestry and Fisheries; Institute of Wood Research; Leuschnerstrasse 91, 21031 Hamburg, Germany

^d Fraunhofer Wilhelm-Klauditz-Institut WKI, Center for Light and Environmentally-Friendly Structures, Bienroder Weg 54E, Braunschweig 38108, Germany

Abstract

This paper investigated the specific compressive strength (specific strength) of fly ash-based geopolymer composites with four hardwood extractives and two softwood extractives, as well as specific wood extractives. Geopolymer paste was mixed with extractives before oven curing at 60 °C for 24 h. The hardened geopolymer paste was stored in a climate chamber (20 °C, 65% RH) for 7 days before finally testing. From the results, the specific strengths of geopolymers with hardwood extractives were not significantly affected. However, geopolymers containing pine extractives showed the most significant reduction in specific strength. Geopolymers with polyphenols (i.e. pycogenol, tannin, and tannic acid) and resin acid (i.e. abietic acid) did not show significant differences in the specific strengths. Generally, geopolymers containing fatty acids (i.e. linoleic and oleic acids) recorded the lowest specific strengths. Since all extractive compounds investigated in this study reduced the specific

strength of the geopolymer, the combined effect of these specific extractives could even be greater.

1.0 Introduction

Inorganic bonded wood composites (IBWC) are one of the major building and construction components. Examples of IBWC include ceramic-bonded, gypsum-bonded, magnesia-bonded and Portland cement-bonded wood composites. Common applications of IBWC include flooring, tiling, prefabricated housing, façade, ceiling, and exterior and partition walls. Wood plays a very important role in IBWC, acting either as an aggregate or reinforcing element serving as to reduce the densities of the products (Sarmin 2016), while also improving tensile strength, flexural strength, toughness and energy absorption capacities through bridging cracks (Shaikh 2013); the inorganic matrix binds the wood particles, providing mechanical strength, low permeability, good chemical resistance, and excellent fire resistance behavior (Bakharev 2005; Ryu et al. 2013; Shehab et al. 2016). Among the IBWC, Portland cement-bonded wood composites dominate the market share (Sarmin et al. 2014). Ordinary Portland cement (OPC) remains the main binding agent in these composites. It is an undisputed fact that the production of OPC continues to be one of the major contributors of CO₂ emissions. With the keen search to finding suitable replacements for this binder, recent researches have shown that geopolymer, an alkali activated cement, serves as a possible alternative (Zhao et al. 2007; Giancaspro et al. 2009; Giancaspro et al. 2010).

Wood is a natural composite comprising mainly of cellulose, lignin and hemicellulose as structural components and non-structural polysaccharides and other extractives. Wood shows different characteristics, which differ in a wide range among species, and even between the same species (Stark et al. 2010). Wood is broadly categorized into softwood and hardwood. In

general, softwoods have a simpler basic structure with relatively less variation in structure compared with those of hardwoods.

Among the structural components of wood, Ye et al. (2018) found that a lower content of cellulose, hemicellulose, and lignin (i.e. 5 wt. %) increases the flexural and compressive strengths of pure metakaolin-based geopolymer composites. Furthermore, the authors observed that both hemicellulose and lignin reduced the composites' compressive and flexural strengths. Alkaline degradation of hemicellulose lowered the degree of geopolymerization (Ye et al. 2018). This drawback asks for different pretreatments and surface modification of wood before utilizing it in high alkaline inorganic matrices. Different pretreatment and modification methods based on alkaline hydrolysis, extraction and retention of sugars and hemicelluloses have been applied to minimize inhibition problems (Zhengtian and Moslemi 1985; Moslemi et al. 1983; Lee and Short 1989). Alkaline hydrolysis degrades hemicelluloses and sugars into non-inhibitory substances, while aqueous extraction removes inhibitory water-soluble substances (Alberto et al. 2000). Retention treatment seals the inhibitory substances in the wood by forming a thin coating layer around the wood preventing the release of the inhibitory substances (Quiroga et al. 2016).

Despite the fact that wood reduces the density and improves on the strength properties of IBWC, their utilization in high alkaline environments causes leaching out of non-structural polysaccharides/low molecular weight carbohydrates, extractives and some structural components like hemicellulose. The kind and amount of these extractives differ by species and the portion of the tree (i.e. sapwood or heartwood), so they may have different inhibitory effects on setting, strength and geopolymerization process. Jorge et al. (2004) established, that the properties of inorganic bonded wood composites are influenced by the addition of wood as

well as the binder type. In the study of the influence of hot water wood pretreatment and fly ash particle size on the performance of geopolymer wood composites (GWC), Asante et al. (2021) determined that forming a GWC with *Eucalypt grandis* wood produced better mechanical and physical properties than those made with *Pinus taeda*. The authors recorded a 3 and 27 % increase in specific strengths of the Eucalypt-based and pine-based GWCs respectively after hot water washing of the wood. This clearly indicates there were some wood extractives hindering the geopolymerization or causing the incompatibility between the wood and the geopolymer. The same authors concluded that the lower specific strength and physical properties of the GWC from pine wood was as a result of the poor incompatibility between the pine and the geopolymer matrix. However, the research was limited to one softwood and one hardwood and as to what group or type of extractives might be causing this incompatibility. Regardless, there is little or no established research about the influence of these inhibitory extractive substances on the properties of geopolymer composites.

The understanding of how extractives from various hardwood and softwood species affect the properties of GWC will serve as the basis for better preparation of these composites, as well as a diverse application of environmentally friendly building materials. Using a fly ash-based geopolymer, extractives from four hardwood species and two softwood species were tested in order to understand how wood extractives affect the specific compressive strength (specific strength) of a geopolymer. Additionally, the effects of sapwood and heartwood extractives as well as specific extractives on the specific strength of fly ash geopolymer were studied. Lastly, the influence of the pretreating of sapwood and heartwood with NaOH on specific strength was also considered.

2. Materials and Methods

2.1 Materials

Class F fly ash (i.e., mass contents of $\text{SiO}_2 + \text{Al}_2\text{O}_3 + \text{Fe}_2\text{O}_3 \geq 70\%$) was obtained from the GK Kiel GmbH power plant in Kiel, Germany. The chemical oxide compositions of the fly ash as detected by X-ray fluorescence (XRF) are shown in Table 3.2.1. Betol 50 T (Na_2SiO_3) was purchased from Woellner, Germany and NaOH (analytical grade) was purchased from VWR, Germany. Betol 50 T and NaOH were used as received to produce the activator solution. Pycogenol, tannic acid, linoleic acid, oleic acid and abietic acid (Sigma Aldrich, Germany) and condensed tannin (from Natural Resource Institute Finland) were used. For the study, four hardwood species (*Eucalypt grandis*, *Eucalypt camaldulensis*, Port Jackson, and Black wattle) and two softwood species (spruce and pine) were used. Fig. 3.2.1 shows the morphology and size of wood particle used for extraction.

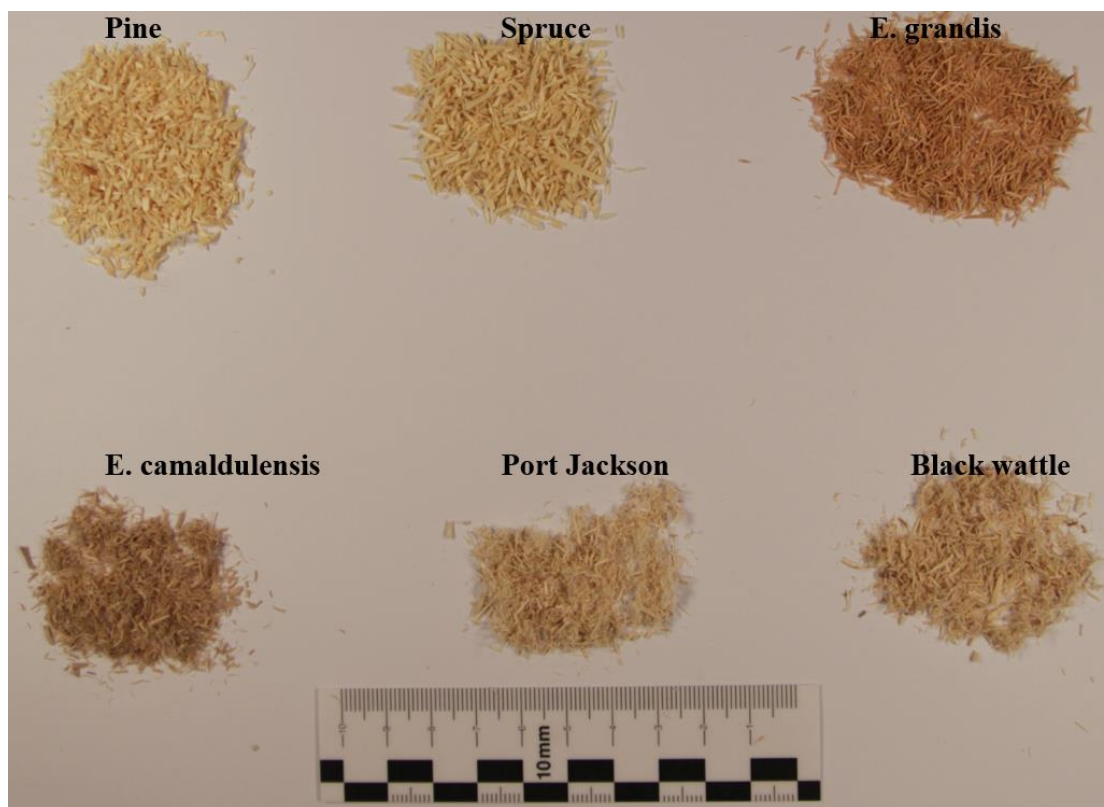


Fig. 3.2.1. The morphology of wood particle used for extraction of wood extractives

Table 3.2.1. Chemical composition of fly ash in weight percentage share (%) by XRF analysis

Component	Al ₂ O ₃	SiO ₂	SO ₃	K ₂ O	Na ₂ O	CaO	TiO ₂	MgO	Fe ₂ O ₃	P ₂ O ₅	LOI*
Share (%)	20.53	54.18	0.01	1.51	0.51	3.36	0.84	1.50	6.31	0.66	4.18

Loss on ignition (LOI*) at 1000 °C.

2.2 Extractives preparation

To study the influence of hardwood and softwood extractives on the strength properties of a geopolymer, wood particles (4 hardwood and 2 softwood species) were mixed with 1% NaOH solution (Table 3.2.2). After 20 min of mixing in the 1% NaOH solution, the wood particle was filtrated to separate the liquid and solid phases. The mass concentration of extractives (i.e. liquid) was measured for each extractive by drying in the oven at 60 °C for 36 h. The extractive was then used to study its effect on specific compressive strength of a pure fly ash geopolymer.

Table 3.2.2. Extraction method

Mass conc. of NaOH (%)	Vol. NaOH (ml)	Mass wood (g)	Contact Time (mins)
1	1000	100	20

2.3 Sample preparation

2.3.1 Geopolymer with softwood and hardwood extractives

The alkaline activator solution for geopolymer was prepared according to the method described by Asante et al. (2022) using Betol 50T (i.e. Na₂SiO₃) and 10 M NaOH in a weight ratio of 2.5:1. The solution was allowed to cool to ambient conditions prior to use. Fig. 3.2.2 shows the manufacturing process for the composites. Fly ash was mixed with the activator solution in a mass ratio of 2:1 for 5 min. Finally, 3% of the extractive solution (i.e. based on fly ash weight)

was added to the mixture for 5 min (Table 3.2.3). The mixture was cast in a cylindrical mold: 50*100 mm² and cured at 60 °C for 24 h. To avoid rapid moisture loss leading to cracks, samples were kept in low density polyethylene plastic before oven curing. The oven-cured samples were kept in the climate chamber (20 °C, 65% RH) for 7 days before compressive strength tests were carried out.

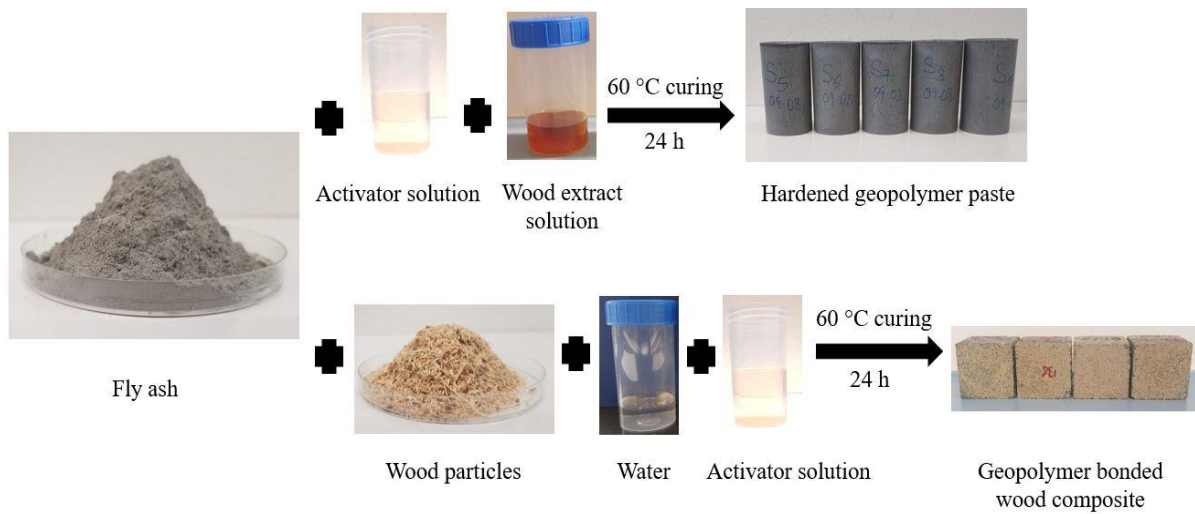


Fig. 3.2.2. Manufacturing process of hardened geopolymer paste and geopolymer bonded wood composite.

Table 3.2.3. The mix design of fly ash geopolymer with wood extractives

	Fly ash: Activator	Na ₂ SiO ₃ : NaOH (Activator)	% Extract
Control	2: 1	2.5: 1	0
Samples with Extract	2: 1	2.5: 1	3

*For the control sample, 3% by mass of fly ash of the NaOH solution used for the extraction was added.

2.3.2 Geopolymer bonded wood composites

To study the influence of the portion of pine wood pretreatment on the properties of a fly ash geopolymer, sapwood and heartwood particles were treated as shown in Table 3.2.1. After 20 mins of mixing in the 1% NaOH solution, the wood particle was filtrated to separate liquid and solid phases. The sapwood and heartwood extractives, collected separately, were used in geopolymer preparation according to Table 3.2.3. The solid particles were dispersed in 2250 mL distilled water (i.e. water: wood particles), before finally washing with 1000 mL distilled water. Finally, wood particles were dried in an oven at 60°C for 36 h and later kept in the climate chamber (20 °C, 65% RH) until the moisture content was, after 7 days, at 10-12%.

The geopolymer wood composite was prepared in accordance with Table 3.2.4 (see Fig. 3.2.2). Fly ash was first mixed with wood (dry mass) for 3 min; water was added and then mixed for 3 min and finally, the mixture was activated for 4 min with the alkaline activator solution. The activated mixture was cast in 50 mm³ molds and cured at 60 °C for 24 h. To avoid rapid moisture loss leading to cracks, samples were sealed in plastic before oven-curing. The oven-cured samples were kept in the climate chamber (20 °C, 65% RH) for 7 days, compressive strength tests being carried out on the 7th day.

Table 3.2.4. Preparation of geopolymer wood composite

Proportion	Fly Ash: activator	Fly ash: wood (dry mass)	Fly ash: additional water
Mass ratio	2:1	4:1	5.3:1

2.3.3 Geopolymer with softwood specific extractives

Pycogenol and condensed tannin were dissolved in water to form a concentration of 0.12%. More details about the condensed tannins can be found in the previous study (Asante et al.

2020). Then, 5 g of abietic and oleic acids were dissolved separately in 20 ml of ethanol, after which 20 ml of 1% NaOH solution was added prior to adding to the geopolymer mortar during sample preparation. 5 g of liquid linoelic acid was used as received, 35 ml of 1% NaOH solution being added hereafter.-Next, 5 g of tannic acid was dissolved in 40 ml of 1% NaOH solution. (NB: To make easy comparisons to control samples, 1% NaOH solution was used for dissolving extract or added to the geopolymer paste after extract addition to keep sodium (Na) ions as close to that of the control samples as possible). The geopolymer paste samples were all prepared according to Table 3.2.3.

2.4 Test conducted

2.4.1 Fourier Transform Infrared Spectroscopy (FTIR)

The FTIR spectra of the untreated and treated pine wood (i.e. sapwood and heartwood) samples were recorded by a Vertex 70 powder FTIR spectrometer equipped with a diamond ATR from (Bruker Optics, Germany) in the range of 4000–500 cm^{-1} .

2.4.2 Analysis of pine sapwood and heartwood extracts

Aliquots (50 ml ea.) of the alkaline extractives of pine sap- and heartwood were acidified with o-phosphoric acid (VWR, purity 85 %) to a pH-value of 7 and extracted with dichloromethane (DCM, Th. Geyer) in a separation funnel by shaking out. The extraction of acidified aliquot was carried out at least three times and the organic phase was combined afterwards. A subsequential extraction stage starts with an additional acidifying step to a pH-value of 2 and extraction as described. After combining the sub-fractions of each extraction step, DCM was removed with a rotary evaporator (IKA RV 10 basic) at atmospheric pressure and a water bath temperature of 45°C. The extractives were removed to a weight flask and weighed out after removal of the residual DCM-phase. Two fractions called “pH 7” and “pH 2” were produced

by liquid-liquid-extraction. During the DCM-extraction, some of the extractive parts sediments due the acidic conditions of the solution. Therefore, a further aliquot (40 ml) of each alkaline extractive sample was precipitated in cold water (1:10, V:V) dropwise and filtered with a cellulose filter. Before weighing out, the residues were dried to mass constancy in a desiccator over silica gel and phosphorus pentoxide subsequently.

The dried extractives were prepared for GC-MS/FID analysis by dissolution in an acetone solution with the internal standard fluoranthene ($\beta=200.06 \mu\text{g/ml}$). The solutions with a concentration of 10 mg/ml DCM-extracts were filtered with a syringe filter (cellulose, $0.45\mu\text{m}$) subsequently. GC/MS-FID analyses (Agilent 6890; Column: VF-1701 (60 m, 0,25 mm ID, $0,25 \mu\text{m}$ Film); 2.0 ml/min He; 45°C , 4 min, 3 K/min, 280°C , 20 min; Split 15:1; FID 280°C , 40 ml/min H_2 , 450 ml/min synth. Air; Recording: 20 Hz; MSD: Agilent 5975B, MSD-Transfer: 280°C , mass range 19 - 550 m/z) were conducted for characterization of the pine wood extractives. Besides the standard characterization of the composition, additional measurements were done for more detailed insights into higher molecular structures which are not detectable by the described characterization. For this purpose, an online derivatization with tetramethylammonium hydroxide (TMAH) on DCM extracts (pH-value of 2) was carried out on a Py-GC/MS-FID system. 10 μl of DCM extracts were weighed into a small pyrolysis cup and 20 μl TMAH solution (10 wt%) was added. The GC/MS-FID measurements of derivatized samples were conducted under the following parameters: Agilent 6890; Column: VF-5ms (60 m, 0,25 mm ID, $0,25 \mu\text{m}$ Film); 1.9 ml/min He; 45°C , 4 min, 3 K/min, 325°C , 20 min; Split 15:1; FID 350°C , 40 ml/min H_2 , 450 ml/min synth. Air; Recording: 20 Hz; MSD: Agilent 5975B, MSD-Transfer: 350°C , mass range 20 - 550 m/z). Quantification of the GC/MS-FID results were carried out using the relative area of the compounds relating the area of the internal

standard for standard measurements. The derivatized samples were evaluated by using the ratio of substance area to total area.

2.4.3 Specific compressive strength testing

The compressive strength of 7 day aged cylindrical samples ($50 \times 100 \text{ mm}^2$) was measured using a hydraulic universal testing machine (UTM) by MTS Systems Corporation (Eden Prairie, Minnesota, US). The MTS UTM was equipped with a Zwick model 1485 control panel (ZwickRoell GmbH & Co. KG, Ulm, Germany). The samples were compressed with a load cell capacity of 250 kN and with a crosshead speed rate of 1 mm/min. The compressive strength was calculated by dividing the maximum force (N) by the cross-sectional area (mm^2) of the sample. The specific strength was calculated by dividing the compressive strength by the density of the geopolymer composite. The average value of five samples was reported for each group.

2.5 Statistical analysis

The statistical analysis was performed using Origin Pro software. An analysis of variance (ANOVA) was conducted to identify differences between the samples' specific compressive strength. Comparisons of means were performed using the Fisher LSD at 5% significance level. The values presented in this study are all means and the error bars represent standard deviations. Means with same letters are not significantly different; $p > 0.05$.

3. Results and Discussion

3.1 Yield of extractives

The yield of all extractives is presented in Table 3.2.5. The yield ranges from 1.54 – 1.96%. Overall, B. wattle (more details of sample code are given in Table 3.2.5) had the highest mass

concentration of extractives with *E. grandis* recording the lowest. The percentage yield of extracts (i.e. dry matter content) of the pine sapwood was slightly lower than that from the heartwood. This comes as no surprise as the sapwood plays the role of sap conduction, storage of photosynthate and synthesis of extractives, the heartwood's function being long-term storage of the extractives in living trees (Rowell 2013). In addition, heartwood is more soluble than sapwood, which suggests that a greater amount of substance can be leached out during the extraction process (Cabangon et al. 2000).

Table 3.2.5. Dry matter content (%) of extractives.

Wood species	Code	Yield (%)
<i>Eucalyt grandis</i>	E. grandis	1.54
<i>Eucalyt camaldulensis</i>	E. camal	1.58
Port Jackson	P. jack.	1.80
Black wattle	B. wattle	1.96
Norway spruce	Spruce	1.73
<i>Pinus sylvestris</i>	Pine	1.81
Pine Sapwood	Sap	1.61
Pine Heartwood	Heart	1.82

3.2 Characterization of pine sapwood and heartwood particles before and after NaOH pretreatment

3.2.1 Morphology

The morphology and appearance of the pine wood particles before and after 1% NaOH treatment are presented in Fig. 3.2.3. Here it can be seen, that the major difference arose from the color change of the wood particles, which changed from pale yellowish to light brown for

the sapwood and from yellowish to dark brown for the heartwood. It is well known that treatment with aqueous NaOH solution removes wood extracts. The color change might be as a result of the removal of extracts and the drying of particles after treatment as a similar observation which was made by Asante et al. (2021).

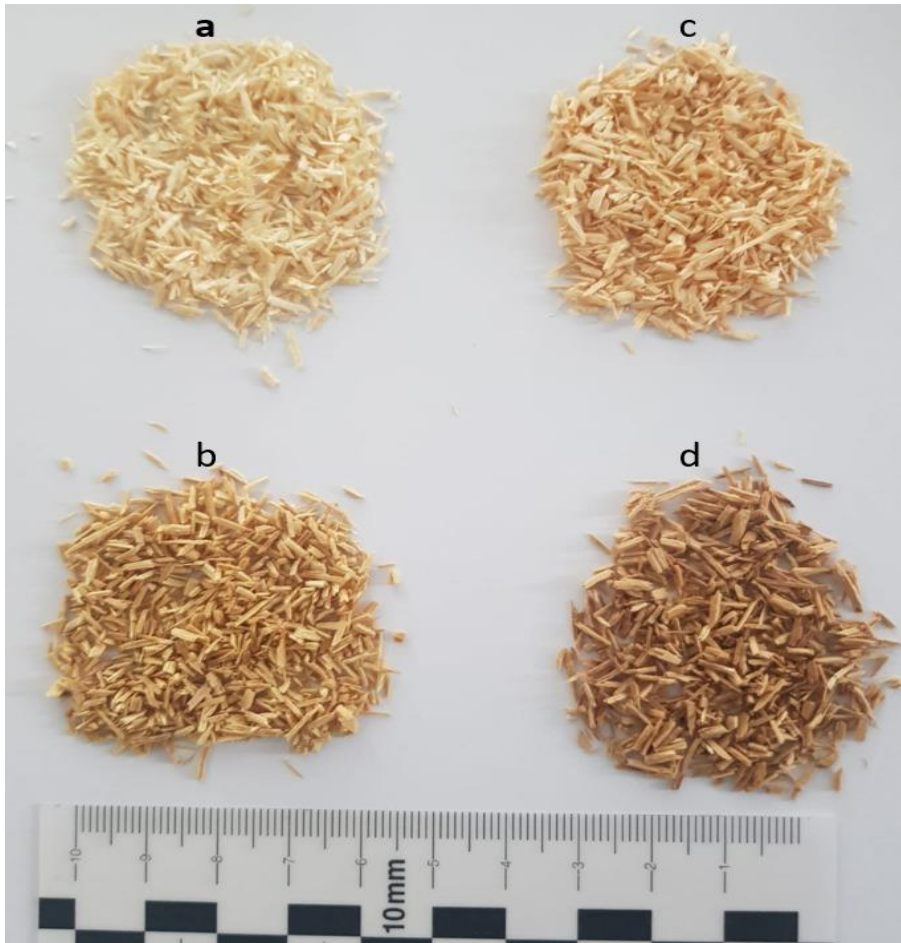


Fig. 3.2.3. Morphology of pine wood particles before and after NaOH treatment: **a** untreated sapwood; **b** treated sapwood; **c** untreated heartwood; **d** treated heartwood

3.2.2 Fourier Transform Infrared Spectroscopy (FTIR)

The structural differences in pine sapwood and heartwood before and after NaOH treatment can be evaluated by Fourier transform infrared spectroscopy (Bhatia and Johri 2016). Fig. 3.2.4 shows the FTIR spectrum for explicating the chemical changes which occur after treating

the pine wood samples with NaOH. In the spectra, the transmittance around 2910-2928 and 1369-1371 cm^{-1} are attributed to the C–H stretching and bending vibration in cellulose (Zhong et al. 2010). The transmittance band of the C–O stretch vibrations in cellulose and hemicelluloses are around 1029- 1033 cm^{-1} , which is the highest intensity band (Barman et al. 2020). Furthermore, the vibrations around 1701 and 1733 cm^{-1} in both untreated sapwood and heartwood respectively, is attributed to the C=O stretching of methyl ester and carboxylic acid (Zhong et al. 2010; Barman et al. 2020). The absence of this spectrum in both the treated sapwood and heartwood represent the major difference in the Fig. 3.2.4. Similar observations were made by Zhong et al. (2010) and Barman et al. (2020) after treating Fir and pine wood respectively with NaOH solution. According to Zhong et al. (2010), this indicated the removal of pectin, waxy and natural oils covering the external surface of the cell wall by the alkali treatment.

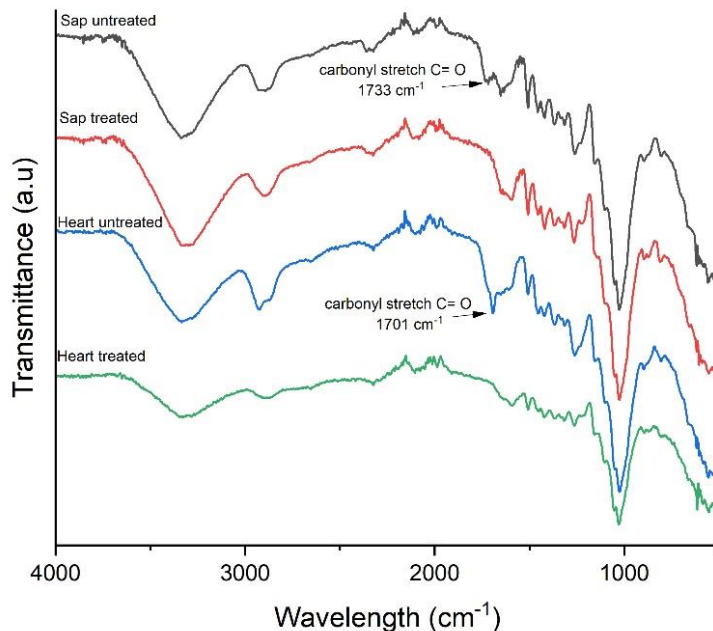


Fig. 3.2.4. FTIR of untreated and NaOH treated pine sapwood and heartwood.

3.3 Effects of pretreatment and portion of pine wood used in geopolymer wood composite.

Since pinewood was mostly affected negatively [see section 3.5], the sapwood and heartwood were used for further analysis. The effect of the portion (i.e. sapwood or heartwood) of pine wood used in geopolymer wood composite production is shown in Fig. 3.2.5. Due to the higher solubility of heartwood vs. sapwood suggesting that a greater amount of substance could be leached out (Cabangon et al. 2000) to disturb the geopolymerization, it was expected that the specific strength of these two composites would be different. This being said, the results in Fig. 3.2.5 show that the specific strength of fly ash based GWCs in both untreated pine sapwood and heartwood was not significantly different.

However, with the 1% NaOH pretreatment, a significant difference was observed between the GWCs from the sapwood and heartwood. The pretreatment of the sapwood and heartwood led to an increase in the specific strengths of both GWCs. Due to their ability to remove extractives and inhibitory contaminants from wood, NaOH increases surface roughness and increases surface wettability (Redzuan et al. 2019). As a result of the NaOH treatment, the wood surface area may have been increased for bonding with the geopolymer, due to the roughness being increased (Redzuan et al. 2019) and therefore the specific strength increasing. Be that as it may, the treatment led to a 21% and 10% increase in the specific strength of GWCs with sapwood and heartwood respectively. This indicates the NaOH treatment was more pronounced in the pine sapwood than the heartwood. In comparing the surface roughness of sapwood and heartwood in *Acacia mangium* after NaOH treatment, Redzuan et al. (2019) observed that the surface roughness of sapwood increased more than that of heartwood (as the cells of sapwood are more permeable to liquid than the heartwood). The authors concluded that the NaOH treatment was more effective for the sapwood than the heartwood. This might have led to the

significant difference between the specific strength of the GWCs with sapwood and the heartwood in this present work.

In contrast to these results, Sarmin et al. (2020) demonstrated with a NaOH treated *Picea abies* veneer, that the debonding strength between the veneer embedded in a blend of fly ash/metakaolin geopolymer was reduced compared to the untreated one. It is possible that the strength of sapwood and heartwood treated samples may increase not only due to the removal of extracts, but also due to the removal of hemicelluloses, as Ye et al. (2018) found that hemicelluloses act as one of the major components of wood that hinders geopolymerization. The increase in strength suggests that washing wood with NaOH solution is one possible way of removing inhibitory substances in wood before use in a GWC. However, this should be further confirmed in the future work.

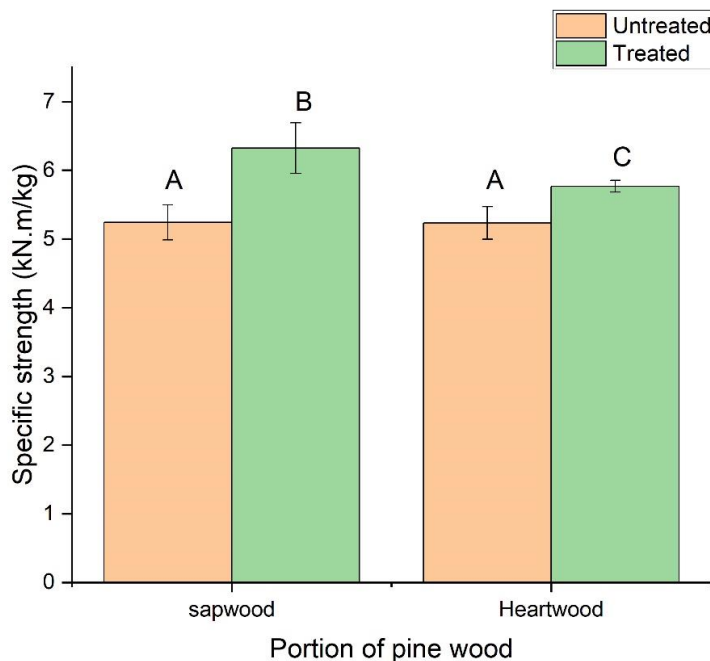


Fig. 3.2.5. Specific compressive strength of fly ash geopolymer wood composite with treated and untreated pine sapwood and heartwood

3.4 Influence of pine sapwood and heartwood extractives on the specific strength

The effect of pine sapwood and hardwood extractives on the pure fly ash-based geopolymer is shown in Fig. 3.2.6. The specific strength of the control sample was significantly different from the geopolymers with pine extractives. This indicates that there are pine specific extractives which hinder the geopolymerization process thereby reducing the strength. However, among the geopolymers with extracts, no significant difference was observed between the specific strengths of the ones containing sapwood and heartwood extractives. According to Cabangon et al. (2000), heartwood has higher solubility than sapwood suggesting larger amounts of substance that could be leached out during the extraction process. Despite the fact that the diversity of compounds is higher in sapwood extracts than in hardwood extracts, some similar compounds were extracted from both the sapwood and the heartwood [section 3.6,], although the amount (i.e. the yield) of the extracts was different (see Table 5). The similar nature of the compounds extracted might have resulted in the strength behaviors of the geopolymer with sapwood extract and the heartwood extract. It is likely that one or a combination of these extracts might have caused the reduction in the specific strength of the geopolymer.

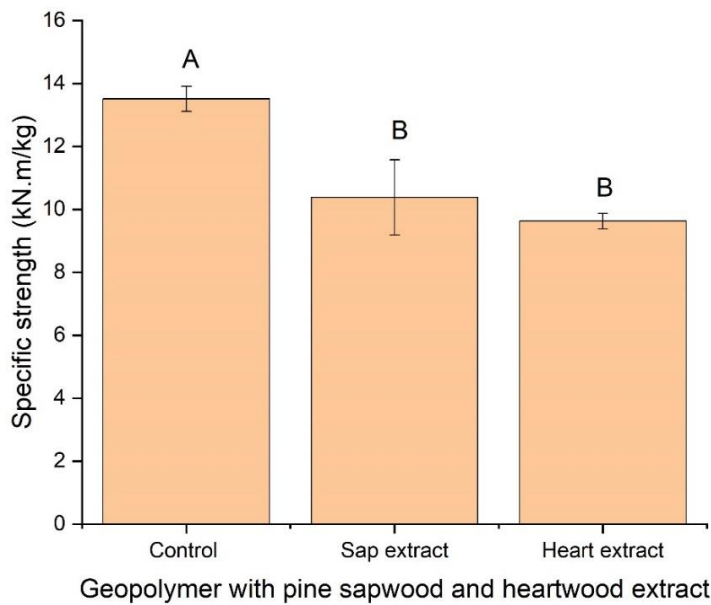


Fig. 3.2.6. Specific compressive strength of pure fly ash geopolymer with pine sapwood and heartwood extracts

3.5 Effects of softwood and hardwood extract on the specific strength of fly ash geopolymer

Fig. 3.2.7 shows the specific strength of a geopolymer with different hardwood and softwood extractives. Specific strength values of 11.11 kN.m/kg and 11.87 kN.m/kg were recorded for geopolymers with pine and spruce softwood respectively, while a range of 12.69 – 13.77 kN.m/kg was recorded for geopolymers with hardwood extractives. In comparison with the control (13.51 kN.m/kg), it can be seen that the specific strength of the geopolymers with hardwood extracts was not significantly affected. However, the specific strength of geopolymers with softwood extractives was significantly affected; with geopolymers containing pine extractive recording the least strength. Similarly, Asante et al. (2021) found that a geopolymer wood composite made of eucalypt wood, would have a higher specific compression strength than one made of pine wood. The same authors concluded that there

might be pine specific extractives hindering the geopolymerization process and therefore causing a reduction in strength.

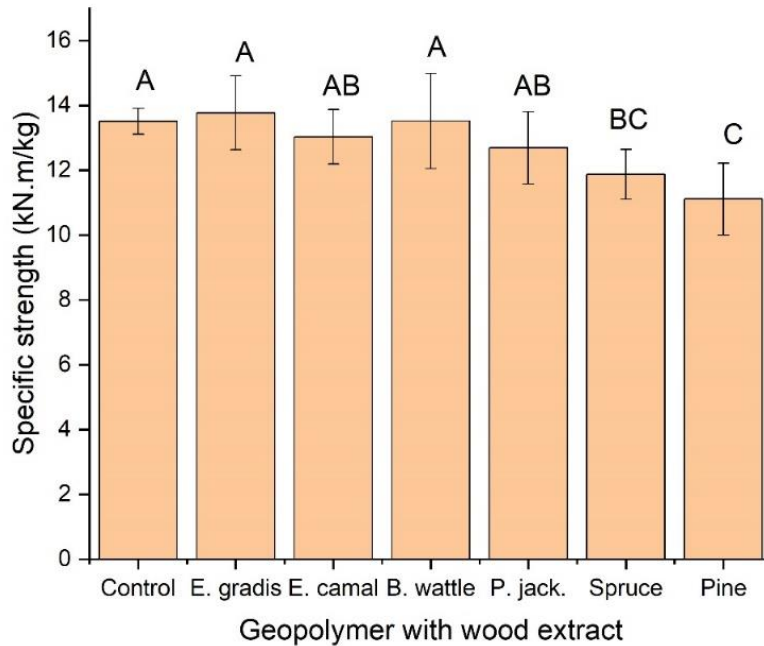


Fig. 3.2.7. Specific compressive strength of pure fly ash geopolymer with hardwood and softwood extractives (Means with same letters are not significantly different; $p > 0.05$).

3.6 GC/MS-FID analysis of pine sapwood and heartwood extractives extracted with NaOH

From the aliquots (50 ml) of alkaline extractive solutions, a portion of DCM-soluble compounds could be extracted in various amounts depending on the pH-value during liquid-liquid extraction. The heartwood sample shows a higher amount of DCM-soluble with approx. 0.6 g considering the aliquot volume. Thereof, 47 % of the DCM-extract from the heartwood sample is attributable to the first extraction step at pH-value 7, while 52 % is accounted to pH-value 2. In the case of sapwood, the amounts of each pH-value step were allocated in reverse

order (pH-value 7: 57 %; pH-value 2: 43 %). Besides the DCM-soluble fractions, solid non-DCM-soluble fractions were found due precipitation from the liquid phase. From these aliquots only small amounts of probably lignin-derived compounds were found (heartwood: 0.1 g, sapwood: 0.005 g).

Table 3.2.6. Semi-quantification of DCM-extractable compounds of alkaline extractives from pine sap- and heartwood at pH-value 7 and 2 in relation to internal standard (IS) area

Order of retention	Compound	relative Area			
		Heartwood		Sapwood	
		pH 2	pH 7	pH 2	pH 7
1	Butanol, 2-methyl-2-	0.032	0.032	0.008	0.014
2	Butanone, 3-methyl-2-	0.034	0.015		
3	1,3-Dioxolane, 2,2,4-trimethyl-		0.005		0.005
4	Acetic acid	0.041		0.023	
5	Isobutyl methyl ketone	0.011	0.011	0.013	0.011
6	Pentanol, 1-				0.015
7	α -Pinene	0.023	0.021		
8	2-Heptanone				0.040
9	3-Carene	0.024	0.023		
10	Hexanoic acid			0.532	
11	Fenchol		0.030		
12	Pinocarveol				0.029
13	cis-Verbenol				0.099
14	unknown Terpene		0.026		

15	(-)-4-Terpineol	0.015	0.082		0.029
16	endo-Borneol	0.015	0.094		0.029
17	similar to α -Terpineol		0.024		
18	α -Terpineol	0.047	0.304		0.027
19	p-Cymen-8-ol		0.054		0.182
20	similar to p-Cymen-8-ol		0.054		0.182
21	cis-Carveol				0.043
22	Guaiacol, 4-vinyl-	0.042			
23	α -Muurolene	0.018	0.012		
24	β -Cadinene	0.010			
25	α -Calacorene	0.006			
26	Vanillin	0.015	0.158		0.705
27	α -Campholenaldehyde				0.055
28	Ethanone, 1-(4-hydroxy-3-methoxyphenyl)				0.027
29	Pimara-8(14),15-diene	0.010			
30	Isobutyl phthalate (softener)	0.010			0.018
31	13-Epi-Manoyl oxide	0.005			
32	Fluoranthene (IS)	1.000	1.000	1.000	1.000
33	Pimaral	0.123	0.095		0.034
34	Naphthalene, 1-phenyl- (impurity IS)	0.013	0.013	0.012	0.014
35	Isopimara-7,15-dienal	0.053	0.040		0.017
36	Pimarol (spectrum not confirmed)	0.074	0.055		0.125
37	Dehydroabietal	0.016	0.012		0.012
38	trans-3,5-Dimethoxystilbene	0.027	0.022		

39	Dehydroabietic acid methyl ester	0.037	0.028	
	Methyl dehydroabietate			0.014
40	Abietal (spectrum not confirmed)	0.019	0.013	
41	Methyl abietate	0.012		
42	Dehydro-4-epiabietol			0.017
43	4'-Methoxy-2-hydroxystilbene	0.684	1.309	

Table 3.2.6 shows the composition of the DCM-soluble extracts from the alkaline extractives corresponding to their pH-value. It can be seen, that the alkaline extractives consist of terpenoid compounds like pinene, carene as monomeric terpenes, terpineol and borneol as representatives of alcohols of monocyclic and bicyclic terpenes respectively. Aside from this, nonspecific low molecular weight substances like alcohols, ketones and acids (only in pH=2 samples) also occur in each sample. Furthermore, typical compounds for pine wood extractives like salts and esters of abietic acid and stilbenes, also occur predominantly in the heartwood samples, whereas high amounts of vanillin, p-Cymen-8-ol and pimarol were found at the acidic fraction of sapwood extractives.

Table 3.2.7. Semi-quantification of DCM extractable compounds of alkaline extractives from pine sap- and heartwood at pH-value 2 after derivatization with TMAH

No.	Compound	relative Area (%)	
		Sapwood	Heartwood
1	Methyl dehydroabietate	26.0	33.6
2	Methyl sandaracopimarate	4.5	19.7
3	Methyl abietate		15.7

4	trans-3,5-Dimethoxystilbene		9.0
5	Nonanedioic acid dimethyl ester	10.3	
6	7-Oxodehydroabietic acid methyl ester	7.7	2.9
7	x-Octadecenoic acid, methyl ester	6.7	
8	Cyclotrisiloxane, hexamethyl-	4.2	0.2
9	Cyclotetrasiloxane, octamethyl-	3.9	0.3
10	Methyl 7-methoxyabieta-6,9(11),8(14),12-tetraen-18-oate	3.7	3.7
11	Nonanoic acid, methyl ester	3.7	0.3
12	Hexanoic acid, methyl ester	3.6	0.7
13	Hexadecanoic acid, methyl ester	3.4	2.8
14	Octanoic acid, methyl ester	2.3	0.2
15	Cyclopentasiloxane, decamethyl-	1.9	0.4
16	Methyl abieta-8,13(15)-dien-18-oate		1.8
17	Hexadecanoic acid, 14-methyl-, methyl ester	1.8	0.4
18	Stigmasta-3,5-dien-7-one	1.7	
19	similar to Methyl sandaracopimarate		1.7
20	Benzaldehyde, 3,4-dimethoxy-	1.7	0.4
21	Hexanal	1.3	
22	Octanedioic acid, dimethyl ester	1.1	
23	Decanedioic acid, dimethyl ester	1.0	
24	Octadecanoic acid, methyl ester	1.0	0.7
25	Cyclohexasiloxane, dodecamethyl-	1.0	0.6
26	Heptanoic acid, methyl ester	0.9	
27	Benzoic acid, 3,4-dimethoxy-, methyl ester	0.9	0.2
28	Undecanedioic acid, dimethyl ester	0.8	

29	Cycloheptasiloxane, tetradecamethyl-	0.7	0.2
30	Cyclooctasiloxane, hexadecamethyl-	0.6	
31	Decanoic acid, 9-oxo-, methyl ester	0.5	
32	Decanoic acid, methyl ester	0.5	0.2
33	Tetradecanoic acid, methyl ester	0.5	0.2
34	Cyclononasiloxane, octadecamethyl-	0.4	
35	Benzoic acid, methyl ester		0.4
36	Siloxane compound	0.3	
37	Heptadecanoic acid, methyl ester	0.3	
38	Cyclodecasiloxane, eicosamethyl-	0.3	
39	alpha-Terpineol		0.3
40	x,y-Octadecadienoic acid methyl ester	0.3	
41	Acetophenone, 3,4-dimethoxy-	0.2	
42	Tetradecanoic acid, x-methyl-, methyl ester	0.2	

Table 3.2.7 shows the distribution of higher molecular compounds, which are detectable due derivatization of the alkaline pine wood extractives. For this method, mainly aliphatic carboxylic acids can be detected by forming the corresponding methyl esters. Thereby a typical distribution between the composition of the heartwood and the sapwood extractives can be seen. The GC-detectable compounds of sapwood extractives consist of up to 39 wt% of saturated and unsaturated fatty acids while terpenoids and resin acids accounts for an amount of 26 wt%; in the extractives from heartwood, terpenoids and resin acids occur predominantly, with an amount of up to 51 wt% of the GC-detectable substances. Meanwhile aliphatic carboxylic acids represent only a small amount (up to 5 wt%) of the extractives. The diversity of compounds is higher in sapwood samples than in hardwood samples. The five compounds

with the highest amounts represent, in the case of heartwood, up to 78 wt% of the GC-detectable compounds, these compounds representing only 41 wt% in the sapwood samples.

3.7 Effect of softwood specific extracts on the specific compressive strength of pure fly ash geopolymer

It is a well-established fact that in high alkaline environments, non-structural wood compounds such as polyphenolics (tannins), dyes, simple sugars, resin and fatty acids are dissolved from wood (Doczekalska and Zborowska 2010; Huang and Yan 2013). One of the major differences in extract composition between the sapwood and heartwood of pine is their proportion of fatty and resin acids (section 3.6). The sapwood contains more fatty acids while the heartwood contains more resin acids as was also observed by Back and Allen (2000). For these reasons, in order to understand the influence of specific extractives on the strength of a fly ash based geopolymer, the authors of the present work considered two fatty acids (linoleic and oleic acids), one resin acid (i.e. abietic acid) and three polyphenols (i.e. condensed tannins, pycogenol and tannic acids).

A lower specific strength was recorded for all the tested specific extractives when compared to the control group (Fig. 3.2.8). There was no significant difference between geopolymer composites containing polyphenols (i.e. pycogenol, tannin and tannic acid) and resin acids (abietic acid). Generally, geopolymers containing linoleic and oleic acids (fatty acids) recorded the lowest specific strengths. Although Portland cement differs from a geopolymer in some ways, similar observations were made by Tugrul Albayrak et al. (2005), who found that oleic acid and sunflower oil (containing oleic and linoleic acids) decrease the compressive strength of concrete.

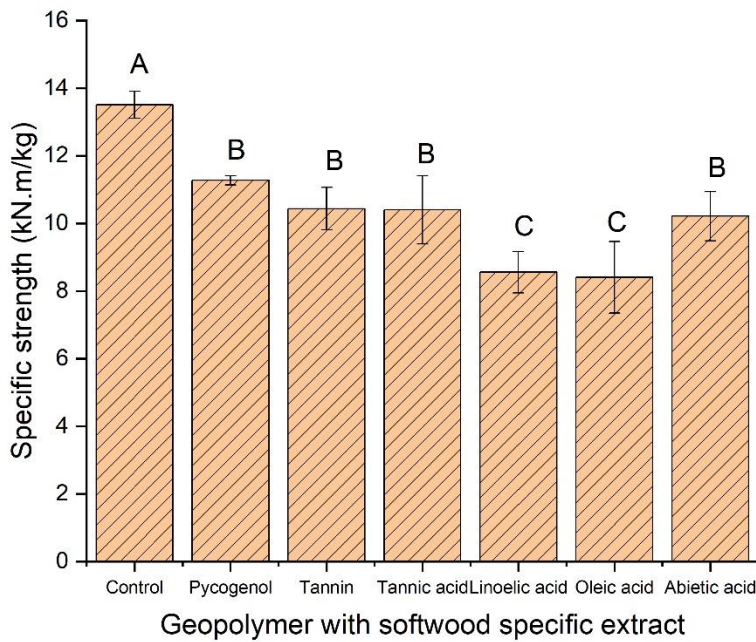


Fig. 3.2.8. Specific compressive strength of pure fly ash geopolymer with softwood specific extracts

In a process called saponification, Shill et al. (2020) and Shill et al. (2022) found that esters of fatty acids reacted at high temperatures with free sodium hydroxide in a fly ash geopolymer to produce sodium carboxylate, which is a salt. Furthermore, Shill et al. (2020) determined that soap and salt compounds, such as sodium carboxylate and sodium phosphates, were present in the fly ash geopolymer mortar after saponification had occurred. The authors defined this process of the formation of soap compounds on a geopolymer as saponification of a geopolymer. It is believed that the formation of soap compounds on the geopolymer took place when the fatty acids (i.e. linoleic and oleic acids) were exposed to the geopolymer at 60 °C, resulting in the saponification of the geopolymer. This caused the geopolymer to weaken and lose its specific compressive strength, as was also observed by Shill et al. (2020).

It was discovered that geopolymers containing fatty acids and resin acid/polyphenols differed significantly in specific compressive strength. Since all extractive compounds investigated in this study reduced the specific strength of the geopolymer, the combined effect of these specific extractives could even be greater. However, this might depend on other factors, such as the amount and nature of wood extractives present in the mixture as observed in cement (Sandermann et al. 1960; Biblis and Lo 1968; Fischer et al. 1974; Liu and Moslemi 1985).

4. Conclusions

In this study, fly ash based geopolymer composites were produced to investigate the influence of four (4) hardwoods and two (2) softwoods extractives on the specific compressive strength.

The following conclusions were made from the study:

- The specific compressive strengths of geopolymers with hardwood (i.e. *E. grandis*, *E. camaldulensis*, *P. jackson* and *B. wattle*) extracts were not affected, while those with softwood (i.e. spruce and pine) were reduced.
- The highest specific strength reduction was observed in geopolymer composites with pine extracts.
- The diversity of compounds is higher in sapwood extract than in hardwood extract.
- All the tested specific extracts (i.e. pycogenol, tannin, tannic acid, abietic acid, linoleic and oleic acids) recorded lower specific compressive strengths when compared to the control, suggesting that the combined effect of these specific extractives could even be greater on the GWC strength and geopolymer-wood compatibility.
- Among the single pure compounds investigated in this present study, the fatty acids (i.e. linoleic and oleic acids) led to the greatest reduction in specific strength in the geopolymer.

- With NaOH pretreatment of pine wood prior to its use in a geopolymer wood composite, the specific strength of a geopolymer sapwood composite was higher than that with heartwood.

Acknowledgements

The authors are grateful for the financial support provided by the BioHome project funded by the Bundesministerium für Bildung und Forschung (BMBF) [grant number 01DG17007A] and the DAAD project [grant number 57359374] and Fachagentur Nachwachsende Rohstoffe e. V. (FNR, Agency for Renewable Resources) founded by Bundesministerium für Ernährung und Landwirtschaft (BMEL), under the Grant Award No.: 22011617. The authors want to thank Silke Radtke for the technical support.

References

Alberto, M.; Mougel, E.; Zoulalian, A. (2000): Compatibility of some tropical hardwoods species with Portland cement using isothermal calorimetry. In *Forest Product Journal* 50 (9), pp. 83–88.

Asante, Bright; Schmidt, Goran; Teixeira, Ronaldo; Krause, Andreas; Savastano Junior, Holmer (2021): Influence of wood pretreatment and fly ash particle size on the performance of geopolymer wood composite. In *Eur. J. Wood Prod.* 79 (3), pp. 597–609. DOI: 10.1007/s00107-021-01671-9.

Asante, Bright; Sirviö, Juho A.; Li, Panpan; Lavola, Anu; Julkunen-Tiitto, Riitta; Haapala, Antti; Liimatainen, Henrikki (2020): Adsorption of bark derived polyphenols onto functionalized nanocellulose: Equilibrium modeling and kinetics. In *AIChE J* 66 (2). DOI: 10.1002/aic.16823.

Asante, Bright; Ye, Hanzhou; Nopens, Martin; Schmidt, Goran; Krause, Andreas (2022): Influence of wood moisture content on the hardened state properties of geopolymer wood composites. In *Composites Part A: Applied Science and Manufacturing* 152, p. 106680. DOI: 10.1016/j.compositesa.2021.106680.

Back, Ernst L.; Allen, Lawrence H. (2000): Pitch control, wood resin and deresination. Atlanta, Ga.: Tappi.

Bakharev, T. (2005): Resistance of geopolymer materials to acid attack. In *Cement and Concrete Research* 35 (4), pp. 658–670. DOI: 10.1016/j.cemconres.2004.06.005.

Barman, Dharendra Nath; Haque, Md. Azizul; Hossain, Md. Murad; Paul, Shyamal Kumar; Yun, Han Dae (2020): Deconstruction of Pine Wood (*Pinus sylvestris*) Recalcitrant Structure Using Alkali Treatment for Enhancing Enzymatic Saccharification Evaluated by Congo Red. In *Waste Biomass Valor* 11 (5), pp. 1755–1764. DOI: 10.1007/s12649-018-00547-z.

Bhatia, Latika; Johri, Sonia (2016): FTIR Analysis and Optimization of Simultaneous Saccharification and Fermentation Parameters for Sustainable Production of Ethanol from Peels of *Ananas cosmosus* by *Mucor indicus* MTCC 4349. In *Waste Biomass Valor* 7 (3), pp. 427–438. DOI: 10.1007/s12649-015-9462-4.

Biblis, E. L.; Lo, C. F. (1968): Sugars and other wood extractives: Effect on setting of southern pine cement mixtures. In *Forest Prod. J.* 18 (8), 28-34.

Cabangon, R. J.; Eusebio, D. A.; Soriano, F. P.; Cunningham, R. B.; Donnelly, C.; Evans, P. D. (2000): Effect of post-harvest storage on the suitability of *Acacia mangium* for the manufacture of wood-wool cement boards. In: *Wood-cement composites in the Asia-Pacific region*, Canberra, Australia., 97-104.

Doczekalska, B.; Zborowska, M. (2010): Wood chemical composition of selected fast growing species treated with naoh part i: structural substances. In *Wood Research* 55 (1), 41-48.

- Fan, Mizi; Ndikontar, Maurice Kor; Zhou, Xiangming; Ngamveng, Joseph Noah (2012): Cement-bonded composites made from tropical woods: Compatibility of wood and cement. In *Construction and Building Materials* 36, pp. 135–140. DOI: 10.1016/j.conbuildmat.2012.04.089.
- Fischer, F.; Wienhaus, O.; Ryssel, M.; Olbrecht, J. (1974): The water soluble carbohydrates of wood and their influence on the production of light weight wood wool boards. In *Holztechnologie* 15 (1), pp. 12–19.
- Giancaspro, James; Papakonstantinou, Christos; Balaguru, P. (2009): Mechanical behavior of fire-resistant biocomposite. In *Composites Part B: Engineering* 40 (3), pp. 206–211. DOI: 10.1016/j.compositesb.2008.11.008.
- Giancaspro, James W.; Papakonstantinou, Christos G.; Balaguru, P. N. (2010): Flexural Response of Inorganic Hybrid Composites With E-Glass and Carbon Fibers. In *Journal of Engineering Materials and Technology* 132 (2). DOI: 10.1115/1.4000670.
- Huang, Z.; Yan, N. (2013): Characterization of major components in barks from five canadian tree species. In *Wood and Fiber Science* 46 (2), pp. 167–174.
- Jorge, F. C.; Pereira, C.; Ferreira, J. M. F. (2004): Wood-cement composites: a review. In *Holz Roh Werkst* 62 (5), pp. 370–377. DOI: 10.1007/s00107-004-0501-2.
- Lee, A.W.C; Short, P. H. (1989): Pretreating hardwood for cement-bonded excelsior board. In *Forest Product Journal* 39 (10), pp. 68–70.
- Liu, Z.; Moslemi, A. A. (1985): Influence of chemical additives on the hydration characteristics of western larch wood-cementwater mixtures. In *Forest Prod. J.* 7 (7/8), pp. 37–43.
- Moslemi, A. A.; Garcia, J.F; Hofstrand, A. D. (1983): Effect of various treatments and additives on woodeportland cementewater systems. In *Wood Fiber Science* 15 (2), 164-76.

- Quiroga, A.; Marzocchi, V.; Rintoul, I. (2016): Influence of wood treatments on mechanical properties of wood–cement composites and of *Populus Euroamericana* wood fibers. In *Composites Part B: Engineering* 84, pp. 25–32. DOI: 10.1016/j.compositesb.2015.08.069.
- Redzuan, M. S.J.; Paridah, M. T.; Anwar, U. M.K.; Juliana, A. H.; Lee, S. H.; Norwahyuni, M. Y. (2019): Effects of surface pretreatment on wettability of *Acacia mangium* wood. In *JTFS* 31 (2), pp. 249–258. DOI: 10.26525/jtfs2019.31.2.249258.
- Rowell, Roger M. (2013): Handbook of wood chemistry and wood composites. 2nd ed. Boca Raton: Taylor & Francis.
- Ryu, Gum Sung; Lee, Young Bok; Koh, Kyung Taek; Chung, Young Soo (2013): The mechanical properties of fly ash-based geopolymer concrete with alkaline activators. In *Construction and Building Materials* 47, pp. 409–418. DOI: 10.1016/j.conbuildmat.2013.05.069.
- Sandermann, W.; Preusser, H. J.; Schweers, W. (1960): The effect of wood extractives on the setting of cement-bonded wood materials. In *Holzforschung* 14 (3), 70-77.
- Sandermann, Wilhelm; Brendel, Manfred (1956): Studien über mineralgebundene Holzwerkstoffe—Zweite Mitteilung: Die „zementvergiftende“ Wirkung von Holzinhaltstoffen und ihre Abhängigkeit von der chemischen Konstitution. In *Holz Roh Werkst* 14 (8), pp. 307–313. DOI: 10.1007/BF02605217.
- Sarmin, Siti Noorbaini (2016): The Influence of Different Wood Aggregates on the Properties of Geopolymer Composites. In *KEM* 723, pp. 74–79. DOI: 10.4028/www.scientific.net/KEM.723.74.
- Sarmin, Siti Noorbaini; Rahman, Wan Mohd Nazri Wan Abdul; Mohd Yunus, Nor Yuziah; Ahmad, Nurrohana (2020): Determination of the Bond Strength of Wood Veneer and Geopolymer Matrix by Means of a Pull-Out Test. In *MSF* 981, pp. 162–168. DOI: 10.4028/www.scientific.net/MSF.981.162.

Shaikh, Faiz Uddin Ahmed (2013): Review of mechanical properties of short fibre reinforced geopolymer composites. In *Construction and Building Materials* 43, pp. 37–49. DOI: 10.1016/j.conbuildmat.2013.01.026.

Shehab, Hamdy K.; Eisa, Ahmed S.; Wahba, Ahmed M. (2016): Mechanical properties of fly ash based geopolymer concrete with full and partial cement replacement. In *Construction and Building Materials* 126, pp. 560–565. DOI: 10.1016/j.conbuildmat.2016.09.059.

Shill, Sukanta Kumer; Al-Deen, Safat; Ashraf, Mahmud; Garcez, Estela Oliari; Subhani, Mahbube; Hossain, Muhammad Monowar (2022): Resistance of Geopolymer, Epoxy and Cement Mortar to Hydrocarbon-Based Synthetic Engine Lubricant, Hydraulic Fluid, Jet Fuel and Elevated Temperatures. In *Construction Materials* 2 (1), pp. 15–26. DOI: 10.3390/constrmater2010002.

Shill, Sukanta Kumer; Al-Deen, Safat; Ashraf, Mahmud; Hutchison, Wayne (2020): Resistance of fly ash based geopolymer mortar to both chemicals and high thermal cycles simultaneously. In *Construction and Building Materials* 239, p. 117886. DOI: 10.1016/j.conbuildmat.2019.117886.

Tugrul Albayrak, Ali; Yasar, Muzaffer; Gurkaynak, M. Ali; Gurgey, Ismet (2005): Investigation of the effects of fatty acids on the compressive strength of the concrete and the grindability of the cement. In *Cement and Concrete Research* 35 (2), pp. 400–404. DOI: 10.1016/j.cemconres.2004.07.031.

Weatherwax, R. C.; Tarkow, H. (1964): Effect of wood on the setting of Portland cement. In *Forest Products Journal* 14 (12), pp. 567–570.

Ye, Hanzhou; Zhang, Yang; Yu, Zhiming; Mu, Jun (2018): Effects of cellulose, hemicellulose, and lignin on the morphology and mechanical properties of metakaolin-based geopolymer. In *Construction and Building Materials* 173, pp. 10–16. DOI: 10.1016/j.conbuildmat.2018.04.028.

Zhao, Q.; Nair, B.; Rahimian, T.; Balaguru, P. (2007): Novel geopolymer based composites with enhanced ductility. In *J Mater Sci* 42 (9), pp. 3131–3137. DOI: 10.1007/s10853-006-0527-4.

Zhengtian, L.; Moslemi, A. A. (1985): Influence of chemical additives on the hydration characteristics of western larch wood cement water mixtures. In *Forest Product Journal* 35 (7), pp. 37–43.

Zhong, Li; Shi, Tiejun; Guo, Liying (2010): Preparation and morphology of porous SiO₂ ceramics derived from fir flour templates. In *J Serb Chem Soc* 75 (3), pp. 385–394. DOI: 10.2298/JSC090410010Z.

CHAPTER 4

Influence of wood moisture content on the hardened state properties of geopolymer wood composite (**Paper 2**)

Authors' contribution

	CD	EX	ED
Bright Asante	70%	60%	50%
Hanzhou Ye	10%	20%	20%
Martin Nopens	5%	10%	10%
Goran Schmidt	0%	5%	10%
Andreas Krause	15%	5%	10%

CD: Conceptual Design

EX: Conducting experiments

ED: Editing



Prof. Andreas Krause

(Supervisor)

Originally published in: Composites Part A: Applied Science and Manufacturing. Volume 152. Published Online 16 October 2021. <https://doi.org/10.1016/j.compositesa.2021.106680>.

Changes to original published work

To conform to the systematic numbering in the present thesis, all figures and tables in the original published work are preceded by the thesis chapter number.

Fig. 3, 4, 5 and 6a were modified with a brighter version for the purpose of this thesis.

NB: These changes might have moved some text positions.



Influence of wood moisture content on the hardened state properties of geopolymer wood composites

Bright Asante^{a,*}, Hanzhou Ye^{a,b}, Martin Nopens^a, Goran Schmidt^c, Andreas Krause^c

^a University of Hamburg, Institute of Wood Sciences, Leuschnerstrasse 91, 21031 Hamburg, Germany

^b Ministry of Education Key Laboratory of Wooden Material Science and Application, Beijing Forestry University, Tsinghua East Road 35, 100083 Beijing, China

^c Johann Heinrich von Thünen Institute, Federal Research Institute for Rural Areas, Forestry and Fisheries, Institute of Wood Research, Leuschnerstrasse 91, 21031 Hamburg, Germany

ARTICLE INFO

Keywords:

Ceramic-matrix composites (CMCs)

Strength

Porosity

Microstructures

ABSTRACT

Geopolymer wood composites (GWC) serve as an emerging green alternative to Portland cement wood composites in the construction sector. The wood's moisture content upon being introduced into the GWC formulation alters the content of water, which is one of the key factors influencing the strength and structure in the geopolymerization process. This study investigates the influence of initial wood moisture content on the material properties of GWC. The prepared GWC were made using 20 wt% wood flour with five different wood moisture contents (i.e. 1, 12, 27, 60 and 90 wt%). Generally, the GWC had structurally bound water, free water and cell wall water; the latter two waters can evaporate with time or temperature. Forming GWC with wood of a higher moisture content led to 30–wt% of the initial water being structurally bound. Density and compressive strength of the GWC were higher when using dry wood while porosity was reduced.

1. Introduction

Geopolymer consists of aluminosilicate raw material (such as meta-kaolin, coal fly ash, high calcium containing slags) and activator solution (e.g. sodium hydroxide and sodium silicate) [1]. In combination with wood (fibers, particles, flour) it forms geopolymer wood composites (GWC). During the manufacturing process, the aluminosilicate, upon contact with the activator solution, undergoes dissolution, hydrolysis of Al³⁺ and Si⁴⁺ compounds and a subsequent polycondensation reaction forms an amorphous to semi-crystalline solid geopolymer network [2]. The wood component binds mechanically to the geopolymer surface and forms a solid based composite [3].

The wood in GWC serves as a means for reducing density and thermal conductivity [4,5], whereas the geopolymer matrix binds the wood particles, providing mechanical strength, low permeability, good chemical resistance and excellent fire resistance behavior [6–8]. The alkali activator solution commonly used in the geopolymer binder synthesis is sodium hydroxide (NaOH), with or without sodium silicate (Na₂SiO₃) [9]. Different molar concentrations of NaOH/ Na₂SiO₃ have been used in geopolymerization, where the alkali hydroxide pellets have been dissolved in water. However, the diverse concentrations introduce different amounts of water into the mixture [10,11], which can have

adverse effects on the formation and properties of the GWC.

Water is essential in the geopolymerization process as it plays an important role in the strength and geopolymer product development. Pure water cannot activate aluminosilicate particles, except for those containing a considerable OH⁻ anion concentration. Water provides an environment for dissolution of aluminosilicates, movement of ions, hydrolysis of Al³⁺ and Si⁴⁺ compounds and polycondensation of various aluminum and silicon hydroxyl compound groups [12–14]. Therefore, water has a high influence on the geopolymer gel structure and product characteristics. Even though water provides a suitable environment and medium, too much water could reduce the geopolymerization rate during the period of dissolution to hydrolysis for its dilution effect [14] and contribute to the porosity of the material, making it too loose to use it for construction.

Perera et al. [15] studied the disposition of water in meta-kaolinite-based geopolymer and showed the existence of water in cured geopolymer in three forms. First, the intergranular water, also called free water: existing as a thin nanoscale surface layer, which is removed between room temperature and 150 °C. The authors stated that most of the water exists as free water constituting about 60% of the initial water. Secondly, interstitial water, which is related to the activating cation and can be removed between 150 °C and 300 °C. Lastly, the bound water

* Corresponding author.

E-mail address: bright.asante@uni-hamburg.de (B. Asante).

<https://doi.org/10.1016/j.compositesa.2021.106680>

Received 19 July 2021; Received in revised form 26 July 2021; Accepted 10 October 2021

Available online 16 October 2021

1359-835X/© 2021 Elsevier Ltd. All rights reserved.

originating from OH-groups, which may remain in the hardened geopolymer. It was shown that almost all three forms of water are lost at about 700 °C [15]. In contrast to the 60% of free water stated earlier [15] that could be removed between room temperature and 150 °C, Pouhet et al. [16] showed that 90% of the initial water mass could be removed after drying at 105 °C. However, the amount and mechanism of water removal is expected to be more complex in geopolymer wood composites.

Wood consists mainly of cellulose, hemicellulose and lignin. These main compounds possess an abundant number of OH-groups. Therefore, wood is a hydrophilic material, which is capable of holding water. Below the so-called “fiber saturation”, water is only located within the cell walls, above the fiber saturation threshold (moisture content of around 30%, depending on species) water is located in the porous structure as free water [17]. During composite preparation, this water (held in the wood) may be available for the interaction during the mixing and consolidation of the composite. In a case where the wood is dry or not saturated with water, it is likely to absorb water from the inorganic paste. For this reason, when adding wood to a composite, extra water is needed to complete the mixing process. Finding the correct amount of additional water needed is key in developing the composite. Mixing wood particles directly with inorganic mineral binder could potentially affect the water/binder ratio; this could limit the water available for geopolymerization due to migration of water into the wood particles [18]. Hence, Tamba et al. [19] proposed fully saturating the wood with water before use in mineral bonded composites. This shows that wood moisture content (MC) may play a key role in the movement of water (containing ions) within the composite before the final hardening of the GWC. In addition, Berzins et al. [20] stated that the high proportion of liquid in the GWC moistens the wood and allows for better compression of the composite.

The role of water in geopolymerization has been studied previously for fly ash- and kaolinite-based [21], metakaolinite-based [15,22,23], calcined kaolin-based [14], fly ash based [24] and flash calcined metakaolin based [16] with none of the studies focusing on the GWC as a whole. Several studies report on the properties of GWC where the researchers increased the amount of water or liquid activator with increase in wood content. The main purpose of the increase in water or liquid activator was to facilitate workability of the mix. However, these studies did not consider the influence of wood MC, additional liquid activator or water in the composite mixture [18,20,25,26]. Unlike Portland cement, water is considered not to be incorporated directly in the geopolymer. However, a small percentage of water remains as interstitial water in the geopolymer [27]. This fact combined with the water requirement of wood to mix the GWC can easily alter the amount of water available for geopolymerization or influence the amount of free or bound water in the composite.

Porosity as a pore structure feature is known as the important property to describe a porous ceramic material as it allows indicating the volume of voids or cavity [28]. According to Khalili et al. [29] porosity quantification is essential to obtain parameters such as thermal conductivity, mass transfer, diffusion coefficient and permeability. However, the composition of the ceramic matrix, as well as heating are factors that influence the porosity [30,31]. It is a well-established fact that an increase in the porosity reduces the strength of geopolymer; nevertheless, the magnitude of this effect depends greatly on inner structure properties such as pore size, shape and distribution [32–34].

One potential option to gain information about the inner structure of materials is the application of thermoporosimetry (TP). Fully water-saturated samples are cooled down below the freezing temperature of water and then heated up; the size and shape of the inner pores influencing the melting behavior of the water. This technique is common for inorganic materials like silica materials and organic ones like cellulose [35–37]. Within the wood cell wall no pores exist which can be detected by TP [38]. However, the TP is expected to detect the pores occurring in the geopolymer matrix. The pore analysis is based on the fact that the

water held in a porous geopolymer material will have a depressed melting point [39]. The basic principle is that the known relationships between the pore size and the melting temperature depression, and the pore volume and melting enthalpy can be exploited to determine the pore size distribution [37]. Therefore, TP is ideal for investigating the porosity of GWC.

This study tested the hypothesis that the MC of wood has a significant effect on the properties of the formed GWC. This was done by producing GWC using softwood flour (dry to wet wood MC). The strength, porosity (i.e. using TP method) and density of the resulting GWC were assessed. In addition, the composite mass loss and water released over time from the GWC and the interface between wood and geopolymer matrix were evaluated.

2. Materials and methods

2.1. Materials

Class F fly ash ($\text{SiO}_2 + \text{Al}_2\text{O}_3 + \text{Fe}_2\text{O}_3 \geq 70\%$) was obtained from the GK Kiel GmbH power plant in Kiel, Germany. The chemical oxides compositions of the fly ash as detected by X-ray fluorescence (XRF) are shown in Table 4.1. Betol 50 T (Na_2SiO_3) was purchased from Woellner, Germany and NaOH (analytical grade) was purchased from VWR, Germany. Betol 50 T and NaOH were used as received to produce the activator solution. Wood flour (Arbocel C100) was obtained from Rettenmaier & Söhne GmbH + Co KG, Rosenberg, Germany. Deionized water was used throughout the experiment.

2.2. Sample preparation

Liquid alkaline solution for activation was prepared using solutions Betol 50 T (Na_2SiO_3) and 10 M NaOH in a weight ratio of 2.5:1. The solution was mixed and cooled to ambient condition at least a day prior to use. For the influence of wood MC on the composites, no additional water was added to the mixture. The mixtures were designed in such a way that all contained equal mass of fly ash, wood, and activator solutes, with the differences arising from the water in the wood. The samples were formed by mixing 80 wt% fly ash and 20 wt% wood flour (dry matter) with different MC (1.3, 11.6, 26.8, 58.5 and 89.6%) for 3 min, followed by alkaline activation of the mixture for 5 min. The ratio of fly ash to activator was kept constant at 1.6 for all mixtures. The mixture was cast in 50 mm cube molds, cold pressed at 80 bars. The pressure was held for 20 s after which the mold with the sample was sealed in a low-density polyethylene bag. The sealed samples were oven cured at 60 °C for 24 h. The cured samples were conditioned in the climate chamber 20 °C and 65% relative humidity (RH) for further tests. For easy identification and description, the composite samples were given the identification code as in Table 4.2.

2.3. Test conducted

2.3.1. Composite mass loss and residual water

The water content of each mixture was determined using the oven dry method to compare with the calculated water content. Calculated water content was estimated based on the assumption that the total initial water in the mixture is the sum of water in the activator solution and that in the wood (as no additional water was introduced to the mixture).

Whilst storing at under 20 °C/65% RH, the composite mass changes were monitored to study the water released (as moisture) from the composites. The mass of each sample cast (day 0), after oven curing i.e. before climate conditioning (day 1), and every day during storing in climate chamber (day 2–day 61) was measured. The mass changes as a result of water released (NM) was normalized based on the initial mass of material cast since a different initial amount was cast for the GWC group during sample preparation (Eq. (1)). After 60 days of climate

Table 4.1
Chemical composition of fly ash from XRF.

Component	Al ₂ O ₃	SiO ₂	SO ₃	K ₂ O	Na ₂ O	CaO	TiO ₂	MgO	Fe ₂ O ₃	P ₂ O ₅	LOI*
Share (%)	20.53	54.18	0.01	1.51	0.51	3.36	0.84	1.50	6.31	0.66	4.18

LOI* at 1000 °C.

Table 4.2
Composites with their code.

Code	Geopolymer wood composite (GWC type)
GC1	GWC formed with wood MC 1.3%
GC12	GWC formed with wood MC 11.6%
GC27	GWC formed with wood MC 26.8%
GC60	GWC formed with wood MC 58.5%
GC90	GWC formed with wood MC 89.3%

chamber aging, the measurement of total evaporable and residual water (g) was measured by oven drying GWC at 103 ± 2 °C until the change in mass was less than 0.01% within 48 hrs. Seven replicates were used for each variant. The total composite mass loss over time (ML) at 60 days and after oven drying was calculated using Eq. (2).

$$NM (\%) = \frac{Mt}{Mi} \times 100 \quad (1)$$

$$ML (\%) = \frac{Mi - Mt}{Mi} \times 100 \quad (2)$$

where M_i and M_t were the initial mass of the sample cast and mass of the sample at the day of measurement, respectively.

2.3.2. Density

Climate chamber cured (20 °C/65% RH) GWC was used for the density estimation. The average of four samples per group was used for determination of density. Density of the samples was found by measuring the mass (M_o) of the samples on a balance. The length, width and height of the samples were measured with a caliper. The volume (V_o) was calculated by multiplying the length, width and height of the samples. The density of 7 and 28 days old GWC was calculated by dividing the M_o by the V_o .

2.3.3. Porosity (Thermoporosimetry)

Thermoporosimetry measurements were performed with a Mettler Toledo (DSC 3+ STAR^e System). A cylindrical sample of size 4 mm diameter and 4 ± 1 mm height was prepared by cutting out of the GWC material by punching. Measurements were carried out in sealed Mettler Toledo aluminum pans. All GWC groups were measured, each having three samples. Instrument calibration was performed with an indium metal standard. Afterwards, the DSC measurement sample mass was determined by storing the opened pan at 103 °C for 72 h. Measurements were performed in the isothermal step mode according to Park et al. [35] in the range between 198 nm and 2 nm (corresponding temperature -20 to -0.2 °C). Melting enthalpy was determined by integrating each endothermic peak with left starting horizontal baseline and following summation of all peaks.

2.3.4. Compressive strength

The compressive strength of 7 day aged GWC samples cubes ($50 \times 50 \times 50$ mm³) was measured using a hydraulic universal testing machine (UTM) by MTS Systems Corporation (Eden Prairie, Minnesota, US). The MTS UTM was equipped with a Zwick model 1485 control panel (ZwickRoell GmbH & Co. KG, Ulm, Germany). The samples were compressed with a load cell capacity of 250 kN and with a crosshead speed rate of 1 mm/min. The compressive strength was calculated by dividing the maximum force (N) by the cross-sectional area (mm²) of the sample. The average of four samples was reported for each group.

Specific strength with structurally bound water was calculated by dividing the compressive strength by the density of the samples at the time of testing. Specific strength without structurally bound water was calculated by dividing the compressive strength by the density, which was reduced by the mass of structurally bound water.

2.3.5. Microstructure analysis

The morphology and microstructure of the different composites was assessed using a field emission scanning electron microscope (FESEM) Quanta FEG Type 250, FEI Electron Optics (SN: D9122), Netherlands. Specimens for surface analysis were prepared by cutting a $3-5 \times 2$ mm² piece from the GWC samples with a diamond saw. The specimens were oven dried and gold coated before imaging.

3. Results and discussion

3.1. The state transformation of initial water in the hardened GWC

Fig. 4.1 shows the changes occurring in the state of initial water to final composite structure after the two different curing conditions (i.e. climate chamber aging and oven drying). From Fig. 4.1, the cast shows the initial water arising from the activator and wood in the composite mixtures. However, after 60 days of climate chamber aging, this water was reduced in all composites. After drying until no change in composite's mass, the remaining water is no longer defined as water but as a structural component, as it constitutes part of the final product formed.

From Table 4.3, composite mass loss increases with increasing wood MC for both curing conditions. After 60 days of aging in the climate chamber, the greatest mass loss occurs in GC90 while the least change was recorded in GC1. With drying, the same trend of mass loss was recorded as in climate chamber (Table 4.3). Assuming the solid content (i. e. masses of wood and geopolymer) remain the same from casting to the final drying at 103 °C, then composite mass loss over time is attributed to the moisture released through the state transformation of the initial water in the composite.

A conceptual model was developed in connection with the water forms and state transformation of the initial water in the geopolymer wood composites during a curing process, illustrated in a schematic in

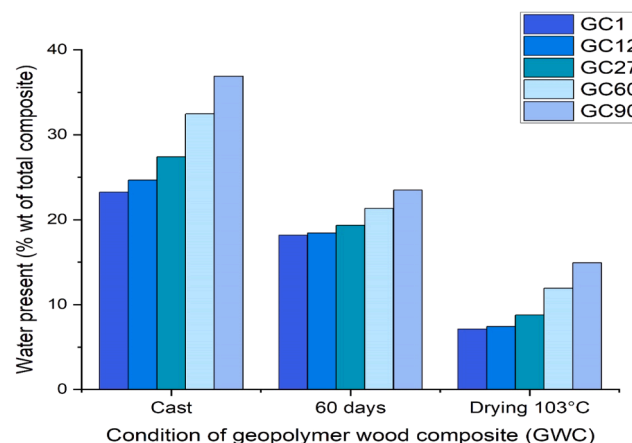


Fig. 4.1. State transformation of initial water in the final composites after aging and drying conditions. (For interpretation of the references to colour in this figure legend, the reader is referred to the web version of this article.)

Table 4.3

Composite mass loss due to water evaporation from casting – 60 days aging in climate chamber and drying at 103 °C.

Composite mass loss (%)	Type of geopolymer wood composite (GWC)				
	GC1	GC12	GC27	GC60	GC90
60 days	6.2	7.6	10.0	14.1	17.6
103 °C	17.3	18.6	20.4	23.3	25.8

Fig. 4.2. The authors estimated three water types in the GWC: namely free water, cell wall water and structurally bound water (Fig. 4.2). Free water is physically bonded in the geopolymer [40]. Free water in the GWC exists in the liquid state but in two different locations. It originates partly from the wood (i.e. when the wood is wet enough / above the FSP of wood) [41] and the geopolymer matrix [15]. Removal of free water from the GWC induces pores in the geopolymer matrix [22] and causes a significant reduction in the mass of the composite, as the majority of the water in the GWC exists in this state [15]. Hence, more free water leads to higher the amount of pore structures in the composite as this water was already filling up the voids in the composite. With long-term drying at ambient conditions or at temperatures up to 200 °C, all free water will be removed [22,42]. However, how fast this water is removed depends on the conditions of curing or temperature during removal.

Cell wall water is the water bound in wood cell walls. Under ambient conditions, such as those used in a climate chamber, this water will interact with its surroundings and the percentage of MC of this water will be between 0% and 30% [43]. However, this water will be zero after drying of the GWC at 103 °C. Reduction of this water leads to wood shrinkage. The shrinkage would cause drying stresses, eventually resulting in the delamination of the wood from the geopolymer matrix or a gap at the interface between the wood and geopolymer matrix [3] (i.e. the part of the wood with weaker bonding to the geopolymer matrix becomes separated). The third type of water in the GWC is the structurally bound water. It is important to note that the authors used the term ‘structurally bound water’ to mean water that could not escape after drying at 103 °C. Structurally bound water is somehow bound to the composite material.

Table 4.3 and Fig. 4.1 suggest that composite mass loss and wt% of water forming a structurally bound water after curing and aging/drying is dependent on the wood MC used in composite formulation. Also the results in Fig. 4.1 suggest that the amount of water that could not escape after drying at 103 °C (i.e. structurally bound water) is higher in samples with higher wood MC. Table 4.3 and Fig. 4.1 show that most of the water was expelled out of the composite structure after drying at 103 °C. Re-searches by Davidovits [40] and White et al. [42] show that most of the water that evaporates at temperatures lower than 200 °C is free water or physically bound water that exists in cured geopolymer when water is entrapped in large pores. Approximately, there was a relative loss of about 70–75% of the initial water mass in all GWC.

It was expected that after drying at 103 °C, the amount of structurally bound water would be the same for all GWC irrespective of the initial wood MC as reported for pure geopolymer paste (i.e. geopolymer without wood) [16,22]. Contradictorily, it was found that this water tends to increase with increasing wood MC. Since all mixture compositions were kept constant with the only difference arising from the wood MC, this behavior might be from the different contribution of the wood MC. Recent publication by Davidovits [1] has shown that water is pre-present in geopolymer at temperatures only below 150–200 °C. The author further explained that this water is essentially in the form of –OH groups associated with SiQ3 (3Si, 1OH) and SiQ2 (2Si, 2OH) species. These –OH groups are located primarily on the surface of the nano-particulates, and each particulate is surrounded with some physically bonded water and some siloxonate hydrate molecules. Davidovits [40] showed that water remains entrapped in the pores or bonded to the developed 3-D geopolymer network and/or possibly to silanol and aluminol groups within the structure, after geopolymerization is completed.

White et al. [42] showed by Neutron Pair Distribution Function that this water might be entrapped in the small framework pores and/or as terminal hydroxyl groups. The authors also found that with varying initial water content the amount of interstitial water entrapped in the small framework pores and/or as terminal hydroxyl groups remained the same for all geopolymers. They further explained that all free water entrapped in pores or intergranular space can be completely lost by

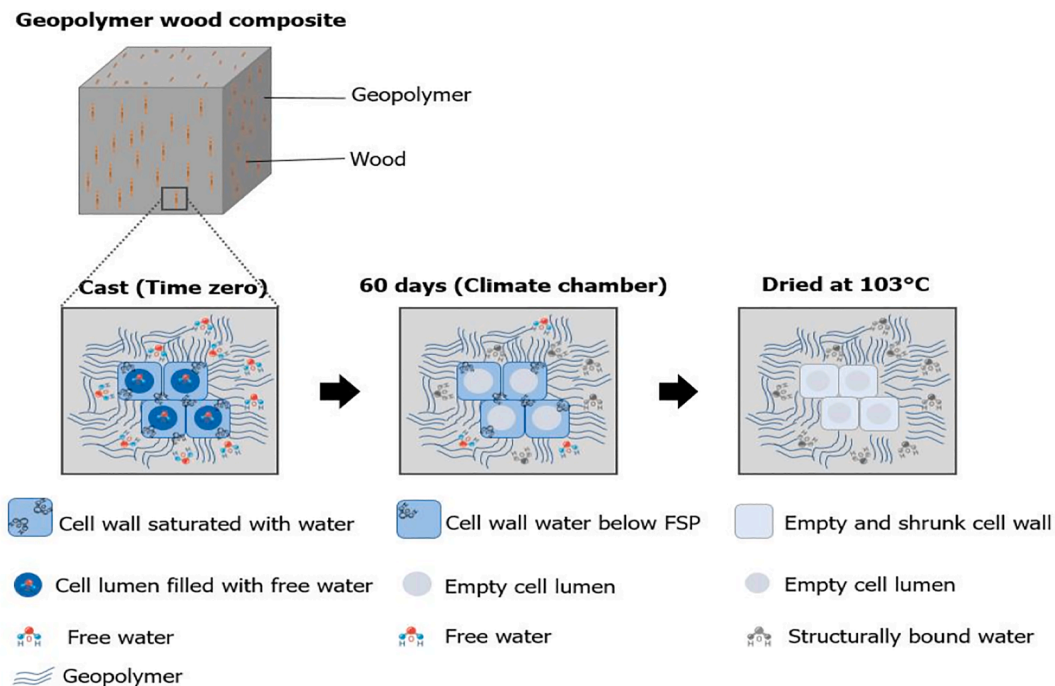


Fig. 4.2. Illustration of water forms and state transformation of initial water in the geopolymer wood composites. (For interpretation of the references to colour in this figure legend, the reader is referred to the web version of this article.)

drying the geopolymer at 200 °C. It is likely that the interstitial water was the same for all the GWC, however, the wood MC contributed different amount of additional water to the composites. Thus, increasing wood MC increased the amount of water and drying at 103 °C did not get rid of all the free water, as 200 °C is required. The different amount of the residual free water might have added to the interstitial water causing an increase in the water entrapped in the GWC with increase in wood MC. The residual free water and the interstitial water together forms the structurally bound water in this present research.

These findings indicate that the tightly incorporated water molecules (i.e. about 25–30% of the initial water) are partly inaccessible and cannot be completely removed from the GWC. Kobera et al. [44] also found that the immobilized water that does not leave the aluminosilicate network forms amorphous aluminosilicate hydrates in which water molecules are strongly bound to the matrix. However, Davidovits [40] and Perera et al. [15] showed that additional weight loss (due to water removal) could occur in the geopolymer at temperature 300 °C and above. Thus, the structurally bound water might be removed at elevated temperatures; however, said temperature increase might lead to greater mass loss due to decomposition of the wood. Generally, the GWC had structurally bound water, free water and cell wall water; the latter two waters can evaporate with time or temperature.

3.2. Water released from GWC from casting – 60 days of aging in a climate chamber

The normalized mass changes from casting to 60 days of aging of the GWC in the climate chamber are shown in Fig. 4.3. The percentage mass of all GWCs decreased sharply with age from casting to 10 days of aging in the climate chamber. However, this decrease was sharper in GWCs with a higher wood MC signifying that higher initial wood MC allowed for a greater quantity of water to be removed with the climate chamber aging. After 10 days, the masses of GC1, GC12 and GC27 stabilized, while there was a gradual decrease in GC60 and GC90.

The observed relationship between the water released from casting – 60 days of aging in the climate chamber, was well fitted to a first order exponential decay function with a high determination ($R^2 > 0.99$).

$$y = A \cdot \exp(-kx) + y_0 \tag{3}$$

where y_0 is the dry mass of the material cast, A is the water released (predominantly free water with some cell wall water), k is the drying rate constant that dictates the rate of decrease of $A + y_0$ into y_0 , with x being the time of measurement and y_0 the final weight of GWC after water removal (i.e. solid material, structurally bound water and partly cell wall water that could not be removed after 60 days of aging).

The decay rate constant (k) shows the rate at which a quantity will

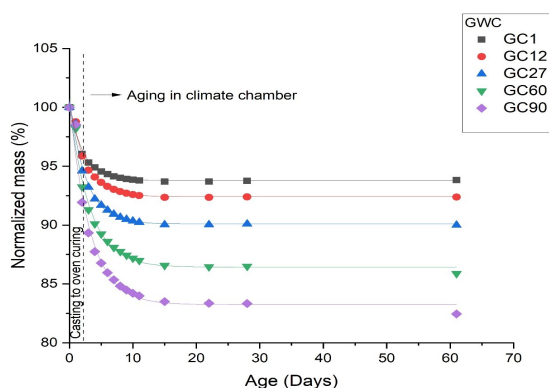


Fig. 4.3. Water released from a GWC from casting-60 days of aging in a climate chamber. (For interpretation of the references to colour in this figure legend, the reader is referred to the web version of this article.)

disappear, a larger k value signifying more rapid drying [45]. In Table 4.4 it can be seen, that the higher the rate constant (k) is, the faster the drying of the composite will be, while a lower k, leads to slower drying. This supports why the water loss curve stabilized earlier in GWCs with lower wood MC compared to the others. The k values showed that it took a shorter amount of time for water to disappear in the GC1 > GC12 > GC27 > GC60 > GC90. However, the amount of free water released (A) was greater in GWCs with a higher wood MC. It can be deduced that when the amount of free water was increased, the decay rate constant was reduced.

It was expected that the GWCs with a higher wood MC would release water at a faster speed (i.e. yield higher k value) due to more spaces (pores) occupied by water. Our results, however, suggest that this is not the case. Even though, GWCs with a higher wood MC had higher pore volume after drying, these pores were only present after the water had left the composite and did not contribute much at the time of moisture release. Thus, it can be said, that a high porosity (i.e pore volume) does not essentially imply a high permeability. There are pores, but they do not necessarily form a continuous path for water to move from the core to the edge. The differing water release speeds means the material structure and behavior is different for the composites. The speed and amount of water released might be a function of the how much water is present, as well as the location and state of the water in the GWC and not just the spaces (pores) occupied by water in the GWC.

3.3. Density

Density reduced with increasing wood MC in the composites at all ages (Fig. 4.4). Density of the GWC ranged from 1.22 to 1.25 g/cm³ (7 days) and 1.19–1.24 g/cm³ (28 days). The differences in densities at 7 days of age was less compared to after 28 days. There was a formation of new phase material (–Si–O–Al–O–) as a result of the continuous dissolution of residual solid ash particles with its associated poly-condensation reaction in the geopolymer matrix [14]. However, there was also a continual release of water (free and cell wall water) from the whole composite (i.e. the matrix and the wood). In general, forming a GWC with a higher wood MC led to a less dense composite material. After geopolymerization free water consisting as a majority of the water are entrapped in large pores [15,40]. During prolonged aging, the water evaporates [22] and the spaces previously occupied by water, become pores, making the composite less dense. Furthermore, observed differences in densities between 7 and 28 days composites can be explained by the different amount of water that was present at the time of measurement. In view of the results below, the wood MC was one dominant factor affecting the GWC density.

3.4. Porosity

The cumulative pore volume of the different sample groups can be seen in Fig. 4.5. The pore volume (displayed as pore water in gg⁻¹ sample) increased with the increasing wood MC in the GWC. This result was in accordance with the decrease in density seen when the moisture content of the initial state was increased. The higher porosity of the GWC with a higher wood MC could be explained by the empty pores

Table 4.4
Exponential decay function fitted to composite mass loss data.

Model	One phase exponential decay (Orthogonal distance regression Pro)				
	GC1	GC12	GC27	GC60	GC90
Plot					
y_0	93.79 ± 0.05	92.41 ± 0.06	90.09 ± 0.07	86.42 ± 0.11	83.23 ± 0.16
A	6.55 ± 0.33	8.09 ± 0.34	10.61 ± 0.47	13.77 ± 0.71	17.27 ± 0.71
k	0.46	0.39	0.38	0.31	0.31
Reduced Chi-Sqr	0.018	0.019	0.025	0.063	0.106
R-Square	0.999	0.999	0.999	0.999	0.999

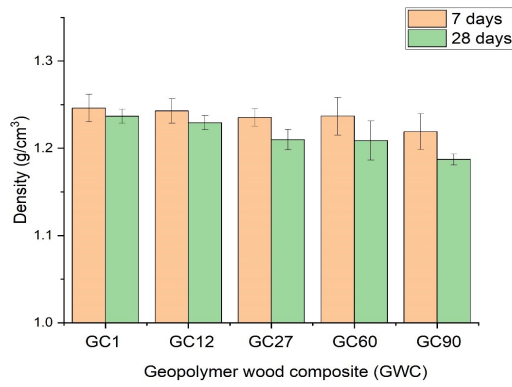


Fig. 4.4. Density development of geopolymer wood composites with wood of different MC. (For interpretation of the references to colour in this figure legend, the reader is referred to the web version of this article.)

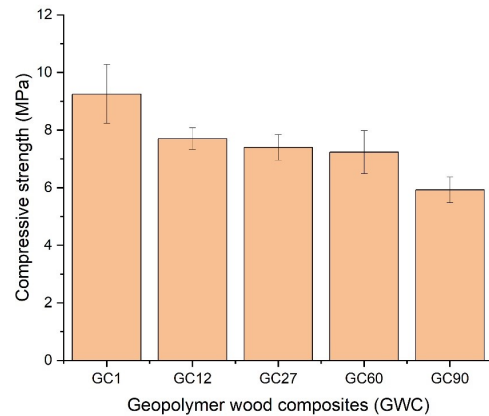


Fig. 4.6a. 7 days compressive strength of geopolymer wood composites with different wood MC. (For interpretation of the references to colour in this figure legend, the reader is referred to the web version of this article.)

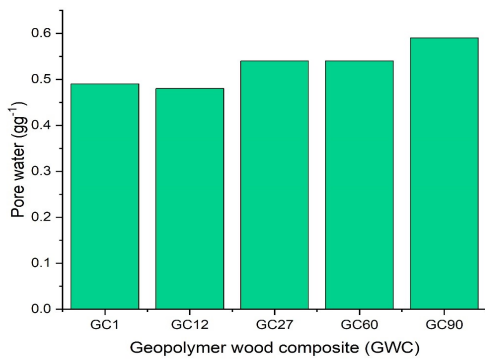


Fig. 4.5. 7 days cumulative pore volume of geopolymer wood composites with different wood MC. (For interpretation of the references to colour in this figure legend, the reader is referred to the web version of this article.)

created from the additional spaces initially occupied by water (i.e. predominantly free water). Additionally, at a later curing age, the release of water might have not only created pores but also microcracks through contraction and cracking [46–48], which might make the material more porous and reduce the strength properties of the composite (Section 3.5).

Due to the mixture of inorganic raw materials within the GWC, the usage of TP to determine precise pore size distributions was limited. Inorganic compounds diluted in water change the corresponding melting points. Additionally, the presence of structurally bound water limits TP measurements as the water bound in confined spaces was not detectable by the melting behaviour due to pore sizes below 2 nm [49,50].

3.5. Compressive strength

Fig. 4.6a shows the compressive strength of 7 day old GWC formulated with different wood MC. Generally, compressive strength reduced with increasing wood MC as the highest strength (9.25 MPa) was recorded for GC1 and the lowest (5.92 MPa) for GC90. The strength of the GWC reduced gradually in composites with wood MC of approximately 12% to 60% and decreased sharply after increasing the wood MC from 60% (GC60) to 90% (GC90). The strength difference of the GWC might be attributed to the wood MC and its contribution to the different structurally bound water, and to some extent the density of the composite at the time of strength testing.

In this work, all mixture compositions were kept the same, with the only difference arising from the water held in the wood. At constant activator to binder ratio, the increasing wood MC as in GC1–GC90, means increasing water to total solid ratio. The increasing water content in the wood can interfere in the mechanical performance because of combined effects such as (i) higher porosity/pore volume (including porous size distribution) of the composite because of the water gradually released by the wood particles. An increase in porosity reduces the strength in ceramic or concrete-like materials [32–34]; (ii) poor adhesion with the hardened matrix due to the shrinkage of the wood particles during the water release. Ye et al. [3] found out that during GWC curing process, wood experience dimensional changes (first swelling and later shrinkage) while the geopolymer is transformed from paste to geopolymer solid. However, the magnitude of dimension change in the wood is dependent on the moisture content. Wood shrinkage in the geopolymer causes an interfacial weakening or a gap at the interface between the geopolymer matrix and the wood [3]; (iii) contamination of the released water with water-soluble wood extractives that could interfere in the polycondensation kinetics of the geopolymer, as Asante et al. [51] observed that leached extracts led to lower strength in GWC.

Water has become part of the structural component of the composite to a certain degree. Compressive strength has not gone down solely due to density or porosity differences. Fig. 4.6b shows the specific strength with and without the structurally bound water. Specific strength lowered in all

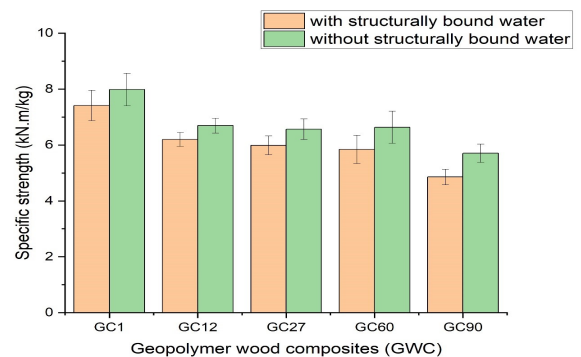


Fig. 6b. 7 days specific strength of geopolymer wood composites with and without structurally bound water. (For interpretation of the references to colour in this figure legend, the reader is referred to the web version of this article.)

GWC with increasing wood MC. It comes as no surprise that specific strength with the structurally bound water was lower than without the structurally bound water. However, it was expected that the GWC with a higher wood MC would produce higher specific strength (without structurally bound water) than the GWC with a lower wood MC since their compressive strength was divided by lower density. This clearly shows that 24.5–30% of the initial water forming a structural component (i.e. structurally bound water), contributed to the weight of the GWC but not to the strength. Too much water increased the GWC mass, causing an increase in the density but a reduction in strength, as the water does not contribute to the strength of the GWC. This response occurs with a higher wood MC as more water is structurally bound to the GWC.

3.6. Microstructure analysis

Over the course of the curing process, the geopolymer was transformed from a geopolymer paste (gel) to a geopolymer solid, while the wood experienced some dimensional changes (first swelling and later shrinking) due to a change in the moisture content [3]. The morphology of the composites with different initial wood MC was assessed using a FESEM (Fig. 4.7). It can be seen on all images that parts of a wood particle remained attached to the geopolymer matrix, while a gap due to wood shrinkage was found in other parts of the very same wood particle. However, the gaps tended to increase with increasing wood MC in the composite formulation. This phenomenon might be due to the non-uniform shrinkage of wood particles within the geopolymer matrix. Fig. 4.7 shows that GWC formulated with a lower wood MC had a compact and better geopolymer-wood bonding interface with fewer micro cracks.

The FESEM images illustrate that more micro cracks occurred in GWC formulated with a higher wood MC. The movement of free water out of the composites might have created these pathways for water removal and hence the existence of micro cracks. The enhanced geopolymer-wood interface bonding, combined with a lower amount of micro cracks in GWCs with a lower wood MC, are believed to have increased the maximum load transfer capacity [52,53] and hence contributed to the higher strength (also see Fig. 4.6a).

4. Conclusion

Stability and the long-term properties of composites are very important when considering the application and use of materials. This study investigated for the first time, the effect of wood MC on the hardened properties of a GWC. The prepared GWCs were made using 20 % dry wood with five different wood MC.

Water became part of the GWC structure. Part of the initial water could not be removed by drying at 103 °C. Forming a GWC using a higher wood moisture content led to a greater amount of structurally bound water in the composite, irrespective of the porosity of the GWC.

Early-stage density was less affected by the wood MC, as a range of 1.22–1.25 g/cm³ was recorded for GC1 → GC90. However, increased aging time showed that the density was greatly affected by the wood MC, as more water was lost from both matrix and wood, which can also be seen by an increase in cumulative porosity. The results also revealed that the composite mass loss in hardened GWC increased with increasing wood MC.

Compressive strength reduced when the initial wood MC was

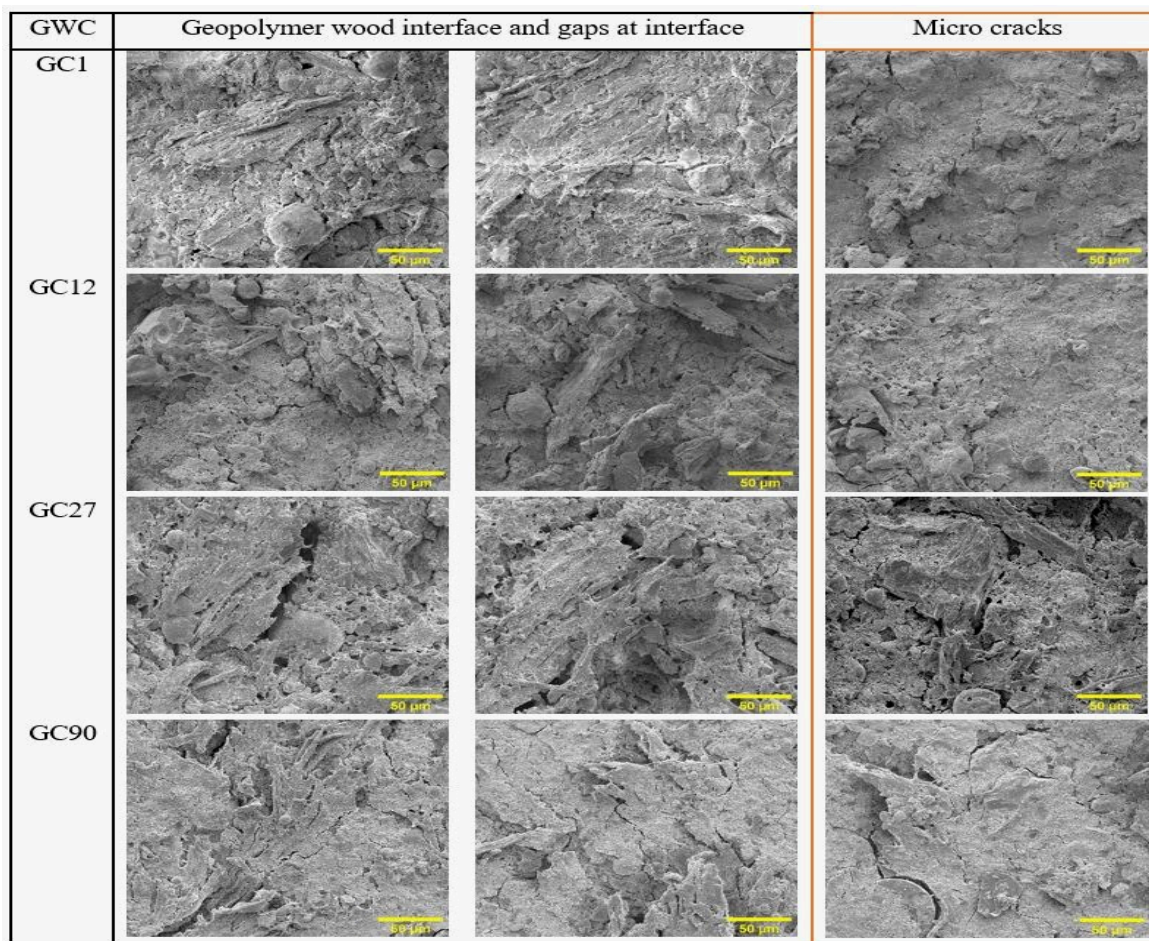


Fig. 4.7. FESEM images of geopolymer wood composites (GWC) interfaces formed with different wood MC. (For interpretation of the references to colour in this figure legend, the reader is referred to the web version of this article.)

increased, as the range of 9.25–5.92 MPa was recorded for GC1 → GC90. The structurally bound water contributed to the weight of the GWC but not the strength. This water weakened the GWC materials and reduced the strength.

Forming GWCs using a higher wood MC led to inferior interface bonding (gaps) between the geopolymer matrix and the wood. This decreased the maximum load transfer capacity and led to a lower strength.

Initial wood MC, climate chamber aging and drying conditions all affected the rate of water loss from the GWC. The differing water release speeds and the amount of structurally bound water in the GWC, indicates different composite material structures.

Generally, GWCs manufactured with a low amount of initial wood MC performed better than those with a high MC. Density, porosity and the specific compressive strength of the geopolymer wood composites (GWC) were favorable with dry wood. When producing GWC with high strengths, a low wood moisture content should be introduced in practice. However, the wood component does not have to be completely pre-dried, saving energy and production costs. For optimal endurance of the GWC, it is important to keep the raw materials as dry as possible.

CRedit authorship contribution statement

Bright Asante: Conceptualization, Methodology, Investigation, Writing– original draft. **Hanzhou Ye:** Investigation, Visualization, Writing– original draft. **Martin Nopens:** Methodology, Writing– original draft, Visualization. **Goran Schmidt:** Visualization, Writing – review & editing. **Andreas Krause:** Funding acquisition, Visualization, Supervision.

Declaration of Competing Interest

The authors declare that they have no known competing financial interests or personal relationships that could have appeared to influence the work reported in this paper.

Acknowledgments

This work was supported by the German Federal Ministry of Education and Research, under the grant number 01DG17007A and in DAAD project 57359374.

References

- Davidovits J. Review Geopolymers: Ceramic-Like Inorganic Polymers. *J Ceram Sci Technol* 2017;8(3):335–50.
- Sambucci M, Sibai A, Valente M. Recent advances in geopolymer technology. A potential eco-friendly solution in the construction materials industry: A review. *J Compos Sci* 2021;5(4):1–30.
- Ye H, Asante B, Schmidt G, Krause A, Zhang Y, Yu Z. Interfacial bonding properties of the eco-friendly geopolymer-wood composites: influences of embedded wood depth, wood surface roughness, and moisture conditions. *J Mater Sci* 2021;56(12):7420–33.
- Meng QK, Hetzer M, De Kee D. PLA/clay/wood nanocomposites: nanoclay effects on mechanical and thermal properties. *J Compos Mater* 2011;45(10):1145–58.
- Sarmin SN, Welling J, Krause A, Shalabafan A. Investigating the possibility of geopolymer to produce inorganic-bonded wood composites for multifunctional construction material – A review. *BioResources* 2014;9(4):7941–50.
- Bakharev T. Resistance of geopolymer materials to acid attack. *Cem Concr Res* 2005;35(4):658–70.
- Ryu GS, Lee YB, Koh KT, Chung YS. The mechanical properties of fly ash-based geopolymer concrete with alkaline activators. *Constr Build Mater* 2013;47:409–18.
- Shehab HK, Eisa AS, Wahba AM. Mechanical properties of fly ash based geopolymer concrete with full and partial cement replacement. *Constr Build Mater* 2016;126:560–5.
- Provis JL. Green concrete or red herring? – Future of alkali-activated materials. *Adv Appl Ceram* 2014;113(8):472–7.
- Görhan G, Kürklü G. The influence of the NaOH solution on the properties of the fly ash-based geopolymer mortar cured at different temperatures. *Compos Part B: Eng* 2014;58:371–7.
- Livi CN, Repette WL. Effect of NaOH concentration and curing regime on geopolymer. *Revista IBRACON de Estruturas e Materiais* 2017;10(6):1174–81.
- Hanzlicek T, Steinerova-Vondrakova M. Investigation of dissolution of aluminosilicates in aqueous alkaline solution under laboratory conditions. *Ceram Slik* 2002;46(3):97–103.
- Sagoe-Crentsil K, Weng L. Dissolution processes, hydrolysis and condensation reactions during geopolymer synthesis: Part II. High Si/Al ratio systems. *J Mater Sci* 2007;42(9):3007–14.
- Zuhua Z, Xiao Y, Huajun Z, Yue C. Role of water in the synthesis of calcined kaolin-based geopolymer. *Appl Clay Sci* 2009;43(2):218–23.
- Perera DS, Vance ER, Finnie KS, Blackford MG, Hanna JV, Cassidy DJ. Disposition of Water in Metakaolinite Based Geopolymers. In: Bansal NP, Singh JP, Kriven WM, editors. *Advances in Ceramic Matrix Composites XI*. Hoboken, NJ, USA: John Wiley & Sons, Inc; 2006. p. 225–36.
- Pouhet R, Cyr M, Bucher R. Influence of the initial water content in flash calcined metakaolin-based geopolymer. *Constr Build Mater* 2019;201:421–9.
- Engelund ET, Thygesen LG, Svensson S, Hill CAS. A critical discussion of the physics of wood–water interactions. *Wood Sci Technol* 2013;47(1):141–61.
- Alomayri T, Low IM. Synthesis and characterization of mechanical properties in cotton fiber-reinforced geopolymer composites. *J Asian Ceram Soc* 2013;1(1):30–4.
- Tamba S, Jauberthie R, Lanos C, Rendell F. Lightweight wood fibre concrete. *Concr Sci Eng* 2001;3(9):53–7.
- Berzins A, Morozovs A, Gross U, Iejavs J. Mechanical properties of wood-geopolymer composite. In: *Engineering for rural development-16th international scientific conference*. Latvia University of Agriculture, May, 2017. p. 1167–73.
- van Jaarsveld JGS, van Deventer JSJ, Lukey GC. The effect of composition and temperature on the properties of fly ash- and kaolinite-based geopolymers. *Chem Eng J* 2002;89(1-3):63–73.
- Lizcano M, Gonzalez A, Basu S, Lozano K, Radovic M, Viehland D. Effects of Water Content and Chemical Composition on Structural Properties of Alkaline Activated Metakaolin-Based Geopolymers. *J Am Ceram Soc* 2012;95(7):2169–77.
- Wang H, Li H, Yan F. Synthesis and mechanical properties of metakaolinite-based geopolymer. *Colloids Surf, A: Physicochem Eng Asp* 2005;268(1-3):1–6.
- Xie J, Kayali O. Effect of initial water content and curing moisture conditions on the development of fly ash-based geopolymers in heat and ambient temperature. *Constr Build Mater* 2014;67:20–8.
- Sarmin SN, Welling J. Lightweight geopolymer wood composite synthesized from alkali-activated fly ash and metakaolin. *Jurnal Teknologi* 2016;78(11).
- Al Bakri Abdullah MM, Izzat AM, Muhammad Faheem MT, Kamarudin H, Khairul Nizar I, Bnhussain M, et al. Feasibility of Producing Wood Fibre-Reinforced Geopolymer Composites (WFRGC). *AMR* 2012;626:918–25.
- Perera DS, Uchida O, Vance ER, Finnie KS. Influence of curing schedule on the integrity of geopolymers. *J Mater Sci* 2007;42(9):3099–106.
- Youmou M, Fongang RTT, Sofack JC, Kamseu E, Melo UC, Tonle IK, et al. Design of ceramic filters using Clay/Sawdust composites: Effect of pore network on the hydraulic permeability. *Ceram Int* 2017;43(5):4496–507.
- Khalili A, Morad MR, Matyka M, Liu B, Malekmohammadi BR, Weise J, et al. Porosity variation below fluid-porous interface. *Chem Eng Sci* 2014;107:311–6.
- Liang L, Li JB, Lin H, Yang XZ, Guo GF, He MS. Relation between porosity and permeability of ceramic membrane supports. *AMR* 2006;11-12:39–42.
- Félix LCM, Munoz LAB. Representing a relation between porosity and permeability based on inductive rules. *J Pet Sci Eng* 2005;47:23–34.
- Shi C. Strength, pore structure and permeability of alkali-activated slag mortars. *Cem Concr Res* 1996;26(12):1789–99.
- O'Farrell M, Wild S, Sabir BB. Pore size distribution and compressive strength of waste clay brick mortar. *Cem Concr Res* 2001;23(1):81–91.
- Wen CE, Yamada Y, Shimojima K, Chino Y, Hosokawa H, Mabuchi M. Compressibility of porous magnesium foam: Dependency on porosity and pore size. *Mater Lett* 2004;58(3-4):357–60.
- Park S, Venditti R, Jameel H, Pawlak J. Changes in pore size distribution during the drying of cellulose fibers as measured by differential scanning calorimetry. *Carbohydr Polym* 2006;66(1):97–103.
- Findenegg GH, Jahnert S, Akcakayiran D, Schreiber A. Freezing and melting of water confined in silica nanopores. *ChemPhysChem* 2008;9(18):2651–9.
- Maloney TC. Thermoporosimetry of hard (silica) and soft (cellulosic) materials by isothermal step melting. *J Therm Anal Calorim* 2015;121(1):7–17.
- Nopens M, Sazama U, König S, Kaschuro S, Krause A, Fröba M. Determination of mesopores in the wood cell wall at dry and wet state. *Sci Rep* 2020;10(1):9543.
- Landry MR. Thermoporosimetry by differential scanning calorimetry: experimental considerations and applications. *Thermochim Acta* 2005;433(1-2):27–50.
- Davidovits J. *Geopolymer Chemistry and Applications*, 2nd ed. Geopolymer Institute, Saint-Quentin: France; 2008.
- Gezici-Koc Ö, Erich SJF, Huinink HP, Van der Ven LGJ, Adan CGO. Bound and free water distribution in wood during water uptake and drying as measured by 1D magnetic resonance imaging. *Cellul* 2017;24:535–53.
- White CE, Provis JL, Proffen T, Deventer JSJV. The effect of temperature on the local structure of metakaolin-based geopolymer binder: a neutron pair distribution function investigation. *J Am Ceram Soc* 2010;93(10):3486–92.
- Kucharczyk A, Pawlik K. Modelling and experimental study of moisture transport in wood, taking into account diffusion and the accompanying adsorption of water vapour by cell walls. *Mater (Basel)* 2020;14(1):17. <https://doi.org/10.3390/ma14010017>.
- Kobera L, Slavík R, Koloušek D, Urbanová M, Kotek J, Brus J. Structural stability of aluminosilicate inorganic polymers: influence of the preparation procedure. *Ceram Slik* 2011;55(4):343–54.
- Khanday MA, Rafiq A, Nazir K. Mathematical models for drug diffusion through the compartments of blood and tissue medium. *Alexandria J Med* 2017;53(3):245–9.

- [46] Rashad AM. Alkali-activated metakaolin: A short guide for civil Engineer – An overview. *Constr Build Mater* 2013;41:751–65.
- [47] Arellano-Aguilar R, Burciaga-Díaz O, Gorokhovskiy A, Escalante-García JI. Geopolymer mortars based on a low grade metakaolin: Effects of the chemical composition, temperature and aggregate:binder ratio. *Constr Build Mater* 2014;50:642–8.
- [48] Sá Ribeiro RA, Sá Ribeiro MG, Kriven WM. A review of particle- and fiber-reinforced metakaolin-based geopolymer composites. *J Ceram Sci Technol* 2017;8(3):307–22.
- [49] Jähnert S, Vaca Chávez F, Schaumann GE, Schreiber A, Schönhoff M, Findenegg GH. Melting and freezing of water in cylindrical silica nanopores. *Phys Chem Chem Phys* 2008;10(39):6039–51.
- [50] Mietner JB, Brieler FJ, Lee YJ, Fröba M. Properties of water confined in periodic mesoporous organosilicas: nanoimprinting the local structure. *Angew Chem Int Ed Engl* 2017;56(40):12348–51.
- [51] Asante B, Schmidt G, Teixeira R, Krause A, Savastano Junior H. Influence of wood pretreatment and fly ash particle size on the performance of geopolymer wood composite. *Eur J Wood Wood Prod* 2021;79(3):597–609.
- [52] Wu H-C, Sun P. New building materials from fly ash-based lightweight inorganic polymer. *Constr Build Mater* 2007;21(1):211–7.
- [53] Chen R, Ahmari S, Zhang L. Utilization of sweet sorghum fiber to reinforce fly ash-based geopolymer. *J Mater Sci* 2014;49(6):2548–58.

CHAPTER 5

Interfacial bonding properties of the eco-friendly geopolymer-wood composites: influences of embedded wood depth, wood surface roughness, and moisture conditions (**Paper 3**)

Authors' contribution

	CD	EX	ED
Hanzhou Ye	50%	40%	40%
Bright Asante	40%	30%	30%
Goran Schmidt	5%	5%	10%
Andreas Krause	5%	20%	0%
Yang Zhang	0%	5%	10%
Zhiming Yu	0%	0%	10%

CD: Conceptual Design

EX: Conducting experiments

ED: Editing



Prof. Andreas Krause

(Supervisor)

Originally published in: Journal of Materials Science. Volume 56. First published online 21 January 2021. <https://doi.org/10.1007/s10853-021-05775-8>.

Changes to original published work

To conform to the systematic numbering in the present thesis, all figures and tables in the original published work are preceded by the thesis chapter number.

The text 'figure' in full was shortened to Fig. Other than this, no changes were made to the text.

NB: These changes might have moved some text positions.



Interfacial bonding properties of the eco-friendly geopolymer-wood composites: influences of embedded wood depth, wood surface roughness, and moisture conditions

Hanzhou Ye^{1,2,3}, Bright Asante³, Goran Schmidt^{3,4}, Andreas Krause⁴, Yang Zhang^{1,2,*} , and Zhiming Yu^{1,2}

¹ Ministry of Education Key Laboratory of Wooden Material Science and Application, Beijing Forestry University, Beijing 100083, China

² Beijing Key Laboratory of Wood Science and Engineering, Beijing Forestry University, Beijing 100083, China

³ Institute of Wood Science, University of Hamburg, 21031 Hamburg, Germany

⁴ Institute of Wood Research, Johann Heinrich von Thünen Institute, 21031 Hamburg, Germany

Received: 20 November 2020

Accepted: 3 January 2021

© The Author(s), under exclusive licence to Springer Science+Business Media, LLC part of Springer Nature 2021

ABSTRACT

With environmental friendliness, the sustainability of natural resources, and sustainable utilization of geopolymers considered in the building industry, interfacial bonding strength of geopolymer-wood composites was enhanced environmental-friendly by increasing embedded depth of wood, sanding wood surface, and controlling moisture conditions during curing process. Beech and spruce were compared as different wood species. Pullout test was modified by using a wood veneer to determine the interfacial bonding strength of geopolymer-wood composites. It was found that geopolymer exhibited higher interfacial bonding strength with spruce rather than with beech. Interfacial bonding strength increased with an increase in the embedded depth of the wood veneer, but reaching a plateau when the depth exceeded 25 mm. A higher interfacial bonding strength caused by strong mechanical interlocking at the interface was successfully created by improving the wood surface roughness via sanding with 60-grit sandpaper. Interfacial bonding strength was higher by curing under wet conditions comparing to dry conditions. However, the influence of initial wood moisture content on the interfacial bonding strength can be ignored. The results of this study serve as the basis for better preparation of geopolymer-wood composites and a diverse application of environmentally friendly building materials.

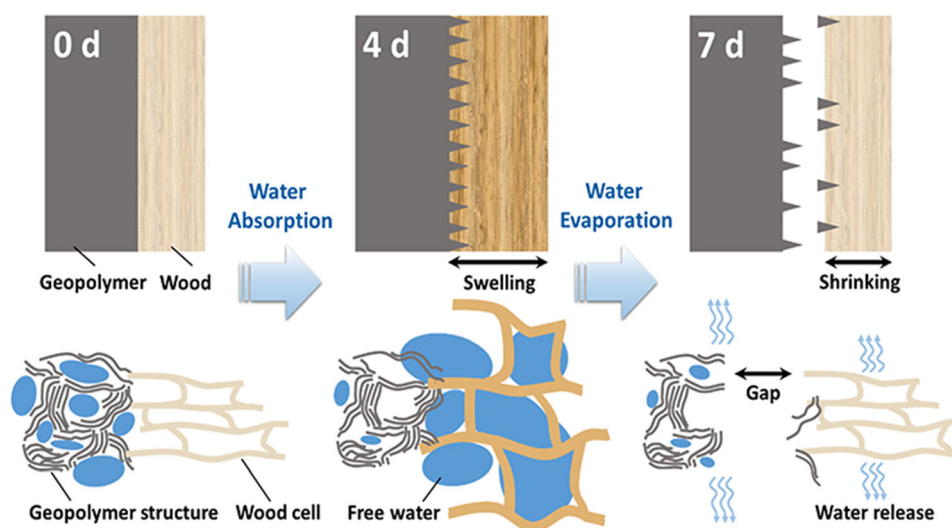
Handling Editor: Stephen Eichhorn

Address correspondence to E-mail: bjfuzhangyang@bjfu.edu.cn

<https://doi.org/10.1007/s10853-021-05775-8>

Published online: 21 January 2021

GRAPHICAL ABSTRACT



Introduction

With growing concerns about the finite resources and the environmental impact of the building industry, synthetic reinforcements are being substituted by the lignocellulose fibers due to their sustainable, low cost, non-toxic, lightweight, and biodegradable properties [1–4]. Inorganic bonded wood composites have been widely used in various building material applications [5]. Different from traditional wood-based composites made with formaldehyde or isocyanate-containing resins, inorganic composites do not release volatile toxic substances and have become attractive building materials, especially for the interior uses [6]. Commercial products, such as wood-wool cement board (WWCB), wood cement-bonded board (WCB), and cement-bonded particleboard distinguish themselves from wood-based materials by high durability, dimensional stability, toughness, strength, rapid and low-cost production, good acoustic and thermal insulation properties, and a great fire resistance [5–9].

The widely used Ordinary Portland Cement (OPC) contributes 5–8% of CO₂ to the global emission [10]. Geopolymers, the potentially low impact alternative

to the OPC, cause less CO₂ emissions and offer considerable economic benefits, while at the same time possessing the advantages of cement-based materials [11–14]. Geopolymers can be derived from a wide range of little-used secondary resources, such as mineral soils (metakaolin [15], red mud [16, 17], and clay waste [18]), industrial wastes (fly ash [19, 20], bottom ash [21], aluminum-waste [22], quarry dust waste [23], and furnace slag [24–26]), and biomass ashes (wood [27], coconut [28], and rice husk [29]).

Geopolymers are brittle materials that have low toughness and poor crack resistance properties. To prevent the crack generation, restrain crack-propagations, and enhance the mechanical properties of the geopolymer, fibers from metals, polymers, minerals, animals, and natural plants have been widely incorporated as the reinforcements into the geopolymer-based matrices [30, 31]. Specifically, the composites with a geopolymer matrix were successfully reinforced with a range of lignocellulosic fibers, such as bamboo [32], luffa cylindrical fiber [33], cotton, and flax [34], and they can also be used as environmentally friendly inorganic binders and flame-resistant coatings for wood-based composites [35–38].

A weak interfacial bonding was detected between geopolymer and high-content wood in our previous

works [39]. Mechanical characterization of the interface is an important part of the composite research, since the interface between the two components (geopolymer and wood) plays a key role in the performance of the geopolymer-wood composites [37]. Interface properties of composites are routinely measured by various tests: the fiber pullout test, the microbond test, fiber fragmentation test, microtension test, microcompression test, fiber push-out test, the microdebond test, and the microindentation [40–42]. Among them, the fiber pullout test, especially the single fiber pullout test, is the most popular, direct, and reliable method for developed interfacial bonding strength (interfacial shear strength) [43]. Nevertheless, it is difficult to evaluate and represent the whole wood material based on a single fiber pullout test due to the naturally non-uniform morphology of the wood fibers.

Pullout test was developed by using a wood veneer for this study to determine the interfacial bonding strength of geopolymer-wood composites. Influences of wood embedded depth, wood species, surface roughness, and moisture contents on the interfacial bonding strength of the geopolymer-wood composites were mainly studied. A conceptual model was then proposed for the interfacial bonding mechanism during the curing process in the geopolymer-wood composites.

Materials and methods

Materials

A commercial metakaolin (MK) (Metamax®, BASF SE, Germany) was used as the aluminosilicate source. Sodium silicate (Na_2SiO_3) solution (Betol 50 T, Woellner GmbH, Germany) and sodium hydroxide (NaOH) pellets (98.0%, VWR, Germany) were used as the alkaline activator for geopolymer. The activator and geopolymer paste were prepared as described in our previous studies [39, 44].

Norway spruce (*Picea abies*) and common beech (*Fagus sylvatica* L.) veneers were used in this work. The two veneer surfaces were sanded by a sanding machine (Bütfering Schleiftechnik GmbH, Germany) using 180 grit sandpaper (#180). For wood sample preparations (as used in Sect. “Influence of surface roughness on bonding between geopolymer and wood”), the surfaces were sanded to obtain different

surface roughness by #60, #100, and #180 sandpapers, respectively.

After sanding, the wood veneers were cut into same size pieces (117 mm × 20 mm × 1 mm) and stored in a climate chamber (Pharma 1300, Weiss Technik, Germany) at a constant temperature of 20 ± 2 °C and $65 \pm 5\%$ relative humidity (RH) for at least two weeks. Different initial wood moisture conditions before the curing process and various environmental humidity conditions during the curing process are shown in Table 5.1. The different initial wood moisture conditions of the spruce and beech veneers used in Sect. “Influence of moisture on bonding between geopolymer and wood during curing” were achieved with four different pretreatment processes:

- (1) Dry condition (-d): oven-dried at 103 ± 2 °C for 48 h and stored in a dry desiccator before use;
- (2) Wet condition (-85): stored in the climate chamber at 20 ± 2 °C and $85 \pm 5\%$ RH for more than 2 weeks;
- (3) Room condition (-65): stored in the climate chamber at 20 ± 2 °C and $65 \pm 5\%$ RH for more than 2 weeks;
- (4) Condition of wood cell wall fully water-saturated without compounds leaking (-w): wood veneers were spread on a plastic net above water in a sealed plastic box to absorb moisture without touching water for several days (around 7 days for spruce and 5 days for beech) until the wood moisture content was $30 \pm 2\%$.

Sample preparations for the pullout testing

Geopolymer paste (320 g) was poured into an open cylindrical plastic mold ($d = 50$ mm, $h = 100$ mm). The wood veneer was embedded into the geopolymer paste at a certain depth to prepare the samples. The same embedded depth (50 mm) of wood veneer in the geopolymer matrix was applied to the sample preparations used for investigating the influence of surface roughness and wood moisture content on the interfacial bonding strength.

A cap was fixed on the plastic mold to keep the wood veneer in a vertical position. The molds were sealed with a cap to prevent any surface cracks of the geopolymer matrix at an early stage and improve the initial strength of the geopolymer by slowing the water escape from the geopolymer matrix. The cap

Table 5.1 Initial moisture conditions before curing and the environmental humidity conditions during curing of the spruce and beech veneers

Samples	Initial wood moisture conditions before curing	Environmental humidity conditions during curing
Beech (Spruce)-d-35	Dry	Dry
Beech (Spruce)-w-35	Fully water-saturated	Dry
Beech (Spruce)-d-85	Dry	Wet
Beech (Spruce)-w-85	Fully water-saturated	Wet
Beech (Spruce)-85-85	Wet	Wet
Beech (Spruce)-65-65	Room condition	Indoor humidity

was removed when the samples were cured in the climate chamber for 1 day.

The samples were then cured in a plastic mold without the caps in an RH climate chamber at 20 ± 2 °C/ $65 \pm 5\%$ for another 6 days (total of 7 days curing time) before the pullout testing. At this stage, different curing conditions were used for the samples described in Sect. “[Dimensional change analysis](#)” in the climate chambers for 7 days with the same temperature (20 ± 2 °C) but different relative humidity (dry condition: $35 \pm 5\%$ RH, indoor humidity: $65 \pm 5\%$ RH, and wet condition: $85 \pm 5\%$ RH, respectively) as shown in Table 5.1.

Pullout testing

Pullout testing was used to evaluate the interfacial bonding strength between wood veneer and geopolymer matrix with a Zwick/Roell universal

testing machine (Zwick/Roell, Germany). A gripping jaw clamped the wood veneer and a purpose-built fixed base (illustrated in Fig. 5.1) held down the geopolymer block. The crosshead speed rate was set at 1 mm/min. The maximum pullout force was recorded with a 5-kN load cell. Only the pullout force value of the intact wood was recorded; the value of damaged wood was discarded. The test of each group of samples was repeated at least five times. The interfacial bonding strength in this study is defined by the pullout force per unit of the interfacial attached area of wood veneer in the geopolymer matrix. The interfacial attached area of wood veneer is related to the depth of wood embedded in the geopolymer matrix.

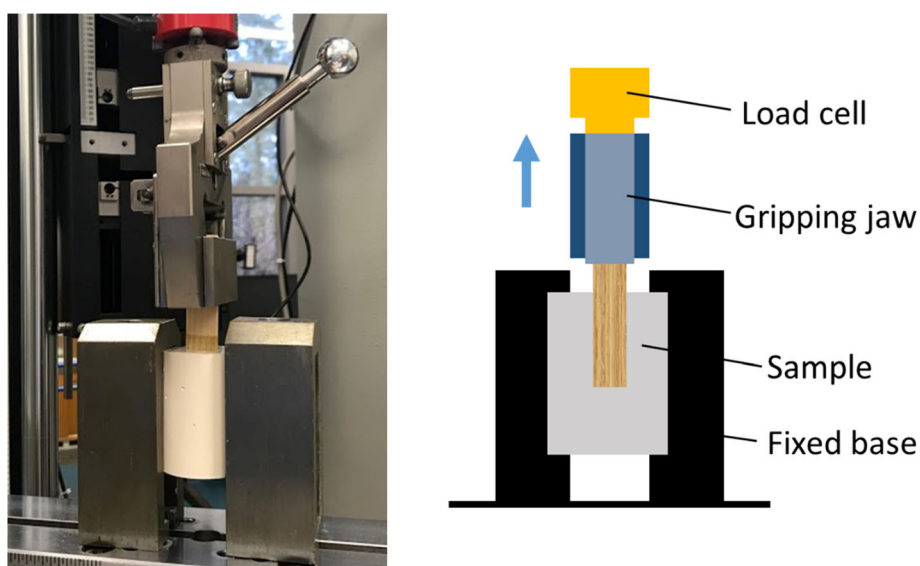


Figure 1 Pullout testing setup for the geopolymer-wood composites.

Surface roughness measurements

The parameters of average roughness (R_a), mean peak-to-valley height (R_z), and maximum roughness (R_{max}) are commonly used for determining surface roughness. The surface roughness (R_a , R_z , and R_{max}) of both front and back surfaces of wood veneers after sanding was measured according to the standard ISO 4287 [45] by a surface roughness tester (TR200, TIME, China). Measurements were made perpendicular to the wood fibers at five different points on each sample at 20 ± 2 °C and $65 \pm 5\%$ RH environment conditions. The detailed descriptions of the surface roughness measurements are available in previous studies [46, 47]. The parameters of the device were set to the measurement length (λ_c) = 0.8 mm with five measurement numbers as a cut-off value, and the surface roughness profile treated with a Gaussian filter.

Moisture content (MC) measurements of wood veneer

A wood veneer without the visible geopolymer was taken out from the geopolymer matrix immediately after a certain time of curing. The wood samples for MC measurements were cut from the portions of the wood veneer that were embedded in the geopolymer matrix. The initial weight (W_0) of the wood veneer was measured immediately. After the weight measurement was taken, the samples were dried in an oven at 103 °C for 48 h. The dry weight (W_d) of the samples was measured after they cooled in a dry desiccator for 2 days. The measurement was replicated with at least three specimens per group, and the average of the values was used. The moisture content of the wood veneer was calculated using the following equation:

$$MC = \left(\frac{W_0 - W_d}{W_d} \right) \times 100\% \quad (1)$$

Dimensional change rate measurements

The dimensional change rate (DCR) was measured for the pure geopolymer samples and the embedded wood veneers. The DCR of geopolymer (DCR_G) was calculated with the following equation:

$$DCR_G = \left(\frac{d - d_0}{d_0} \right) \times 100\% \quad (2)$$

where d_0 is the inner diameter of the plastic mold and d is the diameter of solid pure geopolymer after the curing process.

After being embedded and cured in the geopolymer, the wood veneer was removed, and its thickness was measured immediately. The dimensional change rate of wood veneer (DCR_W) was calculated with the following equation:

$$DCR_W = \left(\frac{THK - THK_0}{THK_0} \right) \times 100\% \quad (3)$$

where THK_0 is the initial thickness of the wood veneer measured before testing and THK is the thicknesses of the wood veneer after curing.

The dimensional change rate difference (Δ_d) of the samples was calculated with the following equation:

$$\Delta_d = DCR_{7d} - DCR_{4d} \quad (4)$$

where the DCR_{4d} and the DCR_{7d} are the dimensional change rates of the wood veneer and the geopolymer cured for 4 and 7 days, respectively.

Morphology characteristics of the interface

Samples with a 2-mm thickness were cut from the cross section of the geopolymer-wood block for observation. The samples were then polished with 800-grit sandpaper to investigate the influences of wood surface roughness on the interface morphology properties. Morphology images of the interface between wood and geopolymer were acquired with a stereomicroscope (SZX16, Olympus, Japan) equipped with a 1 × objective lens (SDF PLAPO 1XPF, Olympus, Japan) and a camera (AxioCam 208 color, Zeiss, Germany).

Scanning electron microscopy (SEM, LEO 1525, Oberkochen, Germany) was also applied to evaluate the microstructures of geopolymer and wood at the interface. The geopolymer surface at the interface and the cross sections of the wood veneers (both spruce and beech) after pullout testing were used for the examinations. All the samples were coated with platinum (Pt) before using. The detailed description of the methods is presented in the previous studies [39, 44].

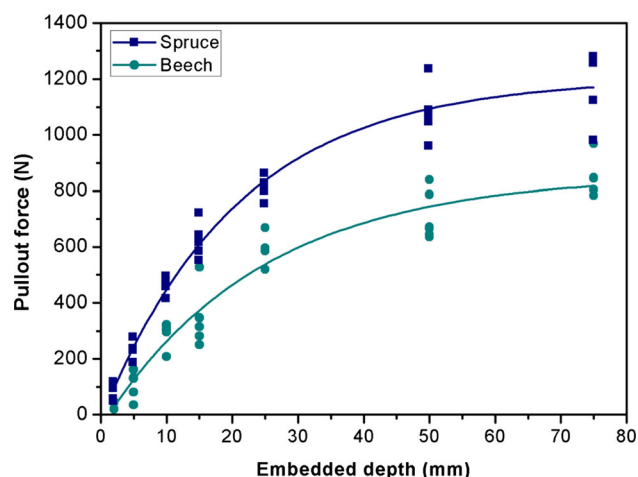


Fig. 5.2 Pullout force of spruce and beech veneers at different embedded depths.

Results and discussion

Interfacial bonding strength analysis by pullout testing

Influence of embedded depths on pullout force

Pullout testing was used to investigate the interfacial mechanical properties of the geopolymer-wood composites. Relationships between the embedded depth of the veneer and the pullout force for both spruce and beech are shown in Fig. 5.2. Spruce showed consequently higher pullout force than beech due to the better interfacial bonding caused by the rougher surface (illustrated in detail in Sect. “Influence of surface roughness on bonding between geopolymer and wood”). Further, in both spruce and beech samples, the pullout force had a steeper slope at an embedded depth < 25 mm. The slope then flattened and approximated constancy at an embedded depth > 50 mm. A comparable relationship between the pullout force and the embedded depth was detected in the pullout testing of steel fiber from an asphalt binder, showing plateaus around the peak pullout force [48]. The contribution of the end-grain wood cross-sectional area to the pullout force was negligible. It means that the relevant load during the pullout was transferred to the geopolymer matrix through the faces of the veneer and not through its end-grain. As the depth of embedment increased in both beech and spruce, the interfacial bonding force asymptotically approached a constant.

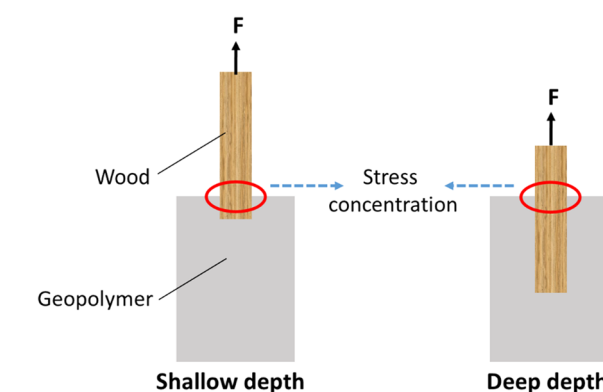
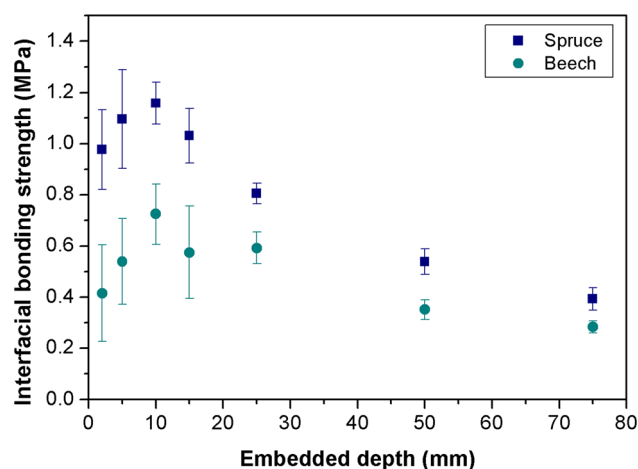


Fig. 5.3 Relationship between embedded depth and interfacial bonding strength for spruce and beech.

Influence of embedded depths on interfacial bonding strength

The relationships between the embedded depths and the interfacial bonding strengths for spruce and beech veneers are shown in Fig. 5.3. A similar trend to the influence of embedded depths on pullout force was detected for the interfacial bonding strength for both spruce and beech samples. Both spruce and beech gained interfacial bonding strength as the embedded depth increased from 2 to 10 mm, reaching peak values at roughly 1.2 and 0.7 MPa, respectively. Then, the interfacial bonding strengths gradually declined as the depth of the wood veneers increased. The lowest interfacial bonding strength for both spruce and beech was detected at the maximum embedded depth of 75 mm. The nonlinear distribution between the interfacial bonding strength and the depth of the embedded wood veneers was due to the concentration of stress near the top surface of the geopolymer matrix (circled in Fig. 5.3). This concentration

of stress presumably reduced with an increase in embedded length, and the stress distributions became generally flatter [48]. A similar stress concentration phenomenon in pullout testing was also reported for fiber (steel and wood) and cement [49, 50]. The stress concentration could be caused by a stronger bond between the wood and geopolymer at the top surface resulting from the denser structure and higher strength of the geopolymer surface due to a lower water content [51, 52].

Influence of surface roughness on bonding between geopolymer and wood

Sanding is an easy and common way to steer the surface roughness in the actual wood veneer production. Surface roughness parameters of spruce and beech veneers sanded with grit sizes of 60, 100, and 180 are presented in Table 5.2. The highest surface roughness was detected after being sanded with grit size 60, whereas the lowest value was detected with grit size 180. Based on the values of R_a , R_z , and R_{max} determined from the surface of spruce and beech veneers, the surface roughness of the wood veneers was improved significantly by decreasing the grit size of sandpaper. Further, in all samples, the roughness parameters of the back surfaces of the wood veneers measured consistently higher than those of the front surfaces. This occurred due to the fabrication method. The back surface of the veneer experienced superficial cracks that formed as a result of compression tearing on one side of the wood surface during rotary peeling [53]. Also, when sanded with the same grit size, beech samples presented a smoother surface than spruce samples, which is consistent with results reported in other research [54].

Table 5.2 Surface roughness values of spruce and beech veneers

Samples	Parameters of surface roughness (μm)					
	Front surface of wood veneer			Back surface of wood veneer		
	R_a	R_z	R_{max}	R_a	R_z	R_{max}
Spruce-60	9.00 ± 0.89	50.64 ± 5.72	66.97 ± 9.07	11.57 ± 0.83	62.02 ± 6.06	79.40 ± 17.62
Spruce-100	6.40 ± 0.62	38.74 ± 4.30	47.52 ± 7.12	6.64 ± 0.71	38.96 ± 3.41	48.01 ± 7.89
Spruce-180	2.23 ± 0.85	15.69 ± 5.70	18.84 ± 5.88	4.97 ± 1.21	32.47 ± 7.85	44.89 ± 13.84
Beech-60	6.37 ± 0.49	39.18 ± 7.09	52.39 ± 15.95	9.99 ± 0.77	56.64 ± 5.63	71.38 ± 11.60
Beech-100	3.28 ± 0.05	24.91 ± 0.97	31.31 ± 1.84	6.22 ± 0.53	34.60 ± 4.32	45.77 ± 8.49
Beech-180	2.51 ± 0.13	19.13 ± 2.46	24.88 ± 2.82	3.20 ± 0.16	24.07 ± 2.85	29.64 ± 3.36

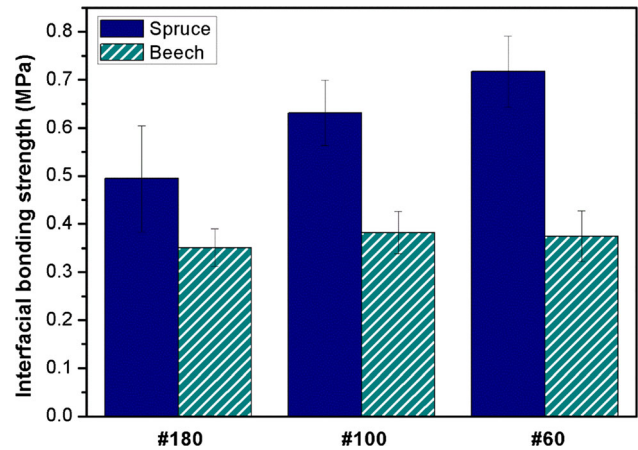


Fig. 5.4 Interfacial bonding strength between geopolymer and wood veneers sanded with grit sizes 60, 100, and 180.

This is because compared to spruce, beech generally has higher density and more regular distribution of anatomical elements, such as libriform fibers [55].

The interfacial bonding strengths of geopolymer and wood veneers sanded with different grit sizes are shown in Fig. 5.4. Under the same general sanding treatment, the interfacial bonding strength of the geopolymer is higher with spruce than with beech. The surface of the spruce samples was generally rougher than that of the beech sanded with the same grit size (also see Table 5.2). The higher interfacial bonding strength of spruce was presumably due to the stronger mechanical interlocking between the rougher wood surface and the geopolymer. This could also be seen in the microscope images of the interface morphology between the geopolymer and wood sanded by grit sizes 60 and 180, respectively (see Fig. 5.5a–b). Grit sizes had little effect, however, on the enhancement of interface bonding between beech and geopolymer due to the slighter roughness

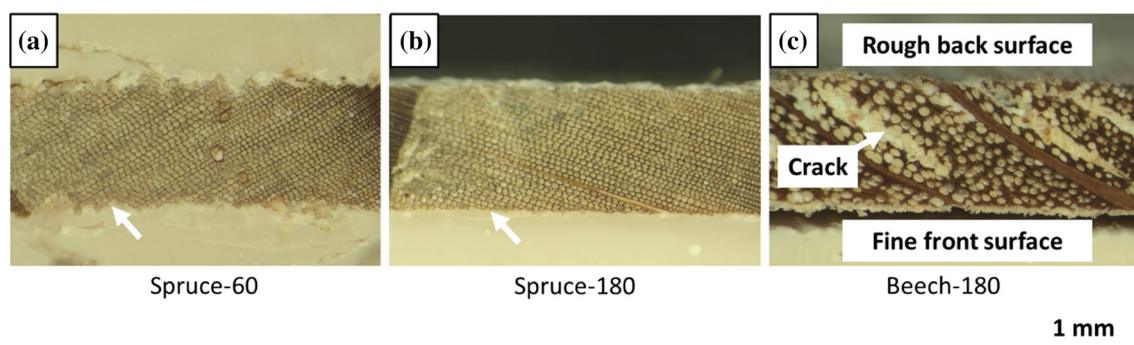


Figure 5 Microscope images of the interface between wood and geopolymer: **a** spruce-60; **b** spruce-180; **c** beech-180.

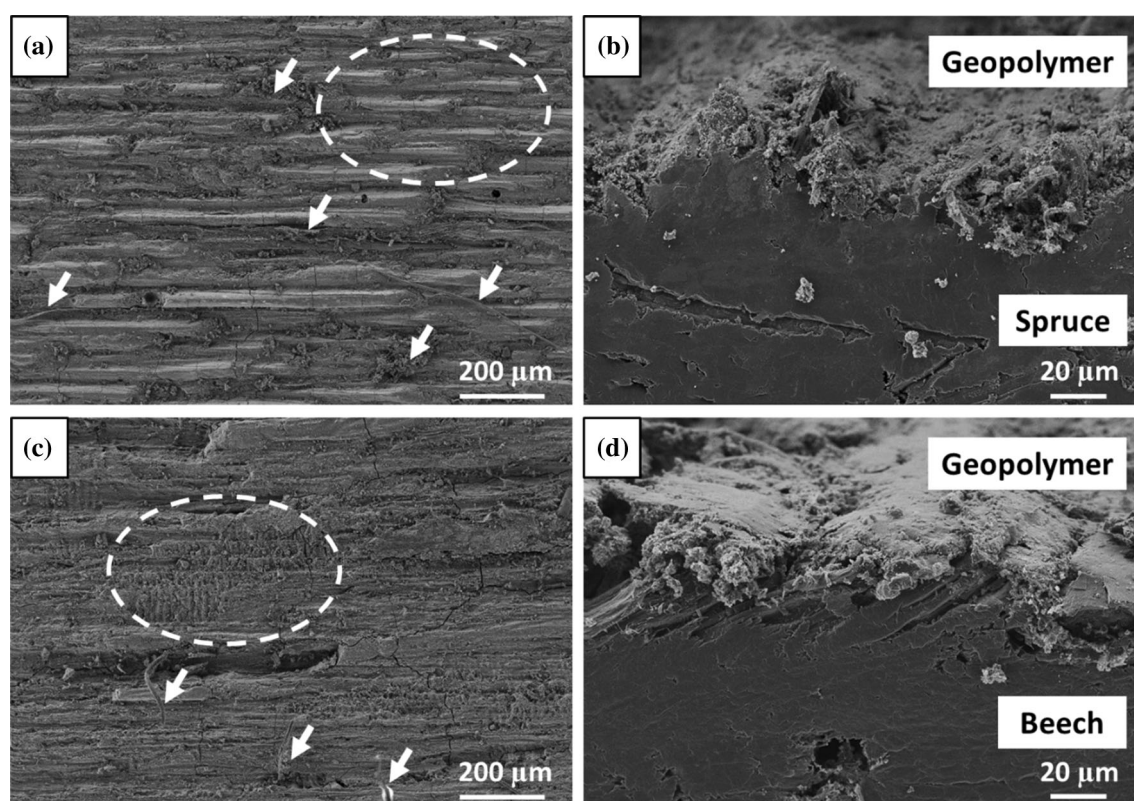


Fig. 5.6 SEM images of geopolymer and wood surfaces at the interface after pullout tests: **a** spruce fibers attached to the geopolymer; **b** geopolymer penetrated the spruce veneer; **c** beech fibers attached to the geopolymer; **d** geopolymer penetrated the beech veneer.

differences created by different sandpapers. Specifically, samples sanded with 180 grit size showed a visible gap between the geopolymer matrix and the wood veneer after 7 days of climate chamber curing. Interestingly, those gaps only occurred between geopolymer and the finer surfaces of wood veneers. The veneer detachment due to the asymmetric bonding behavior between the finer wood surfaces and cement was also detected in prior research [49].

The rough-cut surfaces of the spruce and beech veneers presented in Table 5.2 have led to robust interfacial interlocking between geopolymer and wood, with the geopolymer hooking solidly into the cracks of the back surfaces of the wood veneers (Fig. 5.5c).

The SEM images of the interfaces of geopolymer and wood after the pullout tests are presented in Fig. 5.6. It was found that wood fibers were attached to the

geopolymer (narrowed in Fig. 5.6a and c); in an adjacent area, the geopolymer was embedded in both the rough and smooth surfaces of the wood veneer (pointed out in Fig. 5.6b and d). Also, contact between the fiber and the matrix can be evidenced by the imprint of the fibers on the geopolymer matrix after the fiber pullout [56]. In this study, the imprint of spruce and beech fibers (circled in Fig. 5.6a and c) was detected on the geopolymer. Interestingly, a gap between the finer wood surface and geopolymer was then detected after 7 days of curing. A possible reason for this is that the finer wood and geopolymer were once attached, but later separated from each other.

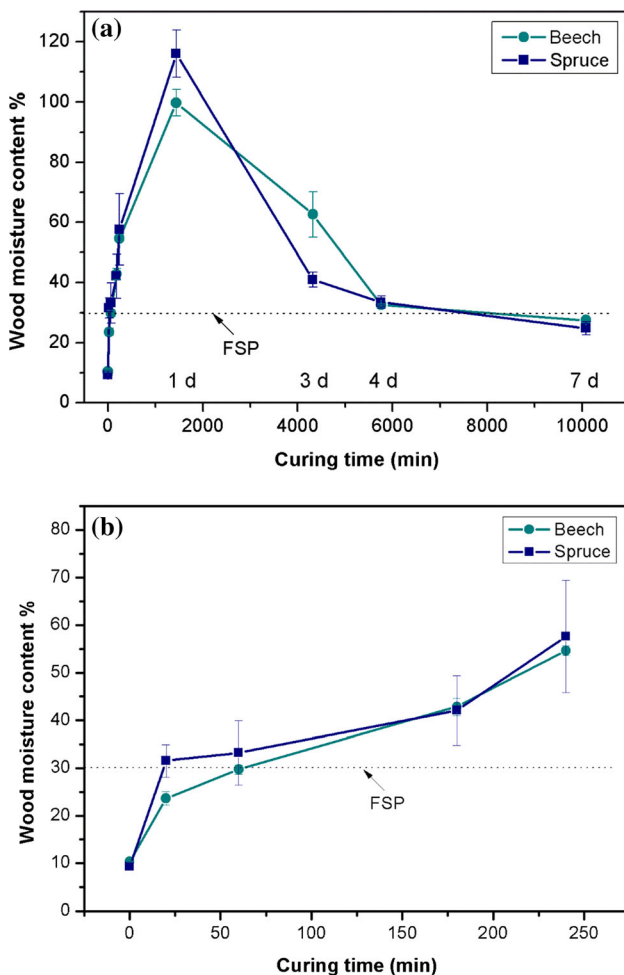


Figure 7 Influence of curing time on the wood moisture content in the geopolymer matrix: **a** from 0 to 7 days and **b** the magnification from 0 to 4 h.

Influence of moisture on bonding between geopolymer and wood during curing

Moisture content analysis

Moisture content (MC) of spruce and beech based on the curing time of 0–7 days and its magnification of 0–4 h are shown in Fig. 5.7. The dimensional change of wood was influenced by its moisture content during the curing process. The wood moisture content around 30% is considered to be a fiber saturation point (FSP), where the wood cell wall is saturated with bound water and without free water in lumens [57]. Wood shrinks when the moisture content of its cell walls drops below the FSP and swells until the MC passes the FSP [58]. The following illustrations about the relationship between the moisture content and the dimensional change in wood were based on this theory. Figure 7 shows that initially, while below FSP, the water absorption was faster in spruce than in beech, leading to a faster swelling (20 min for spruce and 60 min for beech). After that, the MC of both wood samples stayed continually above the FSP as the excess water entered into the wood lumens, and there were no dimensional changes during the 4 days of curing. The MC of spruce and beech increased gradually within 1 day of curing and reached its highest value of above 100% mainly due to the sealing effect of molds. Once the cap on the mold was released in the climate chamber after 1 day of curing, MC started to decrease. At this stage, the water evaporated mainly from the wood lumen. Wood veneer dimensions remained the same, while their MC stayed above the FSP. After curing for 3 days, it was noticed that MC decreased faster in spruce than in beech. After 4 days of curing, the MC of both reached the FSP. This could be defined as the starting point of the shrinking of wood during the curing process. After that, the MC of the wood samples continued to decrease until it reached a balance with the surrounding environment, while the wood experienced a deeper degree of shrinking after 7 days of curing.

Water in liquid form was detected on the surface of geopolymer samples at the curing age of 24 h due to the condensation process during geopolymerization that expels interstitial water that cannot stay within the framework of geopolymer [10, 59]. Indeed, more than 90% of the initial mixing water in the

Table 5.3 Dimensional change rate of geopolymer and embedded wood after curing for 4 and 7 days

Samples	Initial MC %	DCR _{4d} %	DCR _{7d} %	Δ_d %
Spruce-65	9.31	+ 13.89*	+ 9.56	- 4.33*
Spruce-w	31.95	+ 6.20	+ 5.03	- 1.17
Beech-65	10.42	+ 7.84	+ 4.54	- 3.30
Beech-w	30.48	+ 2.08	+ 1.98	- 0.10
Geopolymer		- 0.14	- 0.30	- 0.16

*Positive (+) and negative (-) symbols mean the swelling and shrinking of the samples, respectively

geopolymer was not bonded to its structure but remained free and related to the voids and the high transfer coefficients on the geopolymer [60]. The free water that leached from the geopolymer could be absorbed by the wood and then evaporated into the environment under low relative humidity at ambient temperature.

Dimensional change analysis

Table 5.3 shows the dimensional changes in geopolymer and the embedded wood veneer after 4 and 7 days of curing, respectively. The dimensional changes in wood were influenced by the wood MC during the curing process. For the wood veneers prepared wet or at 65% RH, the initial MC was

around 10% and 31%, respectively. It was detected that both spruce and beech veneers swelled slightly in the geopolymer paste during the curing that took place between day 4 and 7 of the process compared to the initial veneers before embedding. Geopolymer shrank slightly from day 4 to 7 of the curing process. The drying shrinkage of the geopolymer resulted from the high capillary pressure generated between the wet and dry areas of the micropore network due to the excessive free water evaporation [61]. The Δ_d of the samples was used to illustrate the dimensional change rate differences between days 4 and 7 of curing. It was found that spruce-w and beech-w veneers shrank slightly less than spruce-65 and beech-65. The shrinking of the geopolymer was negligible in comparison with wood.

A conceptual model was developed about the influence of moisture on bonding at the interface between geopolymer and wood during a curing process, illustrated in a schematic in Fig. 5.8. During the curing process, wood experienced some dimensional changes (first swelling and later shrinking) due to a change in the moisture content, while geopolymer transformed from geopolymer paste (gel) to geopolymer solid. The initial and final setting times of pure geopolymer were around 100 min and 145 min, respectively, as investigated in the previous studies [38]. Although introducing wood veneer could prolong the setting time of geopolymer, it was

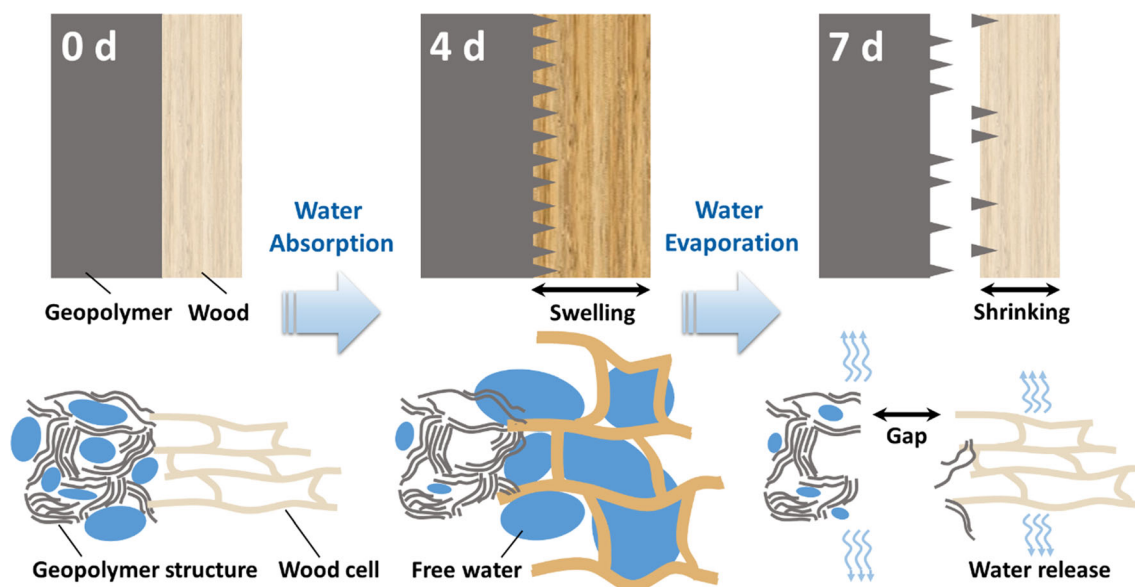


Figure 8 Schematic diagram of the influences of moisture on bonding at the interface between geopolymer and wood during the curing process.

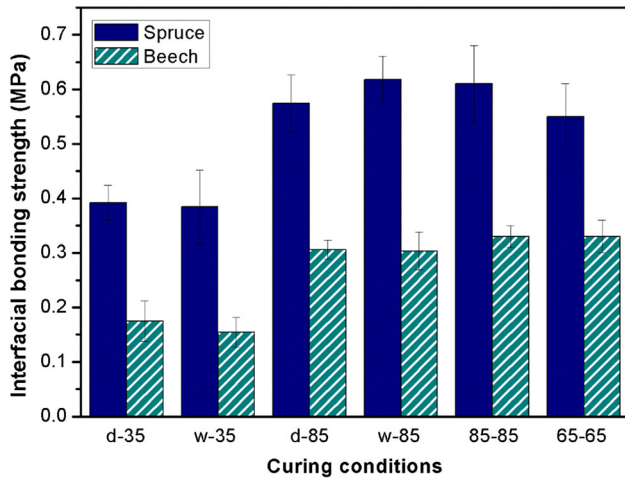


Figure 9 Interfacial bonding strength of geopolymer-wood composites under different curing conditions.

noticed in the experiment that geopolymer became solid within 1 day of curing. Wood shrank, however, beginning on the fourth day of the curing process. The dimensional changes in geopolymer between days 4 and 7 can be ignored in comparison with the wood shrinkage because when the wood started to shrink after curing for 4 days, the dimension of geopolymer was nearly consistent. Thus, the interfacial weakening (i.e., the gap at the interface between wood and geopolymer) was mainly due to the shrinking of the wood veneer.

Applications of the moisture content control

Spruce and beech veneers with different initial moisture conditions were further used to investigate the interfacial bonding strength between wood and geopolymer under different curing conditions. Different environmental humidity conditions at 35%, 85%, and 65% were applied during the curing process to simulate different manufacturing conditions like dry, wet, and common indoor humidity conditions, respectively. The interfacial bonding strengths of geopolymer-wood composites under different curing conditions are shown in Fig. 5.9. Lower interfacial bonding strength values were detected in spruce-d-35, beech-d-35, spruce-w-35, and beech-w-35 cured under dry environmental conditions. Nevertheless, taking the groups of spruce-d-85, spruce-w-85, and spruce-85-85 as an example, it was shown that pre-treatments of different wood moisture conditions before curing had a slight influence on the interfacial

bonding strength of the samples under the same environment conditions during the curing process. No visible gaps were detected at the interface of the geopolymer and wood veneer when the samples were cured under a wet condition (20 °C/85% RH). A visible gap, however, was detected in the spruce-d-35, beech-d-35, spruce-w-35, and beech-w-35 samples after curing in a dry environment (20 °C/35% RH) for 7 days. The similar interfacial bonding strength was detected in the samples cured under 65% RH (common indoor humidity condition) as compared to the samples cured under 85% humidity. Thus, controlling wood moisture conditions before the curing process is not necessary for the improvement of higher interfacial bonding properties of wood and geopolymer.

Conclusions

In this study, interfacial bonding strength of the geopolymer-wood composites were improved environmental-friendly by increasing embedded depth, sanding wood surface, and controlling curing conditions. Beech and spruce were compared as different wood species. A pullout test method was developed for the analysis of interfacial bonding strength between the geopolymer and wood. It was found that the pullout force increased with an increase in embedded depth of the wood veneer, and a plateau was detected at the depth of 25 mm. The bottom end of the wood veneer carried only a negligible load during the pullout testing. Compared to beech, spruce showed a higher interfacial bonding strength between wood and geopolymer. Strong mechanical interlocking at the interface was successfully achieved by sanding wood surface with grit size 60 sandpaper. Moreover, interfacial bonding strength was increased under wet curing conditions (20 °C/85% RH). Weak interface was mainly caused by the wood shrinking under dry conditions (20 °C/35% RH) during curing process. Influence of initial wood moisture content, however, can be ignored on the interfacial bonding strength between wood and geopolymer. A conceptual model was proposed explaining the moisture influence on the interfacial bonding mechanism of the geopolymer-wood composites during the curing process.

Acknowledgements

The authors are grateful for the financial support provided by the National Natural Science Foundation of China [grant number 31800485], the Beijing Outstanding Talent Training Foundation [grant number 2017000020124G092], the China Scholarship Council [No. 201806510025], and the BioHome project funded by the German Federal Ministry of Education and Research [grant number 01DG17007A] and the DAAD project [grant number 57359374].

Compliance with ethical standards

Conflicts of interest The authors declare that they have no conflicts or competing interests.

References

- [1] Li M, Khelifa M, Khennane A, El Ganaoui M (2019) Structural response of cement-bonded wood composite panels as permanent formwork. *Compos Struct* 209:13–22. <https://doi.org/10.1016/j.compstruct.2018.10.079>
- [2] Kochova K, Caprai V, Gauvin F, Schollbach K, Brouwers H (2020) Investigation of local degradation in wood stands and its effect on cement wood composites. *Constr Build Mater* 231:117201. <https://doi.org/10.1016/j.conbuildmat.2019.117201>
- [3] Zhang S, Xiang A, Tian H, Rajulu AV (2018) Water-blown castor oil-based polyurethane foams with soy protein as a reactive reinforcing filler. *J Polym Environ* 26(1):15–22. <https://doi.org/10.1007/s10924-016-0914-0>
- [4] Furtos G, Silaghi-Dumitrescu L, Pascuta P, Sarosi C, Korniejenko K (2019) Mechanical properties of wood fiber reinforced geopolymer composites with sand addition. *J Nat Fibers* 06:1–19. <https://doi.org/10.1080/15440478.2019.1621792>
- [5] Quiroga A, Marzocchi V, Rintoul I (2016) Influence of wood treatments on mechanical properties of wood–cement composites and of *Populus Euroamericana* wood fibers. *Compos B Eng* 84:25–32. <https://doi.org/10.1016/j.compositesb.2015.08.069>
- [6] Wang L, Chen SS, Tsang DC, Poon C-S, Shih K (2016) Recycling contaminated wood into eco-friendly particle-board using green cement and carbon dioxide curing. *J Clean Prod* 137:861–870. <https://doi.org/10.1016/j.jclepro.2016.07.180>
- [7] Karade S (2010) Cement-bonded composites from lignocellulosic wastes. *Constr Build Mater* 24(8):1323–1330. <https://doi.org/10.1016/j.conbuildmat.2010.02.003>
- [8] Wei YM, Tomita B (2001) Effects of five additive materials on mechanical and dimensional properties of wood cement-bonded boards. *J Wood Sci* 47(6):437–444
- [9] de la Gree GD, Yu Q, Brouwers H (2014) Wood-wool cement board: optimized inorganic coating. In: Proceedings of the 14th International Inorganic-Bonded Fiber Composites Conference (IIBCC). Da Nang, Vietnam, September, pp 15–19.
- [10] Li Z, Zhang S, Zuo Y, Chen W, Ye G (2019) Chemical deformation of metakaolin based geopolymer. *Cement Concrete Res* 120:108–118. <https://doi.org/10.1016/j.cemconres.2019.03.017>
- [11] Singh NB (2018) Fly ash-based geopolymer binder: a future construction material. *Minerals* 8(7):299. <https://doi.org/10.3390/min8070299>
- [12] Aly AM, El-Feky M, Kohail M, Nasr E-SA (2019) Performance of geopolymer concrete containing recycled rubber. *Constr Build Mater* 207:136–144. <https://doi.org/10.1016/j.conbuildmat.2019.02.121>
- [13] Hassan A, Arif M, Shariq M (2019) Use of geopolymer concrete for a cleaner and sustainable environment—a review of mechanical properties and microstructure. *J Clean Prod* 223:704–728. <https://doi.org/10.1016/j.jclepro.2019.03.051>
- [14] Singh N, Middendorf B (2020) Geopolymers as an alternative to Portland cement: an overview. *Constr Build Mater* 237:117455. <https://doi.org/10.1016/j.conbuildmat.2019.117455>
- [15] Medri V, Papa E, Lizion J, Landi E (2020) Metakaolin-based geopolymer beads: production methods and characterization. *J Clean Prod* 244:118844. <https://doi.org/10.1016/j.jclepro.2019.118844>
- [16] Nie Q, Hu W, Huang B, Shu X, He Q (2019) Synergistic utilization of red mud for flue-gas desulfurization and fly ash-based geopolymer preparation. *J Hazard Mater* 369:503–511. <https://doi.org/10.1016/j.jhazmat.2019.02.059>
- [17] Li Y, Min X, Ke Y, Liu D, Tang C (2019) Preparation of red mud-based geopolymer materials from MSWI fly ash and red mud by mechanical activation. *Waste Manage* 83:202–208. <https://doi.org/10.1016/j.wasman.2018.11.019>
- [18] Dassekpo J-BM, Ning J, Zha X (2018) Potential solidification/stabilization of clay-waste using green geopolymer remediation technologies. *Process Saf Environ* 117:684–693. <https://doi.org/10.1016/j.psep.2018.06.013>
- [19] Gunasekara C, Law D, Bhuiyan S, Setunge S, Ward L (2019) Chloride induced corrosion in different fly ash based geopolymer concretes. *Constr Build Mater* 200:502–513. <https://doi.org/10.1016/j.conbuildmat.2018.12.168>
- [20] Shang J, Dai J-G, Zhao T-J, Guo S-Y, Zhang P, Mu B (2018) Alternation of traditional cement mortars using fly ash-based

- geopolymer mortars modified by slag. *J Clean Prod* 203:746–756. <https://doi.org/10.1016/j.jclepro.2018.08.255>
- [21] Zhu W, Rao XH, Liu Y, Yang E-H (2018) Lightweight aerated metakaolin-based geopolymer incorporating municipal solid waste incineration bottom ash as gas-forming agent. *J Clean Prod* 177:775–781. <https://doi.org/10.1016/j.jclepro.2017.12.267>
- [22] Leiva C, Luna-Galiano Y, Arenas C, Alonso-Fariñas B, Fernández-Pereira C (2019) A porous geopolymer based on aluminum-waste with acoustic properties. *Waste Manage* 95:504–512. <https://doi.org/10.1016/j.wasman.2019.06.042>
- [23] Kürklü G, Görhan G (2019) Investigation of usability of quarry dust waste in fly ash-based geopolymer adhesive mortar production. *Constr Build Mater* 217:498–506. <https://doi.org/10.1016/j.conbuildmat.2019.05.104>
- [24] Bouaissi A, Li L-y, Abdullah MMAB, Bui Q-B (2019) Mechanical properties and microstructure analysis of FA-GGBS-HMNS based geopolymer concrete. *Constr Build Mater* 210:198–209. <https://doi.org/10.1016/j.conbuildmat.2019.03.202>
- [25] Hu Y, Tang Z, Li W, Li Y, Tam VW (2019) Physical-mechanical properties of fly ash/GGBFS geopolymer composites with recycled aggregates. *Constr Build Mater* 226:139–151. <https://doi.org/10.1016/j.conbuildmat.2019.07.211>
- [26] Phummiphan I, Horpibulsuk S, Rachan R, Arulrajah A, Shen S-L, Chindaprasit P (2018) High calcium fly ash geopolymer stabilized lateritic soil and granulated blast furnace slag blends as a pavement base material. *J Hazard Mater* 341:257–267. <https://doi.org/10.1016/j.jhazmat.2017.07.067>
- [27] Abdulkareem OA, Ramli M, Matthews JC (2019) Production of geopolymer mortar system containing high calcium biomass wood ash as a partial substitution to fly ash: an early age evaluation. *Compos Part B: Eng* 174:106941. <https://doi.org/10.1016/j.compositesb.2019.106941>
- [28] Hassan HS, Abdel-Gawwad H, García SV, Israde-Alcántara I (2018) Fabrication and characterization of thermally-insulating coconut ash-based geopolymer foam. *Waste Manage* 80:235–240. <https://doi.org/10.1016/j.wasman.2018.09.022>
- [29] Kaur K, Singh J, Kaur M (2018) Compressive strength of rice husk ash based geopolymer: the effect of alkaline activator. *Constr Build Mater* 169:188–192. <https://doi.org/10.1016/j.conbuildmat.2018.02.200>
- [30] Liu S, Rawat P, Chen Z, Guo S, Shi C, Zhu D (2020) Pullout behaviors of single yarn and textile in cement matrix at elevated temperatures with varying loading speeds. *Compos Part B: Eng* 108251. <https://doi.org/10.1016/j.compositesb.2020.108251>
- [31] Korniejenko K, Łach M, Dogan-Saglamtimur N, Furtos G, Mikula J (2020) The overview of mechanical properties of short natural fiber reinforced geopolymer composites. *Environ Res Technol* 3(1): 28–39. <https://doi.org/10.35208/ert.671713>
- [32] Ribeiro RAS, Ribeiro MGS, Sankar K, Kriven WM (2016) Geopolymer-bamboo composite—a novel sustainable construction material. *Constr Build Mater* 123:501–507. <https://doi.org/10.1016/j.conbuildmat.2016.07.037>
- [33] Alshaaer M, Mallouh SA, Al-Faiyz Y, Fahmy T, Kallel A, Rocha F (2017) Fabrication, microstructural and mechanical characterization of Luffa Cylindrical Fibre-Reinforced geopolymer composite. *Appl Clay Sci* 143:125–133. <https://doi.org/10.1016/j.clay.2017.03.030>
- [34] Wongs A, Kunthawatwong R, Naenudon S, Sata V, Chindaprasit P (2020) Natural fiber reinforced high calcium fly ash geopolymer mortar. *Constr Build Mater* 241:118143. <https://doi.org/10.1016/j.conbuildmat.2020.118143>
- [35] Bahrami M, Shalbafan A, Welling J (2019) Development of plywood using geopolymer as binder: effect of silica fume on the plywood and binder characteristics. *Eur J Wood Wood Prod* 77(6):981–994. <https://doi.org/10.1007/s00107-019-01462-3>
- [36] Shalbafan A, Thoemen H (2020) Geopolymer-bonded laminated veneer lumber as environmentally friendly and formaldehyde-free product: Effect of various additives on geopolymer binder features. *Appl Sci* 10(2):593. <https://doi.org/10.3390/app10020593>
- [37] Berzins A, Morozovs A, Van den Bulcke J, Van Acker J (2017) Softwood surface compatibility with inorganic geopolymer. *Adv Mater Proc*, 793–798. <https://doi.org/10.5185/amp.2017/913>
- [38] Ye H, Pan D, Tian Z, Zhang Y, Yu Z, Mu J (2020) Preparation and properties of geopolymer/soy protein isolate composites by *in situ* organic-inorganic hybridization: a potential green binder for the wood industry. *J Clean Prod*, 123363. <https://doi.org/10.1016/j.jclepro.2020.123363>
- [39] Ye H, Zhang Y, Yu Z (2018) Wood flour's effect on the properties of geopolymer-based composites at different curing times. *BioResources* 13(2):2499–2514. <https://doi.org/10.15376/biores.13.2.2499-2514>
- [40] Piggott M (1993) The single-fibre pull-out method: its advantages, interpretation and experimental realization. *Compos Interface* 1(3):211–223. <https://doi.org/10.1163/156855493X00086>
- [41] Revol BP, Thomassey M, Ruch F, Bouquey M, Nardin M (2017) Single fibre model composite: Interfacial shear strength measurements between reactive polyamide-6 and cellulosic or glass fibres by microdroplet pullout test. *Compos Sci Technol* 148:9–19. <https://doi.org/10.1016/j.compscitech.2017.05.018>

- [42] Monteiro SN, Satyanarayana KG, Margem FM et al (2011) Interfacial shear strength in lignocellulosic fibers incorporated polymeric composites, In: Kalia S, Kaith BS, Kaur I (eds) Cellulose fibers: bio-and nano-polymer composites. Springer, Berlin, pp 241–262. https://doi.org/10.1007/978-3-642-17370-7_9
- [43] Sydenstricker TH, Mochnaz S, Amico SC (2003) Pull-out and other evaluations in sisal-reinforced polyester biocomposites. *Polym Test* 22(4):375–380. [https://doi.org/10.1016/S0142-9418\(02\)00116-2](https://doi.org/10.1016/S0142-9418(02)00116-2)
- [44] Ye H, Zhang Y, Yu Z, Mu J (2018) Effects of cellulose, hemicellulose, and lignin on the morphology and mechanical properties of metakaolin-based geopolymer. *Constr Build Mater* 173:10–16. <https://doi.org/10.1016/j.conbuildmat.2018.04.028>
- [45] ISO E 4287 (1997) Geometrical product specifications (GPS). Surface texture. Profile method. Terms, definitions and surface texture parameters. International Organization for Standardization, Geneva.
- [46] Bekhta P, Sedliačik J, Jones D (2018) Effect of short-term thermomechanical densification of wood veneers on the properties of birch plywood. *Eur J Wood Wood Prod* 76(2):549–562. <https://doi.org/10.1007/s00107-017-1233-4>
- [47] Budakçı M, İlçe AC, Korkut DS, Gurleyen T (2011) Evaluating the surface roughness of heat-treated wood cut with different circular saws. *BioResources* 6(4):4247–4258
- [48] Park P, El-Tawil S, Naaman AE (2017) Pull-out behavior of straight steel fibers from asphalt binder. *Constr Build Mater* 144:125–137. <https://doi.org/10.1016/j.conbuildmat.2017.03.159>
- [49] Frybort S, Mauritz R, Teischinger A, Müller U (2012) Investigation of the mechanical interactions at the interface of wood-cement composites by means of electronic speckle pattern interferometry. *BioResources* 7(2):2483–2495
- [50] Kabir MR, Islam MM (2014) Bond stress behavior between concrete and steel rebar: critical investigation of pull-out test via finite element modeling. *Int J Civ Struct Eng* 5(1):80–90. <https://doi.org/10.6088/ijcser.2014050008>
- [51] Xie J, Kayali O (2014) Effect of initial water content and curing moisture conditions on the development of fly ash-based geopolymers in heat and ambient temperature. *Constr Build Mater* 67:20–28. <https://doi.org/10.1016/j.conbuildmat.2013.10.047>
- [52] Zuhua Z, Xiao Y, Huajun Z, Yue C (2009) Role of water in the synthesis of calcined kaolin-based geopolymer. *Appl Clay Sci* 43(2):218–223. <https://doi.org/10.1016/j.clay.2008.09.003>
- [53] Corder SE, Atherton GH (1963) Effect of peeling temperatures on Douglas fir veneer. Oregon State University Information circular 18.
- [54] Papp EA, Csiha C (2017) Contact angle as function of surface roughness of different wood species. *Surf Interfaces* 8:54–59. <https://doi.org/10.1016/j.surfin.2017.04.009>
- [55] Kminiak R, Gaff M (2015) Roughness of surface created by transversal sawing of spruce, beech, and oak wood. *BioResources* 10(2):2873–2887. <https://doi.org/10.15376/biores.10.2.2873-2887>
- [56] Alzeer M, MacKenzie KJ (2012) Synthesis and mechanical properties of new fibre-reinforced composites of inorganic polymers with natural wool fibres. *J Mater Sci* 47(19):6958–6965. <https://doi.org/10.1007/s10853-012-6644-3>
- [57] Telkki V-V, Yliniemi M, Jokisaari J (2013) Moisture in softwoods: fiber saturation point, hydroxyl site content, and the amount of micropores as determined from NMR relaxation time distributions. *Holzforschung* 67(3):291–300. <https://doi.org/10.1515/hf-2012-0057>
- [58] Reeb JE (1995) Wood and moisture relationships. Oregon State University. Oregon.
- [59] Park S, Pour-Ghaz M (2018) What is the role of water in the geopolymerization of Metakaolin? *Constr Build Mater* 182:360–370. <https://doi.org/10.1016/j.conbuildmat.2018.06.073>
- [60] Pouhet R, Cyr M, Bucher R (2019) Influence of the initial water content in flash calcined metakaolin-based geopolymer. *Constr Build Mater* 201:421–429. <https://doi.org/10.1016/j.conbuildmat.2018.12.201>
- [61] Kuenzel C, Vandepierre LJ, Donatello S, Boccaccini AR, Cheeseman C (2012) Ambient temperature drying shrinkage and cracking in metakaolin-based geopolymers. *J Am Ceram Soc* 95(10):3270–3277. <https://doi.org/10.1111/j.1551-2916.2012.05380.x>

Publisher's Note Springer Nature remains neutral with regard to jurisdictional claims in published maps and institutional affiliations.

CHAPTER 6

Additional work

Preliminary studies on the influence of processing (mixing) parameters on the properties of geopolymer wood composite

Bright Asante^a, Andreas Krause^b

^a University of Hamburg, Institute of Wood Sciences, Leuschnerstrasse 91, 21031 Hamburg, Germany

^b Johann Heinrich von Thünen Institute; Federal Research Institute for Rural Areas, Forestry and Fisheries; Institute of Wood Research; Leuschnerstrasse 91, 21031 Hamburg, Germany

Abstract

Class F fly ash and metakaolin aluminosilicate materials were used as separate precursor materials in the preparation of geopolymer wood composites (GWC). Different mixing parameters were investigated, as to what stage during the manufacture of GWC to add alkaline activator solution, wood (fibers or flour) and/or water. Using compressive strength and density profiles, the properties of the resulting GWC were characterized. From the results, the five different mixing parameters did not influence the strengths of fly ash-based and metakaolin-based GWCs with wood fibers or flour. In addition, fly ash-based and metakaolin-based GWCs showed a nearly constant density profile. The density profiles show that the wood fibers were evenly mixed in the both geopolymer matrices. In conclusion, the similar density profiles and strengths give more flexibility in mixing during the manufacture of fly ash-based and metakaolin-based GWCs.

1.0 Introduction

Geopolymers are produced by alkali activation of aluminosilicate materials such as slag, metakaolin, coal ash etc. Geopolymer wood composites (GWC) consist of aluminosilicate raw

material, wood particles and alkaline solution. When all materials are mixed, the aluminosilicate material, upon contact with the activator solution, undergoes dissolution, hydrolysis and a polycondensation reaction to form a solid product that encases the wood particles/ fibers.

Water provides a suitable environment for the dissolution of aluminosilicates, movement of ions, hydrolysis of Al^{3+} and Si^{4+} compounds and polycondensation of various aluminum and silicon hydroxyl compound groups i.e. indicating a great influence on the geopolymer gel structure and product characteristics (Hanzlicek and Steinerova-Vondrakova 2002; Sagoe-Crentsil and Weng 2007; Zuhua et al. 2009). Nevertheless, adding water to the geopolymer binder or mixture of aluminosilicate and wood could also reduce the geopolymerization rate during the period of dissolution to hydrolysis for its dilution effect (Zuhua et al. 2009). Owing to these reasons, the need to determine when (what stage) and how to add water as well as the proper amount of additional water needed is key in developing a geopolymer wood composite.

Wood and inorganic binders have a long history, where wood fibers are used mostly for reinforcement, and flour and particles as fillers in inorganic bonded wood composites. Wood is a hydrophilic material, capable of holding water. In composite preparation, this water may or may not be available to the mixture during the mixing. For this reason, when adding wood fiber or particles to a composite, extra water is sometimes needed to complete the mixing process. Mixing wood directly with a geopolymer could potentially affect the water:geopolymer binder ratio; this could limit the water and ions available for geopolymerization due to migration of water/ions into the wood (Alomayri and Low 2013). Direct mixing of wood with the aluminosilicate material could also limit the amount/ area of contact between the activator solution and the aluminosilicate precursor material. These

indicates that when to add what material during GWC fabrication may be critical for the resulting composite.

Throughout literature, two different mixing technologies in the fabrication of geopolymer wood composites are displayed. The first pertains to dry mixing of the wood and aluminosilicate source before alkaline activation (Alomayri and Low, 2013; Sarmin and Welling, 2016; Sarmin, 2016; Malenab et al., 2017; Furtos et al., 2021). In these cases, this mixing is to allow homogeneity in solid materials before binding by the geopolymer. The second involves the activation of the aluminosilicate source with the alkaline activator before adding the fibers (Sá Ribeiro et al. 2016; Tan et al. 2019; Berzins et al. 2017). This is to activate as many particles from the precursor source as possible, making them available for the binding of fibers. The activation of both ordinary Portland cement and geopolymer cement occur under an alkaline environment, however, each chemical reaction and binding effect is different. Amongst the key factors affecting the quality of a cement wood composite are the organic filler type, type of binder and technological and manufacturing factors such as method of fabrication of the composite (Sanaev et al. 2016; Yel et al. 2020).

Although simple processing technology is required for cement bonded wood composites (Fan et al. 2012), the aforementioned reasons make it clear, that the smallest mistake in the process technology of geopolymer wood composite fabrication can affect the properties of the resulting product. Wood of every size and form are used in the manufacture of cement wood based composites. However, the geometry of the wood has a strong effect on the properties of the product formed (Frybort et al. 2008). This implies that the appropriate process technology may vary among wood flour/ particles and fibers. GWC process technology leading to poor or low composite properties may limit the practical application of the geopolymer wood composite.

Therefore, maximizing the best composite properties through research on the appropriate mixing technologies attract extensive attention.

Until now, no account has been found in relation to analysis on the influence of varying the mixing parameters of a geopolymer wood composite with wood fibers/particles or flour. This paper aims at providing fundamentals and an essential database for process technologies for geopolymer wood composites used in construction. In this study, we report the results of the impact of wood type (wood fibers and flour) and how variation in the mixing parameters affects the properties of the geopolymer wood composite. On route to achieving this, five different mixing procedures and the addition of water at different stages in composite formation were assessed. In addition, the research was conducted using both fly ash and metakaolin as separate aluminosilicate precursor materials.

2.0 Materials and Methods

2.1 Materials

Class F Fly ash was obtained from GK Kiel GmbH power plant in Kiel, Germany. Betol 50T (Na_2SiO_3) from Woellner, Germany and analytic grade of NaOH pellets from VWR, Germany were used for the activator solution. Wood flour (Arbocel C100, Rettenmaier & Söhne GmbH + Co KG, Rosenberg- Germany) and wood fibers. Deionized water was used throughout the experiment. The chemical compositions of the fly ash are tabulated in Table 6.1.

Table 6.1. Chemical composition of fly ash from XRF

Component	Al ₂ O ₃	SiO ₂	SO ₃	K ₂ O	Na ₂ O	CaO	TiO ₂	MgO	Fe ₂ O ₃	P ₂ O ₅	LOI*
Share (%)	20.53	54.18	0.01	1.51	0.51	3.36	0.84	1.50	6.31	0.66	4.18

LOI* at 1000 °C.

2.2 Mixture proportion and sample preparation

The alkaline solution for geopolymer was prepared using solutions Betol 50T (Na₂SiO₃) and 10 M NaOH in a weight ratio of 2.5:1; it was subsequently allowed to cool to ambient conditions prior to use. For the study of the variation in the mixing procedure, mixed softwood wood flour and fibers were used. Table 6.2a-b shows the proportion of materials used in preparation of the composite. Five (5) types of mixing variations (Mix A- E) were used for the study. The variations were done in relation to when to add what material during the composite preparation. Sample preparations were done according to Table 6.3. For Mix D and E, the water was added to the wood and the mix then sealed in low-density polyethylene (LDPE) plastic for 7 days before using in the composite preparation. This was to help the wood attain equilibrium prior to its use. Water to solid ratio and total mixing time were kept at constant for all mixtures. Samples were casted in 50 mm cube mold, cold pressed at 80 bars for 30 s and sealed in LDPE plastic. The sealed samples were oven cured at 60 degrees in the plastic for 24 h. The cured samples were conditioned in the climate chamber 20⁰C/ 65% RH for further testing.

Table 6.2a. Composite mixture by mass ratio for geopolymer wood flour composites.

Proportion	Fly Ash: Wood flour	Fly Ash: Activator	Fly Ash: water
Ratio	9:1	1.5:1	27:1

Table 6.2b. Composite mixture by mass ratio for geopolymer wood fiber composites.

Precursor	aluminosilicate: Wood fiber	aluminosilicate: Activator	aluminosilicate: water
FA	19:1	2:1	23:1
MK	19:1	1.5:1	4:1

*NB: FA = fly ash aluminosilicate material and MK= metakaolin aluminosilicate material

Table 6.3. Manufacturing process for geopolymer wood composites

Mix A	Mix B	Mix C	Mix D	MIX E
Fly ash and wood are mixed for 3 min.	Fly ash and wood are mixed for 3 min.	Activate fly ash for 4 min.	Fly ash and the moist wood are mixed for 3 min.	Activate fly ash for 4 min.
Add alkaline activator and mix for 4 mins	Add water and mix for 3 min.	Add wood and mix for 3 min.	Add alkaline activator and mix for 7 min.	Add the moist wood and mix for 6 min
Add water and mix for 3 min.	Add alkaline activator and mix for 4 min.	Add water and mix for 3 min.		

2.3 TEST CONDUCTED

2.3.1 Density profile

Density profiles were measured using a DENSE-LAB X made by Electronic Wood Systems GmbH. Geopolymer wood fiber composites of dimensions 50 mm³ were used for the measurements. Before loading the samples into the machine, an electronic caliper was used to measure all three dimensions of each sample, and an electronic scale was used to determine

their weight. Using these measurements, the overall density of each sample was calculated by dividing the samples mass by volume.

2.3.2 Compressive strength and specific compressive strength

The compressive strength of 28 day aged cube samples (50 mm^3) were measured using a hydraulic universal testing machine (UTM) by MTS Systems Corporation (Eden Prairie, Minnesota, US). The MTS UTM was equipped with a Zwick model 1485 control panel (ZwickRoell GmbH & Co. KG, Ulm, Germany). The samples were compressed with a load cell capacity of 250 kN and with a crosshead speed rate of 1 mm/min. The compressive strength was calculated by dividing the maximum force (N) by the cross-sectional area (mm^2) of the sample. The average of four samples was reported for each group.

3.0 RESULTS AND DISCUSSION

3.1 Effect of mixing variations on the specific compressive strength

The specific strength of geopolymer wood composites with mixing variations are shown in Fig. 6.1- 6.3. Here it can be seen, that specific strength ranges from 6.8- 7.36 kN.m/ kg for the fly ash based geopolymer wood flour composites, 26.38- 28.10 kN.m/ kg for fly ash based geopolymer wood fiber composites and 9.01- 9.51 kN.m/ kg for the metakaolin-based geopolymer wood fiber composites. The minimal differences in the strength ranges shows that there is more flexibility during mixing or composite formation. Even though Asante et al. (2022) found that using wood with low moisture content gives a higher strength, Mix D and E recorded similar strength as Mix A- C. This shows practically, that in order for Mix D and E to achieve a strength similar to Mix A- C, there is no need to completely dry the wood to a very low moisture content prior to composite formation. This might help cut down production cost in both fly ash-based and metakaolin-based geopolymer wood composites. It can be concluded

that the water in the wood adds up to the total water content in the mixture and, as much as the total water to solid content and other mixing parameters are the same, will lead to similar strength.

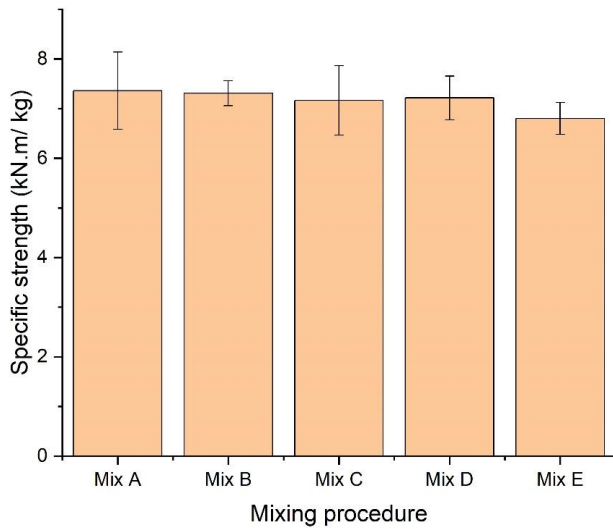


Fig. 6.1. Effect of different mixing procedures on fly ash-based geopolymer wood flour composite.

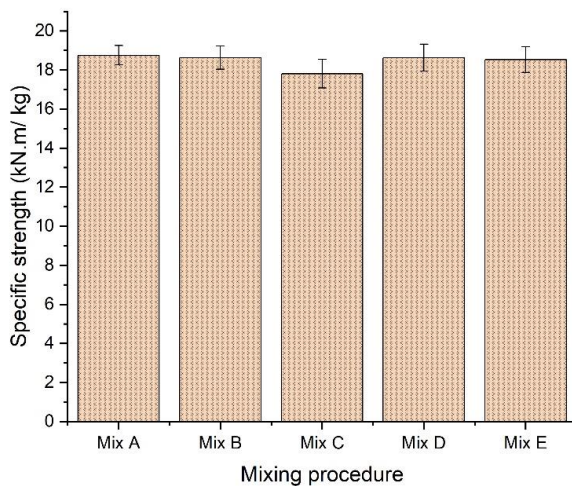


Fig. 6.2. Effect of different mixing procedures on fly ash-based geopolymer wood fiber composite.

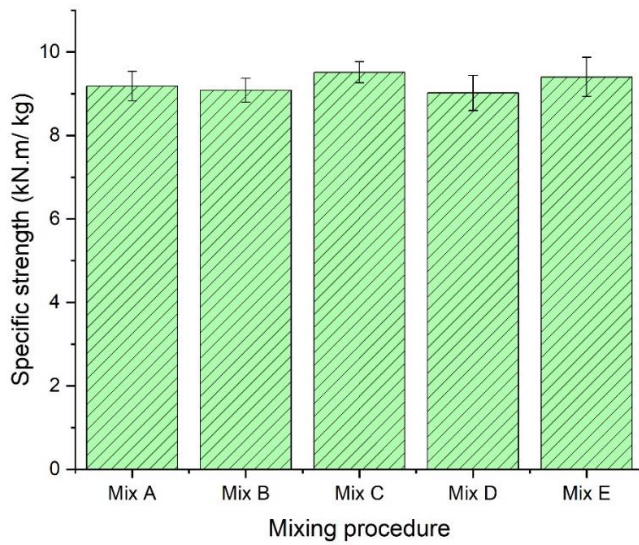
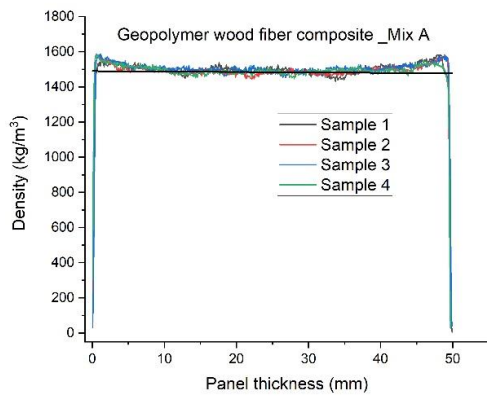


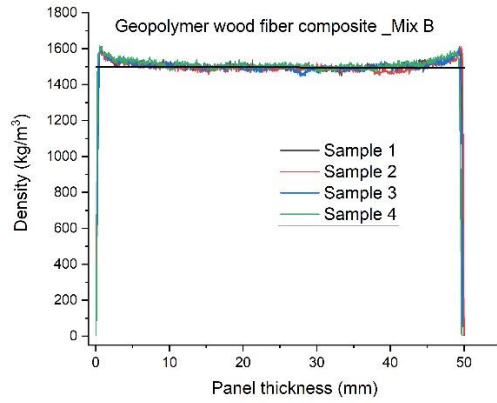
Fig. 6.3. Effect of different mixing procedures on metakaolin-based geopolymer wood fiber composite.

3.2 Density profiles for the different mixing variations

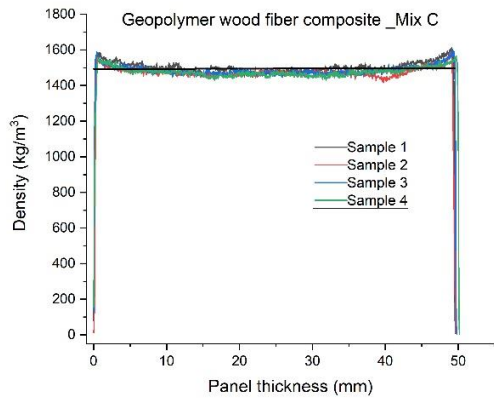
Due to the discrepancy in density between the less dense wood fiber and the denser geopolymer, the different mixing and distribution of fibers in the fly ash-based and metakaolin-based geopolymer wood fiber composites can be assessed using density profiles. The higher the density is, the higher the ratio of geopolymer to wood. Similar density profiles were observed across the five different mixes for both fly ash-based and metakaolin-based geopolymer wood fiber composites (Fig. 6.4 and 6.5). The high peaks in density at the edges (i.e. about 2-3 mm) of the samples confirm the presence of geopolymer close to the surface, which can be seen in all mix groups (A-E). However, the distances between the edges showed evenly mixed and fairly distributed wood fibers within the mixes across all sample groups and can be explained by the surface roughness, as the x-rays used to measure the local densities only intersect with parts of the uneven surfaces.



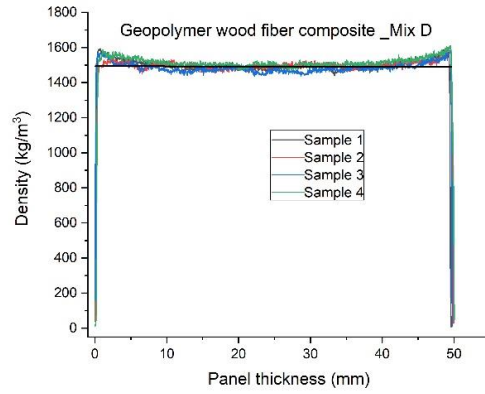
Mix A



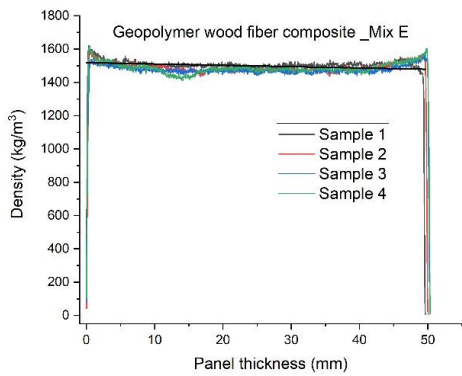
Mix B



Mix C

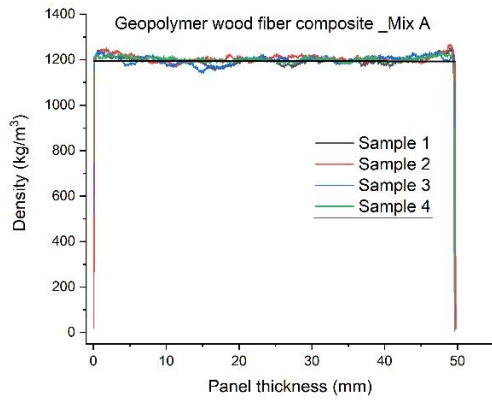


Mix D

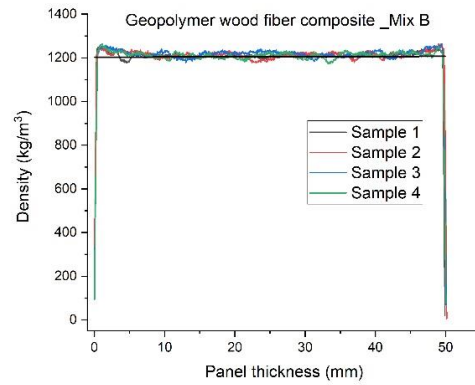


Mix E

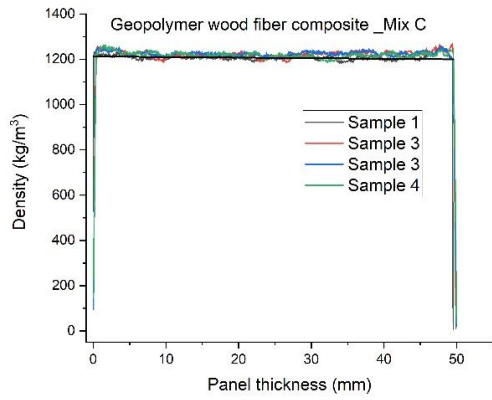
Fig. 6.4. Density profiles of fly ash-based geopolymer wood fiber composite (Mix A-E)



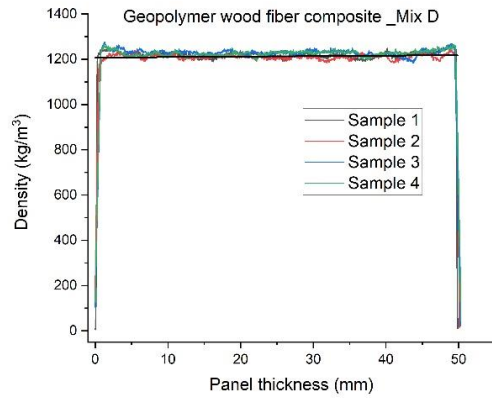
Mix A



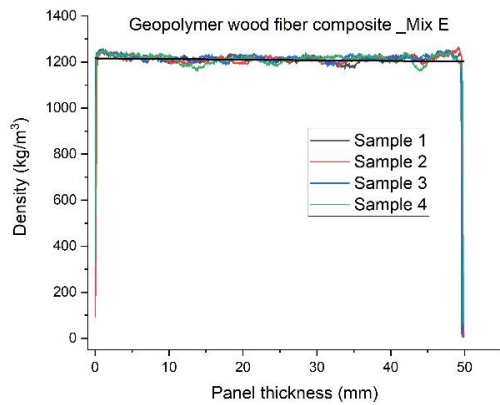
Mix B



Mix C



Mix D



Mix E

Fig. 6.5. Density profiles of metakaolin-based geopolymer wood fiber composite (Mix A-E)

4.0 Conclusion

This study presents the influence of different raw material mixing on the strength and density of both fly ash-based and metakaolin-based geopolymer wood fiber composites. Specific compressive strength and density profiles were used as a means of comparing the influence of the mixing variations. From the study, similar strength and density profile were recorded for both fly ash-based and metakaolin-based geopolymer wood fiber composites. It can be concluded that when to add what raw material does not really matter in the formulation of geopolymer wood fiber/ flour composites, on the condition that the mixing time and amount of raw materials remain the same. This gives more flexibility during composite formulation or production.

Acknowledgements

The authors are grateful for the financial support provided by the BioHome project funded by the Bundesministerium für Bildung und Forschung (BMBF) [grant number 01DG17007A] and the DAAD project [grant number 57359374].

Reference

Alomayri, T.; Low, I. M. (2013): Synthesis and characterization of mechanical properties in cotton fiber-reinforced geopolymer composites. In *Journal of Asian Ceramic Societies* 1 (1), pp. 30–34. DOI: 10.1016/j.jascer.2013.01.002.

Asante, B.; Ye, H.; Nopens, M.; Schmidt, G.; Krause, A. (2022). Influence of wood moisture content on the hardened state properties of geopolymer wood composites. *Composites Part A*, 152 <https://doi.org/10.1016/j.compositesa.2021.106680>

Berzins, A.; Morozovs, A.; Gross, U.; Iejavs, J. (2017): Mechanical properties of woodgeopolymer composite. In: Engineering for rural development-16th international scientific conference. Latvia University of Agriculture, May, 2017. pp. 1167–1173.

Fan, Mizi; Ndikontar, Maurice Kor; Zhou, Xiangming; Ngamveng, Joseph Noah (2012): Cement-bonded composites made from tropical woods: Compatibility of wood and cement. In *Construction and Building Materials* 36, pp. 135–140. DOI: 10.1016/j.conbuildmat.2012.04.089.

Frybort, S.; Mauritz, R.; Teischinger, A.; Müller, U. (2008): Cement bonded composites review. In *BioResources* 3 (2), pp. 602–626.

Furtos, G.; Silaghi-Dumitrescu, L.; Pascuta, P.; Sarosi, C.; Korniejenko, K. (2021): Mechanical Properties of Wood Fiber Reinforced Geopolymer Composites with Sand Addition. In *Journal of Natural Fibers* 18 (2), pp. 285–296. DOI: 10.1080/15440478.2019.1621792.

Hanzlicek, T.; Steinerova-Vondrakova, M. (2002): Investigation of Dissolution of Aluminosilicates in Aqueous Alkaline Solution under Laboratory Conditions. In *Ceramics – Silikáty* 46 (3), pp. 97–103.

Malenab, R. A. J.; Ngo, J. P. S.; Promentilla, M. A. B. (2017): Chemical Treatment of Waste Abaca for Natural Fiber-Reinforced Geopolymer Composite. In *Materials (Basel, Switzerland)* 10 (6). DOI: 10.3390/ma10060579.

Sá Ribeiro, R. A.; Sá Ribeiro, M. G.; Sankar, Kaushik; Kriven, W. M. (2016): Geopolymer-bamboo composite – A novel sustainable construction material. In *Construction and Building Materials* 123, pp. 501–507. DOI: 10.1016/j.conbuildmat.2016.07.037.

Sagoe-Crentsil, K.; Weng, L. (2007): Dissolution processes, hydrolysis and condensation reactions during geopolymer synthesis. Part II. High Si/Al ratio systems. In *Journal of Materials Science* 42 (9), pp. 3007–3014. DOI: 10.1007/s10853-006-0818-9.

Sanaev, V. G.; Zaprudnov, V. I.; Gorbacheva, G. A.; Oblivin, A. N. (2016): Factors affecting the quality of wood-cement composites. *Bulletin of the Transilvania University of Braşov Series II: Forestry • Wood Industry • Agricultural Food Engineering* 9 (58), pp. 63–70.

Sarmin, S. N. (2016): The Influence of Different Wood Aggregates on the Properties of Geopolymer Composites. In *Key Engineering Materials* 723, pp. 74–79. DOI: 10.4028/www.scientific.net/KEM.723.74.

Sarmin, S. N.; Welling, J. (2016): Lightweight geopolymer wood composite synthesized from alkali-activated fly ash and metakaolin. In *Jurnal Teknologi* 78 (11), pp. 49–55.

Tan, J.; Lu, W.; Huang, Y.; Wei, S.; Xuan, X.; Liu, L.; Zheng, G. (2019): Preliminary study on compatibility of metakaolin-based geopolymer paste with plant fibers. In *Construction and Building Materials* 225, pp. 772–775. DOI: 10.1016/j.conbuildmat.2019.07.142.

Yel, H.; Cavdar, A.D.; Torun, S. B. (2020): Effect of press temperature on some properties of cement bonded particleboard. In *Maderas, Cienc. tecnol.* (ahead), p. 0. DOI: 10.4067/S0718-221X2020005000108.

Zuhua, Z.; Xiao, Y.; Huajun, Z.; Yue, C. (2009): Role of water in the synthesis of calcined kaolin-based geopolymer. In *Applied Clay Science* 43 (2), pp. 218–223. DOI: 10.1016/j.clay.2008.09.003.

CHAPTER 7

DISCUSSION OF THE CONDUCTED RESEARCH

Since there are no commercially available products of GWCs, the results of this work will be compared to other GWCs and cement wood composites from other research works. Discussion in this chapter is based on the two research scopes stated in the introduction part.

7.1 Evaluation of how wood's inherent properties affect properties of geopolymer wood composites

Overall, the effect of wood's inherent properties were identified in Chapters 3 (3.1 and 3.2). Based on the findings, it can be concluded that wood's inherent properties affect both the physical and compressive strength properties of fly ash based geopolymer wood composites. However, in this present studies, the extent of these effects depend on:

- Wood species
- Portion of wood
- Type of extractives

7.1.1 Effect of wood species on the properties of geopolymer wood composite

To achieve appropriate and acceptable composite properties in IBWC, the wood has to be properly mixed with an inorganic matrix and has to be properly encased in the matrix. This calls for proper compatibility between the matrix and the filler/reinforcement. The results from Chapter 3.1 (Fig. 3.1.5, Table 3.1.3) showed that Eucalypt was more compatible for fly ash-based GWCs than Pine. The geopolymer wood composites (GWCs) based on eucalypt had a significantly higher dry bulk density and lower water absorption compared to those from pine. A plausible reason for this behavior can be explained by the roles of the densities of eucalypt and pine. Eucalypt wood used in the study had an apparent density of 0.56 g/cm^3 while pine

had 0.39 g/cm³. These densities contributed to the overall bulk density of their respective GWCs. Wood density, which is a measure of the quantity of cell wall material contained in a specific volume, had been found to be one of the factors influencing the overall density and water absorption of the IBWC's (Amiandamhen 2017). However, with hot water pre-treatment of both eucalypt and pine wood, the bulk densities and water absorption remained the same with no difference between the treated and untreated GWCs. A chemical analysis of the wood after the treatment showed that the extracts in both eucalypt (from 4.08% to 1.33%) and pine (from 2.74% to 1.47%) were reduced. However, the structural components of the wood remained the same (Chapter 3.1, Table 3.1.4). In addition, wood density is known to affect the permeability of wood and wood based products (Syofuna et al. 2012). It has been reported that extractives in wood can range from 1 – 20 % of the dry weight and can there affect the wood density (Singleton et al. 2003). It is possible that the change in the extracts' content (67.4% and 46.4% for eucalypt and pine respectively), did not affect the density of the wood materials after the hot water pre-treatment and therefore had no influence on the bulk densities of the GWCs. Although high amount of extracts were removed from eucalypt wood as compared to pine after the hot water extraction, the water absorption of GWCs with eucalypt was lower. This resistance could be attributed to their high densities, meaning that they are able to remain durable even after extractive removal (Syofuna et al. 2012). It has also been reported that the crystalline regions of the cellulose increase with wood density (El-Osta 1971) and these crystalline regions of the cellulose are inaccessible to water molecules (Hernández 2007). These might have contributed to the reduced water absorption for the GWC with eucalypt wood.

7.1.2 Effect of wood extractives on the properties of geopolymer wood composite

The reduction in extracts content by the hot water treatment (Chapter 3.1, Table 3.1.4) led to a significant difference in specific compressive strength of the composites with untreated and treated wood. There was a 3% and 27% increase in specific strength of the GWC with eucalypt and pine wood respectively, indicating improved compatibility after the extract removal. Although the matrix properties of cement are different from a geopolymer (see Chapter 1, section 1.6.2), Garcez et al. (2016) found that eucalypt wood was more compatible with cement than pine. Even though softwoods have been found to be more compatible with cement than hardwoods (Weatherwax and Tarkow 1964), this was not in the case with the fly ash-based geopolymer. To clarify these notions, four hardwoods (two eucalypt species and two acacia species) and two softwoods extractives (i.e. extracts from pine and spruce) were used in pure fly ash-based geopolymers (Chapter 3.2). It could be seen that the addition of spruce and pine extractives lowered the compressive strength, while the four hardwoods extractives geopolymer had similar strength compared to the control (Chapter 3.2, Fig. 3.2.7). However, the greatest strength reduction was observed in samples with pine extractives. This leads to the conclusion that there were pine specific extracts causing the reduction in strength.

A GC-MS/FID analysis was performed on pine sapwood and heartwood extracts extracted with NaOH. The GC-detectable compounds of sapwood extractives consist of up to 39 wt% of saturated and unsaturated fatty acids while terpenoids and resin acids accounts for an amount of 26 wt%; in the extractives from heartwood, terpenoids and resin acids occur predominantly, with an amount of up to 51 wt% of the GC-detectable substances. The diversity of compounds is higher in sapwood extract than in hardwood extract (Chapter 3.2, Table 3.2.7). From the GC-MS/ FID analysis, one of the major difference in extracts composition between the sapwood and heartwood of pine is their proportion of fatty and resin acids.

The sapwood contains more fatty acids while the heartwood contains more of resin acids (Back and Allen 2000). This was also confirmed in these present studies (Chapter 3.2, Table 3.2.7). Both fatty acids and resin acids are composed of different compounds and molecules. Owing to this, in order to understand the influence of specific extractives on the strength of fly ash-based geopolymer, the present work considered two fatty acids (linoleic and oleic acids), one resin acid (i.e. abietic acid) and three polyphenols (i.e. condensed tannins, pycogenol and tannic acids). All the geopolymers with specific extractives recorded lower specific strengths when compared to the control (Chapter 3.2, Fig. 3.2.3). Geopolymers with pycogenol, tannin and abietic acid (resin acid) recorded similar strength to the geopolymers with sapwood or heartwood extract. Nonetheless, geopolymers with linoleic and oleic acids (Fatty acids) recorded lower strengths. Although Portland cement is different from a geopolymer, similar observations were made by Tugrul Albayrak et al. (2005), who found that oleic acid and sunflower oil (containing oleic and linoleic acids) decreases the compressive strength of concrete.

Shill et al. (2020) and Shill et al. (2022) found that esters of fatty acids reacted with free NaOH in fly ash geopolymers at high temperatures to produce sodium carboxylate, which is a salt, in a process known as saponification. Shill et al. (2020) also identified the presence of soap and salt compounds, e.g., sodium carboxylate and sodium phosphates in the fly ash based geopolymer mortar after the saponification occurrence. The authors defined this process of the formation of soap compounds on geopolymer as saponification of a geopolymer; this occurred when fatty acids (linoleic and oleic acids) were exposed to the geopolymer at a high temperature. Saponification significantly weakened the top layer of the geopolymer mortar and resulted in a reduction in the compressive strength (Shill et al. 2020).

As all the tested specific extracts had an influence on the strength property investigated, the combined effect of these specific extractives could even be greater. Nevertheless, the extent of this variation might depend, among other factors, on the amount and nature of wood extractives present in the mixture (Sandermann et al. 1960; Biblis and Lo 1968; Fischer et al. 1974; Liu and Moslemi 1985) as observed in cement and the combination of the specific extracts and compounds.

7.1.3 Effects of the portion of wood and pretreatment on the properties of geopolymer wood composite

The portion of wood (i.e. sapwood or heartwood) is another influencing factor for the interaction between the geopolymer and the wood. Due to the higher solubility of heartwood vs. sapwood suggesting that a greater amount of substance could be leached out (Cabangon et al. 2000) to disturb the geopolymerization, it was expected that the strength of the GWC formed with the sapwood and heartwood would be different. In contrast, the results in Chapter 3.2 (Fig. 3.2.4) showed that forming a fly ash-based GWC with both untreated pine heartwood and sapwood yielded the same specific strength. This contradicts the findings by (Semple and Evans 2000), who found that the heartwood of radiata pine severely inhibited cement hydration, and the wood-cement boards made with the heartwood had little structural integrity, while boards made from the sapwood have been made industrially and commercialized. However, with pretreatment a clear difference was observed between the GWCs made from sapwood and heartwood.

Hot water pretreatment of pine wood led to an increase in the strength of the composites (Chapter 3.1). Similar observations were made when the pine sapwood and heartwood were pretreated with a NaOH solution (Chapter 3.2). These increases in strength might be related to

the enhanced compatibility between the wood and the fly ash geopolymer matrix. In contrast to these results, research by (Sarmin et al. 2020) showed that NaOH pretreatment of wood decreases compatibility between the wood and geopolymer matrix. The authors worked with spruce (*Picea abies* veneer) and a blend of fly ash/metakaolin geopolymer, which might be the reasons for these differences with NaOH pretreatment. However, compared to cement wood composites, both hot water and NaOH pretreatment are known to increase strength properties, with the latter being most effective (Sutigno 2000). This suggests that the issues of pretreatment for compatibility as well as interface problems are much more complicated when dealing with GWCs compared to other IBWCs. Hence, pretreatment for improved compatibility and strength in GWCs might directly relate to the wood species, portion of wood as well as the geopolymer matrix material.

7.2 Evaluation of material preprocessing of geopolymer wood composites

In the present thesis, it is indicated, that there is a lack of systematic processes in place to fully exploit the potential use of wood fibers and particles as reinforcement and fillers respectively in geopolymer wood bonded composites. Chapters 4, 5 and 6 show the effect material preprocessing and the effect of different mixing processes during the manufacturing of GWC. The results of the conducted study, are summarized as follows:

- a) Water molecules become part of the fly ash-based GWC structure, which could not be removed by drying. The different wood moisture contents used in the GWC manufacture contributed differently to the amount of water that remained after GWC drying.
- b) Preparation of wood veneer surface by sanding led to an increase in interfacial bonding strength between the wood and the metakaolin-based geopolymer matrix.
- c) The different mixing and processing technologies had no effect on the properties of both fly ash-based and metakaolin-based GWCs, as long as the amount of raw materials and

mixing time for the different processes was kept constant. That is to say, it did not matter when to add what raw material during composite formulation as all the different processes resulted in the same density and compressive strength.

7.2.1 Effect of wood moisture content on the properties of geopolymer wood composite

The differing amount of water held in the wood (wood moisture content) contributed differently to the structural bound water (i.e. water that could not be evaporated and remained in the final GWC), density, porosity, compressive strength and the specific compressive strength of the fly ash-based GWC (Chapter 4, Fig. 4.1, 4.3, 4.4, 4.5 and 4.6). Wood consists mainly of cellulose, hemicellulose and lignin as structural components. These components possess an abundant number of hydroxyl (OH-groups) (Wang and Piao 2011). Thus, wood is a hydrophilic material, which is an intrinsic property of wood and its affinity for water (Wang and Piao 2011). Water is only found in the cell walls below fiber saturation (i.e. bound water), yet it is located in the pores of cells, cell lumens or cavities as free water above fiber saturation threshold (moisture content of about 30%, depending on species) (Engelund et al. 2013). The hydrophilicity and porosity of wood cause it both to absorb liquid water and absorb moisture vapor from the air. According to Wang and Piao (2011) the interactions between wood and water vapor, and wood and liquid water have profound impacts on the physical properties, mechanical properties, and utility in wood and wood-based products. As a result, controlling moisture in wood is crucial for ensuring fly ash-based GWC performance.

Generally, composites manufactured with a low amount of initial wood moisture content performed better than those with a high moisture content i.e. density, porosity, compressive strength and the specific compressive strength of the composites were favorable with dry wood (Chapter 4). Lizcano et al. (2012) stated that in a Na-activated pure metakaolin-based

geopolymer, about 15–20 wt% remained as residual or non-evaporable water with most of the water evaporated during 21 days curing and aging in ambient conditions. However, this could not be confirmed in the present study. Even with heating to 103°C, the present findings indicate about 25–30% of the initial water molecules were tightly incorporated and partly inaccessible and could not be removed from the fly ash-based GWC. Kobera et al. (2011) also found that the immobilized water that does not leave the aluminosilicate network, forms amorphous aluminosilicate hydrates in which water molecules are strongly bound to the matrix. Contrastingly, Davidovits (2008) and Perera et al. (2006) showed that additional weight loss (due to water removal) could occur in the geopolymer at temperatures of 300 °C and above. Thus, the tightly incorporated water molecules might be removed at elevated temperatures. However, said temperature increase might lead to greater mass loss due to decomposition of the wood, as wood product's performance is affected by the thermal degradation of its chemical components as it reaches elevated temperatures. Between 100 °C and 200 °C, the wood components in wood products dehydrates, generating water vapor and other noncombustible gases and liquids, such as CO₂, formic acid, acetic acid, and water. With prolonged exposures at higher temperatures, wood can become charred. As the temperature rises above 200 °C, thermal decomposition (i.e. pyrolysis) occurs for hemicelluloses (between 200-300 °C) and for lignin components (between 225- 450 °C) (White and Dietenberger, 2001).

7.2.2 Effect of wood surface roughness on the properties of geopolymer wood composite

The process of bonding wood to geopolymer is essentially completed after transition of the geopolymer binder from gel or slurry to solid form. In bonding wood to other materials such as geopolymer, penetration and surface roughness are among the most important factors to consider (Cheng and Sun 2006; Sulaiman et al. 2009). Cheng and Sun (2006) stated an appropriate penetration depth into the wood surface is necessary for a strong bond to be formed.

In wood, penetration occurs when a binding agent enters the lumen/ cavities, or cell wall as a result of fluid, gel, or slurry movement (Marra 1992). The interface region of the bond is defined as the volume containing both wood cells and binding agent. It is created when the binding agent penetrates into the wood's cavities and partially fills them. In addition to wood-related parameters such as the diameter of the lumen/ cavity and the portion of the bisected lumen/ cavity on the wood surface, the properties of the binding agent (Kamke and Lee 2007), the bonding processing parameters, hardening time and curing rate of the binding agent (Resnik et al. 1997) all play a role.

The surface texture of wood is composed of anatomical roughness (such as the presence of extracts and oil, waxes etc.) as well as the roughness due to processing (such as cutting, peeling and planning) (Okumura and Fujiwara 2007; Sulaiman et al. 2009). According to Petri (1987), surface roughness affects the bonding because it increases the total contact area between binding agent and substrate. It could also provide an interlocking effect, trapping the binding agent in the cavities and acting as an anchor. The roughness of wood surface could be improved to a certain extent by sanding; Taylor et al. (1999) mentioned that surface roughness is influenced by its anatomical structure, particularly the cell cavities. That could be caused by its non-homogeneous structure. Cross grain, annual ring width, rays, knots, reaction wood, and the proportion of earlywood to latewood were other factors that affected it.

According to Coelho et al. (2008.), sanding is the operation that makes the wood surface more homogeneous, reducing the influence of the anatomical structure on the roughness profile. It has the ability to make the wood surfaces more uniform and later to absorb or allow for better penetration of the binding agent (Sulaiman et al. 2009). However, Moura and Hernández (2006) stated that in sanding the wood, the sanding grains act as small knives on the wood

surface producing dust with different exit angles. Hernández and Cool (2008) showed in a visual analysis, the occurrence of raised fibers caused by the abrasive action of sanding on the sanded surface. For Meijer (2004), sanding could negatively affect wood bonding by reducing the number of open cell capillaries.

In this present thesis, the highest surface roughness was detected after being sanded with grit size 60, whereas the lowest value was detected with grit size 180. Based on the roughness values (Chapter 5, Table 5.2) determined, from the surface of spruce and beech veneers, the surface roughness of the wood veneers was improved significantly by decreasing the grit size of sandpaper. It is probable that the P60 grits size sandpaper might have created deeper cavities on the wood surfaces as reported by Gurau et al. (2019). The increased surface roughness of the wood when using P60 sandpaper might have caused enough penetration into the wood cavities and improved mechanical interlocking (i.e. between the wood and the metakaolin-based geopolymer), leading to a higher interfacial bonding strength as observed in this present thesis (Chapter 5, Fig. 5.5). Additionally, beech samples showed a smoother surface than spruce samples when sanded with the same grit size, which is consistent with the findings of earlier studies (Papp and Csiha 2017). This is due to the fact that beech, as compared to spruce, typically has a higher density and more regular distribution of anatomical components, like libriform fibers (Kminiak and Gaff 2015). Moreover, Magross (2015) observed that sanding caused a clogging effect on the surface and decreased the number and size of the beech's anatomical cavities.

Several authors have also reported an inverse relationship between wood density and surface roughness, that is, the lower the density, the greater the roughness, which is in line with the results obtained in this study (Aguilera and Muñoz 2011; Dias Júnior et al. 2013; Laina et al.

2017; Silva et al. 2016). Although density may be a rough indicator, it can be used to estimate the bondability of a wide range of wood species, as was previously mentioned (Forest Products Laboratory 1999). High density woods are difficult to bond for several reasons. Binding agents cannot easily penetrate due to thicker cell walls and a smaller lumen volume. Therefore, significant mechanical interlocking of binding agents and wood is only possible to a depth of one or two cells (Forest Products Laboratory 1999). To attain the highest interfacial bonding strength, the geopolymer must penetrate and mechanically interlock several cell cavities (Chapter 5, Fig. 5.5a–b). In conclusion, both the type of wood and sanding under different conditions have an effect on the surface roughness and interfacial bonding strength between the wood and the metakaolin-based geopolymer.

7.2.3 Effect of dimensional instability in wood on the interfacial bonding strength

Moreover, interfacial bonding strength was increased under wet curing conditions (20 °C / 85% RH), while a weak interface was mainly caused by the wood shrinking under dry conditions (20 °C / 35% RH) during the curing process. Another key factor affecting the interfacial bonding strength is wood shrinkage and swelling (i.e. dimensional instability in wood). As already mentioned above, water exists as free or bound in wood. Instabilities in wood's dimensions (swelling and shrinking) result from changes in bound water. The total amount of bound water depends on the ambient temperature and relative humidity, and as a result of hysteresis whether the water is being absorbed or adsorbed. It is worth mentioning that water sorption is a time-dependent process, and the amount of bound water will also depend on the conditioning time and size of the piece of wood being conditioned. As a result of constant temperature and relative humidity, wood eventually reaches equilibrium moisture content (EMC), a constant moisture content. Wood swells and shrinks because of changes in the

amount of bound water, but does not develop dimensional instabilities when the amount of free water changes (Arzola-Villegas et al. 2019).

During the curing of the metakaolin geopolymer wood composites, the wood experienced some dimensional changes (first swelling and later shrinking) due to a change in the moisture content, while the geopolymer transformed from paste (gel) to solid (Chapter 5, Table 5.3 and Fig. 5.7). In the swollen state, the wood veneer was incorporated optimally in the geopolymer with no evidence of a visible gap between the interface of geopolymer and wood. However, the wood shrank, beginning on the fourth day of the curing process. The dimensional changes in the geopolymer between days 4 and 7 can be ignored in comparison with the wood shrinkage, as when the wood started to shrink after curing for 4 days, the dimension of the geopolymer was nearly consistent. Thus, the interfacial weakening (i.e. the gap at the interface between wood and geopolymer) was mainly due to the shrinking of the wood veneer. However, when the geopolymers with the veneer were cured at a higher relative humidity, the dimensions of the wood might have been stable or experienced minimal to negligible change and therefore resulted in a higher interfacial bonding strength.

7.2.4 Influence of different mixing and manufacturing process on the density and strength of geopolymer wood composite

Mixing wood directly with a geopolymer could potentially affect the water:geopolymer binder ratio; this could limit the water and ions available for geopolymerization due to migration of water/ions into the wood (Alomayri and Low 2013). Direct mixing of wood with the aluminosilicate material could also limit the amount/ area of contact between the alkaline activator solution and the aluminosilicate precursor material. This indicates that when to add what material during GWC fabrication may be crucial to the resulting composite. GWC process

technology leading to poor or low composite properties, may limit the practical application of a geopolymer wood composite. However, the results in Chapter 6 show that the five (5) different mixing variations resulted in similar strength/ minimal difference in strength and density profile. The minimal differences in the strength ranges shows that there is more flexibility during mixing or composite formation.

Even though the results in Chapter 4 showed that using wood with a high moisture content results in a GWC with a lower strength, saturating the wood flour and fibers (Chapter 6) prior to mixing led to similar strength as when the water was added separately to the mixtures. These same phenomena were recorded for the fly ash-based geopolymer wood flour/fiber composites and metakaolin-based wood fiber composites. Practically speaking, in order for Mix D and E to achieve similar strength to Mix A- C, there is no need to completely dry the wood to a very low moisture content prior to composite formation. This might help cut down production cost in both fly ash-based and metakaolin-based geopolymer wood composites. It can be concluded, that the water present in the wood adds up to the total water content in the mixture and, as much as the total water to solid content and other mixing parameters are the same, will lead to similar strength results.

CHAPTER 8

GENERAL CONCLUSION FROM THE RESEARCH

From the results and discussion of the present thesis, the following conclusions were made:

- The wood species used significantly influenced the fly ash-based GWC's specific compressive strength, as eucalypt-based composites yielded a strength nearly double that of pine ones. Furthermore, the wood species affected the composite's density and played a vital role in the water absorption of the composite. The hot-water pretreatment markedly increased the specific compressive strength of pine-based fly ash-based GWCs, but not those of the eucalypt ones. Hot water washing out the pine-specific extracts led to a improved compatibility between wood and fly ash geopolymer matrix.
- Forming a fly ash-based GWC with both untreated pine heartwood and sapwood yielded the same specific strength. However, NaOH pretreatment of both pine sapwood and heartwood increased the specific strength of fly ash-based geopolymer wood composites. With NaOH pretreatment of pine wood before its use in a geopolymer wood composite, the specific strength of geopolymer sapwood composites were higher than those with heartwood, indicating that the pretreatment was more effective for the sapwood than the heartwood.
- The specific strengths of fly ash-based geopolymers with hardwoods (i.e. *E. grandis*, *E. camaldulensis*, P. Jackson and B. wattle) extracts were not affected, while those with the softwoods (i.e. Norway spruce and pine) were reduced. Specific strengths of fly ash-based geopolymers with pycogenol, tannin, tannic acid, abietic acid, and fatty acids (i.e. linoleic and oleic acids) were reduced. However, the greatest reduction in specific

strengths was observed in the fly ash-based geopolymer containing fatty acids (i.e. linoleic and oleic acids).

- After drying the fly ash-based GWCs at 103 degrees, water became part of the GWC (i.e. structurally bound water). Different wood moisture contents (MC) contributed differently to structurally bound water amounts. Forming fly ash-based GWCs using a higher wood MC led to inferior interfacial bonding (gaps) between the fly ash geopolymer matrix and the wood. This decreased the maximum load transfer capacity and led to a lower compressive strength.
- Initial wood MC, climate chamber aging and drying conditions all affected the rate of water loss from the composites. When producing a fly ash-based GWC with high strengths, a low wood moisture content should be introduced in practice. However, the wood component does not have to be completely predried, saving energy and production costs. For optimal endurance of the GWC, it is important to keep the raw materials as dry as possible.
- It was found that the pullout force increased with an increase in embedded depth of the wood veneer, and a plateau was detected at a depth of 25 mm. Compared to beech, spruce showed a higher interfacial bonding strength between the wood and metakaolin-based geopolymer. Strong mechanical interlocking at the interface was successfully achieved by sanding the wood surface with a grit size 60 sandpaper. A weak interface was mainly caused by the wood shrinking under dry conditions during the curing process.

- Varying the mixing parameters i.e. the timing and order of the addition of the raw material components, does not really affect the density and specific compressive strength of both fly ash based and metakaolin-based GWCs. This allows for more flexibility during the manufacturing of both fly ash based and metakaolin-based GWCs.

Finally, it can be stated, that according to the presented results and conclusions, the geopolymer wood composite behavior is a result of a purposeful raw materials selection, accounting for the mechanical and physical properties of both the geopolymer matrix and the wood, and of their interaction.

LIST OF TABLES

- Table 3.1.1** Chemical composition (% by mass) of fly ash from XRF test.
- Table 3.1.2** Extraction conditions for extractive content.
- Table 3.1.3** Mean comparison (standard deviation) of physical properties of geopolymer wood composites (GWC) from ground fly ash. Means in the same column with same letters (a, b or c) are not significantly different ($p > 0.05$).
- Table 3.1.4** Chemical composition of treated and untreated wood particle (%).
- Table 3.1.5** Effect of fly ash particle size on the mean (standard deviation) of the physical properties of geopolymer wood composites (GWC) made with eucalypt. Means in the same column with same letters (a, b or c) are not significantly different ($p > 0.05$).
- Table 3.1.6** Mean comparison (standard deviation) of eucalypt-based geopolymer wood composite before and after 200 cycles of soak/dry conditions. Means in the same column with same letters (a, b or c) are not significantly different ($p > 0.05$).
- Table 3.2.1** Chemical composition of fly ash in weight percentage share (%) by XRF analysis.
- Table 3.2.2** Extraction method and wood pretreatment.
- Table 3.2.3** The mix design of fly ash geopolymer with wood extractives.
- Table 3.2.4** Preparation of geopolymer wood composite.
- Table 3.2.5** Dry matter content (%) of extractives.

Table 3.2.6	Semi-quantification of DCM-extractable compounds of alkaline extractives from pine sap- and heartwood at pH-value 7 and 2 in relation to internal standard (IS) area.
Table 3.2.7	Semi-quantification of DCM extractable compounds of alkaline extractives from pine sap- and heartwood at pH-value 2 after derivatization with TMAH.
Table 4.1	Chemical composition of fly ash from XRF.
Table 4.2	Composites with their code.
Table. 4.3	Composite mass loss due to water evaporation from casting - 60 days aging in climate chamber and drying at 103°C.
Table 4.4	Exponential decay function fitted to composite mass loss data.
Table 5.1	Initial moisture conditions before curing and the environmental humidity conditions during curing of the spruce and beech veneers.
Table 5.2	Surface roughness values of spruce and beech veneers.
Table 5.3	Dimensional change rate of geopolymer and embedded wood after curing for 4 and 7 days. Positive (+) and negative (-) symbols mean the swelling and shrinking of the samples, respectively.
Table 6.1	Chemical composition of fly ash from XRF.
Table 6.2a	Composite mixture by mass ratio for geopolymer wood flour composites.
Table 6.2b	Composite mixture by mass ratio for geopolymer wood fiber composites.
Table 6.3	Manufacturing process for geopolymer wood composites.

LIST OF FIGURES

- Fig. 1.1** Geopolymer systems based on the number of siloxo Si-O units.
- Fig. 1.2** Geopolymerization reaction process.
- Fig. 1.3** Reinforcement/fiber, matrix and composite material.
- Fig. 3.1.1A** Wood particles before and after hot water treatment: (1a) untreated pine; (1b) treated pine; (1c) untreated eucalypt; (1d) treated eucalypt.
- Fig. 3.1.1B** FESEM images of wood particles before and after hot water treatment: (1e) untreated pine; (1f) treated pine; (1g) untreated eucalypt; (1h) treated eucalypt.
- Fig. 3.1.2** Particle size distribution and SEM for raw (2a- 2b) and ground (2c- 2d) fly ash.
- Fig. 3.1.3** X-ray (powder) diffraction analysis of raw and ground fly ashes.
- Fig. 3.1.4** Specific compressive strength of geopolymer wood composites from ground fly ash.
- Fig. 3.1.5** Effect of fly ash particle size on specific compressive strength of GWC made from eucalypt.
- Fig. 3.2.1** The morphology of wood particle used for extraction of wood extractives.
- Fig. 3.2.2** Manufacturing process of hardened geopolymer paste and geopolymer bonded wood composite.
- Fig. 3.2.3** Morphology of pine wood particles before and after NaOH treatment: **a** untreated sapwood; **b** treated sapwood; **c** untreated heartwood; **d** treated heartwood.
- Fig. 3.2.4** FTIR of untreated and NaOH treated pine sapwood and heartwood.

- Fig. 3.2.5** Specific compressive strength of fly ash geopolymer wood composite with treated and untreated pine sapwood and heartwood.
- Fig. 3.2.6** Specific compressive strength of pure fly ash geopolymer with pine sapwood and heartwood extracts.
- Fig. 3.2.7** Specific compressive strength of pure fly ash geopolymer with hardwood and softwood extractives (Means with same letters are not significantly different, $p>0.05$).
- Fig. 3.2.8** Specific compressive strength of pure fly ash geopolymer with softwood specific extracts.
- Fig. 4.1** State transformation of initial water in the final composites after aging and drying conditions.
- Fig. 4.2** Illustration of water forms and state transformation of initial water in the geopolymer wood composites.
- Fig. 4.3** Water released from a GWC from casting- 60 days of aging in a climate chamber.
- Fig 4.4** Density development of geopolymer wood composites with wood of different MC.
- Fig 4.5** 7 days cumulative pore volume of geopolymer wood composites with different wood MC.
- Fig. 4.6a** 7 days compressive strength of geopolymer wood composites with different wood MC.

- Fig. 4.6b** 7 days specific strength of geopolymer wood composites with and without structurally bound water.
- Fig. 4.7** FESEM images of geopolymer wood composites (GWC) interfaces formed with different wood MC.
- Fig. 5.1** Pullout testing setup for the geopolymer-wood composites.
- Fig. 5.2** Pullout force of spruce and beech veneers at different embedded depths.
- Fig. 5.3** Relationship between embedded depth and interfacial bonding strength for spruce and beech.
- Fig. 5.4** Interfacial bonding strength between geopolymer and wood veneers sanded with grit sizes 60, 100, and 180.
- Fig. 5.5** Microscope images of the interface between wood and geopolymer: a spruce-60; b spruce-180; c beech-180.
- Fig. 5.6** SEM images of geopolymer and wood surfaces at the interface after pullout tests: a spruce fibers attached to the geopolymer; b geopolymer penetrated the spruce veneer; c beech fibers attached to the geopolymer; d geopolymer penetrated the beech veneer.
- Fig. 5.7** Influence of curing time on the wood moisture content in the geopolymer matrix: a from 0 to 7 days and b the magnification from 0 to 4 h.
- Fig. 5.8** Schematic diagram of the influences of moisture on bonding at the interface between geopolymer and wood during the curing process.
- Fig. 5.9** Interfacial bonding strength of geopolymer-wood composites under different curing conditions.

- Fig. 6.1** Effect of different mixing procedures on fly ash-based geopolymer Wood flour composite.
- Fig. 6.2** Effect of different mixing procedures on fly ash-based geopolymer wood fiber composite.
- Fig. 6.3** Effect of different mixing procedures on metakaolin-based geopolymer wood fiber composite.
- Fig. 6.4** Density profiles of fly ash-based geopolymer wood fiber composite (Mix A-E).
- Fig. 6.5** Density profiles of metakaolin-based geopolymer wood fiber composite (Mix A-E).

ABBREVIATIONS

IBWC	Inorganic bonded wood composites
OPC	Ordinary Portland cement
GWC	Geopolymer wood composite
MC	Moisture content
FSP	Fiber saturation point
ANOVA	Analysis of variance
FESEM	Field emission scanning electron microscope
SEM	Scanning electron microscope
XRD	X-ray diffraction
XRF	X-ray fluorescence
FTIR	Fourier Transform Infrared Spectroscopy
DCM	dichloromethane
GCMS	Gas chromatograph – mass spectrometry
FID	Flame Ionization detection
TMAH	Tetramethylammonium hydroxide
TP	Thermoporosimetry
Ra	Average roughness
Rz	Mean peak-to-valley height
Rmax	Maximum roughness
DCR	Dimensional change rate
DCRW	Dimensional change rate of wood veneer
DCRG	Dimensional change rate of geopolymer
Fig.	Figure

References

- Aguilera, A.; Muñoz, H. (2011): Rugosidad superficial y potencia de corte en el cepillado de *Acacia melanoxylon* y *Sequoia sempervirens*. In *Maderas, Ciencia y Tecnología* 13 (1), pp. 19–28. DOI: 10.4067/S0718-221X2011000100002.
- Al Bakri, A.; Mohd, M.; Izzat, Ahmad, M.; Muhammad F. M. T.; Kamarudin, H.; Khairul N. I.; Bnhussain, M. et al. (2012): Feasibility of Producing Wood Fibre-Reinforced Geopolymer Composites (WFRGC). In *Advanced Materials Research* 626, pp. 918–925. DOI: 10.4028/www.scientific.net/AMR.626.918.
- Alberto, M.; Mougel, E.; Zoulalian, A. (2000): Compatibility of some tropical hardwoods species with Portland cement using isothermal calorimetry. In *Forest Product Journal* 50 (9), pp. 83–88.
- Alomayri, T.; Low, I. M. (2013): Synthesis and characterization of mechanical properties in cotton fiber-reinforced geopolymer composites. In *Journal of Asian Ceramic Societies* 1 (1), pp. 30–34. DOI: 10.1016/j.jascer.2013.01.002.
- Amiandamhen, O. S. (2017): Phosphate Bonded Wood and Fibre Composites. Dissertation presented for the degree of Doctor of Philosophy. Stellenbosch University, South Africa. Wood Product Science.
- Arzola-Villegas, X.; Lakes, R.; Plaza, N. Z.; Jakes, J. E. (2019): Wood Moisture-Induced Swelling at the Cellular Scale—Ab Intra. In *Forests* 10 (11), p. 996. DOI: 10.3390/f10110996.
- Asante, B.; Schmidt, G.; Teixeira, R.; Krause, A.; Savastano, J. H. (2021): Influence of wood pretreatment and fly ash particle size on the performance of geopolymer wood composite. In *European Journal of Wood and Wood Products* 79 (3), pp. 597–609. DOI: 10.1007/s00107-021-01671-9.
- Asante, B.; Sirviö, J. A.; Li, P.; Lavola, A.; Julkunen-Tiitto, R.; Haapala, A.; Liimatainen, H. (2020): Adsorption of bark derived polyphenols onto functionalized nanocellulose: Equilibrium modeling and kinetics. In *AIChE J* 66 (2). DOI: 10.1002/aic.16823.
- Back, E. L.; Allen, L. H. (2000): Pitch control, wood resin and deresination. Atlanta, Ga.: Tappi.
- Bakharev, T. (2005a): Geopolymeric materials prepared using Class F fly ash and elevated temperature curing. In *Cement and Concrete Research* 35 (6), pp. 1224–1232. DOI: 10.1016/j.cemconres.2004.06.031.

- Bakharev, T. (2005b): Resistance of geopolymer materials to acid attack. In *Cement and Concrete Research* 35 (4), pp. 658–670. DOI: 10.1016/j.cemconres.2004.06.005.
- Bakharev, T.; Sanjayan, J. G.; Cheng, Y.-B. (1999): Alkali activation of Australian slag cements. In *Cement and Concrete Research* 29 (1), pp. 113–120. DOI: 10.1016/S0008-8846(98)00170-7.
- Barbosa, V. F.F; MacKenzie, K. J. D; Thaumaturgo, C. (2000): Synthesis and characterisation of materials based on inorganic polymers of alumina and silica: sodium polysialate polymers. In *International Journal of Inorganic Materials* 2 (4), pp. 309–317. DOI: 10.1016/S1466-6049(00)00041-6.
- Berzins, A.; Morozovs, A.; Gross, U.; Iejavs, J. (2017): Mechanical properties of woodgeopolymer composite. In: Engineering for rural development-16th international scientific conference. Latvia University of Agriculture, May, 2017. pp. 1167–1173.
- Biblis, E. L.; Lo, C. F. (1968): Sugars and other wood extractives: Effect on setting of southern pine cement mixtures. In *Forest Products Journal* 18 (8), 28-34.
- Bouaissi, A.; Li, L.; Al Bakri A., Mohd M.; Bui, Q.-B. (2019): Mechanical properties and microstructure analysis of FA-GGBS-HMNS based geopolymer concrete. In *Construction and Building Materials* 210, pp. 198–209. DOI: 10.1016/j.conbuildmat.2019.03.202.
- Cabangon, R. J.; Eusebio, D. A.; Soriano, F. P.; Cunningham, R. B.; Donnelly, C.; Evans, P. D. (2000): Effect of post-harvest storage on the suitability of *Acacia mangium* for the manufacture of wood-wool cement boards. In: Wood-cement composites in the Asia-Pacific region, Canberra, Australia. Pp. 97-104.
- Cassagnabère, F.; Diederich, P.; Mouret, M.; Escadeillas, G.; Lachemi, M. (2013): Impact of metakaolin characteristics on the rheological properties of mortar in the fresh state. In *Cement and Concrete Composites* 37, pp. 95–107. DOI: 10.1016/j.cemconcomp.2012.12.001.
- Chawla, K. K. (2012a): Introduction. In Krishan K. Chawla (Ed.): *Composite Materials*. New York, NY: Springer New York, pp. 3–6.
- Chawla, K. K. (2012b): Reinforcements. In Krishan K. Chawla (Ed.): *Composite Materials*. New York, NY: Springer New York, pp. 7–71.
- Chen, L.; Wang, Z.; Wang, Y.; Feng, J. (2016): Preparation and Properties of Alkali Activated Metakaolin-Based Geopolymer. In *Materials (Basel, Switzerland)* 9 (9). DOI: 10.3390/ma9090767.

- Chen, X.; Sutrisno, A.; Struble, L. J. (2018): Effects of calcium on setting mechanism of metakaolin-based geopolymer. In *Journal of American Ceramic Society* 101 (2), pp. 957–968. DOI: 10.1111/jace.15249.
- Cheng, E.; Sun, X. (2006): Effects of wood-surface roughness, adhesive viscosity and processing pressure on adhesion strength of protein adhesive. In *Journal of Adhesion Science and Technology* 20 (9), pp. 997–1017. DOI: 10.1163/156856106777657779.
- Coelho, C. L.; Carvalho, L. M. H.; Martins, J. M.; Costa, C. A. V.; Masson, D.; Me´ausoone, J. P. (2008.): Method for evaluating the influence of wood machining conditions on the objective characterization and subjective perception of a finished surface. In *Wood Science and Technology* 42 (3), pp. 181–195.
- Davidovits J. (2002): 30 years of successes and failures in geopolymer applications. Market trends and potential breakthroughs. In: Geopolymer 2002 Conference, Melbourne, Australia, Geopolymer Institute Library.
- Davidovits, J. (1989): Geopolymers and geopolymeric materials. In *Journal of Thermal Analysis and Calorimetry* 35 (2), pp. 429–441. DOI: 10.1007/BF01904446.
- Davidovits, J. (1991): Geopolymers. In *Journal of Thermal Analysis and Calorimetry* 37 (8), pp. 1633–1656. DOI: 10.1007/BF01912193.
- Davidovits, J. (2008): Geopolymer Chemistry and Applications, 2nd ed. Geopolymer Institute, Saint-Quentin: France;
- Dias J. A. F.; Santos, P. V.; Pace, J. H. C.; Carvalho, A. M.; Latorraca, J. V. F. (2013): Caracterização da Madeira de Quatro Espécies Florestais para Uso em Moveleira. In *Ciência da Madeira (Braz. J. Wood Sci.)* 4 (1), pp. 93–107. DOI: 10.12953/2177-6830.v04n01a08.
- Dimas, D.; Giannopoulou, I.; Pnias, D. (2009): Polymerization in sodium silicate solutions: a fundamental process in geopolymerization technology. In *Journal of Materials Science* 44 (14), pp. 3719–3730. DOI: 10.1007/s10853-009-3497-5.
- Doczekalska, B.; Zborowska, M. (2010): Wood chemical composition of selected fast growing species treated with naoh part i: structural substances. In *Wood Research* 55 (1), 41-48.
- Dönmez, İ. E.; Hafizoğlu, H.; Kılıç, A. (2013): Effect of Altitude on the Main Chemical Composition of Scots pine (*Pinus sylvestris* L.). In *International Caucasian Forestry Symposium, Artvin, Turkey*. Proceedings.
- Douiri, H.; Louati, S.; Baklouti, S.; Arous, M.; Fakhfakh, Z. (2014): Structural, thermal and dielectric properties of phosphoric acid-based geopolymers with different amounts of H₃PO₄. In *Materials Letters* 116, pp. 9–12. DOI: 10.1016/j.matlet.2013.10.075.

- Duan, P.; Yan, C.; Zhou, W.; Luo, W. (2016): Fresh properties, mechanical strength and microstructure of fly ash geopolymer paste reinforced with sawdust. In *Construction and Building Materials* 111, pp. 600–610. DOI: 10.1016/j.conbuildmat.2016.02.091.
- Duxson, P.; Fernández-Jiménez, A.; Provis, J. L.; Lukey, G. C.; Palomo, A.; van Deventer, J. S. J. (2007): Geopolymer technology: the current state of the art. In *Journal of Materials Science* 42 (9), pp. 2917–2933. DOI: 10.1007/s10853-006-0637-z.
- Duxson, P.; Provis, J. L.; Lukey, G. C.; Mallicoat, S. W.; Kriven, W. M.; van Deventer, J. S. J. (2005): Understanding the relationship between geopolymer composition, microstructure and mechanical properties. In *Colloids and Surfaces A: Physicochemical and Engineering Aspects* 269 (1-3), pp. 47–58. DOI: 10.1016/j.colsurfa.2005.06.060.
- Eckelman, C. A. (1998): The shrinking and swelling of wood and its effect on furniture. Purdue University Cooperative Extension Service.
- El-Osta M. L. M. (1971): Influence of some characteristics of coniferous wood tissues on short-term creep. PhD thesis. University of British Columbia, Vancouver.
- Engelhardt, G.; Michel, D. (Eds.) (1987): High Resolution Solid State NMR of Silicates and Zeolites. New York: Wiley.
- Engelund, E. T.; Thygesen, L. G.; Svensson, S.; Hill, C.A.S. (2013): A critical discussion of the physics of wood–water interactions. In *Wood Science and Technology* 47 (1), pp. 141–161.
- Fan, M.; Ndikontar, M. K.; Zhou, X.; Ngamveng, J. N. (2012): Cement-bonded composites made from tropical woods: Compatibility of wood and cement. In *Construction and Building Materials* 36, pp. 135–140. DOI: 10.1016/j.conbuildmat.2012.04.089.
- Fernandez, R.; Martirena, F.; Scrivener, K. L. (2011): The origin of the pozzolanic activity of calcined clay minerals: A comparison between kaolinite, illite and montmorillonite. In *Cement and Concrete Research* 41 (1), pp. 113–122. DOI: 10.1016/j.cemconres.2010.09.013.
- Fernández-Jiménez, A.; Palomo, A. (2003): Characterisation of fly ashes. Potential reactivity as alkaline cements. In *Fuel* 82 (18), pp. 2259–2265. DOI: 10.1016/s0016-2361(03)00194-7.
- Fernández-Jiménez, A.; Palomo, A. (2005): Composition and microstructure of alkali activated fly ash binder: Effect of the activator. In *Cement and Concrete Research* 35 (10), pp. 1984–1992. DOI: 10.1016/j.cemconres.2005.03.003.

- Fernández-Jiménez, A.; Palomo, A.; Sobrados, I.; Sanz, J. (2006): The role played by the reactive alumina content in the alkaline activation of fly ashes. In *Microporous and Mesoporous Materials* 91 (1-3), pp. 111–119. DOI: 10.1016/j.micromeso.2005.11.015.
- Ferreira, C.; Ribeiro, A.; Ottosen, L. (2003): Possible applications for municipal solid waste fly ash. In *Journal of hazardous materials* 96 (2-3), pp. 201–216. DOI: 10.1016/S0304-3894(02)00201-7.
- Fischer, F.; Wienhaus, O.; Ryssel, M.; Olbrecht, J. (1974): The water soluble carbohydrates of wood and their influence on the production of light weight wood wool boards. In *Holztechnologie* 15 (1), pp. 12–19.
- Forest legality Initiative (2022): Risk Tool. Available online at <https://forestlegality.org/risk-tool/species/black-wattle#:~:text=A.,well%20as%20for%20forest%20management>, checked on 7/17/2022.
- Forest Products Laboratory (1999): Wood handbook—Wood as an engineering material. Gen. Tech. Rep. FPL–GTR–113. Madison, WI: U.S. Department of Agriculture, Forest Service, Forest Products Laboratory. 463 p.
- Forest Products Laboratory (2010): Wood handbook—Wood as an engineering material. General Technical Report FPL-GTR-190. Madison, WI: U.S.
- Frederick, W. J.; Lien, S. J.; Courchene, C. E.; DeMartini, N. A.; Ragauskas, A. J.; Iisa, K. (2008): Production of ethanol from carbohydrates from loblolly pine: a technical and economic assessment. In *Bioresource technology* 99 (11), pp. 5051–5057. DOI: 10.1016/j.biortech.2007.08.086.
- Frybort, S.; Mauritz, R.; Teischinger, A.; Müller, U. (2012): Investigation of the mechanical interactions at the interface of wood-cement composites by means of electronic speckle pattern interferometry. In *BioResources* 7 (2), pp. 2483–2495.
- Furtos, G.; Silaghi-Dumitrescu, L.; Pascuta, P.; Sarosi, C.; Korniejenco, K. (2021): Mechanical Properties of Wood Fiber Reinforced Geopolymer Composites with Sand Addition. In *Journal of Natural Fibers* 18 (2), pp. 285–296. DOI: 10.1080/15440478.2019.1621792.
- Garcez, M. R.; Garcez, E. O.; Machado, A. O.; Gatto, D. A. (2016): Cement-Wood Composites: Effects of Wood Species, Particle Treatments and Mix Proportion. In *International Journal of Composite Materials* 6 (1), pp. 1–8. DOI: 10.5923/j.cmaterials.20160601.01.
- Giancaspro, J. W.; Papakonstantinou, C. G.; Balaguru, P. N. (2010): Flexural Response of Inorganic Hybrid Composites with E-Glass and Carbon Fibers. In *Journal of Engineering Materials and Technology* 132 (2). DOI: 10.1115/1.4000670.

- Giancaspro, J.; Papakonstantinou, C.; Balaguru, P. (2009): Mechanical behavior of fire-resistant biocomposite. In *Composites Part B: Engineering* 40 (3), pp. 206–211. DOI: 10.1016/j.compositesb.2008.11.008.
- Guo, C-M.; Wang, K-T.; Liu, M-Y.; Li, X-H.; Cui, X-M. (2016): Preparation and characterization of acid-based geopolymer using metakaolin and disused polishing liquid. In *Ceramics International* 42 (7), pp. 9287–9291. DOI: 10.1016/j.ceramint.2016.02.073.
- Gurau, L.; Irle, M.; Buchner, J. (2019): "Surface roughness of heat treated and untreated beech (*Fagus sylvatica* L.) wood after sanding,". In *BioResources* 14 (2), 4512-4531.
- Halas, O.; Benes, L.; Minar, L. (2011): Sawdust as a filler to alkali-activated fly-ash. In: Annals of DAAAM and proceedings of the 22nd international DAAAM symposium, pp. 797–799.
- Hernández, R. E. (2007): Effects of extraneous substances, wood density and interlocked grain on fiber saturation point of hardwoods. In *Wood Material Science & Engineering* 2 (1), pp. 45–53. DOI: 10.1080/17480270701538425.
- Hernández, R. E.; Cool, J. (2008): Effects of cutting parameters on surface quality of paper birch wood machined across the grain with two planing techniques. In *Holz Roh Werkst* 66 (2), pp. 147–154. DOI: 10.1007/s00107-007-0222-4.
- Huang, F.; Singh, P. M.; Ragauskas, A. J. (2011): Characterization of milled wood lignin (MWL) in Loblolly pine stem wood, residue, and bark. In *Journal of Agricultural and Food chemistry* 59 (24), pp. 12910–12916. DOI: 10.1021/jf202701b.
- Huang, Z.; Yan, N. (2013): Characterization of major components in barks from five canadian tree species. In *Wood and Fiber Science* 46 (2), pp. 167–174.
- Hughes, J. F. (1967): Hughes, J.F. 1967. Density as an index of wood quality with special reference to the development of rapid and efficient methods of estimating density. In: Proceedings of the Tropical Forestry Meeting by Commonwealth Forestry Institution. pp. 1–4.
- Izidoro, J. C.; Fungaro, D. A.; dos Santos, F. S.; Wang, S. (2012): Characteristics of Brazilian coal fly ashes and their synthesized zeolites. In *Fuel Processing Technology* 97, pp. 38–44. DOI: 10.1016/j.fuproc.2012.01.009.
- Izidoro, Juliana de C.; Fungaro, Denise Alves; dos Santos, Fernando S.; Wang, Shaobin (2012): Characteristics of Brazilian coal fly ashes and their synthesized zeolites. In *Fuel Processing Technology* 97, pp. 38–44. DOI: 10.1016/j.fuproc.2012.01.009.
- Jorge, F. C.; Pereira, C.; Ferreira, J. M. F. (2004): Wood-cement composites: a review. In *Holz Roh Werkst* 62 (5), pp. 370–377. DOI: 10.1007/s00107-004-0501-2.

- Kamke, F.; Lee, J. (2007): Adhesive Penetration in Wood—a Review. In *Wood Fiber Science* 39, pp. 205–220.
- Karayannis, V. G.; Moustakas, K. G.; Baklavaridis, A. N.; Domopoulou, A. E. (2018): Sustainable ash-based geopolymers. In *Chemical Engineering Transactions* 63, pp. 505–510.
- Khazaei, J. (2007): Water absorption characteristics of three wood varieties. In *Cercetări Agronomice în Moldova XLI* (2), p. 134.
- Kim, H.; Lee, J.-Y. 2017: Effect of ash particle size on the compressive strength and thermal conductivity of geopolymer synthesized with alkali activated low calcium ground coal bottom ash. In: 2017 World of coal ash. Lexington, KY, Lexington, KY.
- Kminiak, R.; Gaff, M. (2015): Roughness of Surface Created by Transversal Sawing of Spruce, Beech, and Oak Wood. In *BioResources* 10 (2). DOI: 10.15376/biores.10.2.2873-2887.
- Kobera, L.; Slavík, R.; Koloušek, D.; Urbanová, M.; Kotek, J.; Brus, J. (2011): Structural stability of aluminosilicate inorganic polymers: influence of the preparation procedure. In *Ceramics-Silikáty* 55 (4), 343–54.
- Komljenović, M.; Petrašinović-Stojkanović, Lj.; Baščarević, Z.; Jovanović, N.; Rosić, A. (2009): Fly ash as the potential raw mixture component for Portland cement clinker synthesis. In *Journal of Thermal Analysis and Calorimetry* 96 (2), pp. 363–368. DOI: 10.1007/s10973-008-8951-0.
- Komnitsas, K.; Zaharaki, D. (2007): Geopolymerisation: A review and prospects for the minerals industry. In *Minerals Engineering* 20 (14), pp. 1261–1277. DOI: 10.1016/j.mineng.2007.07.011.
- Krivenko, P. V.; Kovalchuk, G. Y. (2007): Directed synthesis of alkaline aluminosilicate minerals in a geocement matrix. In *Journal of Materials Science* 42 (9), pp. 2944–2952. DOI: 10.1007/s10853-006-0528-3.
- Kumar, B.; Tike, G. K.; Nanda, P. K. (2007): Evaluation of properties of high-volume fly-ash concrete for pavements. In *Journal of Materials in Civil Engineering* 19, pp. 906–911.
- Laina, R.; Sanz-Lobera, A.; Villasante, A.; López-Espí, P.; Martínez-Rojas, J. A.; Alpuente, J. et al. (2017): Effect of the anatomical structure, wood properties and machining conditions on surface roughness of wood. In *Maderas, Ciencia y Tecnología* (ahead), p. 0. DOI: 10.4067/S0718-221X2017005000018.
- Lan, T.; Meng, Y.; Ju, T.; Chen, Z.; Du, Y.; Deng, Y. et al. (2022): Synthesis and application of geopolymers from municipal waste incineration fly ash (MSWI FA) as raw ingredient

- A review. In *Resources, Conservation and Recycling* 182, p. 106308. DOI: 10.1016/j.resconrec.2022.106308.
- Lassinantti G. M.; Romagnoli, M.; Pollastri, S.; Gualtieri, A. F. (2015): Inorganic polymers from laterite using activation with phosphoric acid and alkaline sodium silicate solution: Mechanical and microstructural properties. In *Cement and Concrete Research* 67, pp. 259–270. DOI: 10.1016/j.cemconres.2014.08.010.
- Lee, A. W. C; Short, P. H. (1989): Pretreating hardwood for cement-bonded excelsior board. In *Forest Product Journal* 39 (10), pp. 68–70.
- Leiva, C.; Luna-Galiano, Y.; Arenas, C.; Alonso-Fariñas, B.; Fernández-Pereira, C. (2019): A porous geopolymer based on aluminum-waste with acoustic properties. In *Waste management (New York, N.Y.)* 95, pp. 504–512. DOI: 10.1016/j.wasman.2019.06.042.
- Li, Y.; Min, X.; Ke, Y.; Liu, D.; Tang, C. (2019a): Preparation of red mud-based geopolymer materials from MSWI fly ash and red mud by mechanical activation. In *Waste management (New York, N.Y.)* 83, pp. 202–208. DOI: 10.1016/j.wasman.2018.11.019.
- Li, Z.; Zhang, S.; Zuo, Y.; Chen, W.; Ye, G. (2019b): Chemical deformation of metakaolin based geopolymer. In *Cement and Concrete Research* 120, pp. 108–118. DOI: 10.1016/j.cemconres.2019.03.017.
- Lingyu, T.; Dongpo, H.; Jianing, Z.; Hongguang, W. (2021): Durability of geopolymers and geopolymer concretes: A review. In *Reviews on Advanced Materials Science* 60 (1), pp. 1–14. DOI: 10.1515/rams-2021-0002.
- Liu, Z.; Moslemi, A. A. (1985): Influence of chemical additives on the hydration characteristics of western larch wood-cementwater mixtures. In *Forest Products Journal* 7 (7/8), pp. 37–43.
- Magross, E. (2015): Evaluation of Selected Properties of Alder Wood as Functions of Sanding and Coating Progress Report No.3, Published by the Department of Wood Engineering, University of West Hungary Sopron. Lóvér-Print Nyomdaipari Kft, Sopron, Hungary, p 18.
- Malenab, R. A. J.; Ngo, J. P. S.; Promentilla, M. A. B. (2017): Chemical Treatment of Waste Abaca for Natural Fiber-Reinforced Geopolymer Composite. In *Materials (Basel, Switzerland)* 10 (6). DOI: 10.3390/ma10060579.
- Mallick, P. K. (2012): Advanced materials for automotive applications: an overview. In : *Advanced Materials in Automotive Engineering*: Elsevier, pp. 5–27.
- Marra, A. (1992): Technology of wood bonding. Principles in Practice. New York. NY.: Van Nostrand Reinhold.

- Mathivet, V.; Jouin, J.; Parlier, M.; Rossignol, S. (2021): Control of the aluminosilico-phosphate geopolymers properties and structures by the phosphorus concentration. In *Materials Chemistry and Physics* 258, p. 123867. DOI: 10.1016/j.matchemphys.2020.123867.
- Medri, V.; Papa, E.; Lizion, J.; Landi, E. (2020): Metakaolin-based geopolymer beads: Production methods and characterization. In *Journal of Cleaner Production* 244, p. 118844. DOI: 10.1016/j.jclepro.2019.118844.
- Meier, E. (2022): The Wood database. Available online at <https://www.wood-database.com/black-wattle/>, checked on 7/17/2022.
- Meijer, M. de (2004): A review of interfacial aspects in wood coatings: wetting, surface energy, substrate penetration and adhesion,” in: COST E18- Proceedings of the Final European Seminar on High Performance Wood Coatings Exterior and Interior Performance 26-27th April 2004, Paris, France,, 1-16.
- Meng, Q. K.; Hetzer, M.; Kee, D. de (2011): PLA/clay/wood nanocomposites: nanoclay effects on mechanical and thermal properties. In *Journal of Composite Materials* 45 (10), pp. 1145–1158. DOI: 10.1177/0021998310381541.
- Mertens, O. (2018): Performance and processing evaluation of thermoplastic wood fiber composites. Doctoral thesis. University of Hamburg, Hamburg, Germany. Institute for Wood Science.
- Missengue, R. N. M.; Losch, P.; Sedres, G.; Musyoka, N. M.; Fatoba, O. O.; Louis, B. et al. (2017): Transformation of South African coal fly ash into ZSM-5 zeolite and its application as an MTO catalyst. In *Comptes Rendus Chimie* 20 (1), pp. 78–86. DOI: 10.1016/j.crci.2016.04.012.
- Morla, P.; Gupta, R.; Azarsa, P.; Sharma, A. (2021): Corrosion Evaluation of Geopolymer Concrete Made with Fly Ash and Bottom Ash. In *Sustainability* 13 (1), p. 398. DOI: 10.3390/su13010398.
- Moslemi, A. A.; Garcia, J.F; Hofstrand, A. D. (1983): Effect of various treatments and additives on wood/portland cement/water systems. In *Wood Fiber Science* 15 (2), 164-76.
- Moura, L. F. de; Hernández, R. E. (2006): Effects of abrasive mineral, grit size and feed speed on the quality of sanded surfaces of sugar maple wood. In *Wood Science and Technology* 40 (6), p. 531. DOI: 10.1007/s00226-006-0077-6.

- Nath, P.; Sarker, P. K. (2014): Effect of GGBFS on setting, workability and early strength properties of fly ash geopolymer concrete cured in ambient condition. In *Construction and Building Materials* 66, pp. 163–171. DOI: 10.1016/j.conbuildmat.2014.05.080.
- Nourbakhsh, A.; Ashori, A. (2008): Fundamental studies on wood–plastic composites: Effects of fiber concentration and mixing temperature on the mechanical properties of poplar/PP composite. In *Polymer Composites* 29 (5), pp. 569–573. DOI: 10.1002/pc.20578.
- Nuaklong, P.; Jongvivatsakul, P.; Pothisiri, T.; Sata, V.; Chindapasirt, P. (2020): Influence of rice husk ash on mechanical properties and fire resistance of recycled aggregate high-calcium fly ash geopolymer concrete. In *Journal of Cleaner Production* 252, p. 119797. DOI: 10.1016/j.jclepro.2019.119797.
- Ogundiran, M. B.; Kumar, S. (2015): Synthesis and characterisation of geopolymer from Nigerian Clay. In *Applied Clay Science* 108, pp. 173–181. DOI: 10.1016/j.clay.2015.02.022.
- Okumura, S.; Fujiwara, Y. (2007): Roughness evaluation of machined surfaces of wood. In *Journal of the Japan Wood Research Society (Japan)* 53 (4), pp. 173–179.
- Olayiwola, O. H. (2021): Development of geopolymer bonded wood composites. Dissertation presented for the degree of Doctor of Philosophy. Stellenbosch University, South Africa. Wood Product Science.
- Orwa et al. (2009): Agroforestry Database 4.0. Available online at http://apps.worldagroforestry.org/treedb/AFTPDFS/Eucalyptus_camaldulensis.PDF, checked on 7/21/2022.
- Palomo, A.; Fernández-Jiménez, A.; Criado, M. (2004): "Geopolimeros": una única base química y diferentes microestructuras. In *Materiales de Construcción* 54 (275), pp. 77–91. DOI: 10.3989/mc.2004.v54.i275.249.
- Papp, E. A.; Csiha, C. (2017): Contact angle as function of surface roughness of different wood species. In *Surfaces and Interfaces* 8, pp. 54–59. DOI: 10.1016/j.surfin.2017.04.009.
- Pereira, B. L. C.; Carneiro, A. D. C. O.; Carvalho, A. M. M. L.; Colodette, J. L.; Oliveira, A. C.; Fontes, M. P. F. (2013): Influence of Chemical Composition of Eucalyptus Wood on Gravimetric Yield and Charcoal Properties. In *BioResources* 8 (3). DOI: 10.15376/biores.8.3.4574-4592.
- Perera, D. S.; Vance, E. R.; Finnie, K. S.; Blackford, M. G.; Hanna, J. V.; Cassidy, D. J. (2006): Disposition of Water in Metakaolinite Based Geopolymers. In: Bansal NP, Singh JP, Kriven WM, editors. *Advances in Ceramic Matrix Composites XI*. Hoboken, NJ, USA: John Wiley & Sons, Inc; p. 225–36.

- Petri, E. M. (1987). *Handbook of Adhesives and Sealants*. McGraw-Hill, New York.
- Phair, J. W.; Smith, J. D.; van Deventer, J.S.J. (2003): Characteristics of aluminosilicate hydrogels related to commercial “Geopolymers”. In *Materials Letters* 57 (28), pp. 4356–4367. DOI: 10.1016/S0167-577X(03)00325-2.
- Pong, W. Y.; Waddell, Dale R.; Lambert, Michael B. (1986): Wood density-moisture profiles in old-growth Douglas-fir and western hemlock. Res. Pap. PNW-347.
- Provis, J. L.; Duxson, P.; van Deventer, Jannie S. J. (2010): The role of particle technology in developing sustainable construction materials. In *Advanced Powder Technology* 21 (1), pp. 2–7. DOI: 10.1016/j.appt.2009.10.006.
- Purbasari, A.; Samadhi, T. W.; Bindar, Y. (2018): The Effect of Alkaline Activator Types on Strength and Microstructural Properties of Geopolymer from Co-Combustion Residuals of Bamboo and Kaolin. In *Indonesian Journal of Chemistry* 18 (3), p. 397. DOI: 10.22146/ijc.26534.
- Quiroga, A.; Marzocchi, V.; Rintoul, I. (2016): Influence of wood treatments on mechanical properties of wood–cement composites and of *Populus Euroamericana* wood fibers. In *Composites Part B: Engineering* 84, pp. 25–32. DOI: 10.1016/j.compositesb.2015.08.069.
- Raisanen, T.; Athanassiadis, D. (2013): Basic chemical composition of the biomass components of pine, spruce and birch. In *Forest Refine*. Available online at <https://pdf4pro.com/view/asic-chemical-composition-of-the-biomass-3f69c.html>.
- Redzuan, M. S. J.; Paridah, M. T.; Anwar, U. M. K.; Juliana, A. H.; Lee, S. H.; Norwahyuni, M. Y. (2019): Effects of surface pretreatment on wettability of *Acacia mangium* wood. In *Journal of Tropical Forest Science* 31 (2), pp. 249–258. DOI: 10.26525/jtfs2019.31.2.249258.
- Resnik, J.; Sernek, M.; Kamke, F. A. (1997): High-frequency heating of wood with moisture content gradient. Wood and fiber science. In *Wood and Fiber Science* 29 (3), pp. 264–271.
- Rohde, G. M.; Zwonok, O.; Chies, F.; Silva, N.I.W. (2006): Cinzas de carvão fóssil no Brasil—aspectos técnicos e ambientais. In *CIENTEC, Porto Alegre*, p. 202.
- Rosas-Casarez, C.; Arredondo-Rea, S.; Cruz-Enríquez, A.; Corral-Higuera, R.; Pellegrini-Cervantes, M.; Gómez-Soberón, J.; Medina-Serna, T. (2018): Influence of Size Reduction of Fly Ash Particles by Grinding on the Chemical Properties of Geopolymers. In *Applied Sciences* 8 (3), p. 365. DOI: 10.3390/app8030365.

- Rovnaník, Pavel (2010): Effect of curing temperature on the development of hard structure of metakaolin-based geopolymer. In *Construction and Building Materials* 24 (7), pp. 1176–1183. DOI: 10.1016/j.conbuildmat.2009.12.023.
- Rowell, Roger M. (2013): Handbook of wood chemistry and wood composites. 2nd ed. Boca Raton: Taylor & Francis.
- Ryu, G. S.; Lee, Y. B.; Koh, K. T.; Chung, Y. S. (2013): The mechanical properties of fly ash-based geopolymer concrete with alkaline activators. In *Construction and Building Materials* 47, pp. 409–418. DOI: 10.1016/j.conbuildmat.2013.05.069.
- Sá Ribeiro, R. A.; Sá Ribeiro, M. G.; Sankar, K.; Kriven, W. M. (2016): Geopolymer-bamboo composite – A novel sustainable construction material. In *Construction and Building Materials* 123, pp. 501–507. DOI: 10.1016/j.conbuildmat.2016.07.037.
- Sabhadiya, J. (2022): What Is Composite Material?- Definition And Types. Available online at <https://www.engineeringchoice.com/composite-material/>, checked on 7/10/2022.
- Saidi, N.; Samet, B.; Baklouti, S. (2013): Effect of Composition on Structure and Mechanical Properties of Metakaolin Based PSS-Geopolymer. In *International Journal of Material Sciences* 3 (4), p. 145. DOI: 10.14355/ijmsci.2013.0304.03.
- Sandermann, W.; Preusser, H. J.; Schweers, W. (1960): The effect of wood extractives on the setting of cement-bonded wood materials. In *Holzforschung* 14 (3), 70-77.
- Sandermann, W.; Brendel, M. (1956): Studien über mineralgebundene Holzwerkstoffe—Zweite Mitteilung: Die „zementvergiftende“ Wirkung von Holzinhaltsstoffen und ihre Abhängigkeit von der chemischen Konstitution. In *Holz Roh Werkst* 14 (8), pp. 307–313. DOI: 10.1007/BF02605217.
- Saranpää, P. (1996): Holzatlas. 4th Edition. R. Wagenführ, 688 pp., 1996 [In German]. Fachbuchverlag Leipzig, Germany. ISBN 3-446-00900-0. Available from Carl Hanser Verlag, Postfach 860420, D-81631 München, Germany. In *IAWA J* 17 (3), pp. 343–344. DOI: 10.1163/22941932-90001585.
- Sarmin, S. N.; Welling, J.; Krause, A.; Shalbafan, A. (2014): Investigating the possibility of geopolymer to produce inorganic-bonded wood composites for multifunctional construction material - A Review. In *BioResources* 9 (4), pp. 7941–7950.
- Sarmin, S. N. (2016): The Influence of Different Wood Aggregates on the Properties of Geopolymer Composites. In *Key Engineering Materials* 723, pp. 74–79. DOI: 10.4028/www.scientific.net/KEM.723.74.
- Sarmin, S.N.; Rahman, W. M. N. W. A.; Mohd Yunus, N. Y.; Ahmad, N. (2020): Determination of the Bond Strength of Wood Veneer and Geopolymer Matrix by Means

- of a Pull-Out Test. In *Materials Science Forum* 981, pp. 162–168. DOI: 10.4028/www.scientific.net/MSF.981.162.
- Sarmin, S. N.; Welling, J. (2016): Lightweight geopolymer wood composite synthesized from alkali-activated fly ash and metakaolin. In *Jurnal Teknologi* 78 (11), pp. 49–55.
- Schirp, A.; Stender, J. (2010): Eigenschaften von extrudierten Holz-Kunststoff-Werkstoffen auf Basis von Refiner-(TMP-)Fasern und Hanffasern. In *Holz Roh Werkst* 68 (2), pp. 219–231. DOI: 10.1007/s00107-009-0372-7.
- Schwarzkopf, M. J.; Burnard, M. D. (2016): Wood-Plastic Composites—Performance and Environmental Impacts. In Andreja Kutnar, Subramanian Senthilkannan Muthu (Eds.): *Environmental Impacts of Traditional and Innovative Forest-based Bioproducts*. Singapore: Springer Singapore (Environmental Footprints and Eco-design of Products and Processes), pp. 19–43.
- Seiffarth, T.; Hohmann, M.; Posern, K.; Kaps, C. (2013): Effect of thermal pre-treatment conditions of common clays on the performance of clay-based geopolymeric binders. In *Applied Clay Science* 73, pp. 35–41. DOI: 10.1016/j.clay.2012.09.010.
- Simple, K. E.; Evans, P. D. (2000): Adverse effects of heartwood on the mechanical properties of wood-wool cement boards manufactured from radiata pine wood. In *Wood Fiber Science* 32 (1), pp. 37–43.
- Shaikh, F. U. A. (2013): Review of mechanical properties of short fibre reinforced geopolymer composites. In *Construction and Building Materials* 43, pp. 37–49. DOI: 10.1016/j.conbuildmat.2013.01.026.
- Sharma, A. K.; Bhandari, R.; Aherwar, A.; Rimašauskienė, R. (2020): Matrix materials used in composites: A comprehensive study. In *Materials Today: Proceedings* 21, pp. 1559–1562. DOI: 10.1016/j.matpr.2019.11.086.
- Shehab, H. K.; Eisa, A. S.; Wahba, A. M. (2016): Mechanical properties of fly ash based geopolymer concrete with full and partial cement replacement. In *Construction and Building Materials* 126, pp. 560–565. DOI: 10.1016/j.conbuildmat.2016.09.059.
- Shi, C.; Jiménez, A. F.; Palomo, A. (2011): New cements for the 21st century: The pursuit of an alternative to Portland cement. In *Cement and Concrete Research* 41 (7), pp. 750–763. DOI: 10.1016/j.cemconres.2011.03.016.
- Shill, S. K.; Al-Deen, S.; Ashraf, M.; Garcez, E. O.; Subhani, M.; Hossain, M. M. (2022): Resistance of Geopolymer, Epoxy and Cement Mortar to Hydrocarbon-Based Synthetic Engine Lubricant, Hydraulic Fluid, Jet Fuel and Elevated Temperatures. In *Construction Materials* 2 (1), pp. 15–26. DOI: 10.3390/constrmater2010002.

- Shill, S. K.; Al-Deen, S.; Ashraf, M.; Hutchison, W. (2020): Resistance of fly ash based geopolymer mortar to both chemicals and high thermal cycles simultaneously. In *Construction and Building Materials* 239, p. 117886. DOI: 10.1016/j.conbuildmat.2019.117886.
- Silva, F. A. V. D.; Silva, J. R. M. da; Moulin, J. C.; Andrade, A. C. D. A.; Nobre, J. R.; Castro, J. P.(2016): Qualidade da superfície usinada em pisos de madeiras de Corymbia E Eucalyptus. In *Revista Floresta* 46 (3), p. 397. DOI: 10.5380/rf.v46i3.43936.
- Simatupang, M. H.; Geimer, R. L. (1990): Inorganic Binder for Wood Composites: Feasibility and Limitations. *Proceeding of Wood Adhesive Symposium*, pp. 169–176.
- Sindhunata; van Deventer, J. S. J.; Lukey, G. C.; Xu, H. (2006): Effect of Curing Temperature and Silicate Concentration on Fly-Ash-Based Geopolymerization. In *Industrial & Engineering Chemistry Research* 45 (10), pp. 3559–3568. DOI: 10.1021/ie051251p.
- Singh, B.; Ishwarya, G.; Gupta, M.; Bhattacharyya, S. K. (2015): Geopolymer concrete: A review of some recent developments. In *Construction and Building Materials* 85, pp. 78–90. DOI: 10.1016/j.conbuildmat.2015.03.036.
- Singh, P. S.; Trigg, M.; Burgar, I.; Bastow, T. (2005): Geopolymer formation processes at room temperature studied by ²⁹Si and ²⁷Al MAS-NMR. In *Materials Science and Engineering: A* 396 (1-2), pp. 392–402. DOI: 10.1016/j.msea.2005.02.002.
- Singleton, R.; DeBell, D. S.; Gartner, B. L. (2003): Effect of extraction on wood density of western hemlock (*Tsuga heterophylla* (raf.) sarg.). In *Wood and Fiber Science* 35 (3), pp. 363–369.
- Song, S.; Sohn, D.; Jennings, H. M.; Mason, T. O. (2000). In *Journal of Materials Science* 35 (1), pp. 249–257. DOI: 10.1023/A:1004742027117.
- Stark, N. M.; Cai, Z.; Carll, C. (2010): Wood-based Composites and Panel Products. In: *Wood handbook. Wood as an engineering material*. Forest Products Society, Madison, Wis.
- Stark, N. M.; Rowlands, R. E. (2003): Effects of wood fiber characteristics on mechanical properties of wood/polypropylene composites. In *Wood and fiber science*. 35 (2), pp. 167–174.
- Stevenson, M.; Sagoe-Crentsil, K. (2005): Relationships between composition, structure and strength of inorganic polymers. In *Journal of Materials Science* 40 (16), pp. 4247–4259. DOI: 10.1007/s10853-005-2794-x.

- Sulaiman, O.; Hashim, R.; Subari, K.; Liang, C. K. (2009): Effect of sanding on surface roughness of rubberwood. In *Journal of Materials Processing Technology* 209 (8), pp. 3949–3955. DOI: 10.1016/j.jmatprotec.2008.09.009.
- Sutigno, P. (2000): Effect of aqueous extraction of wood-wool on the properties of woodwool cement board manufactured from teak (*Tectona grandis*). In: Wood-cement composites in the Asia-Pacific region. pp. 24–28.
- Syofuna, A.; Banana, A. Y.; Nakabonge, G. (2012): Efficiency of natural wood extractives as wood preservatives against termite attack. In *Maderas, Ciencia y Tecnología* 14 (2), pp. 155–163. DOI: 10.4067/S0718-221X2012000200003.
- Tamba, S.; Jauberthie, R.; Lanos, C.; Rendell, F. (2001): Lightweight wood fibre concrete. In *Concrete Science and Engineering* 3 (9), pp. 53–57.
- Tan, J.; Lu, Wanli; H. Y.; Wei, Shiju; Xuan, X.; Liu, L.; Zheng, G. (2019): Preliminary study on compatibility of metakaolin-based geopolymer paste with plant fibers. In *Construction and Building Materials* 225, pp. 772–775. DOI: 10.1016/j.conbuildmat.2019.07.142.
- Taylor, J. B.; Carrano, A. L.; Lemaster, R. L. (1999). Quantification of process parameters in a wood sanding operation. *Forest Products Journal* 49 (5), 41–46.
- Tugrul A., Ali; Yasar, M.; Gurkaynak, M. A.; Gurgey, I. (2005): Investigation of the effects of fatty acids on the compressive strength of the concrete and the grindability of the cement. In *Cement and Concrete Research* 35 (2), pp. 400–404. DOI: 10.1016/j.cemconres.2004.07.031.
- Usta, I. (2003): Comparative Study of Wood Density by Specific Amount of Void Volume (Porosity). In *Turkish Journal of Agriculture and Forestry* 27, pp. 1–6.
- van Chanh, N.; Trung, B. D.; van Tuan, D. (2008): Recent research geopolymer concrete. In Proceedings of the 3rd ACF International Conference-ACF/VCA, Ho Chi Minh City, Vietnam, 11–13 November 2008 18, pp. 235–241.
- van Deventer, J. S. J.; Provis, J. L.; Duxson, P.; Lukey, G. C. (2007): Reaction mechanisms in the geopolymeric conversion of inorganic waste to useful products. In *Journal of Hazardous Materials* 139 (3), pp. 506–513. DOI: 10.1016/j.jhazmat.2006.02.044.
- van Jaarsveld, J. G. S.; van Deventer, J. S. J. (1999): Effect of the Alkali Metal Activator on the Properties of Fly Ash-Based Geopolymers. In *Industrial & Engineering Chemistry Research* 38 (10), pp. 3932–3941. DOI: 10.1021/ie980804b.
- van Jaarsveld, J. G. S.; van Deventer, J. S. J.; Lukey, G. C. (2002): The effect of composition and temperature on the properties of fly ash- and kaolinite-based geopolymers. In

- Chemical Engineering Journal* 89 (1-3), pp. 63–73. DOI: 10.1016/S1385-8947(02)00025-6.
- Vassilev, S. V.; Vassileva, C. G. (2009): A new approach for the combined chemical and mineral classification of the inorganic matter in coal. 1. Chemical and mineral classification systems. In *Fuel* 88 (2), pp. 235–245. DOI: 10.1016/j.fuel.2008.09.006.
- Vogt, O.; Ukrainczyk, N.; Ballschmiede, C.; Koenders, E. (2019): Reactivity and Microstructure of Metakaolin Based Geopolymers: Effect of Fly Ash and Liquid/Solid Contents. In *Materials (Basel, Switzerland)* 12 (21). DOI: 10.3390/ma12213485.
- Wan, Q.; Zhang, R.; Zhang, Y. (2022): Structure and Properties of Phosphate-Based Geopolymer Synthesized with the Spent Fluid Catalytic-Cracking (SFCC) Catalyst. In *Gels (Basel, Switzerland)* 8 (2). DOI: 10.3390/gels8020130.
- Wang, C.; Piao, C. (2011): From Hydrophilicity to hydrophobicity: A Critical Review—Part Ii: Hydrophobic Conversion. In *Wood and Fiber Science* 43 (1), pp. 41–56.
- Wang, H.; Li, H.; Yan, F. (2005): Synthesis and mechanical properties of metakaolinite-based geopolymer. In *Colloids and Surfaces A: Physicochemical and Engineering Aspects* 268 (1-3), pp. 1–6. DOI: 10.1016/j.colsurfa.2005.01.016.
- Wang, Y-S.; Dai, J-G.; Ding, Z.; Xu, W-T. (2017): Phosphate-based geopolymer: Formation mechanism and thermal stability. In *Materials Letters* 190, pp. 209–212. DOI: 10.1016/j.matlet.2017.01.022.
- Weatherwax, R. C.; Tarkow, H. (1964): Effect of wood on the setting of Portland cement. In *Forest Products Journal* 14 (12), pp. 567–570.
- Xu, H.; van Deventer, J. S. J. (2002): Geopolymerisation of multiple minerals. In *Minerals Engineering* 15 (12), pp. 1131–1139. DOI: 10.1016/S0892-6875(02)00255-8.
- Ye, H.; Zhang, Y.; Yu, Z.; Mu, J. (2018): Effects of cellulose, hemicellulose, and lignin on the morphology and mechanical properties of metakaolin-based geopolymer. In *Construction and Building Materials* 173, pp. 10–16. DOI: 10.1016/j.conbuildmat.2018.04.028.
- Youngquist, J. A. (1999): Wood-based composites and panel products. Wood handbook: wood as an engineering material. Madison, WI: USDA Forest Service, Forest Products Laboratory, 1999. General technical report FPL; GTR-113;., pp. 1–31.
- Zhang, B.; Guo, H.; Yuan, P.; Deng, L.; Zhong, X.; Li, Y. et al. (2020a): Novel acid-based geopolymer synthesized from nanosized tubular halloysite: The role of precalcination temperature and phosphoric acid concentration. In *Cement and Concrete Composites* 110, p. 103601. DOI: 10.1016/j.cemconcomp.2020.103601.

- Zhang, P.; Gao, Z.; Wang, J.; Guo, J.; Hu, S.; Ling, Y. (2020b): Properties of fresh and hardened fly ash/slag based geopolymer concrete: A review. In *Journal of Cleaner Production* 270, p. 122389. DOI: 10.1016/j.jclepro.2020.122389.
- Zhang, P.; Wang, K.; Li, Q.; Wang, J.; Ling, Y. (2020c): Fabrication and engineering properties of concretes based on geopolymers/alkali-activated binders - A review. In *Journal of Cleaner Production* 258, p. 120896. DOI: 10.1016/j.jclepro.2020.120896.
- Zhao, Q.; Nair, B.; Rahimian, T.; Balaguru, P. (2007): Novel geopolymer based composites with enhanced ductility. In *Journal of Materials Science* 42 (9), pp. 3131–3137. DOI: 10.1007/s10853-006-0527-4.
- Zhengtian, L.; Moslemi, A. A. (1985): Influence of chemical additives on the hydration characteristics of western larch wood cement water mixtures. In *Forest Product Journal* 35 (7), pp. 37–43.
- Zhuang, X. Y.; Chen, L.; Komarneni, S.; Zhou, C. H.; Tong, D. S.; Yang, H. M. et al. (2016): Fly ash-based geopolymer: clean production, properties and applications. In *Journal of Cleaner Production* 125, pp. 253–267. DOI: 10.1016/j.jclepro.2016.03.019.
- Zuhua, Z.; Xiao, Y.; Huajun, Z.; Yue, C. (2009): Role of water in the synthesis of calcined kaolin-based geopolymer. In *Applied Clay Science* 43 (2), pp. 218–223. DOI: 10.1016/j.clay.2008.09.003.

Eidesstattliche Versicherung

Declaration on oath

Hiermit erkläre ich an Eides statt, dass ich die vorliegende Dissertationsschrift selbst verfasst und keine anderen als die angegebenen Quellen und Hilfsmittel benutzt habe.

I hereby declare, on oath, that I have written the present dissertation by my own and have not used other than the acknowledged resources and aids.

Ich versichere, dass ich keine Dissertation mit dem gleichen Forschungsthema schon einmal in einem früheren Promotionsverfahren an einer wissenschaftlichen Hochschule eingereicht habe, die angenommen oder als ungenügend beurteilt worden ist.

I, the undersigned, hereby declare that I have not submitted a dissertation with the same research topic to an academic higher education institution that had been already accepted or evaluated as insufficient in an earlier doctoral procedure.

Ich versichere, dass beide Formen der mit diesem Antrag zur Bewertung eingereichten Dissertation (d.h. die gebundene Dissertationsschrift und die in elektronischer Form eingereichte Dissertation) übereinstimmen.

I, the undersigned, declare that both forms of the dissertation submitted for evaluation (i.e. the dissertation in hard copy and the dissertation submitted in electronic form) are identical.

Hamburg, 22.10.2022



Bright Asante